RL-331
November 1965

THE EXCITATION OF SURFACE CURRENTS ON A PLASMA-IMMERSED CYLINDER BY INCIDENT ELECTROMAGNETIC AND ELECTROKINETIC WAVES

by
Edmund Kenneth Miller

A dissertation submitted in partial fulfillment
of the requirements for the degree of
Doctor of Philosophy in
The University of Michigan
1965

Doctoral Committee:

Associate Professor Andrejs Olte, Chairman
Professor Chiao-Min Chu
Doctor Raymond F. Goodrich
Professor John S. King
Associate Professor Herschel Weil

RL-331 = RL-331

THE EXCITATION OF SURFACE CURRENTS ON A PLASMA-IMMERSED CYLINDER BY INCIDENT ELECTROMAGNETIC AND ELECTROKINETIC WAVES

by Edmund Kenneth Miller

The purpose of this study is to investigate the surface currents excited by plane electromagnetic (EM) and electrokinetic (EK) (or plasma) waves on an infinitely long, perfectly conducting, circular cylinder immersed in a slightly ionized plasma and drawing zero net current from the plasma. The coupling of the EM and EK waves in the inhomogeneous sheath surrounding the cylinder owing to the boundary conditions at the cylinder surface is examined. The primary motivation for this study is to determine the feasibility of detecting the presence of the EK wave in a plasma by a measurement of the surface currents which it might excite on such a cylinder.

The theoretical formulation of the problem is developed by taking the zeroth and first order velocity moments of the collisionless Boltzmann equation for the electrons and ions. Upon introduction of an equation of state and a scalar pressure for the electrons and ions, together with Maxwell's equations, the process of linearization leads to two sets of equations. One set describes the static plasma while the other accounts for the time-varying or dynamic plasma behavior. These equations show that when the dynamic ion motion is neglected two kinds of waves, the EM and EK waves, can propagate independently in a uniform plasma. Variations in the static plasma properties in a region of non-uniform plasma lead to coupling of these waves.

The interaction of the incident EM or EK wave with the cylinder is studied in two ways, both of which take the sheath to extend a finite distance from the cylinder surface. In the first, the inhomogeneous sheath model, the actual variations in static plasma properties are accounted for. The equations describing the dynamic field variation in the inhomogeneous sheath require numerical solution while those applying in the uniform plasma can be solved analytically. The boundary value problem for waves incident on the cylinder at an arbitrary angle with respect to its axis is then set up by applying boundary conditions to the

field quantities at the cylinder surface and the inhomogeneous sheath-uniform plasma interface. An outline for the procedure used in obtaining a numerical solution to the boundary value problem is given. A second approach to the problem involves replacing the actual inhomogeneous sheath by a free-space layer, which is called the vacuum sheath. The boundary value problem associated with this model is also set up and an analytic solution for the various fields is given.

Extensive numerical results for the surface currents are presented. The vacuum sheath results are given for arbitrary angle of incidence while the inhomogeneous sheath results are restricted to normal wave incidence. It is shown that the surface currents for EK wave incidence are exponentially attenuated by the vacuum sheath, with the attenuation increasing as the angle of incidence measured from the cylinder axis becomes smaller. Further it is found that the EK wave is not as efficient in producing surface currents as the EM wave, even when the sheath attenuation is not taken into account. It is also found that the sheath and plasma compressibility have little effect on the currents due to the EM wave for cylinders with radii small compared with the EM wavelength. Finally, the results of the inhomogeneous sheath and vacuum sheath models are found to be in substantial agreement for normal incidence.

We can conclude from the results of this study that: 1) the plasma compressibility and sheath can be neglected when considering the currents excited by EM waves on a plasma-immersed cylinder of small radius compared with the EM wavelength; 2) the sheath appears to quite effectively screen the EK wave from the cylinder; 3) it appears that since the EK wave is less efficient that the EM wave in exciting surface currents on the cylinder, it would be difficult to detect the EK wave in a background of EM radiation, by a measurement of the surface currents which it produces.

ACKNOWLEDGMENT

The author wishes to express his appreciation to the members of his committee for their help and guidance during this study. Special thanks are especially due to Andrejs Olte, the committee chairman, who suggested the problem. He gave invaluable support throughout the course of this work and furnished many helpful suggestions for carrying it through to completion.

This research was supported in part by the National Aeronautics and Space Administration under Grant NsG-472 with the Langley Research Center at Hampton, Virginia. The numerical computations were supported by The University of Michigan Computing Center.

Special thanks are also due to the author's wife for her patience during the course of this work and for rewriting the original manuscript.

TABLE OF CONTENTS

LIST OF FIGURES

CHAPTER I

INTRODUCTION

The dynamic response of a plasma to high frequency electric fields has received considerable attention in recent years. By plasma we mean a partially ionized gas that on the average is electrically neutral. The analysis of the plasma may proceed from the Boltzmann equation and Maxwell's equations together with appropriate boundary conditions and sources. The ultimate solution involves finding the electric and magnetic fields in the plasma as well as the distribution functions for the various plasma species. Because of the great mathematical difficulty, this is seldom possible. Instead, the problem is converted to one involving only macroscopic variables by taking velocity moments of the Boltzmann equation. In many practical problems it is physically reasonable to neglect all moments higher than second order in velocity. This means we introduce as new macroscopic variables the scalar number density, the vector velocity, and the tensor pressure* for each plasma species. The moment equations obtained are nonlinear in these variables. They are linearized by requiring the time varying perturbations of these variables to be small compared with the static parts. Under certain conditions the tensor pressure reduces to scalar pressure. The perturbed pressure is related by an equation of state to the perturbed number density. The problem at this point is one of finding the perturbed number density and velocity of each species, in addition to the electric and magnetic fields.

Studying the plasma equations thus obtained one observes that for a uniform plasma free of static magnetic fields the electric field can be decomposed into a

*The tensor pressure is often referred to as the kinetic stress tensor.

solenoidal and an irrotational part which can be shown independently to satisfy different vector wave equations. The total time-varying magnetic field is then related to the solenoidal electric field and together they form an electromagnetic (EM) wave. The irrotational time varying electric field is associated with the perturbed charge density accumulation (space charge). These two quantities form a wave that has been referred to as the plasma wave, electro-acoustic wave, and electrokinetic (EK)* wave. We will use the latter term. In the EM wave the energy is shared between the solenoidal electric field and the magnetic field. In the EK wave the energy is shared between the time varying irrotational electric field and the ordered kinetic energy of the charged particles.

In the study of plasma, one frequently finds that to a reasonable approximation the plasma under consideration may be divided into uniform plasma regions connected by nonuniform plasma transitions. Or we may find a uniform plasma terminated via a nonuniform plasma (the sheath) into either dielectric, conductor, or free space. In the nonuniform plasma transition regions the EM and EK waves are coupled due to the static electron density variation. This means that an EK wave (for example) propagating into such a region in addition to reflections will suffer a loss of energy into the EM wave and vice versa. A similar energy conversion between the two waves occurs at sharp transition regions such as the boundary between plasma sheath and dielectric (or metal). This is due to the boundary conditions on the tangential electric and magnetic fields and the ordered electron velocity at the interface. The two waves will be significantly coupled

*This name was suggested by G. Hok (1959).

even in uniform plasma if the linearization requirement on the velocity moment equation is relaxed. The same thing is true if an external static magnetic field is present. We are excluding the last two forms of coupling from this discussion.

The energy conversion between the waves is of interest in applications as diverse as astrophysics and radiation or reception by plasma-immersed antennas. Some of the radio emissions from stellar bodies [illegible] explained on this basis. The effect of the wave conversion on transmission and reception properties of the plasma-imbedded antenna is of considerable importance. The latter is our field of interest. Before we present our problem in detail, it is of value to review briefly some of the pertinent work that has been done in this general area. For an orderly discussion it is convenient to arrarge the papers dealing with the conversion problem into two categories: the scattering problem and the radiation problem. Since in our area of interest the high frequency response of plasma presumes a knowledge of the static plasma sheath solution, the work on this topic will be reviewed.

1. 1 Review of Previous Work

1. 1. 1 The Scattering Problem

A discussion of the scattering problem can be carried out conveniently according to the geometry of the transition region. A further classification of this problem can be made of the basis of whether or not the thickness of the transition region is taken to be small compared with the pertinent wavelengths so that it may be considered as an abrupt discontinuity of the plasma properties. When the transition region is assumed thin, the problem is one of considering

propagation in a uniform plasma together with appropriate boundary conditions at the discontinuity. The use of such a representation is an approximation since a real plasma cannot support abrupt changes in its properties, such as those which occur at the walls confining a laboratory plasma for example, without a corresponding transition region where the plasma properties change in some continuous manner. The validity of such an approximation would be dependent in part on the wavelength of the waves incident on such a transition region compared with its thickness. The coupling between the EM and EK waves due to the nonuniformity is thus neglected with this approach. When the transition region is thick the problem requires consideration of the wave propagation in both the uniform plasma and the nonuniform transition region, together with appropriate boundary conditions. This latter problem is obviously much more complex than the former. The boundary conditions which are taken to apply at an arbitrary boundary are the usual ones from electromagnetic theory for the tangential electric and magnetic fields. In addition, conditions analogous to those encountered in acoustics are usually employed for the pressure and velocity, that is, continuity of electron pressure and normal electron velocity across a permeable boundary, or vanishing of normal electron velocity at a rigid boundary. There is no unanimity regarding the latter boundary condition however, and the use of a different boundary condition will be noted.

1.1.1a Plane Boundary

Thin Transition Region. In the first general treatment of EM and EK wave propagation in a plasma, Field (1956) considered the conversion of EK plane waves

to EM plane waves at a sharp plasma - vacuum interface. Field's formulation began without taking into account the static electric field which is present in regions of electron density variation in the plasma, so his discussion of this aspect of the problem is not correct. His requirement that the normal electron velocity vanish at the interface was also incorrect in not allowing for the possibility of a surface charge. However, Field's work was significant in that his treatment established the basic approach followed later by other investigators in decomposing plane waves in uniform plasma into EM and EK components.

A problem similar to that considered by Field was investigated by Kritz and Mintzer (1960), the difference being that their problem involved a sharp plasma-plasma boundary. They took the normal electron velocity across the interface to be continuous. Analytical expressions for the transmitted and reflected electric fields for arbitrary angles of incidence were obtained. Some numerical results showing the reflection and transmission coefficients of the EK wave for an incident EM wave and the reflection and transmission coefficients of the EM wave for an incident EK wave as a function of the angle of incidence are presented. The ratio of the electron density on the two sides of the interface was taken to be 2. The results show that the EM waves are more efficiently converted to EK waves than are EK waves converted to EM waves. It is interesting that the EK wave excites propagating EM waves for only a small angular interval around normal incidence. Otherwise, EM surface waves, decaying exponentially normal to the surface, are produced, due to the large difference in the propagation constants of the EM and EK waves.

Tidman (1960) found the conversion efficiency of EK to EM energy for the case of a plane EK wave at normal incidence on a plasma-plasma discontinuity. A scalar form was used for the static pressure while the dynamic pressure was taken to be a tensor. His boundary condition on the normal electron velocity was different from that of Kritz and Mintzer in that the total current (displacement plus conduction) was taken to be continuous across the interface. A numerical result for the conversion efficiency was obtained for one particular discontinuity where the static electron density changes by a factor of 2 at the interface.

Cohen (1962a) obtained expressions for the reflection coefficients of EK and EM waves incident on a plasma-metal interface. In formulating the boundary condition on the normal electron velocity, he introduced a bilinear admittance relation between the velocity and the perturbed electron density and electric field. The reflection coefficients which are given involve these admittances but no explicit form is given for them, nor is there any discussion of a possible theoretical method for obtaining them.

Tidman and Boyd (1962) extended Tidman's (1960) earlier work on the plasma-plasma interface. They used the same boundary conditions as those previously used by Tidman except for his continuity condition on the dynamic pressure. An integration through the thin transition region was performed on the electron equation of motion, which gave the discontinuity in the dynamic pressure in terms of the static electric field in the transition region. Expressions for the transmission and reflection coefficients for an EK wave incident at an arbitrary angle on such a boundary are obtained

Fedorchenko (1962) examined the reflection of EK and EM waves from a plasma-dielectric interface, assuming elastic reflection of the electrons from the boundary. The transmission coefficient of the EK wave due to an EM wave incident on such a discontinuity from the dielectric side is found as a function of the angle of incidence for various ratios of the plasma frequency to the radio frequency. These results are plotted graphically and indicate transmission coefficients on the order of 10 to 50 times greater than those obtained by Kritz and Mintzer for the plasma-plasma interface.

Thick Transition Region. Tidman (1960) also investigated the EM radiation produced by an EK wave propagating through a transition region thick compared with the EK wavelength. He calculated the conversion efficiency of EK to EM energy as a function of the ratio of the length of the static electron density variation to the EK wavelength. He was able to show that the conversion efficiency becomes exponentially small for EK wavelengths less than a certain scale length of the electron density variation.

1.1.1b. Spherical Boundary

Thin Transition Region. Cohen (1962a) examined the scattering characteristics of a plasma bubble of constant static electron density which is different from that of the surrounding plasma. Formulas were obtained for the scattering coefficients of such a bubble when illuminated by incident EK and EM radiation, assuming the bubble dimensions are much less than the EK wavelength. The results show that the cross section for scattering into the EK wave are on the order of $(v_\ell/v_r)^3$ greater than the corresponding EM scattering cross sections, where

v_r is the electron rms velocity and v_ℓ is the velocity of light in free space.

The scattering of plane EK and EM waves by a spherically shaped discontinuity in plasma density was treated by Yildiz (1963). He considered the situation where the sphere and the surrounding medium were plasmas of different static electron density, and also where the static electron density of either was zero. Expressions for the scattered fields and scattering cross section are obtained

Thick Transition Region The problem of the scattering of plane EK waves by spherically shaped blobs of small amplitude fluctuations in plasma density was investigated by Tidman and Weiss (1961) The EM energy radiated was determined for the case where the electron density variation is Gaussian, decreasing from the center of the blob. It was found that the scattered energy is exponentially dependent on the square of the ratio of the electron density scale length to the EK wavelength, decreasing as the ratio becomes larger.

1.1.2 The Radiation Problem

The radiation problem may be conveniently discussed according to the kind of source involved In physical problems, the radiation source almost always consists of a physical structure or body which is connected by a transmission line to the generator. The generator impresses voltage across parts of the radiating body and produces current on it. These induced sources produce fields for which a solution is desired. For mathematical convenience in many cases a problem is solved by ignoring the body, and finding the radiation from an equivalent distribution of isolated sources. Thus, for example, if the far-zone fields of a thin linear

dipole antenna are desired, one may solve the corresponding problem for a filamentary current source. A solution of the radiation from a body is difficult since appropriate boundary conditions must be satisfied on the surface of the body. The following discussion of the radiation problem is divided therefore into two parts: the first deals with radiation from isolated sources and the second with radiation from bodies.

1.1.2a Radiation from Isolated Sources

Cohen (1962a) considered the fields due to various kinds of surface distribution of sources in a uniform plasma. His analysis was limited to sources distributed uniformly over a plane surface infinite in extent, with plasma on both sides.

In another paper the fields due to an oscillating current filament in a uniform plasma were found by Cohen (1962b). His analysis showed that the EM field is maximum in a plane normal to the filament while the EK field is maximum along the filament axis. The radiation resistence of the current filament was found to be dominated by the effect of the EK wave. Unfortunately, no definite conclusion can be reached about the behavior of an actual linear dipole in a plasma since the sheath effect and the boundary conditions which must be satisfied on the real antenna are not taken into account by the current filament analysis.

Hessel et al (1962) found both types of fields excited within a uniform plasma half-space due to a magnetic line current source located in free space parallel to the plasma-free space interface. In another paper Hessel and Shmoys (1962) considered the excitation of EM and EK waves by a short oscillating current filament in a uniform plasma. Like Cohen (1962b), they conclude that most of the

radiated power is in the form of EK waves.

1.1.2b Radiation from Bodies

In the same paper in which he examined the radiation from an oscillating current filament in a plasma, Cohen (1962b) also set up the problem for radiation from a wire dipole antenna. He obtained two linear integral equations for the radiated fields, but made no attempt to solve them.

Hessel and Shmoys (1962) also considered the fields due to a prescribed current distribution on the surface of a rigid sphere. They obtained some expressions for the far fields and compared them with the results of the short current filament

Wait (1964a, b) solved for the fields produced by a slotted spherical antenna immersed in a uniform plasma He considered two cases, one when the plasma extends to the surface of the sphere, and the other when the sphere is separated from the plasma by a dielectric layer. The latter model is an attempt to account for the sheath. No numerical results are given, but expressions for the impedance and radiated power are obtained. He concludes that the EK waves will be excited by such an antenna.

1.1.3 The Static Sheath Problem

Before the dynamic plasma behavior can be theoretically analyzed insofar as wave propagation is concerned, a knowledge of the static plasma description is required. This is not a problem where the plasma can be reasonably taken to be uniform, as in regions far from perturbing influences such as confining walls, or bodies immersed in the plasma In the regions close to such perturbing

influences, the plasma is not uniform, however. Such regions are referred to as the plasma sheath. A great deal of effort has been devoted to finding the static plasma behavior in such sheaths. Included below are some of the more pertinent analyses which have been made of the static sheath problem.

A solution to the static plasma sheath problem involves finding the electron and ion number densities and the potential as a function of the space coordinates in the sheath. The ion and electron number densities are related to the potential via Poisson's equation. Expressions for these number densities are obtained by appropriately integrating their respective velocity distribution functions over the velocity. Upon putting these expressions (which are functions of the potential) into Poisson's equation, and integrating subject to the appropriate boundary conditions, a solution for the potential is obtained. It is apparent that in order to carry out the procedure outlined, the electron and ion velocity distribution functions must be known. It is usual to assume the electrons have a Maxwellian velocity distribution function, but the ions on the other hand may be taken to possess some other distribution. The choice used depends to a large extent on the particular problem under consideration, as will be discussed in the following. Various other simplifying assumptions may also be made, such as taking the sheath to be sharply defined from the uniform plasma and ignoring collisions in the sheath. It should be observed that since the random electron velocities are much greater than the random ion velocities in the same plasma, due to their difference in mass, the sheath electric field about an insulated boundary will be such as to attract the ions and repel the electrons. This sheath is thus a region

where the ion density exceeds the electron density.

Tonks and Langmuir (1929a) analyzed the low pressure discharge for plane, cylindrical and spherical geometries. They assumed a Maxwellian distribution function for the electron velocities. Ion generation was also taken into account, assuming the ions to be generated at rest, so that their velocities depended only on the potential difference through which they fall after generation. Ion collisions were ignored. Poisson's equation was then used together with knowledge of the ion and electron velocity distribution function to obtain an integral equation for the potential, which was called the complete plasma-sheath equation. This equation exhibits a dependence on the kind of model assumed for the ion generation. It was simplified by assuming that the ion and electron densities are equal to a high degree of accuracy (Tonks and Langmuir called this the plasma equation) and it was solved for two ion-generation models. A solution to the simplified equation is good for the body of the plasma, but it is not, of course, adequate for the sheath region where the densities of the ions and electrons may be very different. Tonks and Langmuir tried to remedy this by matching an approximate sheath solution to the plasma solution. This was only partially successful in that the sheath potential drop is correctly obtained but the potential profile is not accurate.

Other investigations of various aspects of the sheath problem to improve on the works of Tonks and Langmuir have been carried out by Allen et al (1957), Harrison and Thompson (1959), Auer (1961) and Caruso and Cavaliere (1962) among others. Solutions of the sheath problem, such as these, have characteristically been restricted to special cases or subject to limiting approximations

due to the complexity of the plasma sheath equation. Recently, however, with the availability of high speed computers, accurate numerical analyses, valid throughout the plasma, have been carried out. Numerical solutions to the plasma sheath equation have been given for plane geometry by Self (1963) and for cylindrical geometry by Parker (1964), using essentially the analysis of Tonks and Langmuir. Curves for the sheath potential and charge density are given for various sizes of the discharge and ion generation models.

A somewhat different approach from that of Tonks and Langmuir has been followed by Bernstein and Rabinowitz (1959). They analyzed the problem of cylindrical and spherical probes in a plasma on the basis that in the absence of collisions, the general solution of Boltzmann's equation for a particle distribution function is an arbitrary function of the constants of the motion. The constants of the motion which they used are the energy and magnitude of the angular momentum. The electron velocity distribution function was assumed to be Maxwellian while a mono-energetic velocity distribution function was used for the ions. After integrating the distribution functions over the constants of the motion to get the respective particle number densities, a numerical solution of Poisson's equation was obtained for the potential. The essential difference between the analysis of Bernstein and Rabinowitz and that of Tonks and Langmuir is that the former consider the problem of a probe placed in an infinite plasma medium (the exterior problem) while the latter investigated the plasma confined by walls of a given geometry (the interior problem). (An earlier paper by Mott-Smith and Langmuir (1962) developed the theory of probes in a plasma, but did not discuss

the potential variation in the sheath.) The exterior problem is fundamentally different from the interior problem (besides the obvious difference in geometry) in the motion of the particles which are attracted to the boundary. In the exterior problem only those ions with the proper combination of velocity and angular momentum will strike the probe, while in the interior problem, all ions will eventually reach the boundary. This requires a somewhat more elaborate treatment to calculate the ion number density in the exterior problem. An additional difference between the two developments is that Bernstein and Rabinowitz did not allow for ion generation. Finally, both analyses neglect the existence of a net electron current to the boundary. This is an approximation whose validity is reasonable for boundary potentials equal to or less than the potential an insulated body would assume when immersed in the plasma.

An extention of the work of Bernstein and Rabinowitz has been carried out recently by La Frambois (1964). He also considers the probes of spherical and cylindrical geometry but takes the ion velocity distribution function to be Maxwellian rather than mono-energetic, as did Bernstein and Rabinowitz. Lam (1964) has also analyzed the cylindrical and spherical probes following Bernstein and Rabinowitz for the asymptotic limit of a very large probe radius to Debye-length ratio.

Wasserstrom et al (1964) also treated the case of a spherical probe in a plasma. Their method was to assume Maxwellian velocity distribution for both the ions and electrons. These distribution functions were divided into two parts in velocity space according to whether or not the particle velocity vectors in

physical space were directed along a straight line intersecting the sphere. The two parts of the distribution functions were taken to be different unknown functions of the radius variable. The problem was then to find these unknown radial functions for both the ions and electrons by using the zeroth and first order velocity moments of the Boltzmann equations, the results of which could be used with Poisson's equation to find the potential. The effect of collisions was taken into account in this analysis.

1.1.4 Experimental Work

In addition to the theoretical studies which have been made concerning wave propagation in a plasma, a considerable amount of experimental work has been performed in this area. Some of the more pertinent published results, particularly those dealing with the excitation and detection of EK waves, are discussed below.

The first comprehensive experimental investigation into the subject of plasma oscillations is that of Tonks and Langmuir (1929). The purpose of their experiment was to find the electron plasma oscillations which Dittmer (1926) had suggested were responsible for randomizing the velocity of mono-energetic electron beams when interacting with a plasma. Arrangements for detecting plasma oscillations were made by connecting a crystal detector and galvanometer between two electrodes in the plasma. The oscillation frequency was determined by measuring the wavelength on a pair of Lecher wires. Oscillations were found in the range of 1 to 1000 Mc in a spherically shaped mercury plasma. A theoretical expression which was obtained, relating the oscillation frequency to the electron density, was found to satisfactorily account for the oscillations of fre-

quency greater than 1.5 Mc. (The expression which was derived introduced the electron plasma frequency.) Oscillations of frequency less than 1.5 Mc were attributed to the ions. An expression for the ion oscillation frequency was also obtained and the existence of ion sound waves was postulated, but none were found.

Merrill and Webb (1939) also made a careful study of the interaction of direct current electron beams with a plasma. They used a movable thin wire probe for measuring the electron velocity distribution function. The same probe was also used, in conjunction with a Lecher wire system, to measure the frequency of plasma oscillations. The results showed that the beam electrons were scattered in narrow, well-defined regions, and that oscillations at or near the electron plasma frequency also occurred in these regions. No such oscillations were found outside these scattering regions. It was concluded that since the oscillations occur only where the beam electrons undergo scattering, the beam electrons are the source of energy for exciting the oscillations.

A similar experiment was performed by Wehner (1951). He also found that oscillations occur at the plasma frequency when the beam electrons undergo scattering. When the discharge conditions were such that no abrupt scattering of the beam electrons occurred, no oscillations were detectable. By correlating the probe measurements with visual observation, Wehner was able to conclude that the scattering took place in a thin layer at the edge of the ion sheath which surrounded the beam control grid. Wehner suggested that it is reasonable to believe that the excitation of plasma oscillations by an electron beam is always

associated withthe layers near a plasma boundary, i.e., near the edge of an ion sheath.

Further evidence to support Wehner's results was obtained by Looney and Brown (1955). Their experiment differed from that of Merrill and Webb and Wehner mentioned above in one important respect: whereas the former utilized only one cathode to form the discharge and to provide the electrons for exciting plasma oscillations, Looney and Brown used separate cathodes for each function so that the exciting beam and the plasma could be independently controlled. A movable wire probe, which was capacitatively coupled to a superheterodyne receiver, was used to detect the presence of plasma oscillations. It was found that standing wave patterns in plasma oscillations were set up in the region between the exciting beam electrodes. The oscillations occurred near the electron plasma frequency. The presence of sheaths on the exciting beam electrodes was found to be necessary for the excitation of the oscillations. By varying the exciting beam electrode sheath thickness, it was observed that the standing wave pattern always adjusted so as to keep a node of the pattern near the visible sheath edge. A calculation of the phase velocity of the standing wave components indicated that the oscillations are not EM in origin. The authors suggest that it is a longitudinal pressure wave (EK wave) set up in the plasma electrons by the exciting electron beam.

An experiment was performed by Gabor et al (1955) in order to clarify the plasma oscillation question, particularly as related to the sheath. The experiment was motivated by a desire to account for Maxwellian electron velocity distributions

in a plasma even when its dimentions are many times less than the electron mean free path length. It was suspected by the authors that the explanation of this phenomenon would be found to be associated with plasma oscillations. Contrary to the previously mentioned experiments where an electron beam was used to excite oscillations in a plasma, an electron beam was utilized by Gabor to serve as a probe or detector. A direct current electron beam of 1 to 20 KV energy was collimated and arranged to pass perpendicularly through the edge of the cylindrical mercury plasma, and the deflection of the beam was observed by various arrangements. It was found that when the beam was passed through the plasma outside the sheath region, it suffered little deflection. When, however, it was passed through the sheath region near the wall, the beam was deflected in a direction perpendicular to the wall at frequencies on the order of 120 Mc. It was also determined from the experimental data that the static sheath potential was nearly parabolic and hence the reflection time for all electrons is the same. The authors thus conclude that electrons which reflect from the sheath can gain or lose energy depending on their phase relation to the sheath oscillations at the time of entry. The energy which could be gained in this way could be on the order of several electron volts, thus providing an explanation for the existance of high temperature Maxwellian electron velocity distributions in such plasmas. It is relevant to note that the electron plasma frequency outside the sheath region was found to be about 500 Mc. No consideration was given to the possibility that the electron beam may have excited the oscillations.

Subsequent experiments which involved probing the static plasma sheath with

an electron beam were reported by Gierke et al (1961) and Harp and Kino (1963). No evidence of oscillations within the sheath, as reported by Gabor et al, was found. Harp and Kino also performed the electron beam probing experiment when the sheath was subject to an rf electric field directed normally to the sheath. Their measurements on the electric field variation in the sheath were found to be in good agreement with a theory developed by Pavkovich and Kino (1963), formulated from the collisionless Boltzmann equation.

Another aspect of plasma which has received considerable attention is the scattering of plane electromagnetic waves by a cylindrical plasma column. Tonks (1931) showed that a bounded plasma would oscillate at a single frequency proportional to the plasma frequency, with the proportionality constant determined by the size and shape of the discharge, the nature of the mode of oscillation, and the dielectric constant of the material surrounding the plasma. This result was obtained by regarding the plasma as a uniform dielectric with a dielectric constant $\epsilon = \epsilon_o (1-\omega_p^2/\omega^2)$ where ω_p and ω are the electron plasma frequency and the radio frequency respectively. Subsequent experimental results obtained by Romell (1951) and Dattner (1957, 1963) have shown that there is a series of resonances in the scattering cross section of a plasma column, rather than the single resonance predicted by Tonks. These additional resonances could not be explained successfully using a dielectric theory of cold plasma.

Gould (1959) attempted to account for them by taking into account the random thermal motions of electrons in a uniform hot plasma column and allowing for radial EK wave motion based on a scalar electron pressure. His theoretical

xpression for the resonance frequencies showed that the resonances would be more closely spaced, by about an order of magnitude, than those measured experimentally. In a recent paper, Parker et al (1964) have extended Gould's treatment to the case where the plasma column electron density varies in the radial direction. The model for the nonuniformity of the electron density was based on Parker's (1964) results which were mentioned previously. The analysis proceeded from the linearized zeroth and first order velocity moments of the collisionless Boltzman equation and the Maxwell's equations, together with a scalar electron pressure. The quasi-static approximation was invoked for the EM field (this means the electric field is represented by the gradient of a potential) and a fourth order differential equation obtained for the potential. This equation was solved subject to the boundary condition that the radial electron current vanish at the cylindrical plasma boundary. The resonance spectrum for excitation of the radial waves in the cylindrical plasma column by multipole devices (e.g., a split cylinder capacitor) was then calculated. The frequency spectrum was found to depend on the square of the ratio of the plasma column radius to the root-mean-square electron Debye length. Experiments were performed using dipole and quadrupole excitation devices rather than performing the free space plane wave scattering experiment, since the desired multipole mode of the cylindrical column can be preferentially excited by the former arrangement, whereas the latter experiment does not have this advantage. Good agreement was obtained between the experimental and theoretical spectra. This is a significant result

in that it provides a reasonably conclusive demonstration for the coupling of EM and EK waves at a plasma discontinuity as well as in the inhomogeneous plasma itself. The existence of the radial EK wave is, however, only indirectly observed through the agreement in the results, and is not independently established by other experimental observations which would be desirable. It is also obvious that any theoretical treatment intended to account for experimental observations of a laboratory plasma must take into consideration the nonuniform electron density of such a plasma. Thus Gould's (1959) original treatment of a uniform plasma column was not able to explain experimental observations that were successfully accounted for by the Parker et al (1964) treatment of the nonuniform column.

1.2 Problems Remaining To Be Solved

Up to this point, the general subject of wave propagation in a plasma has been considered, and a rather extensive survey of previous work on this topic has been given. It should now be apparent which areas have been the more completely investigated and also where the major unsolved problems lie. We summarize briefly then the previous contributions, particularly as related to the field of plasma-immersed antennas, which is of primary interest to us.

On the theoretical side, the plasma-plasma interface scattering problem has been solved for a variety of boundary models and boundary conditions for plane and spherical boundaries. Tidman and Boyd (1962) and Tidman and Weiss (1961) have probably given the most careful treatment of the problem in the boundary conditions and boundary models used. Problems of this type are of interest primarily to astrophysicists. Solutions to the electrodynamic plasma

sheath problem when the boundary is a solid material such as a dielectric or metal have been confined to the case of a plane boundary where even then the plasma sheath is neglected, except for the cylindrical plasma column. The isolated source problem has been considered for various types of current sources in a uniform plasma with the indication that more power can be radiated as EK waves than as EM waves from filament currents. The radiation from a body has been confined to a consideration of the spherical antenna with the sheath being neglected or replaced by a layer of uniform permittivity.

On the experimental side, the capability of exciting and possibly also of detecting plasma oscillations (which are apparently EK waves) by means of direct current electron beams has been demonstrated. The experimental results of various authors are in general agreement that it is the sheath region which is important in providing an excitation mechanism for electron beams to produce such oscillations. There is experimental evidence that thin wire probes can also be used to detect plasma oscillations excited by electron beams. Indirect experimental evidence has been obtained which indicates that EK waves can be excited in a cylindrical plasma column by EM waves.

Thus, apart from the cylindrical plasma column, no solution has been obtained for either the scattering problem or radiation problem which includes the effect of the nonuniform plasma sheath at the boundary between the plasma and the scattering or radiating body. No solid theoretical understanding of wave propagation in a plasma can be achieved until the sheath effect is taken into account, for the indications are, from the results of the study on the plasma column

resonances as well as other experimental evidence, that the nonuniform sheath region may be the most important single factor in these problems. There are a number of areas that one might consider investigating then in an effort to clarify the sheath influence on wave propagation in a plasma. The scattering characteristics of plane, cylindrical and spherical body-plasma boundaries are of particular interest. These are boundary shapes which are readily handled and which are commonly encountered in dealing with laboratory-generated plasmas. The radiation from spherical and cylindrical dipole antennas is another problem area which is of great interest, particularly since the results of isolated source studies indicate that more power can be radiated in the EK wave than in the EM wave. Both of these are problem areas where theoretical work in connection with carefully performed experiments could make important contributions to the state of our present knowledge.

There is an additional problem area which is a potentially rewarding one on both a theoretical and experimental basis, and which encompasses aspects of both the scattering and radiation problems. It is the subject of the specific excitation and, more importantly perhaps, the detection of EK waves. All of the theoretical considerations devoted to plasma wave propagation to the present time have ultimately been concerned primarily with EM waves, either with the amount of EM radiation converted from EK waves at some plasma transition region, or with the perturbing influence of the EK wave on the radiation characteristics of an antenna structure or source distribution which should be essentially a source of EM waves. No consideration has been given to the topic of plasma-

immersed antennas from the viewpoint of detecting EK waves. An analysis should be carried out to determine if it is possible to detect with an antenna the presence of EK waves in a plasma. This is particularly important if any experiments are to be performed in this area, for the purpose of testing the theory. Presently, the exist of the EK wave can only be inferred indirectly, as, for example, from its theoretical effect on the impedance characteristics of an antenna, or the resonance of the cylindrical plasma column. It would be more desirable to achieve this end directly by some appropriate detection device.

1.3 Problem To Be Investigated

The problem is to devise and analyze promising schemes that may allow the detection of EK waves by a plasma-immersed antenna. Ideally, a device that would measure the divergence of the electric field at radio frequencies is required. For example, the analog for measuring the curl of the electric field is a small loop antenna. In addition, it should be a passive device that does not unduly disturb either the static or the dynamic plasma behavior. Finally, it should be able to accomplish its task in a strong backgroung of EM radiation. A Langmuir probe such as a thin wire suggests itself as one possibility. Thin wire probes have indeed been successfully used in previous experiments to detect plasma oscillations and to measure static electron densities. However, the oscillations which were observed by using such probes were the result of high energy beams driving the plasma into oscillations. Whether or not such a probe could detect EK wave oscillations of such small amplitude that the linearized theory applies would have to be carefully investigated. A capacitor with grid-like wire meshes

or plates might also be considered as a possibly useful device for this application. This would have the drawback that in order to determine the capacitance, which would be a function of the charge between the plates, a voltage would have to be applied across the plates, with a resulting disturbing influence on the plasma. Another method which was previously employed for detecting plasma oscillations utilized the electron beam. Unfortunately, the probing beam could also at the same time excite oscillations.

The question arises now about what other measurement conceivably may be made on the EK wave, if a direct measurement of the divergence of its electric field does not appear practical. If it is recalled that an EK wave which is scattered from a plasma discontinuity may have some of its energy converted into EM radiation, we are provided with one possible mechanism for such a measurement. While the incident EK wave has no magnetic field, the scattered EM wave does possess a magnetic field and so there will be surface currents induced on a conducting scattering obstacle. If these surface currents could be measured and their wavelengths ascertained, then, because EK and EM waves at the same frequency have wavelengths which differ on the order of the ratio of the velocity of light in a vacuum to the plasma electron thermal velocity, an incident EK wave may, theoretically at least, be detected even in the presence of EM radiation. The problem would be to determine whether from theoretical considerations such induced current measurements could be carried out on a practical basis. A cylindrical geometry appears to be an attractive one from both a theoretical and experimental standpoint. On the theoretical side, a formulation of such

problem for the cylindrical geometry is relatively straightforward, and static
heath studies devoted to this geometry are available. An experimental measure-
ment of surface currents induced by incident waves on a hollow metal cylinder
ould be made by terminating transmission lines, which run inside the cylinder,
t slots cut appropriately on the cylinder surface. The specific problem studied theo-
retically in this investigation is the excitation by incident plane EK and EM waves
of surface currents on an infinitely long, metallic circular cylinder immersed in
a plasma, in order to determine the practicality of making surface current
measurements for the purpose of detecting the EK wave.

The remainder of this thesis is divided into two main sections. In the
following, Chapter II, the theoretical formulation of the problem is given.
Chapter III presents the results of the numerical analysis and contains a discussion
on their significance. The main feature of this study and conclusions reached
from it are given in Chapter IV. Several appendices follow which contain detailed
analyses of various aspects of the problem which are not necessary for an under-
standing of the main part of the thesis. The rationalized meter-kilogram-second
(Giorgi) system is used throughout, unless otherwise indicated.

CHAPTER II

FORMULATION

2.1 The Boltzmann Equation

One starting point in the treatment of an assembly of various kinds of charged and uncharged particles such as is found in a partially ionized gas or plasma, is the Boltzmann equation. This equation accounts for the force effects of both contact collisions between particles as well as the macroscopic forces due to electric, magnetic and gravitational fields. Other formulations, such as the Fokker-Planck equation, have been developed in order to overcome some difficulties in accounting for force effects which are not contact collisions but rather long-range Coulomb collisions in highly ionized gases. A typical laboratory plasma however, in which experiments might be performed to check on the results of the following development, will be only slightly ionized, so that the Boltzmann equation approach, which is used here, is a reasonable one.

A completely general treatment of the N-component plasma would now involve N equations of the form

(2.1)

where $f_j = f_j(\underline{r}, \underline{u}, t)$ is the distribution function of the jth component, which gives the density of particles in ordinary space per unit volume of velocity space at space point $\underline{r}$, velocity $\underline{u}$ and time t. m_j is the mass of the jth species, $\underline{F}_j$ is the force acting on it, and ∇_r and ∇_v are gradient operators in physical space and velocity space. The N-equations which result may be coupled through the

collision term and the force term. A solution of the problem would require finding the N distribution functions appearing in the N-equations. Once the distribution functions have been obtained, all the macroscopic physical observables of interest such as density, velocity, pressure, etc. could be generated from moments of the distribution functions. This is a formidable problem and one which can seldom be solved, even when simplifying assumptions are employed. The usual approach is to employ a linearity condition, i.e., the time-varying components of the variables are assumed to be small compared to their static parts. Such phenomenon as Landau damping can be developed following this analysis, which is called the kinetic theory approach.

When the problem under consideration involves in addition, electric and magnetic fields in the plasma, there is required in addition to the system of equations in (2.1) the Maxwell equations

(2.2a)

(2.2b)

(2.2c)

where $\underline{E}$ and $\underline{H}$ are the electric and magnetic fields in the plasma. μ_o and ϵ_o are the permeability and permittivity of free space. The complexity of the problem is increased still further then, and it is obvious that the kinetic theory treatment is unworkable for all but the simplest problems.

An alternative approach to the solution of (2.1) and (2.2) is the hydrodynamic treatment. This involves taking velocity moments over the distribution functions to generate an infinite set of moment equations in which the macroscopic variables of number density, velocity, pressure, etc. are the unknowns. A solution to the problem requires finding the variation in time and space of these quantities for all the plasma components. It is usual to invoke linearity when using the hydrodynamic approach also. There is no essential philosophical difference between an exact solution obtained from the kinetic approach and that obtained from the hydrodynamic approach, since a knowledge of the distribution functions means that all the macroscopic variables can be found. If, on the other hand, all the infinite set of macroscopic variables is known, the distribution function can be constructed. There is, however, a great practical difference between the two methods when one considers the complexity of the mathematics which is encountered, even in solving a problem where many simplifying assumptions can be made. Oster (1960) points out that in order to avoid excessively complicated mathematics in the kinetic theory approach, it is necessary to make such assumptions that it is more reasonable to use the hydrodynamic equations. The hydrodynamic approach is the one to be used here.

Before further developing the formulation, it is appropriate to discuss the assumptions which will be made about the plasma. The plasma will be considered to be of infinite extent and of uniform temperature throughout, and to consist of electrons, positive ions and neutral particles. The electrons and the ions are taken to have the same number densities on the average so that when

the plasma is uniform, it is electrically neutral. Collisions of the electrons with ions and neutrals are ignored, in so far as their effect on collective plasma oscillations is concerned. This seems justifiable since the electron collision frequency in a typical laboratory plasma may be a factor of 100 or so less than the electron plasma frequency. Electron collisions are important however, to the production of a Maxwellian electron velocity distribution which will be used here. This also seems justifiable, in that Maxwellian electron velocity distributions have been found in laboratory plasmas, even when the electron mean free path is longer than the plasma dimensions. The way in which this distribution is produced in such a plasma is referred to as Langmuir's paradox and has been discussed by Gabor (1955). Finally, the plasma is taken to be quiescent, i.e., no charge is being created or destroyed. This assumption primarily affects the static plasma behavior in sheath regions, and simplifies a discussion of that part of the problem.

2.2 Development of the Macroscopic Equations

The procedure to be followed now is to generate macroscropic plasma variables by taking velocity moments of the collisionless Boltzman equations for the ions and electrons, which are

$$\frac{\partial}{\partial t} \left(\quad \right) + \quad = \quad \tag{2.3}$$

$$\frac{\partial}{\partial t} \left(\quad \right) + \quad = \quad \tag{2.4}$$

f_e and f_i are the electron and ion distribution functions, $\underline{u}_e$ and $\underline{u}_i$ are the electron and ion velocities, and m_e and m_i are their respective masses. The force terms are

(2.5a)

(2.5b)

where -e is the electron charge, and $\underline{E}$ is the electric field in the plasma. With this choice for the force term, the subsequent discussion is limited to the case where gravitational and magnetic forces in the plasma may be neglected in comparison with the electric forces. This is justified in a plasma which is not hot enough for relativistic effects to become important. In addition, no external magnetic field is considered to be present.

The first four moments over the distribution function produce, in Cartesian coordinates,

particle density: (2.6a)

particle current: (2.6b)

pressure: (2.6c)

heat flux: (2.6d)

The random velocity is

An infinite number of coupled moment equations, which contain only the macroscopic plasma variables such as given by (2.6) may be generated from (2.3) and (2.4). If it were necessary to deal with this entire set of equations, there would be no inherent advantage of the hydrodynamic approach over the kinetic treatment. However, it is physically meaningful in many practical problems, to terminate the infinite set of moment equations by taking the nth order velocity moment of the distribution function to be zero.

The point at which the moment equations can be terminated is discussed by Parker et al. (1964). When considering the propagation of longitudinal waves in a plasma, it can be shown that retaining the higher order velocity moments when generating the moment equations is equivalent to including the higher terms in the expansion of (radio frequency/electron plasma frequency)^2 in terms of (thermal speed/wave speed)^2 in the dispersion relation for longitudinal waves propagating in a plasma. Parker et al. conclude that moments up to the pressure tensor and possibly the heat flux tensor are required, but none of the higher moments than these will contribute sufficiently to the accuracy of the results to warrant being used.

Accepting as reasonable the termination of the moment equations with the heat flux tensor, the problem has been simplified a great deal but is unfortunately still very difficult. If no further simplifications were possible, one would be required to deal with an equivalent 19th order differential equation. The choice

is made now to also set the heat flux tensor equal to zero, an approximation which is frequently used see for example Tidman and Boyd (1962), Parker et al. (1964), Kritz and Mintzer (1960) .

This reduces the order of the differential equation to 10th order, and implies that the electron and ion velocity distributions are isotropic Rose and Clark (1961), p. 119 . A final assumption, consistent with setting the heat flux tensor equal to zero, and which reduces the differential equation to 8th order, is that of replacing the pressure tensor by a scalar. The view which is thus taken here is that the electrons behave as a continuous fluid and the effect of all the electron interactions is represented by a scalar pressure term.

The use of a scalar pressure is exact for a uniform plasma. In the presence of a plasma inhomogeneity, which is to be considered shortly, it is an approximation. The representation of the electron behavior in the plasma by an isotropic scalar pressure is one which has been widely used Cohen (1962a), Fedorchenko (1962), Field (1955), Parker et al. (1964), Kritz and Mintzer (1960) . Good agreement between theoretical and experimental results has been obtained by Parker et al. (1964), where the theoretical results were based upon the use of a scalar electron pressure. Hence the indications are that this is not an unreasonable approximation.

The moment equations which are to be used then are obtained from the zeroth and first order velocity moments of (2.3) and (2.4) and are

(2.7a)

(2.7b)

(2.8a)

(2.8b)

where the subscript e and i denote quantities associated with electrons and ions respectively. The Maxwell equations can now be written

(2.9a)

(2.9b)

(2.9c)

(2.9d)

This set of equations is completed by an equation of state which relates the pressure to the number densities of the charged particles. The non-time varying or static pressure P_o, from the assumption of Maxwellian velocity distributions, is

(2.10)

where k is Boltzman's constant and T is the temperature. It should be noted that this is the first use to be made of the Maxwellian velocity distribution.

All of the development to follow rests on this assumption. For the dynamic pressure variations P_1 it follows that

$$\frac{}{1} \quad . \quad 1 \tag{2.11}$$

where for one dimensional, adiabatic pressure variations, $\gamma = 3$, (Cohen, 1955). The temperature for a Maxwellian distribution of velocities is given in terms of the root-mean-square (rms) velocity v_r as

$$r \tag{2.12}$$

The set of Eqs. (2.7) to (2.12) constitutes the starting point from which all of the developments to follow are derived. They contain within them the complete static and dynamic plasma description with which this treatment is concerned, subject to the approximations and assumptions which have been pointed out above. These assumptions are again: that the plasma is non-relativistic, of uniform temperature throughout, infinite in extent, and only slightly ionized; the charged particles are electrons and positive ions having Maxwellian velocity distributions; they suffer no collisions and their behavior can be represented by a scalar pressure. The use of these assumptions on the physical nature of the plasma has been discussed above and no further mention will be made of them below in the subsequent theoretical development. There are however, some simplifying approximations which are basically mathematical in nature to be introduced in the following.

2.3 Linearization of the Macroscopic Equations

While a great simplification has been effected in going from the Boltzmann equations to the system of Eqs. (2.7) to (2.12), so that the problem is much more manageable, it is to be noted that these equations exhibit still a major difficulty. That is, of course, the fact that some of these Eqs., (2.7), (2.8) and (2.9c) are non-linear, thus posing a still very complex mathematical problem. This difficulty may be side-stepped by the artifice of linearization, a very commonly used technique in hydrodynamics. This linearization is accomplished by assuming that variations of the plasma variables from equilibrium are small enough that products of these variations can be neglected. The reasonableness of this assumption is dependent upon whether or not the effects produced by perturbing influences which satisfy the linearity requirements are large enough to be seen experimentally. In other words, there is no doubt that linearization can be valid, but the question is, are perturbing influences which do produce measurable effects small enough so that a linearized theory applies. This cannot be answered until some theoretical answers are obtained. The indications are, however, that good success can be obtained with a linearized theory, which is to be employed here, as shown by the results of Parker et. al. (1964) and Pavkovich and Kino (1964).

Before the linearized equations are written, one further observation is made. Since the ratio of the mass of the positive ion to the electron may vary from about 1800 in a hydrogen plasma to 360, 000 in a mercury plasma, then the ion plasma frequency may be from 1/45 to 1/600 that of the electrons. This means that in the radio frequency range to be considered here, where the electron plasma frequency is always less than the radio frequency, that the ions will

contribute negligibly to collective plasma oscillations. Thus for practical purposes the ion motion can be neglected in so far as the time varying behavior of the plasma is concerned.

The linearization of (2.7) to (2.12) is now accomplished by the following substitutions:

(2.13a)

(2.13b)

(2.13c)

(2.13d)

(2.13e)

(2.13f)

The subscript o denotes a quantity which does not change with time (these will subsequently be referred to as static quantities) and the subscript 1 denotes a time-varying quantity (this will be referred to as a dynamic term). With these substitution, Eqs. (2.7) to (2.12) can be written

(2.14a)

(2.14b)

MISSING
PAGE

of equations differs considerably from the incorrect approach used by Field (1955) where the static electron velocity and electric field terms were neglected. It also differs from the formulation used by Parker et. al. (1964) because of their neglect of the static electron velocity. The reason for the appearance of static velocity terms will become apparent in the following discussion. A static magnetic field term was included in (2.14) for generality; it will be shown to be zero below.

An observation of the linearized equations shows that eight of them contain only static quantities, whereas the six remaining equations may contain both dynamic and static terms, exhibiting the influence of the static plasma characteristics on its dynamic behavior. Thus it is necessary that an understanding of the static behavior of the plasma be reached before its dynamic response can be investigated quantitatively. It is for this reason that in the following section, the static plasma characteristics are investigated for the particular geometry with which the remainder of this study will be concerned.

2.4 The Static Plasma Sheath

As was mentioned in the introduction, the purpose of this study is to investigate the surface currents which are excited on an infinitely long plasma immersed circular metallic cylinder by plane electromagnetic (EM) and electrokinetic (EK) waves. The plasma surrounding such a cylinder is changed by its presence, forming an inhomogeneous region called a sheath. Because of the cylinder geometry, the plasma variation in the sheath is a function only of the radius variable ρ. Figure 2.1 shows the cylinder in relation to the coordinate system.

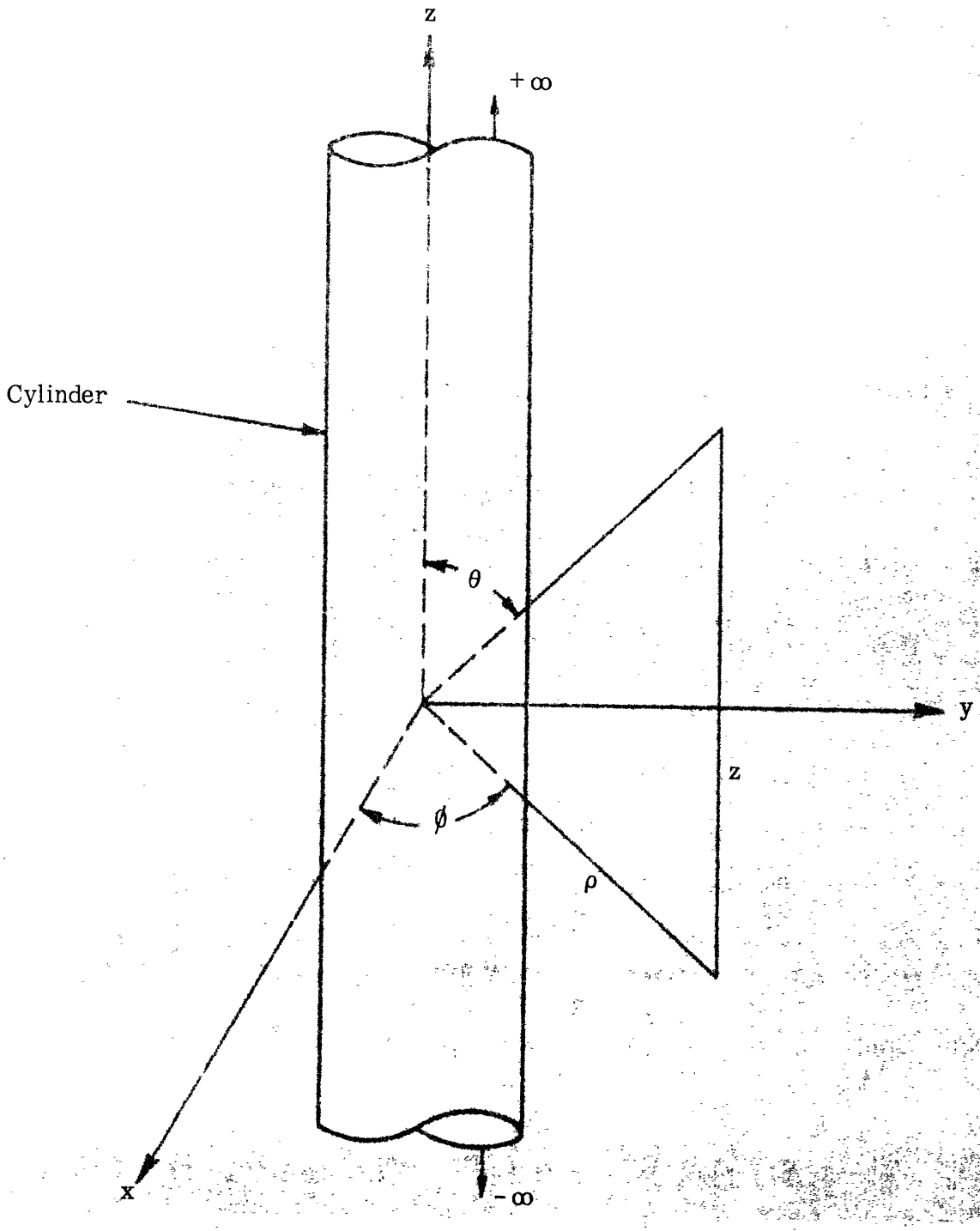

FIG. 2.1: CYLINDER AND COORDINATE SYSTEM

The mechanism for the formation of the inhomogeneous sheath is due to the fact that, since the electrons are lighter than the ions, they have a larger rms velocity, even when they are both at the same temperature. In a typical laboratory plasma the electron temperature may exceed the ion temperature by a factor of 10 to 100, thus, further increasing the velocity discrepancy. Due to this velocity difference, more electrons than ions tend to strike the cylinder per unit time. If the cylinder is insulated, that is allowed to acquire a potential which is determined by the plasma parameters, as will be assumed here, it acquires an excess of electrons which give the cylinder a negative potential. This negative potential repels all but the fastest incoming electrons and it adjusts to the point where the ion and electron currents to the cylinder are equal, i.e. equilibrium is established. This particular sheath is thus a region where there is an excess of positive ions.

The origin of the static ion and electron velocities, which for the cylindrical sheath have radial components only, is thus apparent. Note, however, that there is no net current to the cylinder, and that since as shown by (2.14), the static ion and electron flows are divergenceless, the static electron and ion currents are then everywhere equal. As a result, there is no static magnetic field in the sheath due to these currents, and $\underline{H}_0 = 0$.

This inhomogeneous sheath region extends to infinity on a theoretical basis, since the static currents cannot go to zero, except at an infinite distance from the cylinder, according to the plasma model which is being used here. However, the contribution of the static currents to the plasma inhomogeneity decreases on the order of 1/ radius as the distance from the cylinder increases, so that

from a practical viewpoint the plasma becomes homogeneous in a finite distance. In addition the collisions which occur between electrons and neutrals in a real plasma provide a source for contributing to the electrons and ions which flow to the cylinder, thus further limiting the extent of the inhomogeneous region around it. The picture of the sheath to be used here is that it is of finite extent, the thickness of which is to be established below, and that the plasma outside the sheath can be taken as uniform throughout. Figure 2.2 shows the sheath in relation to the uniform plasma* and the cylinder.

An analysis of the plasma sheath for a planar geometry which was recently carried out by Self (1964) and in which the generation of electrons was taken into account, indicates that the electron and ion densities are within 5 per cent of each other at a distance of 10 to 20 electron Debye lengths (D_ℓ) from the bounding plane wall. (We note that $D_\ell =$ $\left| \right.$. v_{er} is the electron rms velocity.) In another analysis by LaFrambois (1964) for spherical and cylindrical geometries, but in which electron generation was not included, the sheath thickness defined by the same criterion was also found to be on the order of 10 electron Debye lengths. The electron Debye length for a typical laboratory plasma with an electron temperature of 10^4 ^oK and a plasma frequency of 700 Mc is 8.851×10^{-3} cm, so that the sheath thickness is on the order of 1 mm. It is thus very much less than the wavelength of EM waves near the plasma frequency but may be twice the EK wavelength in thickness, as will be verified below.

The fact that there is a static component of electron and ion velocity indicates that the electron and ion velocity distribution functions are not exactly Maxwellian. The departure from a Maxwellian distribution is dependent upon

* The sheath-uniform plasma interface at $\rho = s$ will be referred to in the following as the sheath interface or sheath edge.

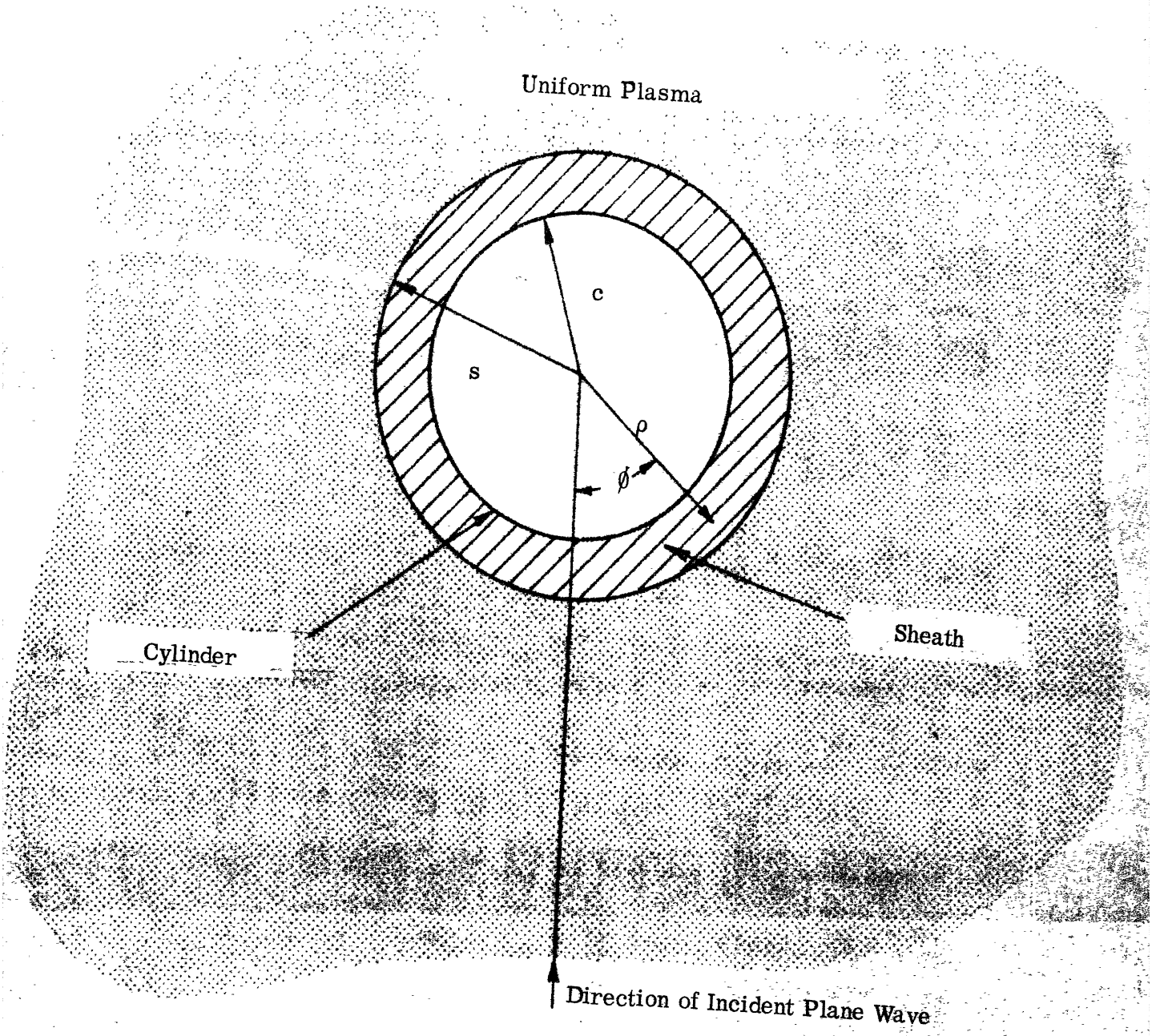

FIG. 2.2. NORMAL CROSS-SECTION OF CYLINDER

the distance from the cylinder. At distances from the cylinder greater than a few electron mean free paths (MFP), the velocity distribution for the electrons will be Maxwellian with a superimposed radial drift velocity due to the static velocity. At distances less than the electron MFP, the electron distribution function will become truncated due to a deficit of fast electrons in the outward direction. This deficit is brought about by the recombination of the electrons and ions which reach the cylinder. Immediately at the cylinder wall, there will be a minimum in the number of outward travelling electrons. The ion velocity distribution becomes almost entirely one-sided as the cylinder is approached since the ions are attracted by the cylinder. It is observed then that the static radial velocities are real drift velocities at large distances from the cylinder. As the observation point is brought closer to the cylinder, the static velocity is primarily caused by the deficit of electrons and ions with outward radially directed velocities.

A qualitative picture of the sheath region has been developed, as a region where there is an excess of positive ions, extending roughly 10 to 20 electron Debye lengths from the cylinder and where the electron and ion velocity distribution functions may differ from Maxwellian. A rigorous quantitative analysis of the sheath requires finding the solution of the Boltzmann equations for the ions and electrons together with Posisson's equation. This is a very complex problem. The usual method is to find expressions for the number densities of the ions and electrons in terms of the potential by integrating the Boltzmann equation. The resulting expressions are then put into Poisson's

equation, from which the potential can be found. The complexity of the equation to be solved for the potential varies widely depending upon the rigor of the treatment. In a report by Chen et. al. (1963) a closed form solution for the potential is obtained for a planar geometry assuming Maxwellian velocity distributions and equal temperatures for both the ions and electrons. On the other hand, La Frambois (1964) when considering spherical and cylindrical probes, had to treat a system of non-linear integral equations in using the orbital analysis of Berstein and Rabinowitz (1959).

In our case, the static sheath solution could be obtained from equations (2.14). The purpose of this study is, however, to examine the dynamic sheath behavior while the static sheath description serves only as a means to that end. Since there are more rigorous static analyses such as that of LaFrambois available in the literature, it is preferable to use some of their results here. Some of the static sheath parameters can be varied when performing the dynamic analysis so that the results which are obtained can reasonably be expected to contain those closest to physical reality. At the same time they will exhibit the sensitivity of the dynamic sheath behavior to the static parameters.

An examination of the theoretical results presented by LaFrambois (1964), and Self (1964), and the experimental findings of Gabor et. al. (1955), Gierke et. al. (1961) and Harp and Kino (1962) shows that the static potential variation in the sheath may be closely represented by

(2.16)

where $_c$ is the potential at the bounding wall, s is the sheath radius, c the cylinder radius, and ρ is the radial co-ordinate. M is an adjustable parameter, the best fit value of M for the experimental results quoted being about 2 and for the theoretical results about 4. Expression (2.16) is, of course, only an approximation since the potential cannot generally be solved for in a closed form. It does, however, give a reasonably accurate fit for the potential variation in the sheath in a form convenient for numerical calculations.

The cylinder potential $_c$, will be calculated from

(2.17)

This form is due to Self (1964) for the planar geometry. An expression due to Chen et. al. (1961), derived for planar geometry, but with assumptions very different from those used by Self yields nearly identical numerical results. Unfortunately, no similar closed form has been found in the literature for the wall potential in the cylindrical geometry. However, values for $_c$ obtained from (2.17) and some graphical results given by LaFrambois (1964) for a cylindrical probe 20 electron Debye lengths in diameter, are in agreement to within 10 percent where LaFrambois graphs may be accurately read. In addition, Parker et. al. (1964) obtained some

numerical values for the wall potential of a cylindrical envelope enclosing a plasma which agree with (2.17) to within 10 percent for envelopes more than a few electron Debye lengths in diameter. Further, their results show the wall potential to be relatively insensitive to the envelope diameter. The evidence indicates that the wall potential is almost independent of cross-sectional geometry so long as the dimensions of the probe or envelope sufficiently exceed the Debye length, the situation in which we shall be interested, thus justifying the use of (2.17). $_{c}$ will be treated as an adjustable parameter through varying m_i so that the effect of a reasonable variation in its magnitude can be observed.

Once the sheath potential variation is known, then it can be observed from equation (2.14) that all the other static sheath parameters can be derived on the basis of the known sheath potential. There is thus obtained

(2.18a)

(2.18b)

(2.18c)

(2.18d)

(2.18d)

(2.18e)

where is the electron and ion density in the uniform plasma, er and ir are the electron and ion rms velocities and I is the electron and ion particle flux density in the sheath.

This is an awkward set of equations to handle, being transcendental in nature. In addition, it does not provide an accurate picture of the ion density and velocity near the cylinder since the use of a scalar pressure for the attracted particles (the ions in this case) becomes increasingly less valid as the attracting surface is approached. Some conclusions about the sheath parameters can be reached from it however. First of all, the electron density can be seen to decrease in the sheath as was previously surmised, since the cylinder potential is negative. A natural question which arises is whether this decrease is due primarily to either or eo, or whether both together have relatively the same influence. Now we observe from equation (2.16a) that v_{eo} is inversely proportional to the product of and n_{eo}. Then since both n_{eo} and decrease in magnitude as the cylinder is approached, we can conclude that v_{eo} must be correspondingly increased with decreasing radius. Thus eo should have its largest value at the cylinder's cylinder surface. If all the incident electrons are absorbed at the cylinder surface, then $V_{eo} \sim V_{er}/2$ there. But from (2.17), the cylinder potential Φ_c is such that varies between 3 and 6, depending upon the ion mass, so that . Since eo decreases approximately as when crossing the sheath away

from the cylinder, which is a faster variation than that of ϕ_o, then

everywhere in the sheath. Consequently

the Boltzmann distribution appears to be a good

approximation for the electron density variation in the sheath. This conclusion is verified by the more detailed analysis of Appendix A.

When the ions are considered, the potential and velocity are seen to have opposing effects on the density variation in the sheath, the potential tending to increase it and the velocity to decrease it. Consequently, nothing further can be concluded about the ion density variation in the sheath unless a specific numerical case is considered.

While it seems that it may be a good approximation to thus neglect the static electron velocity in analyzing the static sheath problem, this may not be justifiable when the dynamic behavior of the sheath is concerned, since the dynamic response is coupled to the static variations. The ion variation in the static sheath is of course not coupled to the dynamic behavior by reason of the large mass of the ions in comparison with the electron mass. In order to give fuller consideration to the static sheath variation, especially from the viewpoint of determining the static electron velocity effect on the dynamic behavior, a semi-quantitative analysis of the static sheath, dealing with those variables related to the electrons only, is carried out in Appendix A. The electron number density, and velocity are obtained there by integrating

a truncated Maxwellian electron velocity distribution, the truncation point being determined by the deficit in outward travelling fast electrons. Expression (2.18b) is also employed to get the static electron density. As a further check, the method of Bernstein and Rabinowitz (1959) is also used to get the electron number density and velocity.

Figures A1 to A4 show the electron number density and velocity in the sheath for some typical plasma parameter values, obtained as outlined in Appendix A. As can be seen from these results, the use of the Boltzman distribution for the static electron density variation in the sheath departs from the other analyses which take loss of electrons to the cylinder into account by less than 5 percent over 85 percent of the sheath. The maximum discrepancy between the various approaches occurs at the cylinder, but the difference is no more than 50 percent. Since the variation between the most rigorous analysis, following Bernstein and Rabinowitz, the semi-quantitative analysis of Appendix A, the expression given by (2.18b), and finally the simplest approach which yields the Boltzmann distribution is negligible over almost all of the sheath, the tentative conclusion reached above, that it is reasonable to use the Boltzmann distribution for the static electron density variation is justified. This is, of course, equivalent to neglecting the loss of electrons to the cylinder, or in other words, regarding the static electron velocity as being equal to zero. Self (1963) arrived at a similar conclusion in analyzing the sheath.

Still unanswered at this point is the question of whether the static electron velocity can be neglected in relation to the dynamic sheath response. This cannot be resolved until some further consideration is given to the dynamic problem. The results of Appendix A for the static electron velocity are used in Appendix B, together with some results to be obtained in section (2.5) to answer this question.

In summary, the static sheath description is based on a representation of the sheath potential by equation (2.16). This potential variation is then used to calculate the static electron density according to equation (2.13b) in which the flow of electrons to the cylinder is neglected. The static electric field is then obtained from the negative gradient of the potential. All of the quantities are functions of the radius variable only, due to the axial and azimuthal symmetry of the sheath.

2.5 The Dynamic Sheath Equations

The equations which contain the description of the dynamic sheath behavior are given by (2.15) and are rewritten here with an harmonic $e^{i\omega t}$ time dependence, as

(2.19a)

(2.19b)

(2.19c)

(2.19d)

(2.19e)

(2.19f)

In order to simplify the notation, and since no ambiguity can now arise, the subscript e is omitted from the quantities dealing with the electrons and the 1 is omitted from the dynamic terms. Equation (2.19a) is the continuity equation for the dynamic component of electron motion, and (2.19b) is the force equation, while (2.19c) to (2.19f) are the usual Maxwell equations. Equations (2.19) exhibit an explicit dependence upon the static sheath variables which, as will be shown below, couple the magnetic field and the dynamic electron density in the sheath.

2.5.1 Uniform Plasma Equations

When the plasma is homogeneous, then these equations take the simpler form

(2.20a)

(2.20b)

(2.20c)

(2.20d)

(2.20e)

Following Field (1955), the total electric field can be broken up into two parts, one part denoted by $\underline{E}_E$ having zero divergence and the other part $\underline{E}_P$, whose curl is zero. Then the set of equations (2.20). exhibits two independently propagating waves, the first having electric field $\underline{E}_E$ corresponding to the usual electromagnetic (EM) wave, and the other with electric field $\underline{E}_P$ being the electrokinetic (EK) wave. The results of this separation of the total electric field are summarized by the following equations:

(2.21a)

(2.21b)

(2.21c)

(2.21d)

(2.21e)

P P

from which (2.22a)

(2.22b)

where (2.23a)

(2.23b)

(2.23c)

(2.23d)

(2.23e)

(2.23f)

and is the velocity of light in free space. The wave equations (2.22) can alternatively be written as

(2.24a)

(2.24b)

This form for the wave equations is more instructive than the first since it emphasizes the independence of the magnetic field and the dynamic electron density

when EM and EK waves propagate in a uniform plasma medium. These are quantities which belong separately to either of the two waves, while each wave possesses an electric field. Equation (2.21) to (2.24) thus serve to describe wave propagation in the uniform medium outside the sheath region.

It should be pointed out that the frequency interval in which the EK wave can propagate unattenuated is limited to . For becomes imaginary so that the waves is exponentially attenuated, and for , the wave may be subject to Landau damping. The EM on the other hand is unattenuated so long as . When both waves together are considered then we require that .

2.5.2 Elimination of the Static Electron Velocity from Dynamic Sheath Equation

We leave this aspect of the problem now and return to the more complex question of the non-uniform medium, as described by the set of equations (2.19). Since a great simplification would be accomplished if the static electron velocity terms were not present in equations (2.19), it is appropriate to consider here whether the magnitude of these terms is such that they might reasonably be neglected in the analysis. A straightforward way of determining the relative importance of these terms is to compare them in magnitude with the other terms in the equation which involve the same dynamic variables. This has the advantage that the dynamic part of these terms

may be factored out, so that the explicit dynamic solution, which is not of course available at this point, is not required. It is thus of interest to compare the ratio of

(2.25a)

(2.25b)

and

(2.25c)

All of these ratios involve radial components only.

Now the dynamic electron density cancels in (2.25a) so that we can obtain the ratio

(2.26)

which involves static quantities only the magnitudes of which are given in Appendix A. In order to similarly factor the dynamic electron velocity from (2.25b), and obtain an expression in the static variables only, the radial derivative of $\underline{V}$ must be approximated in terms of $\underline{V}$ itself. For plane wave propagation in a homogeneous medium, at an angle θ with respect to the z axis of the coordinate system, $\underline{E}$ would be

where K is the propagation constant of the plane wave. It seems reasonable in the present case to replace the [illegible] term in (2.27b) by [illegible], so that an upper bound on this ratio can be expressed as

[illegible] (2.27a)

Similarly, an upper bound on the larger of the two ratios in (2.25c) can be expressed as

[illegible] (2.27b)

The requirement on R_1, R_2 and R_3 in order that terms in [illegible] can be dropped from (2.19) is that they be much less than unity. This is discussed in detail in Appendix B, where it is shown that R_1 and R_2 are less than 0.1 over 85 percent of the sheath, and that it is a reasonable approximation to drop terms in [illegible] from equation (2.19b). It follows as a result, that the terms in [illegible] can be dropped from (2.19a) and (2.19e) with the same degree of approximation as for equation (2.19b), since [illegible].

It should be noted here that the approximations which have been made by omitting the static electron velocity altogether from both the static and dynamic analyses are based on the assumption that the cylinder is insulated and drawing no net current from the plasma. When this assumption is not met, as for example when the cylinder potential is altered by connection to an external source of emf, the argument above may no longer hold. In particular

when the cylinder potential is raised to the plasma potential, there is no sheath, but there is a radial static electron velocity. This velocity provides the only coupling mechanism between the EM and EK waves in this case and thus cannot readily be dropped from equations (2.19). It follows that the relative contributions of the static electric field and static electron density gradient may be comparable at some cylinder potential, so that all the coupling mechanisms must then be considered. At the same time, the static sheath picture becomes more complicated with a variable cylinder potential. The problem of a potential positive with respect to the insulated cylinder potential is not considered in this study. The dynamic equations can now be written

(2.28a)

(2.28b)

(2.28c)

(2.28d)

(2.28e)

while the static sheath variables are simply

(2.29a)

(2.29b)

(2.29c)

This is the final form of the equations which are the basis of the development to follow. No further simplifications or approximations will be made in them. Note that one of the simplifying effects of dropping the static electron velocity terms from (2.19) has been to reduce the order of the set of differential equations. The reason for this is that equations (2.19a) and (2.19d) are redundant, either equation together with (2.19e) serving to derive the other. As a result, either of these two equations are used with the remaining three to form a complete and consistent set of differential equations for the dynamic sheath behavior. Since a derivative of appears only in (2.19a) it is natural to use the other of the two redundant equations, so that becomes a dependent parameter which is determined by the other dependent variables H, E and . If on the other hand, terms in the static electron velocity are retained in the equations, then a derivative of the dynamic velocity appears in (2.19b) as well, so that is then a dependent variable of the differential equations.

2.5.3 Ordered Power Flow in Sheath

A generalization of Poynting's theorem can be obtained from (2.28) in the usual way. We take $\underline{E}^*$ the conjugate of (2.28e) and $\underline{H}^*$ (2.28c) and

upon subtracting obtain

Equation (2.28b) can be used to eliminate the term in , and then upon using (2.28a) to evaluate we get

(2.31)

where

the factor of 1/2 of needed to represent averaging with respect to time. Field (1955) obtained a similar expression without the term. In a uniform plasma, the terms on the left are the average power flow densities in the EM and EK waves respectively, while the first four terms on the right hand side are the time average magnetic and electric energy densities in the EM wave and the kinetic and potential energies in the EK wave. The last term is rather interesting and is considered here in greater detail.

A volume integral of (2.31) leads to a Poynting's theorem for the plasma as

(2.32)

where W_H, W_E, W_K and W_P are real quantities which represent the time average magnetic, electric, kinetic and potential energy, stored in the volume of integration. The real part of the left hand side gives the average power flow across the closed surface bounding the integration volume and the imaginary part is proportional to the difference between the energy stored in the form of magnetic and kinetic energy compared with that in electric and potential energy, within the volume. In a lossless, passive medium, the real part of the surface integral is zero. Since the last term in (2.32) which involves $\underline{E}_o$ can apparently be complex, there is the possibility then that the sheath may be lossy. We define loss to mean a net decrease in the ordered energy content of the plasma, varying with the frequency of the incident wave. Gain is defined as negative loss. Now $n\underline{v}$ is a current flow in the sheath due to charge accumulation, and depending upon the direction of this current flow with respect to $\underline{E}_o$, there can be a gain of energy or loss of energy by the wave in the sheath. This can be accounted for in another way by observing that in the static case, the sheath electrons have a potential energy due to the negative sheath potential. In the presence of the dynamic electron motion, the total electron energy with respect to the static energy, may be increased or decreased, depending upon the displacement of the electron from its static position by the wave. If we rewrite the term in question as

(2.33)

where , and x is the electron displacement from

equilibrium this viewpoint becomes clear.

Thus the term in (2.32) which shows the effect of the static sheath on the dynamic electron motion in the sheath can account for both a reactive energy storage as well as a gain or loss of power in the sheath. Whether or not there is a net gain or loss due to this effect can be determined from the integration of the real part of either the right or left hand side of (2.32).

2.5.4 The Coupled Wave Equations

The decomposition of the electric field into solenoidal and irrotational parts as was done for the homogeneous plasma medium is not meaningful here, in terms of separating the EK and EM waves. This is illustrated by using (2.28b) and (2.28e) to obtain an equation for the electric field , which is

(2.34)

If as before, we attempt to use

(2.35a)

it is apparent that there now is no simple relationship between $\vec{P}$ and ,

and between $\underline{E}_E$ and $\underline{H}$, due to the $\underline{E}_o$ term and the spatial variation of ϵ.

A somewhat more reasonable way to attempt decomposing the total electric field may be using

(2.35b)

(2.35c)

since an EM wave alone propagating in a medium with a variable dielectric constant, satisfies (2.35b) rather than (2.35a). There is thus obtained from (2.35)

(2.36a)

(2.36b)

which does succeed in giving $\underline{E}_E$ in terms of $\underline{H}$ and $\underline{E}_P$ in terms of n. However now

(2.36c)

which shows that $\underline{E}_P$ is not irrotational, thus coupling to the magnetic field.

It is of interest however, to obtain wave equations involving the magnetic field and dynamic electron density, as was done for the homogeneous

medium. This is most simply done by successively taking the curl and divergence of (2.34), and with the new variables

(2.37a)

(2.37b)

there is obtained

(2.38a)

(2.38b)

These equations clearly exhibit the coupling between the magnetic field and the dynamic electron density due to the sheath inhomogeniety. This is in contrast to the case in the uniform plasma where the magnetic field and dynamic electron density satisfy independent wave equations and are quantities associated with only the EM and EK waves respectively. Equations (2.38) reduce to (2.24) when the plasma is uniform, since then $\underline{P}$ and $\underline{E}_o$ become zero.

2.5.5 Specification of the Inhomogeneous Sheath Boundary Value Problem

Since analytical solutions cannot be obtained to equations (2.3[illegible], so that resort must be made to numerical computations, it is preferable to deal with the first order differential equations. For this reason, we return to (2.28) which are rearranged as follows

(2.39a)

(2.39b)

(2.39c)

(2.39d)

A separation of the angular dependence of these variables for the non-uniform plasma follows from the requirement for single valued solutions as varies in increments of 2 radians, in the same way as for the uniform plasma. The variation may be deduced by dividing the sheath region into a number of cylindrical homogeneous shells whose

properties represent an average over that section of the inhomogeneous sheath which they replace. The resultant wave quantities must be periodic in the direction within each shell due to the boundary conditions applied at each shell interface, with the periodicity determined by the incident wave. As the thickness of the shells is taken to be zero in the limit, the variation is seen to be constant through the inhomogeneous sheath. Thus with the azimuthal separation variable or mode number m, which is an integer, and the direction wave number, there is obtained

(2.40a)

(2.40b)

(2.40c)

(2.40d)

The summation is understood to be from to , and is summed over the 3 cylindrical co-ordinates and .

Upon introducing (2.40) into (2.39) and utilizing the orthogonality of the equation with respect to , there is obtained the following set of differential equations

(2.41a)

(2.41b)

(2.41c)

(2.41d)

(2.41e)

(2.41f)

where the prime indicates differentiation with respect to ρ. It should be noted that no derivatives of or appear in these equations. is given by

(2.41g)

and is obtained from

(2.41h)

(2.41i)

(2.41j)

The dynamic sheath behavior is thus specified by a system of 6 first order ordinary differential equations. Before a solution of this system of equations is undertaken, some further consideration must be given to the equations which describe the waves propagating in the uniform plasma, since the waves which are incident on the sheath from the uniform plasma serve as a source for the excitation of the dynamic sheath variation. Now a plane electromagnetic wave of arbitrary polarization, when referred to the plane of incidence in a particular co-ordinate system, can be broken up into two waves of specific polarization, the transverse magnetic (h) and transverse electric (e) waves. In the case of the cylindrical co-ordinate system, the plane of

incidence is taken to be the plane formed by the z axis of the co-ordinate system and the propagation vector of the incident plane wave. The h and e waves are those waves for which the magnetic and electric vectors respectively, are perpendicular to the plane of incidence.

An equally valid criterion which can be used for specifying the polarization is on the basis of the components of the fields. The h wave has no z component of magnetic field and the e wave has no z component of electric field. The fields scattered from the cylindrical sheath can thus also be specified as to their state of polarization as transverse magnetic or transverse electric modes on the basis of a z component of electric or magnetic field. (The scattered fields when mentioned specifically will be referred to as modes since they are functions of the mode number m, and this serves to distinguish them from the incident waves.) We will thus use h and e to refer to the state of polarization of both the incident EM waves and scattered EM modes. The incident EK wave and scattered EK mode will be indicated by p .

As a result of there being three kinds of waves or modes propagating in the uniform plasma, three wave equations are required for that region. Two of the kind given by (2.24a) are required for the EM fields, one each for the h and e polarizations, and the other as given by (2.24b) for the EK wave. It can be seen then, that the complete mathematical description of the dynamic response of the homogeneous plasma and inhomogeneous sheath involves solving a twelfth order system of linear differential

equations, six first order equations for the sheath as given in (2.41) and three second order wave equations as given by (2.24). There are then twelve constants of integration to be determined by the boundary conditions. However, one constant of integration from each of the wave equations for the homogeneous medium will be associated with the incident waves and is therefore an adjustable parameter. This leaves nine constants of integration to be determined, and thus nine scalar boundary conditions are required.

The boundary conditions to be imposed at the interface between the sheath and uniform plasma, assuming no discontinuity in the static plasma variables in crossing the interface, are the usual ones from electromagnetics and acoustics, which can be derived from (2.28). They are: continuity of the tangential electric and magnetic fields, and continuity of the normal dynamic electron velocity and dynamic electron density. The other three boundary conditions are specified at the cylinder surface. Since the cylinder is taken to be infinitely conducting, then the and components of the electric field are zero there.

The final boundary condition must involve in some way, the hydrodynamic aspects of the electron flow. The usual approach is to assume elastic reflection of the incident electrons from the metal surface, so that the normal component of the dynamic electron velocity is set equal to zero. Cohen (1962) discusses this boundary condition in some detail, and concludes that a more realistic way of accounting for the effect of the boundary would be to use

(2.42)

Y_A and Y_B are called bi-linear admittance relations between the velocity, and the electric field and electron pressure. Cohen does not justify this boundary condition except on heuristic grounds, nor suggest any theoretical way for calculating Y_A and Y_B. There is however, from ordinary acoustic theory, some justification for the term in Y_B since the surface effect in acoustics is represented by a surface admittance which relates the normal velocity to the pressure, as in (2.42). A rigid, impenetrable boundary in acoustics is represented by zero surface admittance, while a completely porous boundary has an infinite value of surface admittance. It would seem to be reasonable then to include these two extremes by using as the last boundary condition at the cylinder surface, either zero velocity or zero-pressure, corresponding to Y_B equal to zero or infinity respectively, with Y_A equal to zero. Due to the lengthy numerical calculations which will be required to solve (2.41), it does not seem practical to perform a parametric study on the effects of using other values of Y_A and Y_B.

The nine boundary conditions to be used are written below, with the subscripts 1 and 2 used to denote field quantities in the inhomogeneous sheath and uniform plasma respectively. At the sheath interface ($\rho = s$):

(2.43a)

(2.43b)

(2.43c)

(2.43d)

and at the cylinder ($\rho = c$):

(2.43e)

(2.43f)

This set of boundary conditions completes the specifications of the problem. We wish to find the solution to equations (2.41) which apply to the inhomogeneous sheath, and of (2.24) which apply to the uniform plasma, subject to the boundary conditions (2.43). The boundary conditions (2.43a) to (2.43d) serve as the link between the solutions for the two regions.

Before proceeding to the numerical solutions of (2.41), we first write the analytic solutions for the uniform plasma. It is well known (Stratton (1941) p. 393) that solutions to the vector wave equation can be generated from solutions to the scalar wave equation by the method of potentials. This is due to the fact that, in cylindrical co-ordinates, the component of the vector wave equation is identical to the scalar wave equation. The three possible vector solutions are given by

(2.44a)

(2.44b)

(2.44c)

where , and are solutions to

(2.44d)

for and for

The electric and magnetic fields, in terms of the potentials, are given by

(2.45)

(2.46a)

(2.46b)

(2.47a)

(2.47b)

is the radial direction separation constant, related to and by

(2.48a)

(2.48b)

where is the direction separation constant, given by

(2.49)

^{i} is the angle of incidence measured from the $-$ axis, and ^{i} is the propagation constant of the incident plane wave. η is the plane wave impedance for the EM wave, given by

(2.50)

with the free space impedance.

The potential of the incident plane wave solution of (2.44d) may be expressed in terms of an infinite series of Bessel functions, as

(2.51a)

where ^{i}, ^{i} and λ are subscripted according to the kind of incident plane wave, and is obtained from (2.49). The plane wave is taken to be incident on the cylinder from the direction . The scattered fields have as their potential

(2.51b)

where again ^{s} and λ have subscripts corresponding to the kind of scattered mode. A_{m--} is the Fourier scattering coefficient where the second subscript denotes the kind of incident wave and the third the type of scattered mode. $H_m^{(2)}$ is the Hankel function of the second kind, given by

with J_m and N_m the Bessel and Neumann functions.

Note that and vary in the ratio of so that λ and λ are quite different in value. It should be observed that λ becomes imaginary when an EK wave is incident at an angle such that

or when θ^i is different from normal incidence by approximately radians. When this occurs the Hankel function of second kind with argument $\lambda_E \rho$ becomes a modified Bessel function. The negative imaginary root for λ_E is required so that the fields do not grow as the radial argument increases to infinity, since the medium is passive. Therefore is replaced by , which decreases exponentially with radius for large arguments. This does not occur for EM wave incidence.

Upon using (2.41), (2.43) and (2.51), and eliminating the Fourier scattering coefficients, the boundary conditions at the sheath can be reduced to

(2.52a)

(2.52b)

(2.52c)

(2.52d)

(2.52e)

(2.52f)

In writing these equations, it is assumed that only one wave type is incident, so that two of the three $\quad_i$ must be zero.

The boundary conditions at the cylinder may be written as

(2.52g)

(2.52h)

and

(2.52i)

or

(2.52j)

Q_m being zero is the condition that the dynamic electron pressure be zero at the cylinder wall, while the equation (2.53j) is the condition that the radial dynamic electron velocity is zero at the cylinder. Only one of these two equations is used. Now cylindrical functions of real argument satisfy

(2.53a)

and those of imaginary argument satisfy

(2.53b)

Then by using (2.52) and (2.53), it can be verified that for p and h wave

(2.54a)

and

(2.54b)

For e wave incidence there is obtained

(2.55a)

and

(2.55b)

The dynamic sheath problems has now been reduced to solving the sixth order system of differential equations (2.41) subject to the six boundary conditions (2.52a) to (2.52c) and (2.52g) to (2.52j). It is interesting to observe

that the boundary condition equations at the sheath edge do not involve both EM and EK quantities together in the same equation, as a result of eliminating the Fourier scattering coefficients.

The numerical solution of a set of differential equations with boundary conditions specified at two boundaries is discussed in detail in Appendix C. The basis problem is to obtain the starting values for the numerical integration. This is done by setting, at one boundary, all but one of the modal variables in (2.41) equal to zero, the one remaining being set equal to unity. The boundary conditions are then used to find the values of the derivatives and other variables which may be related to the non-zero input. A numerical integration through the sheath is carried out which yields the output values of the variables and their derivatives at the second boundary. This process is repeated with a new input variable set equal to unity, as many times as there are boundary condition equations at the second boundary. A linear combination of the output values, with a coefficient corresponding to each input, is put into the boundary condition equations at the second boundary, to obtain a matrix, which upon inversion, yields the coefficients of the linear combination. These are the desired starting values for the final numerical integration, which when carried out will produce a solution that satisfies the boundary conditions at both boundaries. The surface currents are then obtained from the tangential components of the magnetic field at the cylinder as

(2.56a)

(2.56b)

A subscript in place of the dash on the current symbol will indicate the kind of incident wave.

An additional complication to the numerical solution of (2.41) is due to the fact that these equations are complex. There are thus effectively twelve real equations, rather than six, to be solved. The computer time required to carry out the numerical calculations involved can become prohibitive, especially when the results are desired to be accurate to three or four significant figures. This degree of accuracy is required since the final results are obtained from summing the Fourier series, where the errors involved in the individual terms in the series are additive.

An interesting feature of equations (2.41) and the boundary condition equations (2.52) is that when , corresponding to normal incidence, these equations break up into two sets. The and components of the velocity and electric field, and the z component of the magnetic field and the electron pressure are in one set, with the component of velocity and electric field and the and components of magnetic field in the other. In other words, the and modes are coupled but independent of the mode equations which stand alone. The coupled and mode equations consist then of four complex differential equations and boundary conditions, with the result that the numerical computation time can be decreased by more than one half. There

is an additional feature in the fact that there are fewer terms in these differential equations with a resultant decrease in the generation of errors.

For these reasons the numerical computations for the inhomogeneous sheath are performed for the case of normal incidence only. It was felt that the problem is an extremely difficult one even for the case of normal incidence and that there would be an increased possibility of better understanding the physics involved, since for a given amount of computer time, more numerical results could be obtained. There is, in addition as discussed in Appendix D, a potentially significant experiment that could be carried out for the case of normal incidence, whereas the case of oblique incidence may not lend itself so easily to experimental investigation. The results for the inhomogeneous sheath solution are contained in Chapter III.

2.6 The Vacuum Sheath Model

It was pointed out above that analytic solutions can be obtained in the homogeneous region outside the sheath. A natural question to consider now is whether the inhomogeneous sheath may be reasonably approximated by replacing it with a homogeneous region with properties which may be different from those of the external uniform plasma. In this way analytic solutions could be obtained everywhere. The results obtained from this model could serve as a measure of the relative importance of the inhomogeneous sheath and the boundary conditions to the coupling of EM and EK waves, when compared with the inhomogeneous sheath solutions. Also, the analytic solutions are easily obtained for arbitrary angles of incidence, in contrast to the case

for the inhomogeneous sheath. A comparison of the results obtained from the two sheath models for normal incidence would serve as an indication of how meaningful are the results obtained for oblique incidence from the homogeneous sheath model.

If the homogeneous sheath region is taken to be a plasma with different properties than the external homogeneous plasma, then in the case of oblique incidence, there will be nine boundary conditions to be satisfied, as was the case for the inhomogeneous sheath. This results in the requirement that a 9 x 9 matrix be inverted for the solution of the Fourier coefficients of the various modes, a task of such complexity that it would have to be carried out numerically. It is felt that there is little loss of generality by using as a sheath model however, a homogeneous region void of plasma, and having the electrical properties of free space, which will be called the vacuum sheath. This reduces the number of boundary conditions from nine to seven, since the p mode will not be transmitted through the vacuum sheath. As a result, the matrix inversion becomes much more manageable, and can be easily carried out analytically, so that the numerical computation become considerably less involved.

In the following discussion the fields scattered from the sheath-plasma interface will be called scattered modes, those which pass through the sheath to the cylinder are denoted as transmitted modes, and those scattered at the cylinder wall are called reflected modes. The latters S, T and R will be used as superscripts on the Fourier coeffecients for the potentials from which the

various field quantities are derived to indicate them as the scattered, transmitted or reflected modes. As before, the subscripts will indicate mode number, the incident wave type and the mode type, in that order.

Six of the boundary conditions to be used are the same as those discussed for the inhomogeneous sheath. They are continuity of the tangential electric and magnetic fields at the sheath edge, and vanishing of the tangential electric field on the cylinder. The last boundary condition for the vacuum sheath should be so chosen as to be consistent with the remaining two conditions at the sheath-plasma interface which were used for the inhomogeneous sheath. There are two possibilities then, corresponding to the continuity of pressure and continuityof normal dynamic electron velocity. Since there is no plasma within the vacuum sheath, these conditions would lead to the vanishing of either the electron pressure or normal electron velocity, at the sheath edge, which are the same conditions mentioned previously for use at the cylinder wall, in connection with the inhomogeneous sheath. The consistency of the boundary conditions used for the two sheath models in thus maintained when the vacuum sheath thickness is taken to be vanishingly small, so that the sheathless case can also be studied with this formulation. The boundary conditions may be stated then, with the sub scripts 1 and 2 used to refer to the vacuum sheath and plasma quantities respectively, at the sheath edge ( )

(2.57a)

(2.57b)

(2.57c)

and at the cylinder ($\rho = c$)

(2.57d)

The field quantities are again generated from their respective potentials, as was done for the analytic solutions in the uniform plasma in connection with the inhomogeneous sheath model. Upon writing the boundary conditions expressed by (2.57), and utilizing the orthogonality of the resulting equations with respect to m, the matrix equation from which the modal Fourier coefficients are obtained can be written

(2.58)

where the prime indicates a derivative with respect to . The middle subscript on the Fourier coefficients, indicated [illegible], will be p, h or e, corresponding to the kind of incident wave determined by the source S. The source terms are given by

(2.59a)

(2.59b)

(2.59c)

where the only which is now zero is that of the particular incident wave. We obtain λ_P, λ_E, and λ_{Eo} (which appears in) from

(2.60a)

(2.60b)

(2.60c)

where the is given by

(2.60d)

when the wave is the incident wave, or

(2.60e)

when the or waves are incident. θ^i the angle of incidence is measured from the positive axis. is given by (2.61) (see insert next page), where $H_m^{(1)}$ and $H_m^{(2)}$ are Hankel functions of the first and second kind.

The observation made about the radial separation constant λ_E possibly becoming imaginary with an incident EK wave in discussing the inhomogeneous sheath model applies here also to λ_E and λ_{Eo}. When this occurs the minus sign must be used on the imaginary roots so that the Hankel functions of the second kind, which represent the scattered fields in the plasma, do not increase in magnitude with increasing radius. Hankel functions of a negative imaginary argument are given by the modified Bessel functions and as

$$
\Delta = \begin{vmatrix}
i\beta H_m^{(2)}(\lambda_P s) & \frac{\lambda_E^2}{K_E} H_m^{(2)}(\lambda_E s) & 0 & -\frac{\lambda_{Eo}^2}{K_{Eo}} H_m^{(1)}(\lambda_{Eo} s) & 0 & -\frac{\lambda_{Eo}^2}{K_{Eo}} H_m^{(2)}(\lambda_{Eo} s) & 0 \\
-\frac{im}{s} H_m^{(2)}(\lambda_P s) & \frac{\beta m}{K_E s} H_m^{(2)}(\lambda_E s) & -H_m^{(2)'}(\lambda_E s) & -\frac{\beta m}{K_E s} H_m^{(1)}(\lambda_{Eo} s) & H_m^{(1)'}(\lambda_{Eo} s) & -\frac{\beta m}{K_{Eo} s} H_m^{(1)}(\lambda_{Eo} s) & H_m^{(2)'}(\lambda_{Eo} s) \\
0 & 0 & \frac{\lambda_E^2}{K_E \eta} H_m^{(2)}(\lambda_E s) & 0 & -\frac{\lambda_{Eo}^2}{K_{Eo} \eta_o} H_m^{(1)}(\lambda_{Eo} s) & 0 & -\frac{\lambda_{Eo}^2}{K_{Eo} \eta_o} H_m^{(2)}(\lambda_{Eo} s) \\
0 & -\frac{1}{\eta} H_m^{(2)'}(\lambda_E s) & \frac{\beta m}{K_E s \eta} H_m^{(2)}(\lambda_E s) & \frac{1}{\eta_o} H_m^{(1)'}(\lambda_{Eo} s) & -\frac{\beta m}{K_{Eo} s \eta_o} H_m^{(1)}(\lambda_{Eo} s) & \frac{1}{\eta_o} H_m^{(2)'}(\lambda_{Eo} s) & -\frac{\beta m}{K_{Eo} s \eta_o} H_m^{(2)}(\lambda_{eo} s) \\
\frac{1}{N^2} H_m^{(2)'}(\lambda_P s) & \frac{i\beta}{K_E} H_m^{(2)'}(\lambda_E s) & -\frac{im}{s} H_m^{(2)}(\lambda_E s) & 0 & 0 & 0 & 0 \\
0 & 0 & 0 & \frac{\lambda_{Eo}^2}{K_{Eo}} H_m^{(1)}(\lambda_{Eo} c) & 0 & \frac{\lambda_{Eo}^2}{K_{Eo}} H_m^{(2)}(\lambda_{Eo} c) & 0 \\
0 & 0 & 0 & \frac{\beta m}{K_{Eo} c} H_m^{(1)}(\lambda_{Eo} c) & -H_m^{(1)'}(\lambda_{Eo} c) & \frac{\beta m}{K_{Eo} c} H_m^{(2)}(\lambda_{Eo} c) & -H_m^{(2)'}(\lambda_{Eo} c)
\end{vmatrix}
\tag{2.61}
$$

(2.62a)

(2.62b)

and vary approximately as and for large . Since the fields transmitted from the sheath interface towards the cylinder vary as , there exists the possibility of a large attenuation in the fields reaching the cylinder, decreasing also the currents excited. This is a significant outcome which is discussed more fully in the next chapter when the numerical results are presented. The angle at which λ_E changes from real to imaginary will be denoted as .

If the boundary condition rather than is used at , then the fifth row of and the fifth row of the source vector on the right hand side of (2.58) are replaced by

(2.63a)

(2.63b)

It is evident with (2.63) put into (2.58) and (2.61), that there is no coupling between the EM and EK waves due to the boundary conditions. But the only

possibility for coupling between the EM and EK waves in a homogeneous plasma terminated by a boundary. Thus we can conclude that the EM and EK waves are not coupled when propagating in a uniform plasma terminated by boundaries at which the electron pressure is zero. This suggests the intriguing possibility of being able to separate the relative contribution of the inhomogeneity and boundary coupling effects in the analysis of the inhomogeneous sheath, since any coupling which is observed when the electron pressure at the cylinder wall is taken to be zero should be due entirely to the sheath inhomogeneity coupling. This point will be discussed further in the presentation of the numerical results which are given in the next chapter.

The solution of (2.58) is straightforward but tedious. The procedure followed was to eliminate four of the coefficients and by solving for them in terms of the other three. A 3 x 3 matrix was generated as a result, from which the desired coefficients were obtained. Results are presented here for the three coefficients found directly from the matrix. Solutions for the other coefficients and a brief outline of the above procedure are given in Appendix E.

Before writing the expressions obtained for the coefficients, some shorthand notation which was used to facilitate writing these rather lengthy expressions is given here. Due to the requirement for boundary conditions to be satisfied at two boundaries, the cylinder wall and the sheath edge, a number of Wronskian-type relations appear in the coefficients, but with Hankel functions

of arguments evaluated at two boundaries. As a consequence, the Wronskian relation cannot be evaluated analytically, as when all the arguments appearing in the expression are the same. In order to avoid writing these numerous relations out in full, they are abbreviated by using

(2.64a)

(2.64b)

(2.64c)

(2.64d)

The prime now indicates differentiation with respect to argument after which the argument is fixed at the indicated value. Note that

Appendix F contains some approximate evaluations of these Wronskians. We will also use

(2.65a)

(2.65b)

(2.65c)

(2.65d)

The determinant D_m of the matrix can then be written

(2.66)

The Fourier coefficients A^{S}_{m-p}, A^{R}_{m-h} and A^{R}_{m-e} are:

Incident p-wave -

(2.57a)

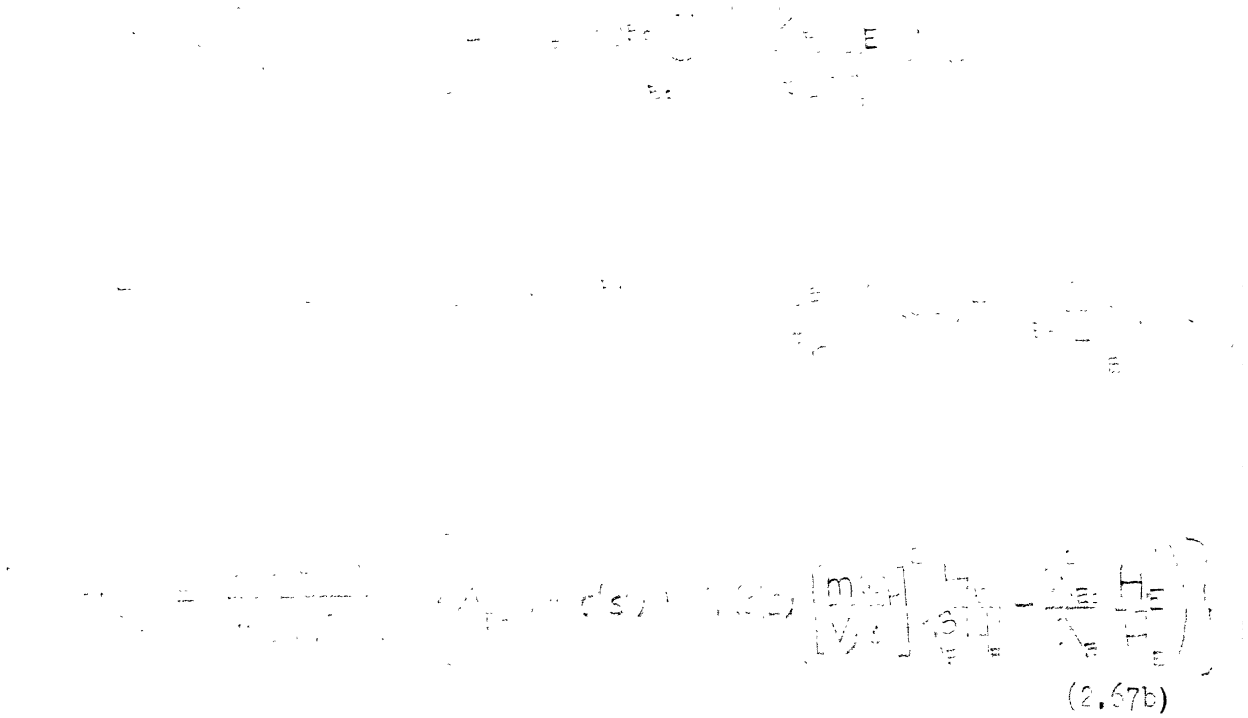

(2.57b)

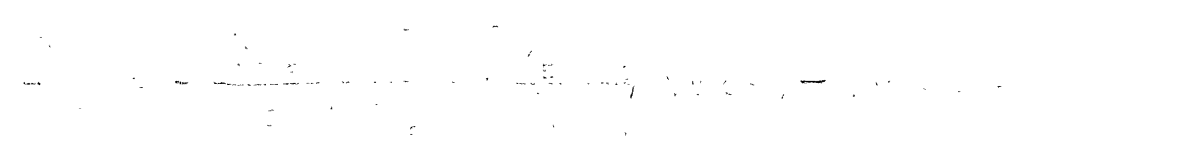

(2.57c)

Incident h-wave -

(2.68a)

(2.68b)

(2.68c)

Incident e-wave -

(2.69a)

(2.69c)

(2.69d)

Upon using (2.53), it can be shown that [illegible] is a property of the Fourier coefficients for the scattered, transmitted and reflected fields of the same type as the incident wave. This is also a property of the coefficient coupling the h and p fields. The coefficients of the other modes dissimilar to the incident wave type have the property $A_{-m} = -(-1)^m A_m$.

The surface currents excited on the cylinder can be written in terms of A^R_{m-h} and A^R_{m-e} as

(2.70a)

(2.70b)

where the dash subscript on the and the will indicate the kind of incident wave. Due to the behavior with change in the sign of m of the various modal coefficients, we observe that

(2.71a)

(2.71b)

These expressions are rather lengthy, and consequently present relatively little interpretable information in their present form. There is however, one interesting feature of the coupling aspect of the problem which can be seen from a consideration of the Fourier coefficients. The coefficients show that the results of the coupling between the incident wave and the various modes can be summarized qualitatively by a matrix C whose elements are proportional to the respective Fourier coefficients as

(2.72a)

where

(2.72b)

There is no distinction made between the scattering, transmission and reflection coefficients for a given mode since all exhibit the same proportionality to the kind of incident wave, denoted by the vector. It is evident for no z variation in the incident field, i.e. for normal incidence, that the h mode decouples from the other two, in agreement with the conclusion reached in the discussion of the inhomogeneous sheath. There is also a decoupling of the e mode from the p and h modes when the azimuthal variation is zero, which corresponds to the cylinder, in the limit of its radius approaching infinity, being replaced by a flat surface. Cohen (1962) and others have pointed this out for scattering from a plane surface.

One additional aspect of this problem can be studied using the results given above. This is the effect of including the EK wave in the formulation upon the scattering properties of the cylinder when illuminated by EM waves.

Or in other words, the results obtained by using a compressible model for the plasma can be compared with those which are gotten from a treatment in which the plasma is incompressible and characterized only by a dielectric constant. The only change in the present formulation to obtain the incompressible plasma results would be to set $A^{S}_{m-p} = 0$ and to eliminate the boundary condition on the normal electron velocity at the sheath edge. A solution of the resulting equations for the new Fourier coefficients is not required since the new coefficients can be obtained directly from (2.68) and (2.69) by setting the terms containing H_p in these expressions equal to zero. This comparison of the compressible and incompressible plasma results should be informative in showing whether it is necessary to allow for compressive plasma effects in the problem of the scattering of EM waves from plasma immersed obstacles.

The calculations which are necessary for obtaining numerical results require the evaluation of Hankel functions of both real and imaginary argument, over a wide range of order and magnitude of argument. This presented a difficult computational problem, and the approach used to solve it is presented in Appendix F. There is also contained in Appendix F a discussion of the limitation on the accuracy of the final results for the surface currents. The limitations on the accuracy of the inhomogeneous sheath results are discussed in Appendix C.

This concludes the formulation of the problem of finding the surface currents excited on an infinitely long, insulated, plasma-immersed circular

metal cylinder by incident plane EM and EK waves. To summarize, the plasma has been taken to be of uniform temperature throughout. The equations which govern its behavior have been obtained from the Boltzmann equation and Maxwell's equations using a linearized theory and a scalar electron pressure. Magnetic force effects are neglected, as are the radio frequency ion motion and the static electron velocity. The inhomogeneous sheath region is assumed to be confined to a layer on the order of several electron Debye lengths thick next to the cylinder surface. Two models are used for the sheath, one taking the sheath inhomogeneity into account, and the other which approximates the sheath with a vacuum layer. Finally, in the boundary condition which relates the electron pressure to the normal electron velocity at a cylinder surface, the surface admittance is taken to have either the value zero or infinity. The numerical results which are obtained from the formulation above follow in Chapter III.

CHAPTER III

RESULTS

The results presented here are given first for the vacuum sheath model, and following, those obtained from the inhomogeneous sheath.

3.1 Vacuum Sheath

Due to the complexity, and hence the time consuming nature of the numerical calculations required for the evaluation of the expressions which give the Fourier coefficients for the various modes arising in the vacuum sheath formulation, it was not practical to carry out a complete parametric analysis involving all the parameters and variables appearing in these expressions. Instead, the following results are obtained as functions of only certain of the parameters and variables, which are given below.

The quantities which are independent parameters in this analysis are

T_e = electron temperature

$\omega = 2\pi f$ = radian radio frequency

V^i = voltage magnitude of incident wave

$\omega_p = 2\pi f_p$ = radian plasma frequency

c = cylinder radius

s = sheath radius

θ^i = angle of incidence of plane wave

The surface current results are obtained as functions of the parameters θ^i, ω_p, c and s. Variations in s are presented as variations in s-c, in units of D_ℓ. The sheath thickness measured in D_ℓ will be denoted by X. The radian plasma

frequency ω_p is varied in terms of N, the ratio of ω_p to ω. The other three parameters are fixed at constant values throughout the calculations. V^i of course, is simply a scale factor for the incident wave, and is set equal to 1.0.*, ω is set at $2\pi \times 10^9$/ sec., corresponding to a frequency of 1 Gc, and T_e is fixed at 10 000°K. This value for T_e corresponds to a typical electron temperature for a cold cathode laboratory discharge. Since the velocity v_r is proportional to the square root of the temperature, a range of temperature variation typical of the cold cathode discharge produces a much smaller change in v_r, so it seems reasonable to fix T_e at this nominal value.

In addition there are the independent variables of the co-ordinate system, ρ, z and ϕ. But since the z variation of all the field components is $e^{i\beta z}$, z can be fixed at a value of zero in the numerical analysis with no loss of generality. Also, since the surface currents, which are of the primary interest, are evaluated at ρ=c, while the field variation in the sheath can be deduced to some extent from the surface current and from observing the asymptotic forms of the field expressions, ρ is fixed at the value of the cylinder radius c. The ϕ variation on the other hand is of importance, and the surface currents will be plotted as a function of ϕ.

Some preliminary calculations were performed to determine what would be the most reasonable nominal values around which the parameter variations could be made. The cylinder radius c, was set at 1 cm for these calculations. It was found that, while the computation time required to obtain a convergent solution for c=1 cm and EK wave incidence was not excessive (on the order of 0.4

*To enable easily comparing the currents due to TM and EM wave incidence, the fields associated with the two waves will not be equal, but are instead chosen to make the power flow density in both waves equal.

seconds per term in the Fourier series), the variation of the surface current with ϕ was so finely structured, as to make plotting the results on 8 1/2 x 11 inch graph paper impractical. Because of this, the nominal radius was decreased to 0.2 cm. The nominal values for the parameters and the range of variation which was investigated is summarized below.

Parameter	Nominal Value	Variation
ω	$2\pi \times 10^9$/sec	None
T_e	$10^{4\,o}$K	None
V^i	1.0	None
$N = f_p/f$	0.7	0.7 to 0.99
θ^i	0.25π	0.05π to 0.5π
c	0.2 cm	0.005 to 1.0 cm
$X = (s-c)/D_\ell$	0; 10	0 to 20 (s-c=0 to 0.177 cm)

Generally, only one parameter at a time was varied from this nominal set of values, except at end points of the range of variation. The situation where the vacuum sheath is taken to be of zero thickness will be referred to in what follows as the sheathless case.

In plotting the surface currents, since they are complex quantities, we can present either their real and imaginary parts, or their magnitude and phase. The latter choice is the one used here, since this is more physically meaningful and laboratory measurements are performed on this basis. The phase of the current is not presented for all the results which follow, however, since the phase behavior can be visualized easily from the few representative curves which are

presented. The surface currents excited by the EK wave are given below, followed by those due to the EM wave in section 3.1.2. The salient features of these results will be commented upon as the various sets of curves are presented, but a detailed discussion of them will be deferred until all the graphs have been given, as there are various features shared in common by the results generated from the different parameter variations.

3.1.1 Incident EK Wave

Figures 3.1 and 3.3 show the magnitude of the z and ϕ directed surface currents $K_p^{(z)}$ and $K_p^{(\phi)}$, excited by the EK wave, for the nominal parameter values. The ordinate on these graphs, as in all the graphs to follow which show the surface currents, is amperes/cm and the abscissa is the azimuthal angle measured (in degrees) from the front of the cylinder. Results are plotted from 0^o to 180^o only, since the curves are symmetric in the ϕ variable. The maximum value of the current will be frequently mentioned; it is the value of the current maximum over the ϕ variation from 0^o to 180^o. In figures 3.2 and 3.4 are plotted the phase of these currents restricted to the interval $-\pi$ to π.

There are two rather striking features exhibited by these curves which compare the cylinder surface currents of the vacuum sheath $10\,D_\ell$ thick, with the sheathless case. The first is the attenuation of the currents by the vacuum sheath, a decrease on the order of 100 - 200 times compared with the sheathless currents. The other principal effect of the vacuum sheath has been to reduce the fluctuations of the currents as a function of the azimuthal angle ϕ. These effects are produced by a sheath of thickness 0.0885 cm, while the EK wave length is 0.0945 cm. The

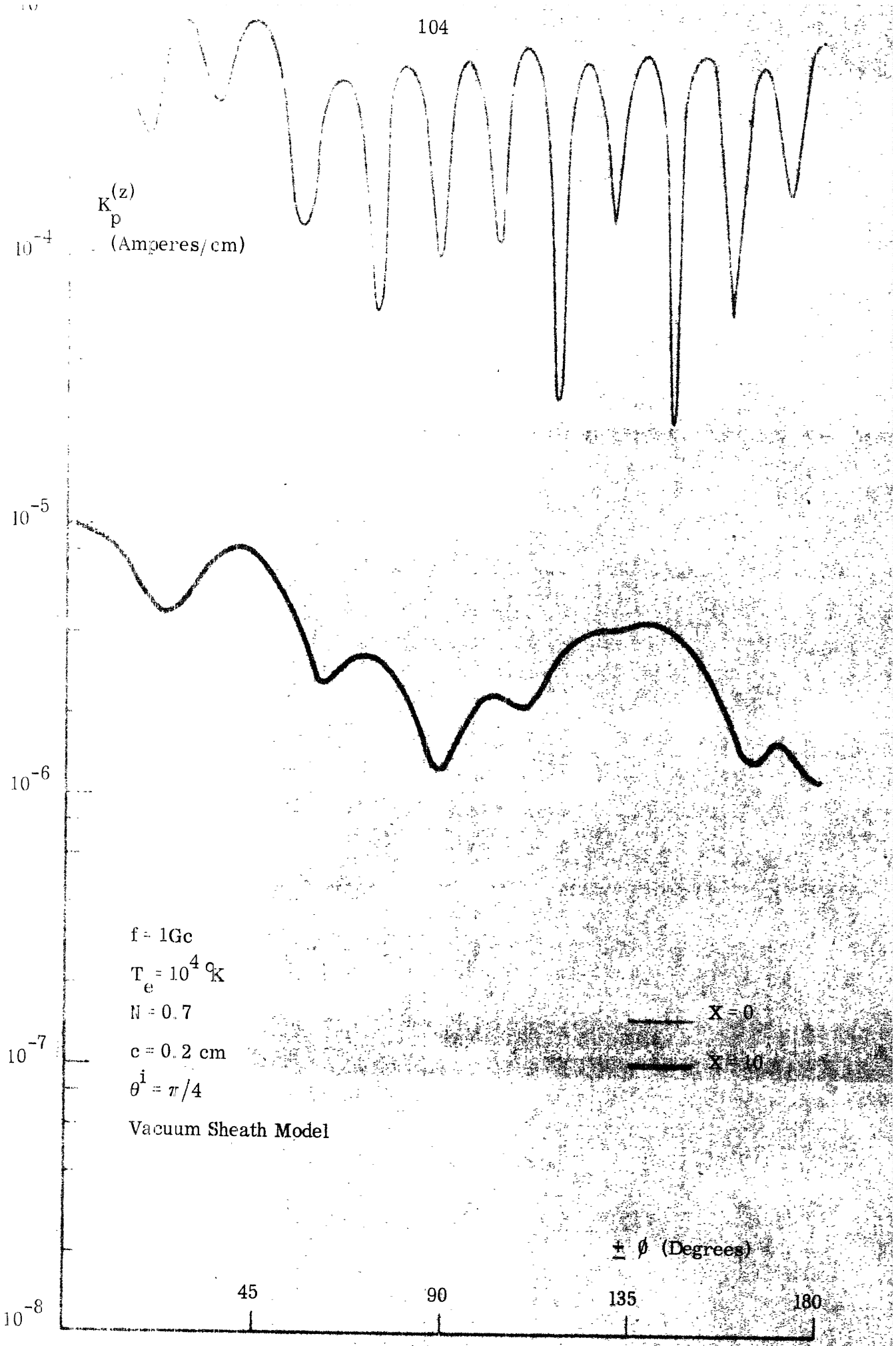

FIG. 3.1: MAGNITUDE OF $K_p^{(z)}$ vs. AZIMUTHAL ANGLE ∅ FOR NOMINAL PARAMETER VALUES.

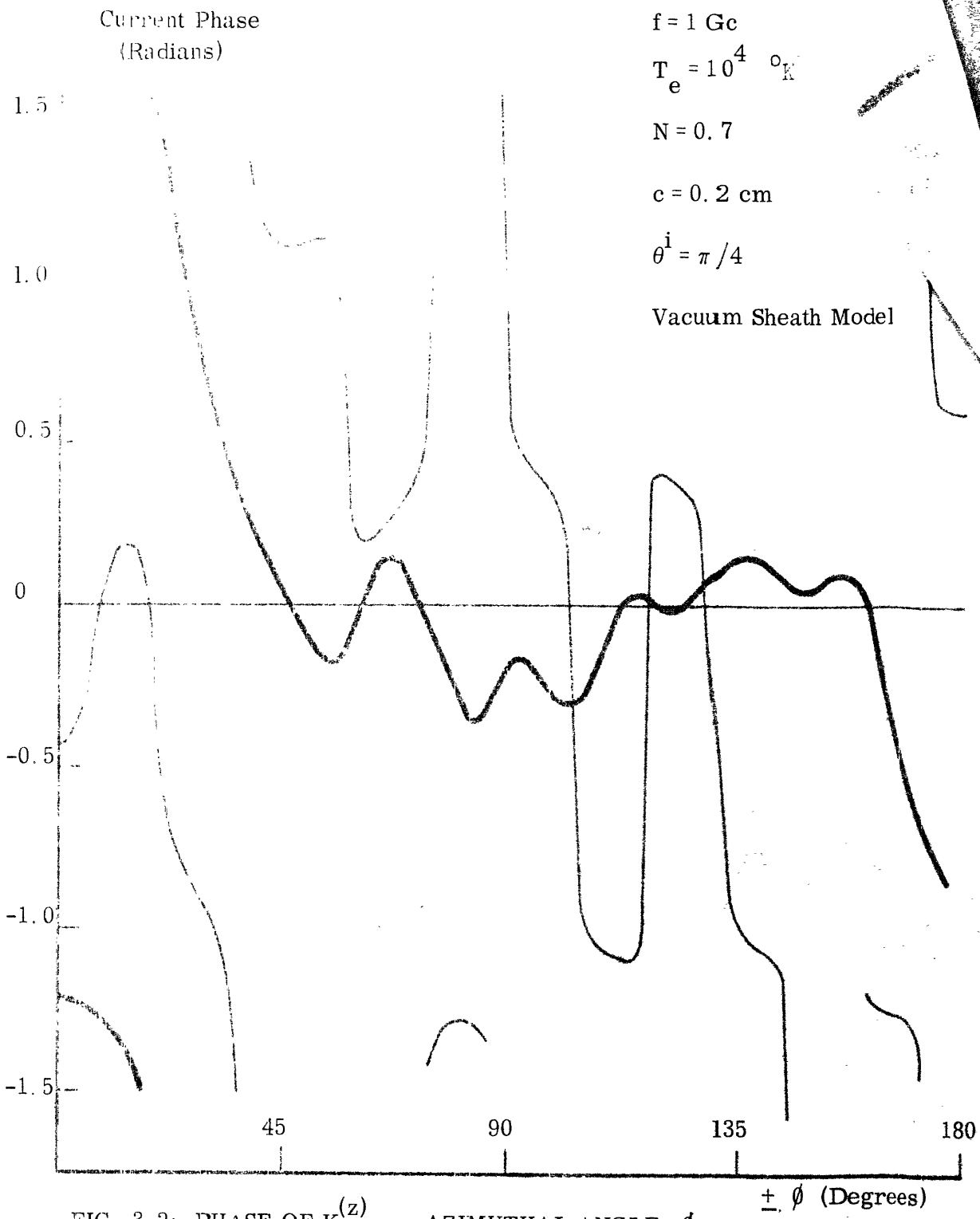

FIG. 3.2: PHASE OF $K_p^{(z)}$ vs. AZIMUTHAL ANGLE ϕ

FOR NOMINAL PARAMETER VALUES

——— X = 0

——— X = 10

MISSING
PAGE

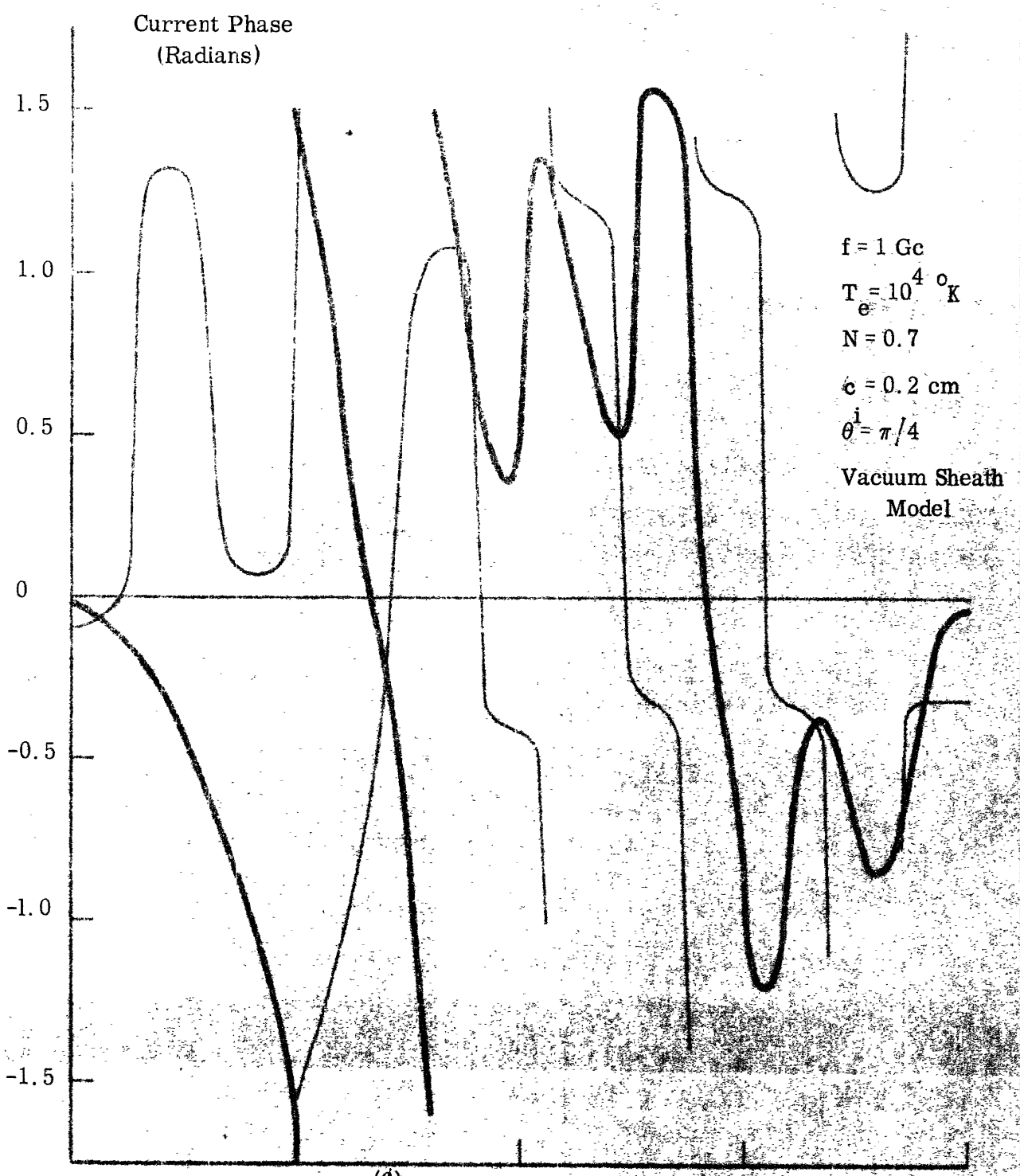

FIG. 3.4: PHASE OF $K_p^{(\phi)}$ vs. AZIMUTHAL ANGLE ϕ FOR NOMINAL PARAMETER VALUES

fluctuations of the current with ϕ for the sheathless case can thus be attributed to interference effects of the incident and scattered fields since the cylinder is approximately 13 EK wave lengths in circumference. The attenuation of the sheath is accounted for by noting that the angle of incidence of the EK wave, $\pi/4$, is less than $\pi/2 - v_r/v_\ell$, the approximate angle at which the scattered EM fields become evanescent. The angle $\pi/2-v_r/v_\ell$ will be referred to as θ_c^i. As a result, the fields which reach the cylinder through the sheath are attenuated, exciting currents of smaller magnitude than those produced when there is no sheath. This effect will be discussed in greater detail at the conclusion of this section, after presenting the other results for the incident EK wave. A comparison of the phase of the currents and the magnitudes reveals that abrupt changes in amplitude are accompanied by corresponding rapid changes in phase. The sheath has the effect of decreasing the phase variation as a function of ϕ.

Figures 3.5 and 3.7 show the current magnitudes, and 3.6 and 3.8 the current phase, again for the nominal parameter values, except that the angle of incidence θ^i is now 89.91 degrees = θ_s, so chosen as to produce a propagating scattered EM mode with a scattering angle equal to $\pi/4$. (See the discussion of Appendix E on the scattering angle). θ^i is not set equal to $\pi/2$ since $K_p^{(z)}$ would then be zero. It is interesting that now $K_p^{(z)}$ is relatively unaffected by the vacuum sheath and is also insensitive to ϕ. This behavior can be verified by the approximate expression for $K_p^{(z)}$ given in (E13a), Appendix E, which shows that in this case $K_p^{(z)}$ is determined primarily by the m = 0 term in the Fourier series. The $K_p^{(\varphi)}$ current on the other hand, is very similar to that for $\theta^i = \pi/4$, for the sheathless case. However, the sheath has considerably less attenuating effect now,

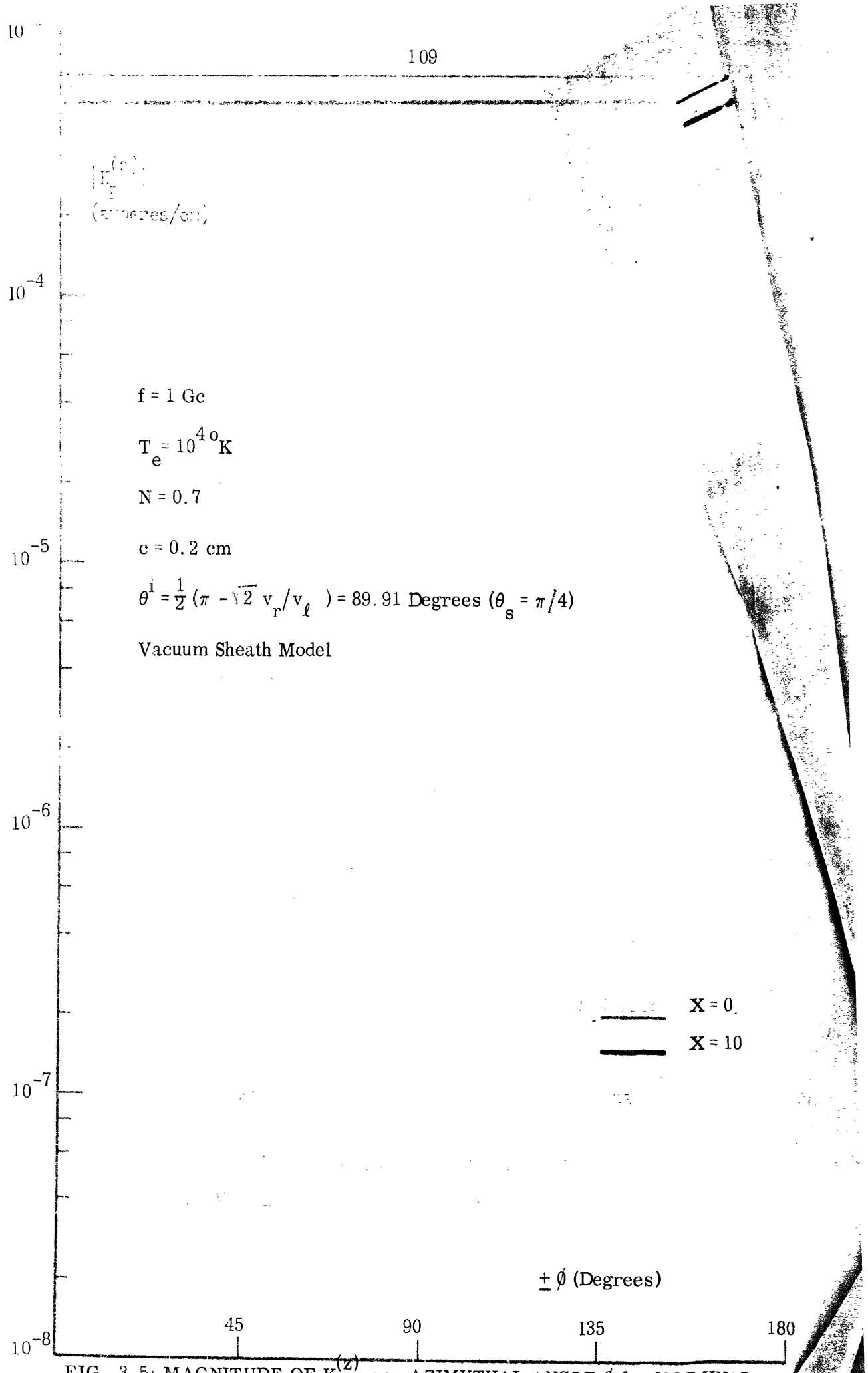

FIG. 3.5: MAGNITUDE OF $K_p^{(z)}$ vs. AZIMUTHAL ANGLE ϕ for NOMINAL PARAMETER VALUES

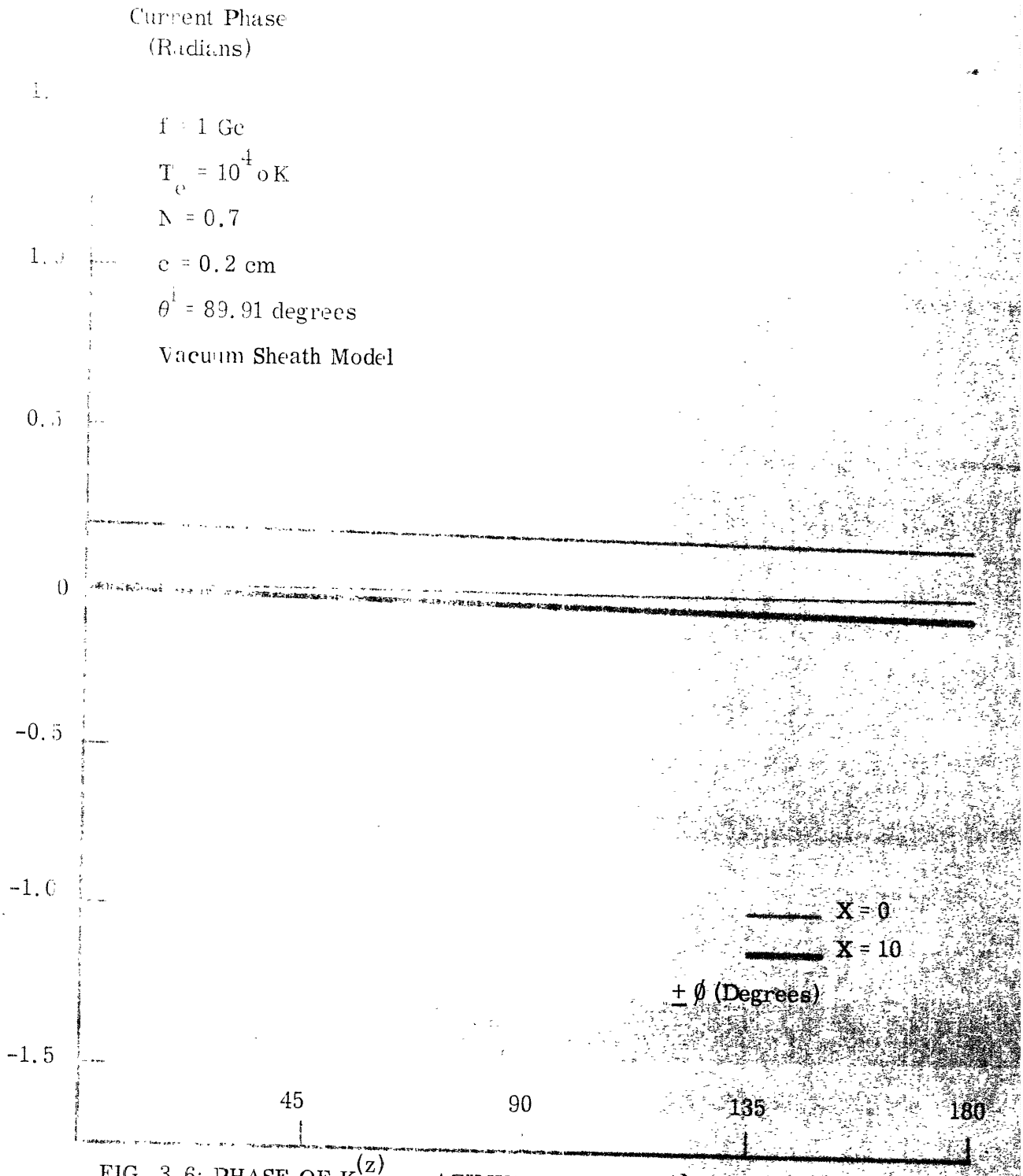

FIG. 3.6: PHASE OF $K_p^{(z)}$ vs. AZIMUTHAL ANGLE ϕ FOR NOMINAL PARAMETER VALUES

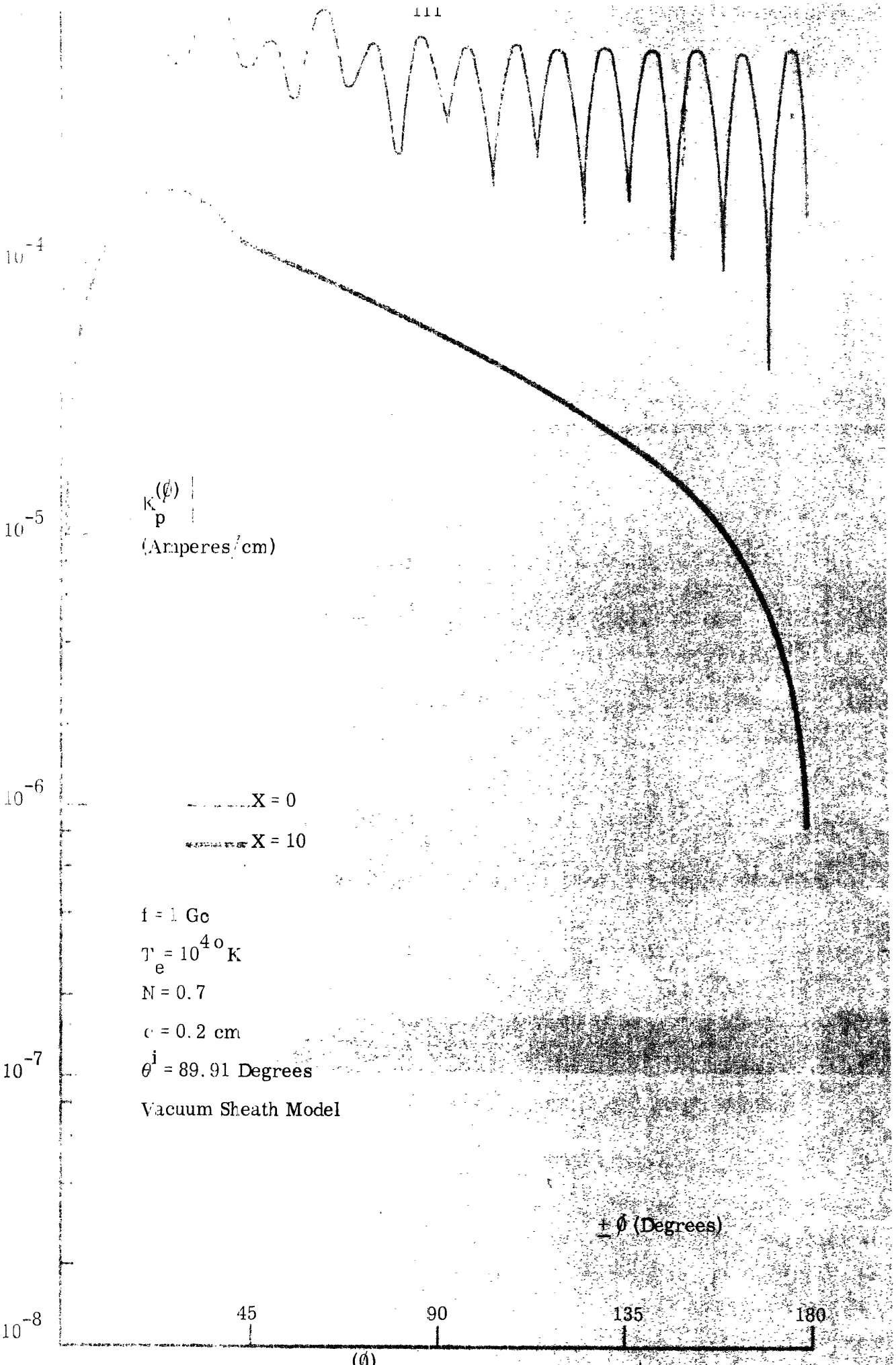

FIG. 3.7: MAGNITUDE OF $K_p^{(\phi)}$ vs. AZIMUTHAL ANGLE ϕ FOR NOMINAL PARAMETER VALUES

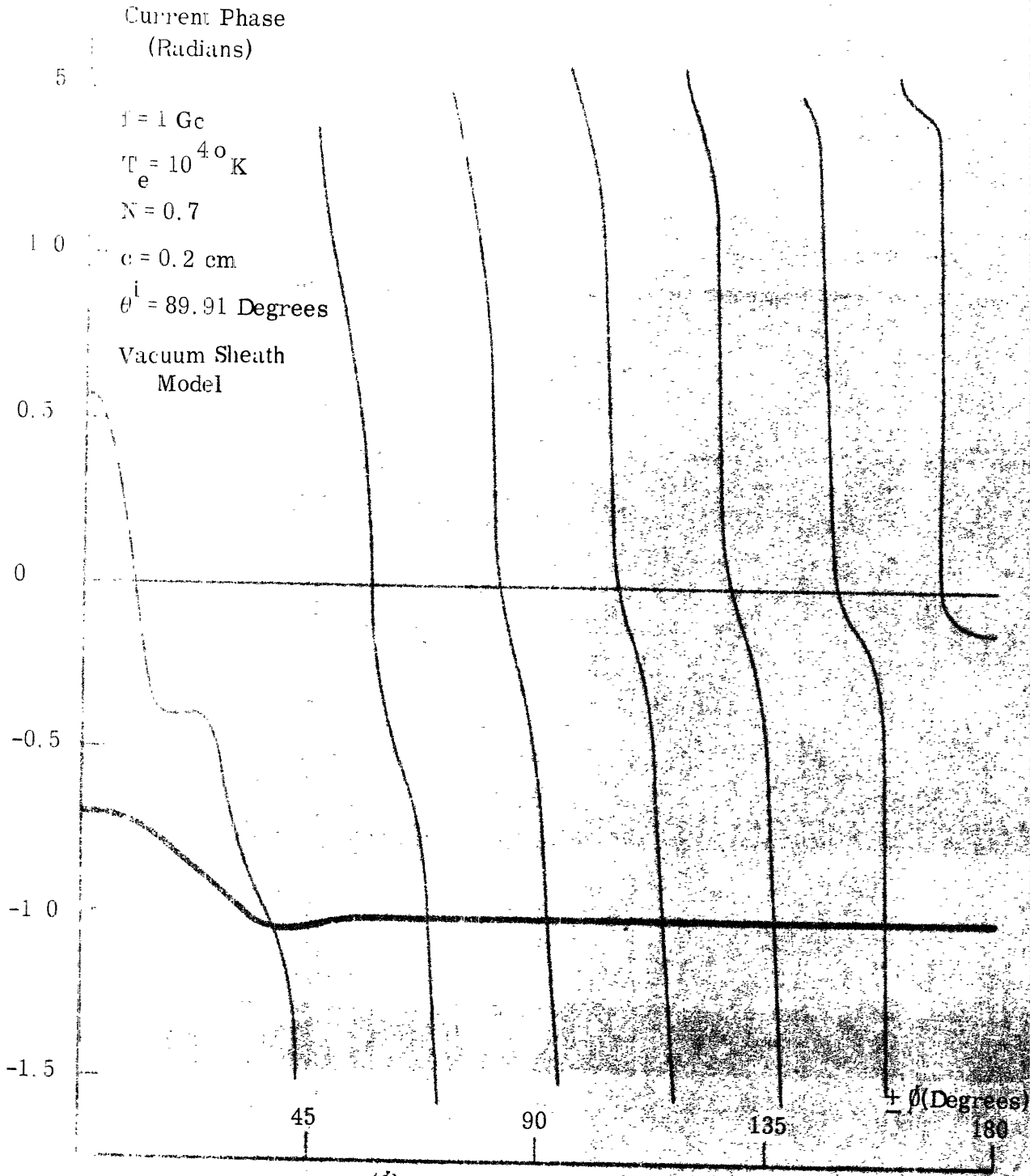

FIG. 3.8: PHASE OF $K_p^{(\phi)}$ vs. AZIMUTHAL ANGLE ϕ FOR NOMINAL PARAMETER VALUES

and has reduced the ϕ fluctuation compared with that for $\theta^i=\pi/4$. As was the case with $\theta^i=\pi/4$, the current phase is observed to fluctuate more rapidly when there are rapid changes in amplitude. This reduction in the ϕ variation of the current by the vacuum sheath is somewhat unexpected. However, the decreased attenuation caused by the sheath is evidently due to the excitation by the EK wave of propagating EM modes which do not decay in the radial direction.

The above graphs serve as a measure of comparison for the curves which follow below and which show the results of the various parameter variations about the nominal values. The results which are given have been selected as providing a representative condensed picture of the computer calculations which were carried out. Some additional graphs will be presented which are derived from the basic curves of the current as a function of angle ϕ, some of which are not included below, as a means of illustrating the more interesting aspects of the results without presenting an excessive amount of detail.

Figures 3.9, 3.11 and 3.13 show the magnitude of the surface currents $K_p^{(z)}$ and $K_p^{(\phi)}$ as the cylinder radius is varied from 0.01 cm to 0.1 cm, for the angle $\theta^i=\pi/4$, and the magnitude of $K_p^{(\phi)}$ for the angle $\theta^i=\theta_s$, and the nominal values of the other parameters. $K_p^{(z)}$ for the latter angle is shown in figure 3.14 as a function of cylinder radius directly, since it is a straight almost horizontal line as a function of ϕ. Graphs of the phase for c=0.1 only are given in figures 3.10 and 3.12 for $\theta^i=\pi/4$.

The most obvious change which occurs when the cylinder radius decreases is the decreasing number of fluctuations in the current magnitude as a function of ϕ.

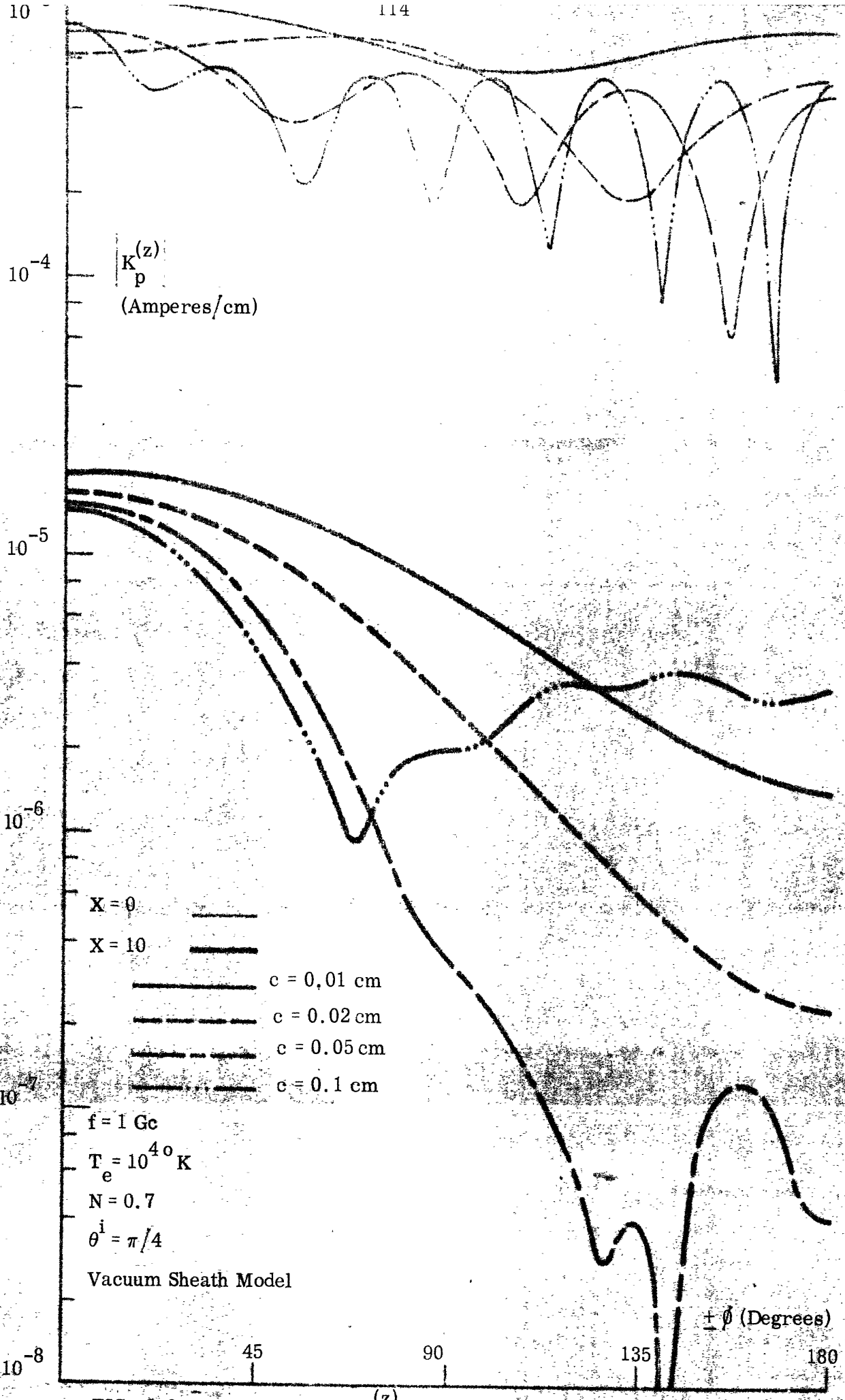

FIG. 3.9: MAGNITUDE OF $K_p^{(z)}$ vs. AZIMUTHAL ANGLE ϕ WITH CYLINDER RADIUS c A PARAMETER

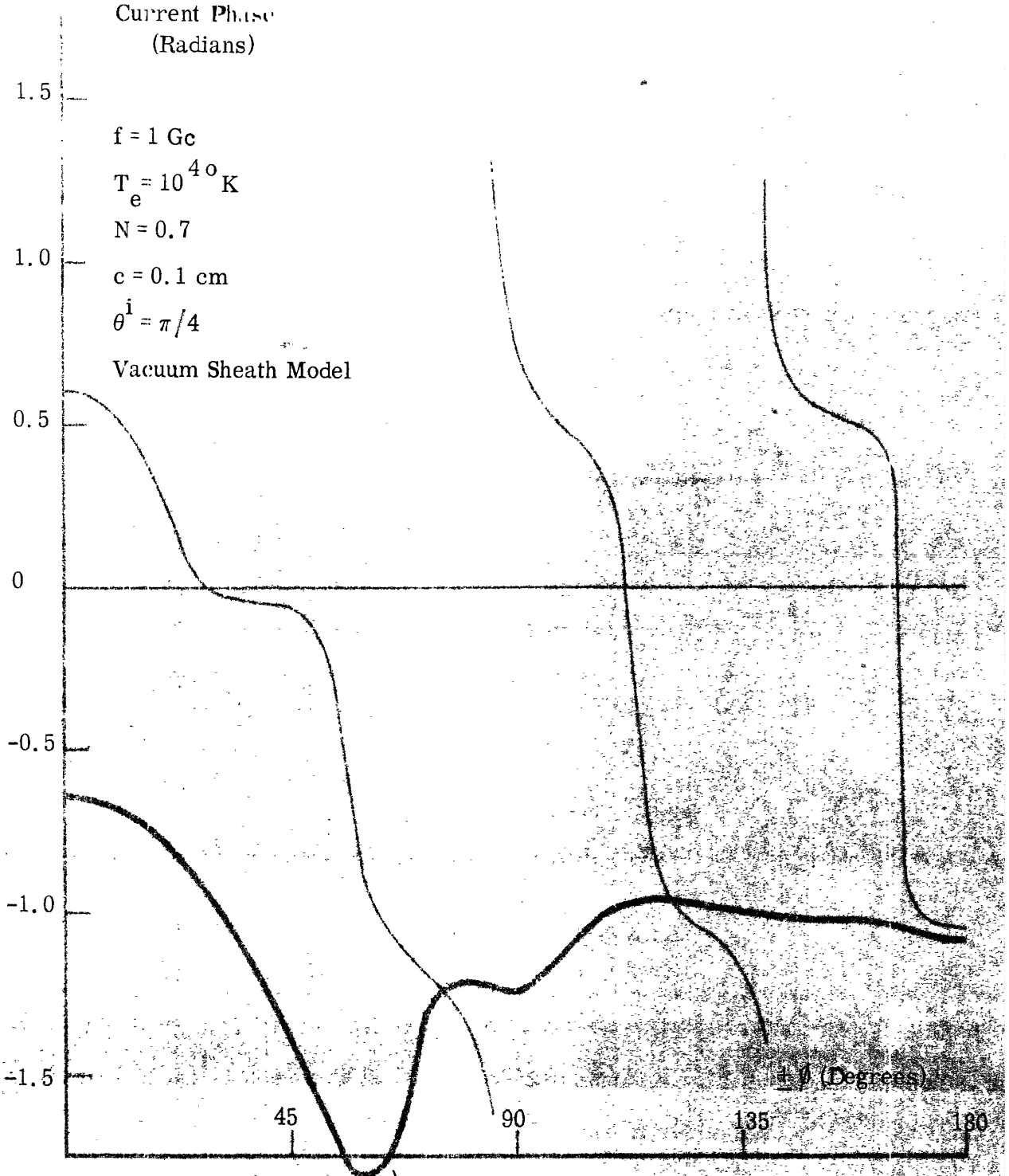

FIG. 3.10 PHASE OF $K_p^{(z)}$ vs. AZIMUTHAL ANGLE ϕ FOR CYLINDER RADIUS c = 0.1 cm

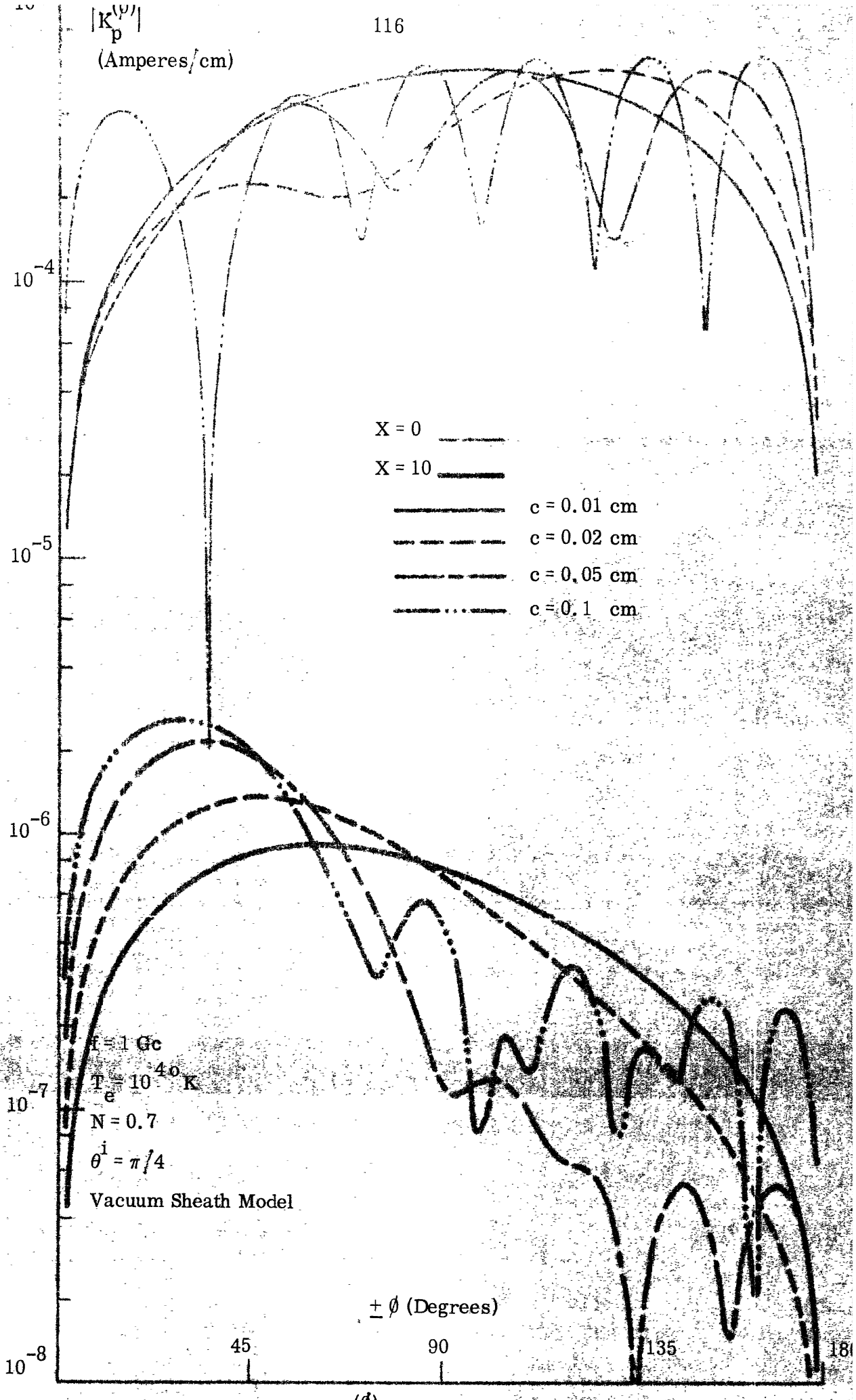

FIG. 3.11: MAGNITUDE OF $K_p^{(\phi)}$ vs. AZIMUTHAL ANGLE ϕ WITH CYLINDER RADIUS c A PARAMETER

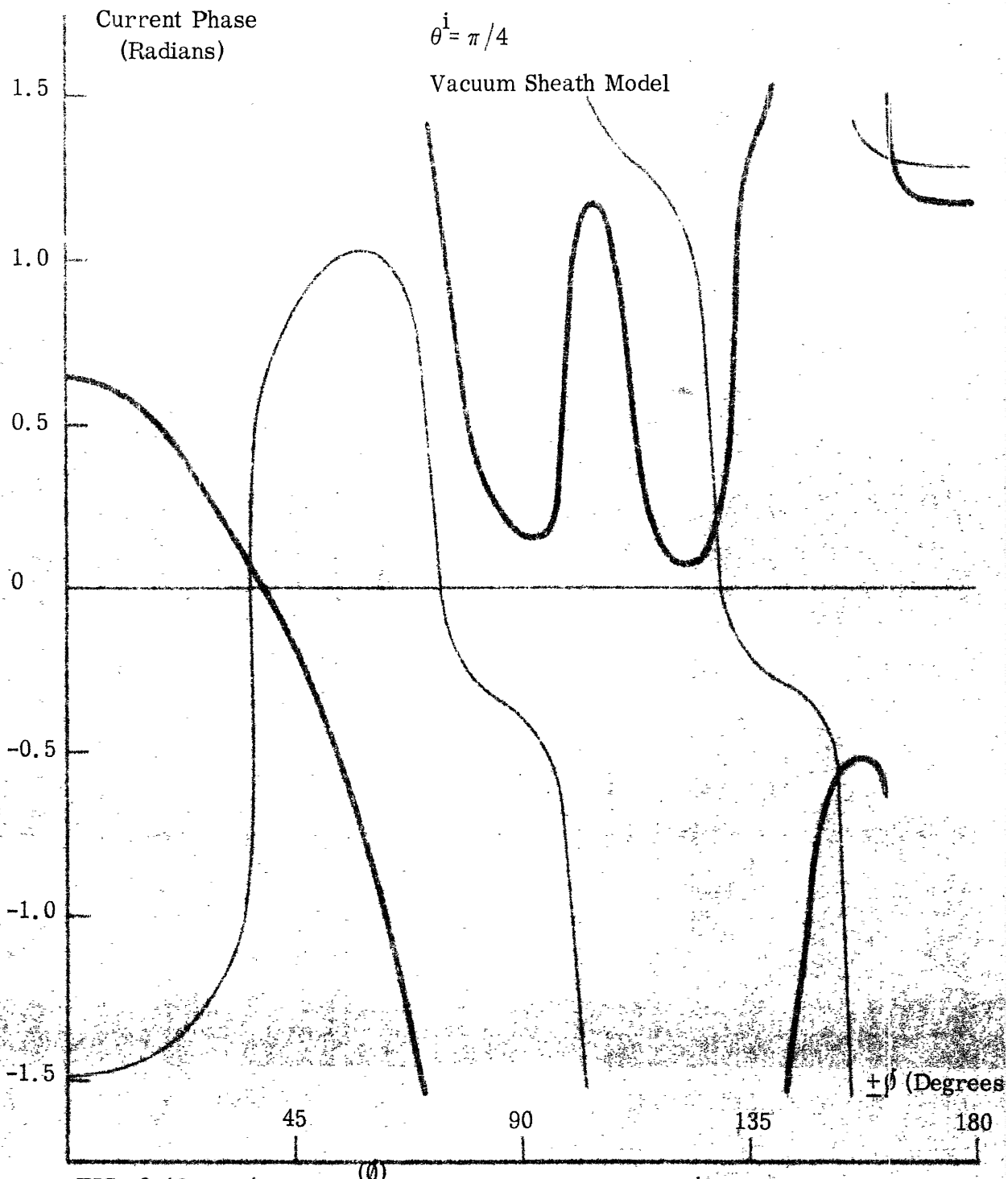

FIG. 3.12: PHASE OF $K_p^{(\phi)}$ vs. AZIMUTHAL ANGLE ϕ
FOR CYLINDER RADIUS c = 0.1 cm

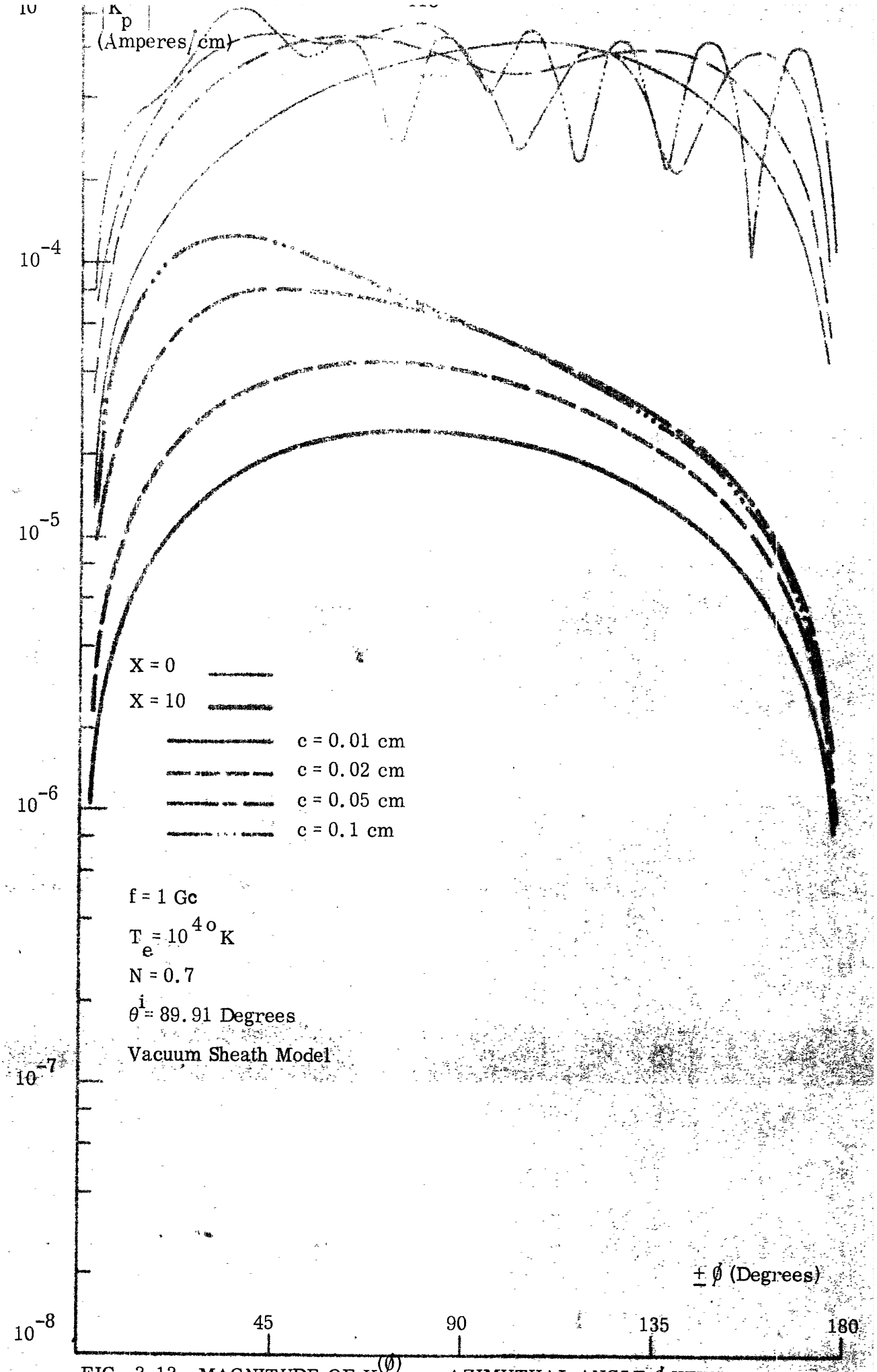

FIG. 3.13: MAGNITUDE OF $K_p^{(\phi)}$ vs. AZIMUTHAL ANGLE ϕ WITH CYLINDER RADIUS c A PARAMETER

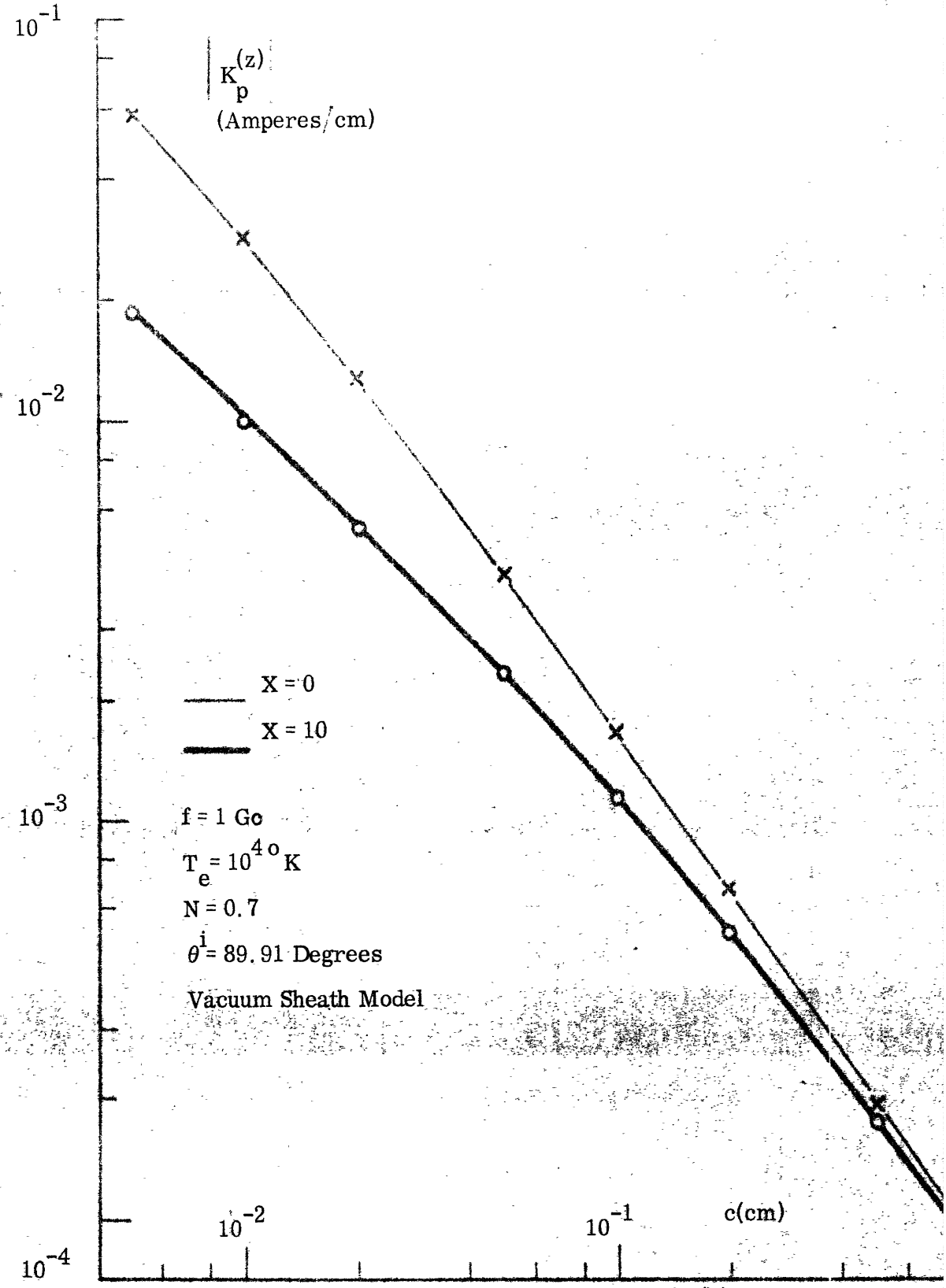

FIG. 3.14: MAGNITUDE OF MAXIMUM VALUE OF $|K_p^{(z)}|$ vs. CYLINDER RADIUS c.

This is reasonable since the cylinder circumference measured in EK wave lengths is decreasing. The attenuation caused by the vacuum sheath however, does not seem to be very sensitive to the cylinder radius. In addition the magnitude of the maximum current also seems rather insensitive to the cylinder radius, except for the z component of current when $\theta^i=\theta_s$. $K_p^{(z)}$ in that case, as shown by figure 3.14 exhibits an inverse relationship to the cylinder radius, varying with the -1 to -3/2 power of the radius, a result which can be deduced from equation (E13a.) in Appendix E. This is an interesting though perhaps not too practically useful result, since a cylinder radius less than 0.1 cm could not likely be used for the experimental measurements suggested in the introduction. In addition, this behavior occurs for only a very narrow angular interval, on the order of 5 to 10 x 10^{-3} radians (0.28 to 0.57 degrees).

The surface currents are shown as a function of the parameter N in figures 3.15 to 3.20, for the angle of incidence $\theta^i=\pi/4$ only. The currents are characterized by decreasing fluctuation as a function of ϕ and decreasing magnitude as N increases. There is also less attenuation due to the vacuum sheath with increasing N, a result to be expected, since as N increases, the EK wave length also increases and the sheath thickness to wave length ratio becomes smaller. It is interesting to note that $K_p^{(z)}$ for N larger than 0.85, exhibits an approximate exponential attenuation in the ϕ variable, characteristic of a surface wave. This occurs with or without the presence of the sheath. The same behavior will be observed as the angle of incidence is varied.

Figures 3.21 to 3.28 present the currents as the angle of incidence θ^i is

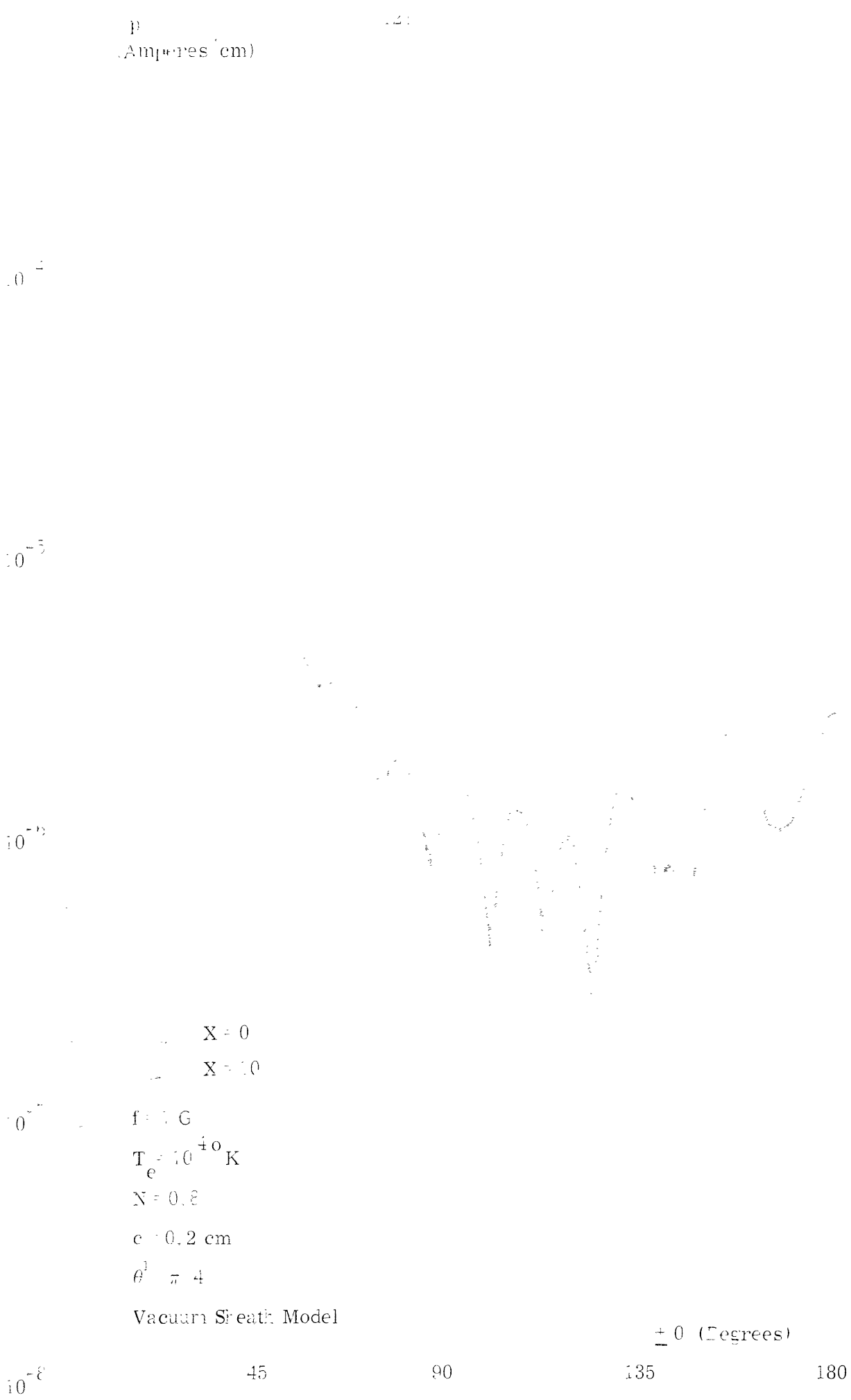

FIG. 3.15: MAGNITUDE OF $K_p^{(z)}$ VS. AZIMUTHAL ANGLE θ FOR N = 0.8 AND NOMINAL VALUES OF OTHER PARAMETERS

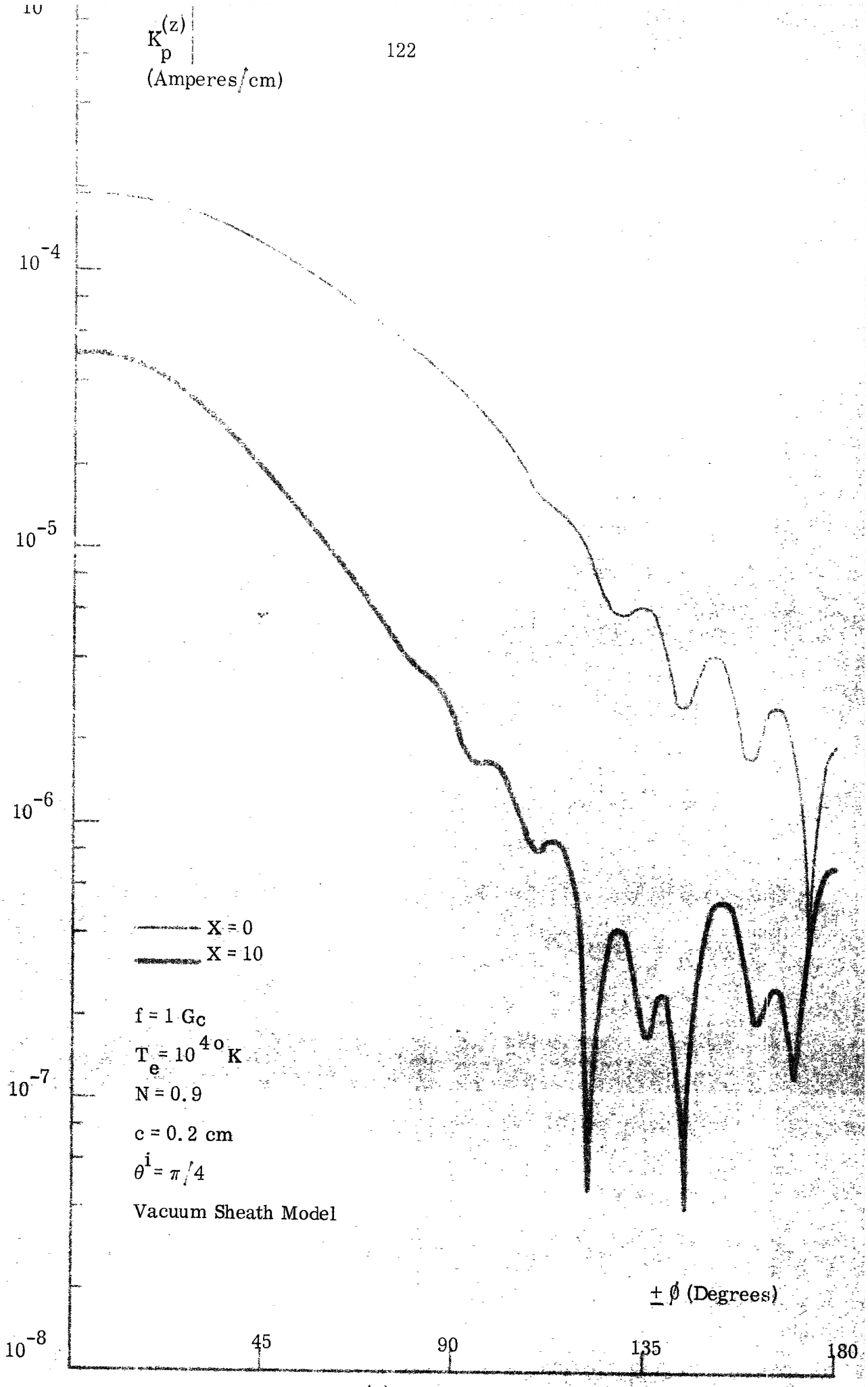

FIG. 3.16: MAGNITUDE OF $K_p^{(z)}$ vs. AZIMUTHAL ANGLE ϕ FOR N = 0.9 AND NOMINAL VALUES OF OTHER PARAMETERS.

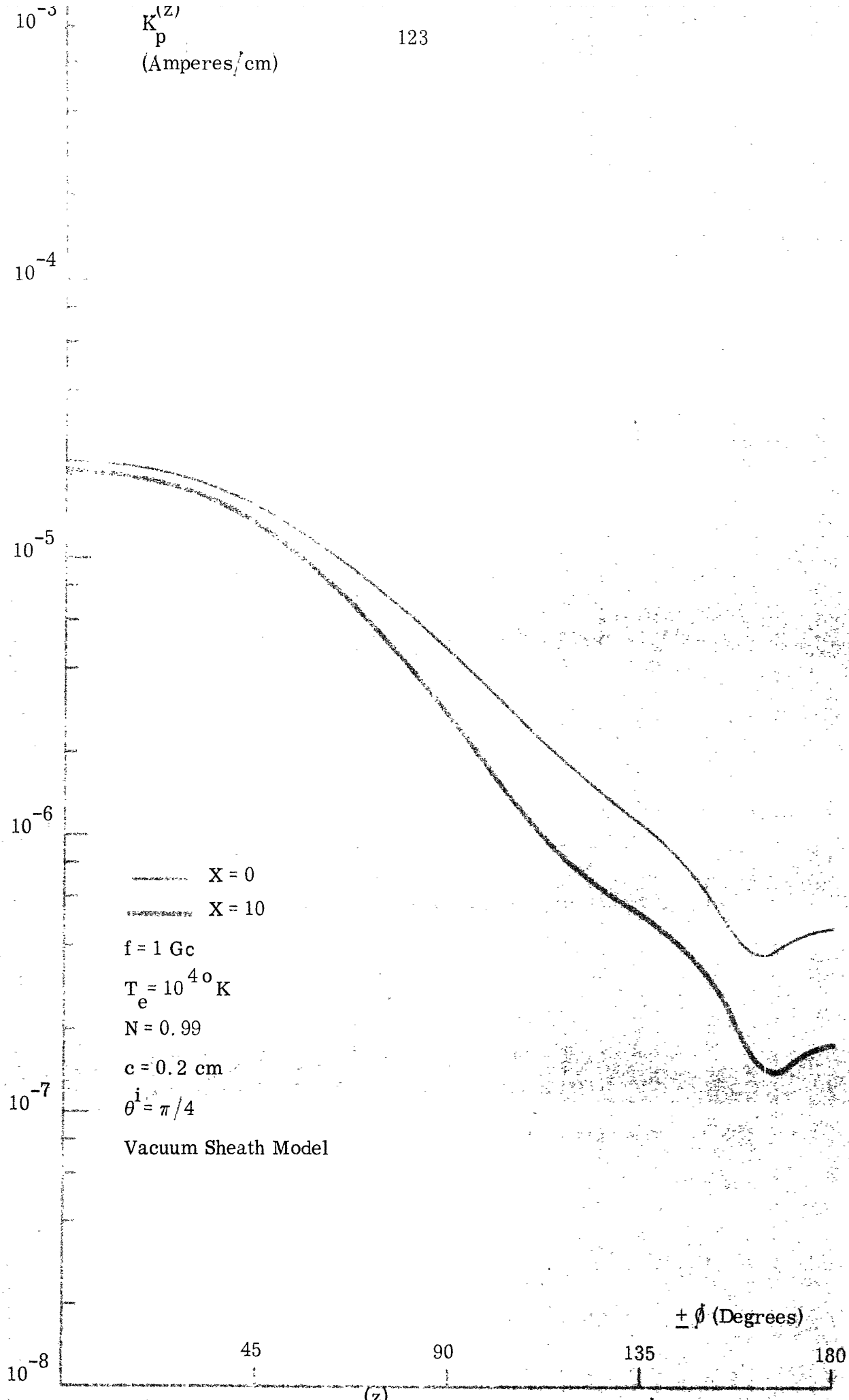

FIG. 3.17: MAGNITUDE OF $K_p^{(z)}$ vs. AZIMUTHAL ANGLE ϕ FOR N = 0.99 AND NOMINAL VALUES OF OTHER PARAMETERS

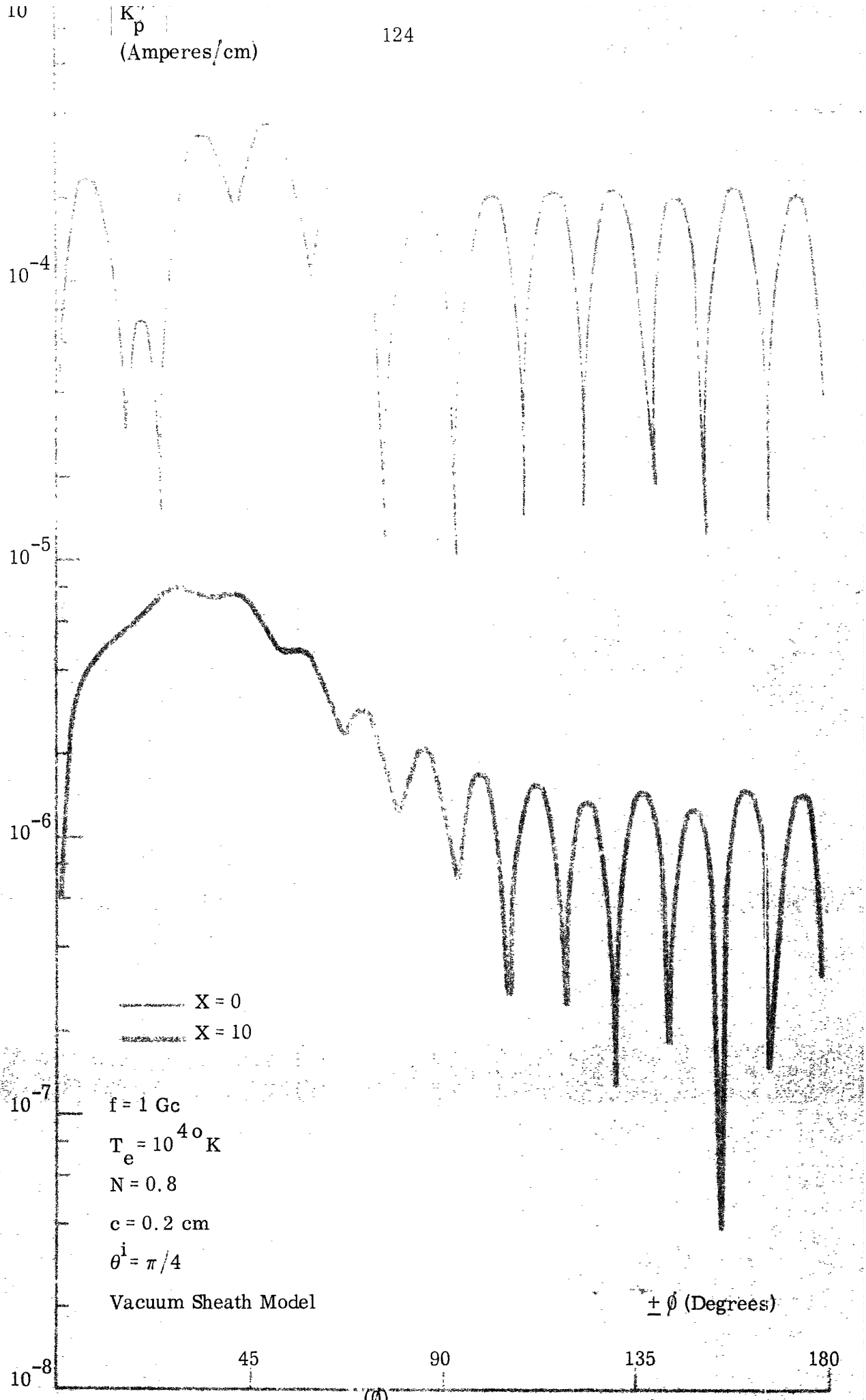

FIG. 3.18: MAGNITUDE OF $K_p^{(\phi)}$ vs. AZIMUTHAL ANGLE ϕ FOR N = 0.8 AND NOMINAL VALUES OF OTHER PARAMETERS

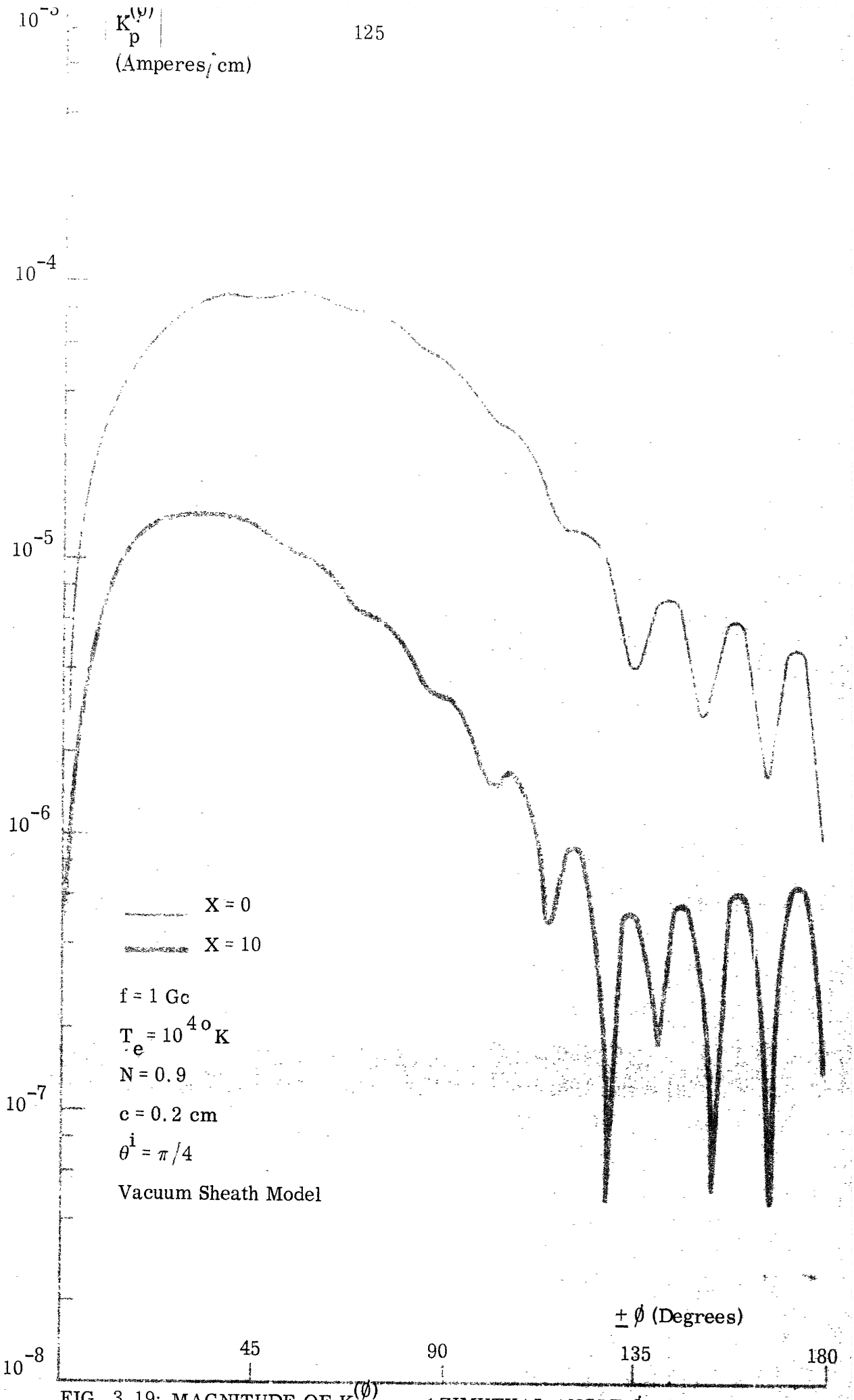

FIG. 3.19: MAGNITUDE OF $K_p^{(\phi)}$ vs. AZIMUTHAL ANGLE ϕ FOR N = 0.9 AND NOMINAL VALUES OF OTHER PARAMETERS

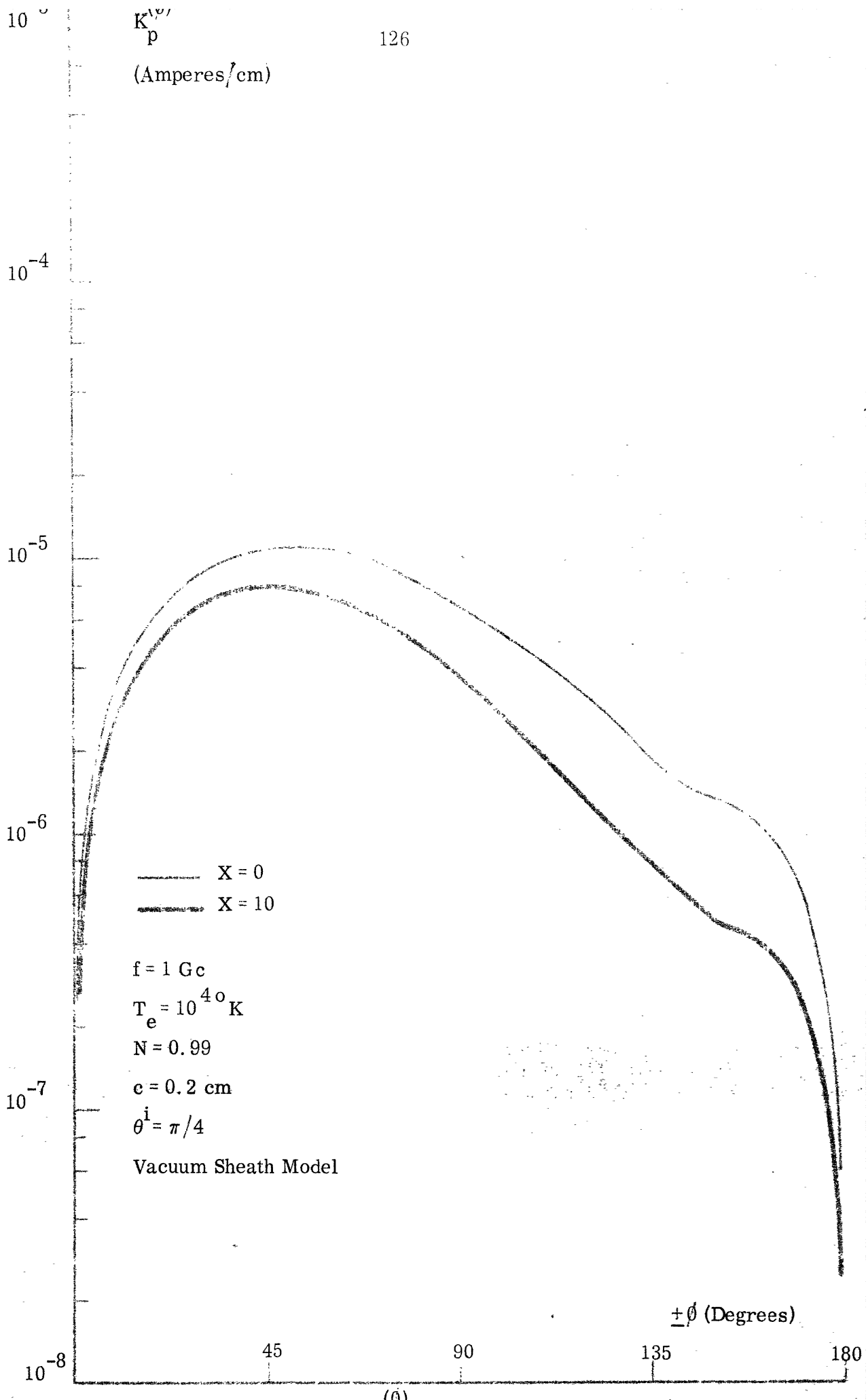

FIG. 3.20: MAGNITUDE OF $K_p^{(\phi)}$ vs. AZIMUTHAL ANGLE ϕ FOR N = 0.99 AND NOMINAL VALUES OF OTHER PARAMETERS

varied in steps of 0.1π from 0.05π to 0.45π. There is generally an increase in the fluctuation of the current magnitude as a function of ϕ with increasing angle of incidence. Also, the attenuation of the maximum current value caused by the vacuum sheath is observed to decrease with increasing angle of incidence. An exponential decrease in $K_p^{(z)}$ as a function of ϕ is observed, for $\theta^i = .45\pi$, again exhibiting a behavior characteristic of a surface wave. $K_p^{(\phi)}$ for this angle of incidence also has an exponential attenuation with ϕ after the maximum value is reached at about $\phi = 20^o$ to 25^o.

There is an additional graph given in figure 3.29 which shows the maximum value of $|K_p^{(z)}|$ for the sheathless case as a function of the angle of incidence on a logarithmic scale, measured from normal incidence. The maximum in $|K_p^{(z)}|$ occurred generally near $\phi = 0$. There is a narrow spike in this curve centered about the angle where $\theta^i = \theta_c^i$. This is caused by the leading term in the Fourier series for $K_p^{(z)}$. No similar peaking occurs for $K_p^{(\phi)}$.

The results for the final parameter variation, that of the sheath thickness expressed in D_ℓ, are shown in figures 3.30 to 3.35 for $\theta^i = \pi/20$, $\pi/4$ and θ_s. The curves for the first two angles of incidence generally show a reduction in amplitude and ϕ variation with increasing sheath thickness. For sheaths of 2 and 5 D_ℓ in thickness, and $\theta^i = \pi/20$, there is however increased ϕ variation in the currents, and at some angles they exceed the sheathless values. The currents for $\theta^i = \theta_s$ are reduced much less in amplitude with increasing sheath thickness, though there is a decrease in the ϕ variation of $K_p^{(\phi)}$ at this angle of incidence also.

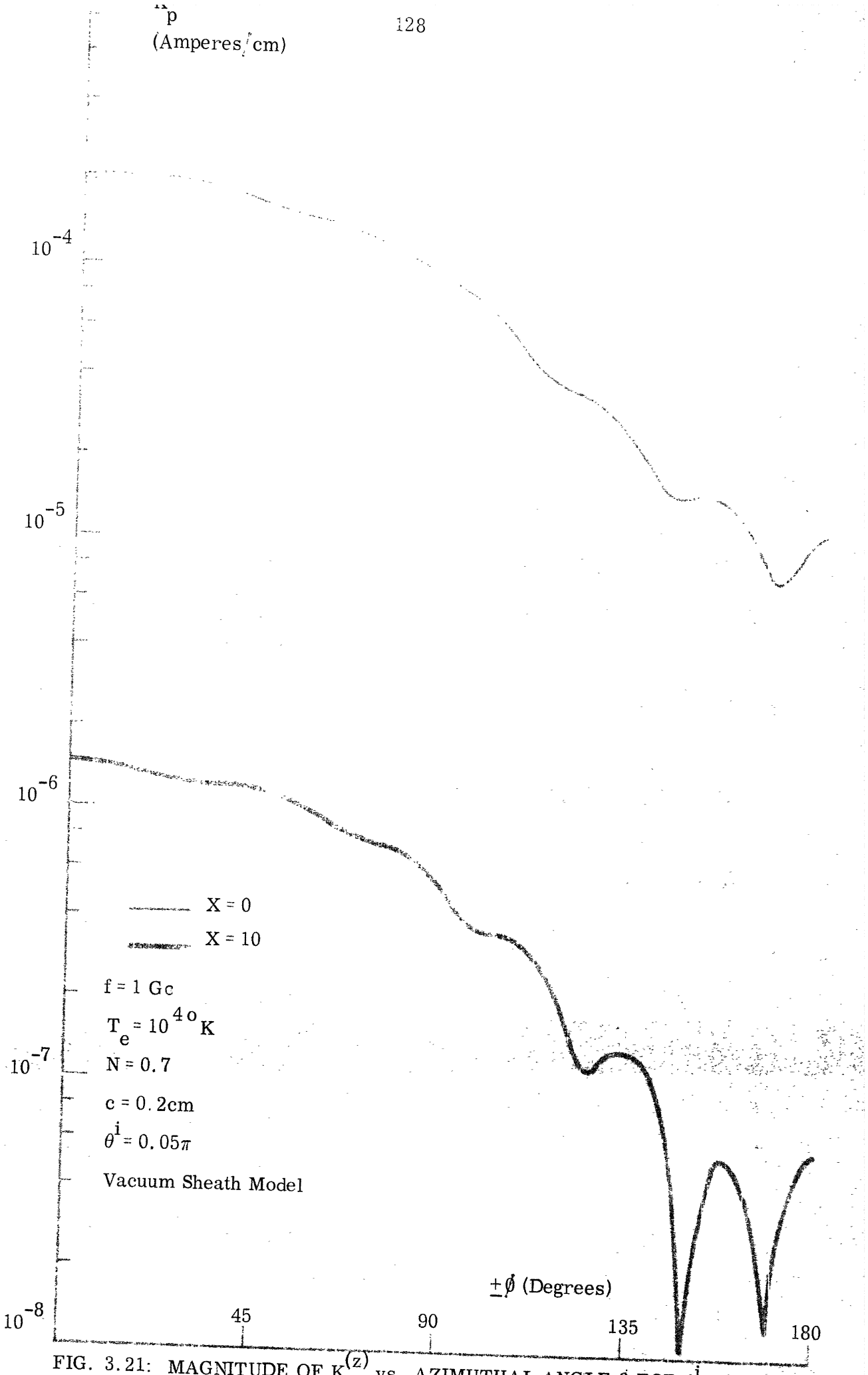

FIG. 3.21: MAGNITUDE OF $K_p^{(z)}$ vs. AZIMUTHAL ANGLE ϕ FOR $\theta^i = 0.05\pi$ AND NOMINAL VALUES OF OTHER PARAMETERS

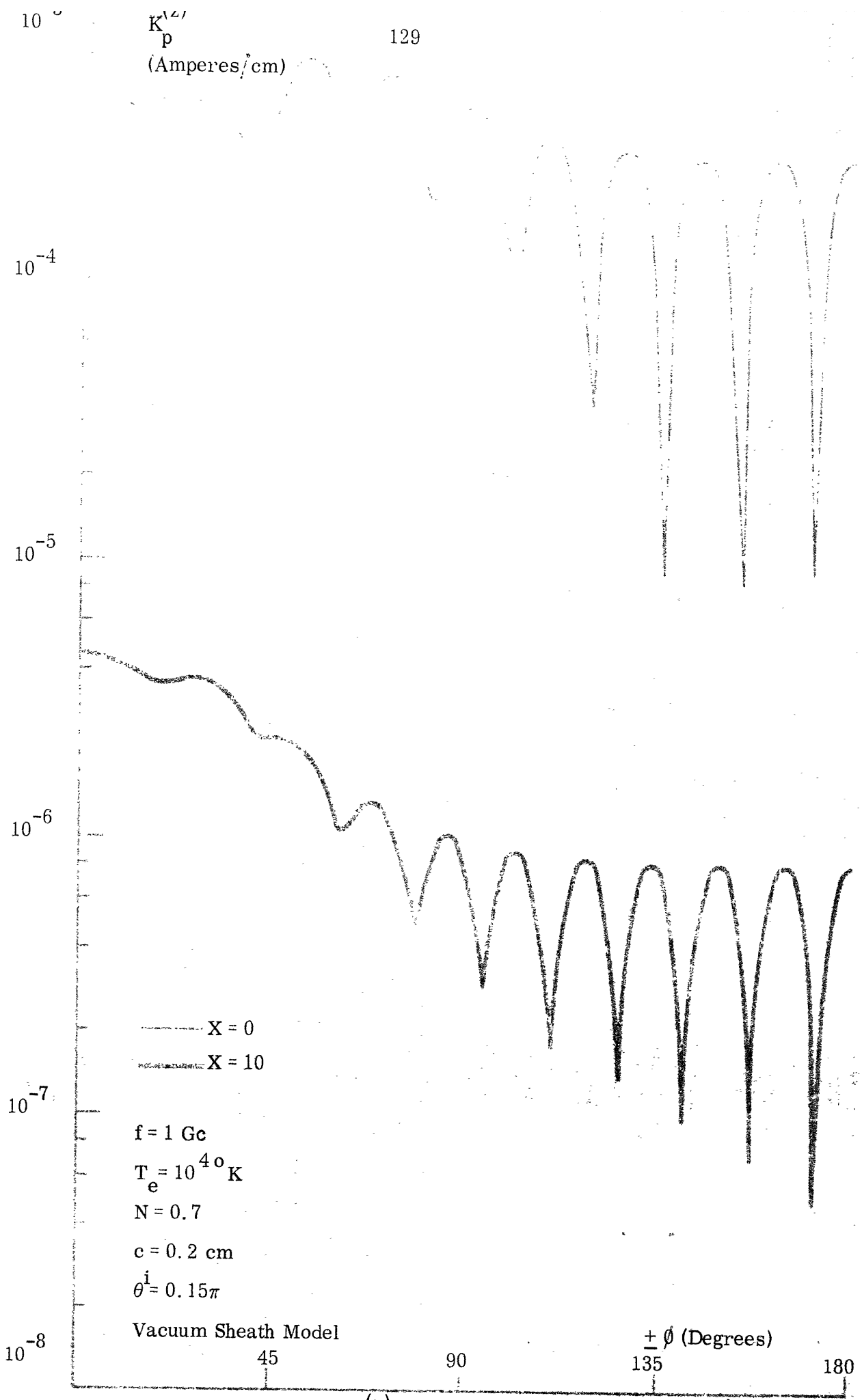

FIG. 3.22: MAGNITUDE OF $K_p^{(z)}$ vs. AZIMUTHAL ANGLE $\emptyset$ FOR $\theta^i = 0.15\pi$ AND NOMINAL VALUES OF OTHER PARAMETERS

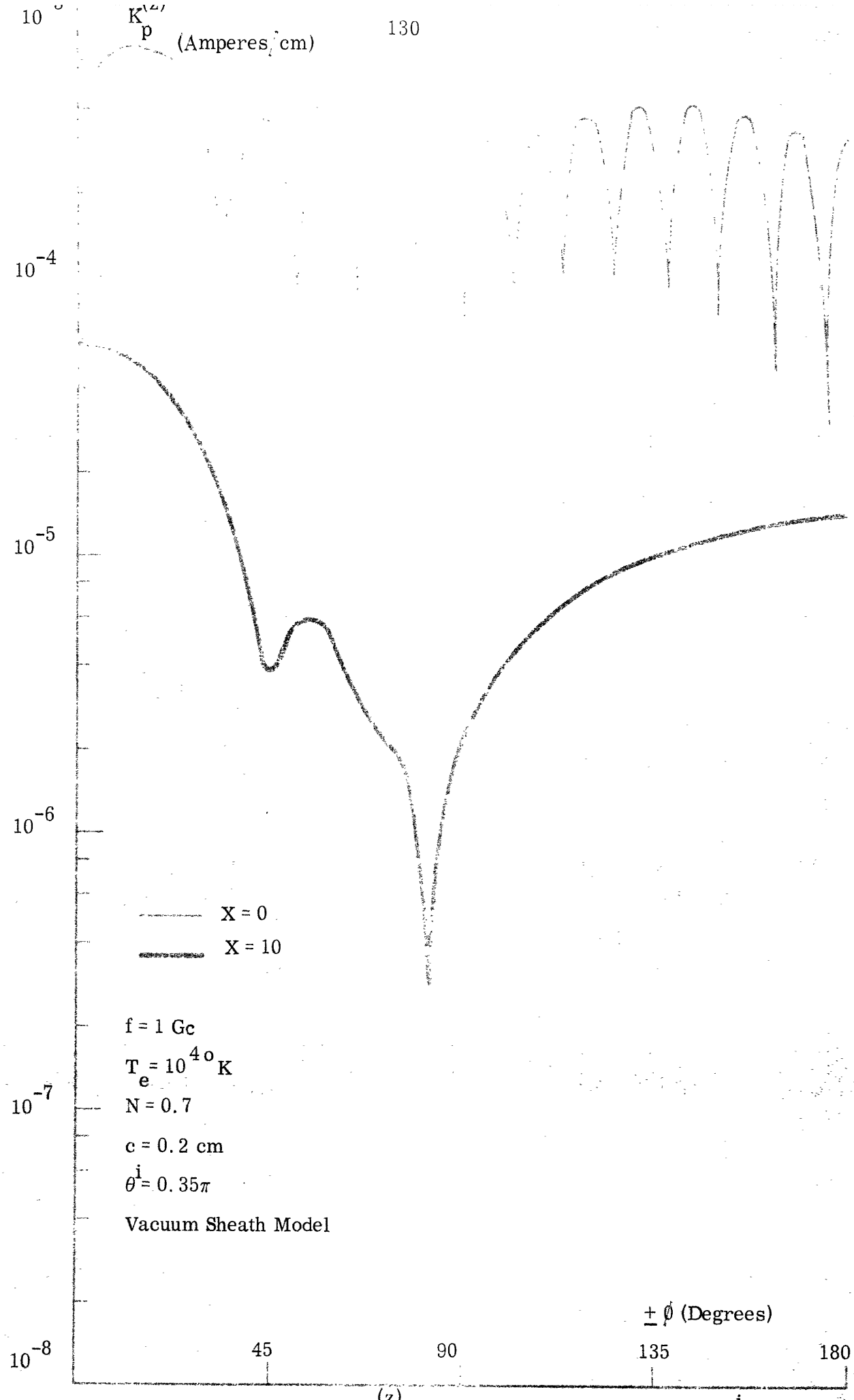

FIG. 3.23: MAGNITUDE OF $K_p^{(z)}$ vs. AZIMUTHAL ANGLE ϕ FOR $\theta^i = 0.35\pi$ AND NOMINAL VALUES OF OTHER PARAMETERS

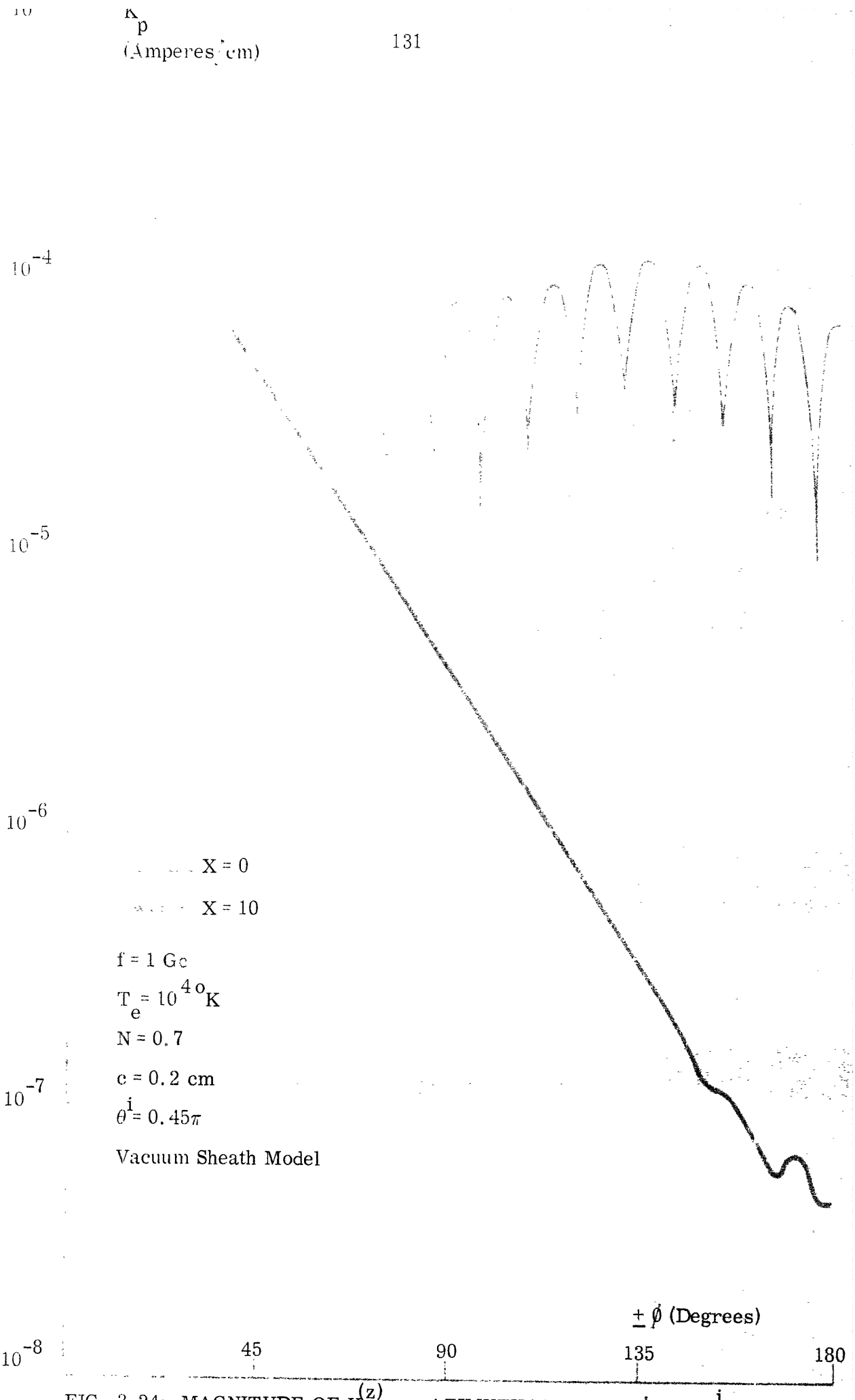

FIG. 3.24: MAGNITUDE OF $K_p^{(z)}$ vs. AZIMUTHAL ANGLE ϕ FOR $\theta^i = 0.45\pi$ AND NOMINAL VALUES OF OTHER PARAMETERS

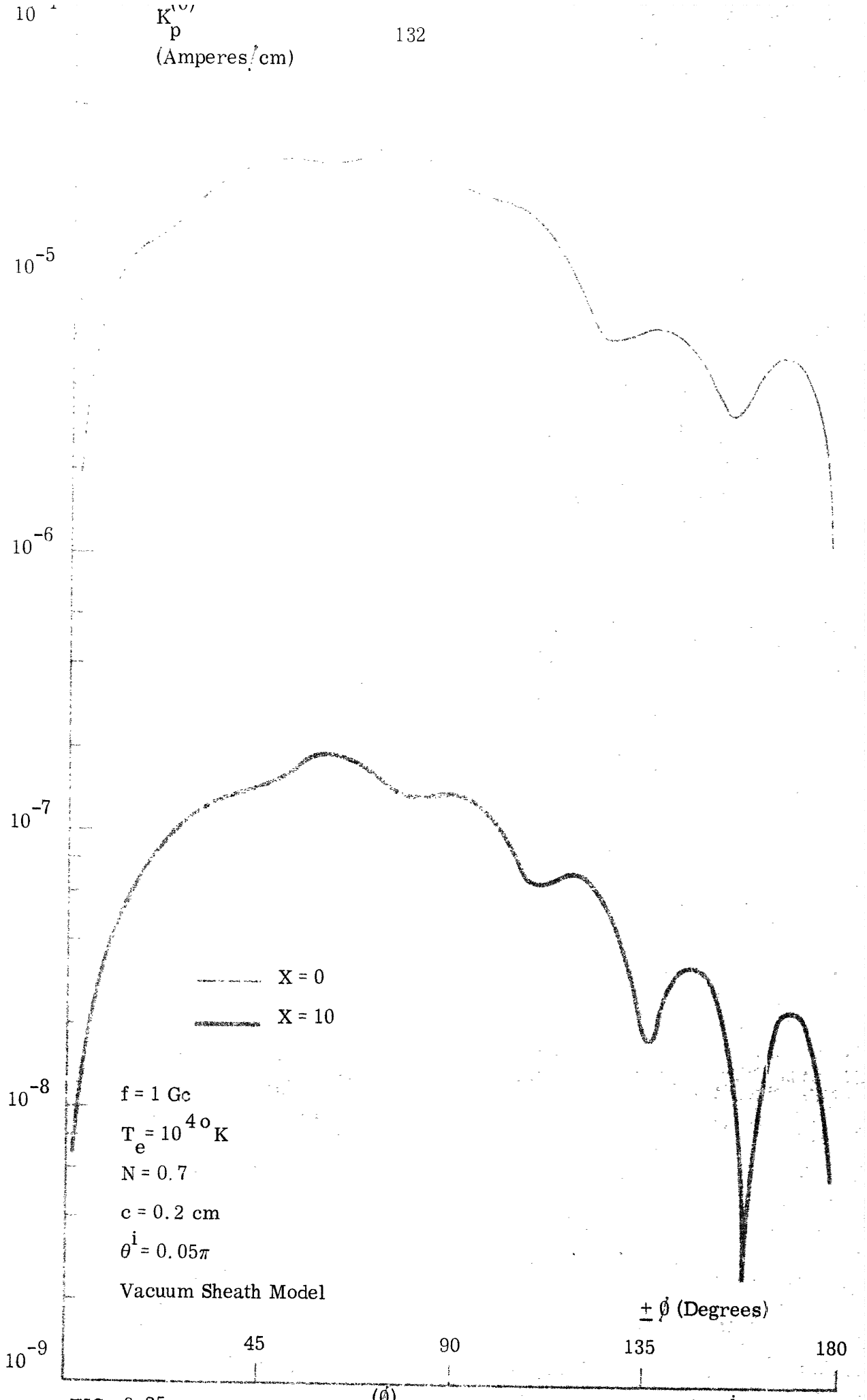

FIG. 3.25: MAGNITUDE OF $K_p^{(\phi)}$ vs. AZIMUTHAL ANGLE ϕ FOR $\theta^i = 0.05\pi$ AND NOMINAL VALUES OF OTHER PARAMETERS

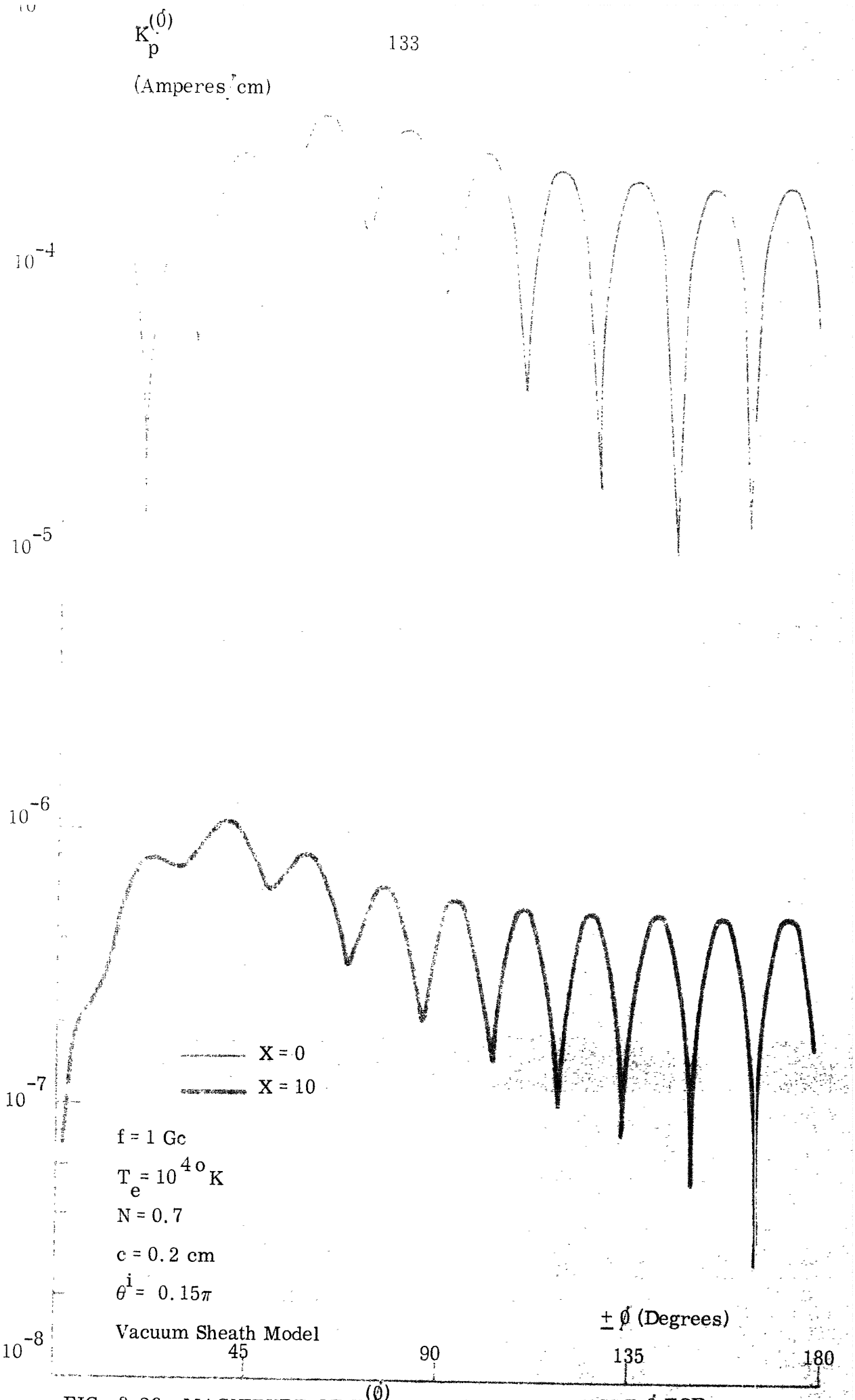

FIG. 3.26: MAGNITUDE OF $K_p^{(\phi)}$ vs. AZIMUTHAL ANGLE ϕ FOR $\theta^i = 0.15\pi$ AND NOMINAL VALUES OF OTHER PARAMETERS

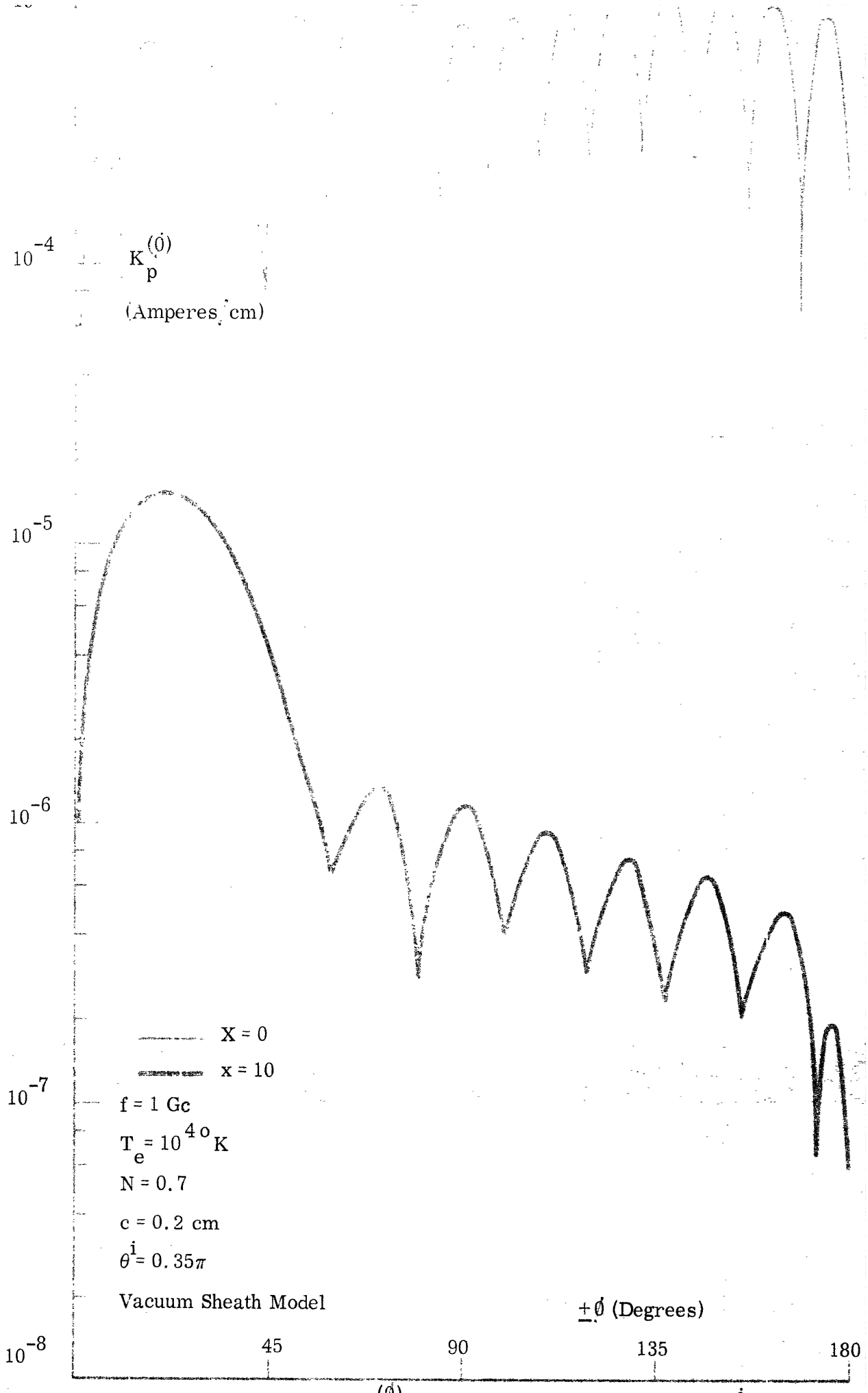

FIG. 3.27: MAGNITUDE OF $K_p^{(\phi)}$ vs. AZIMUTHAL ANGLE ϕ FOR $\theta^i = 0.35\pi$ AND NOMINAL VALUES OF OTHER PARAMETERS

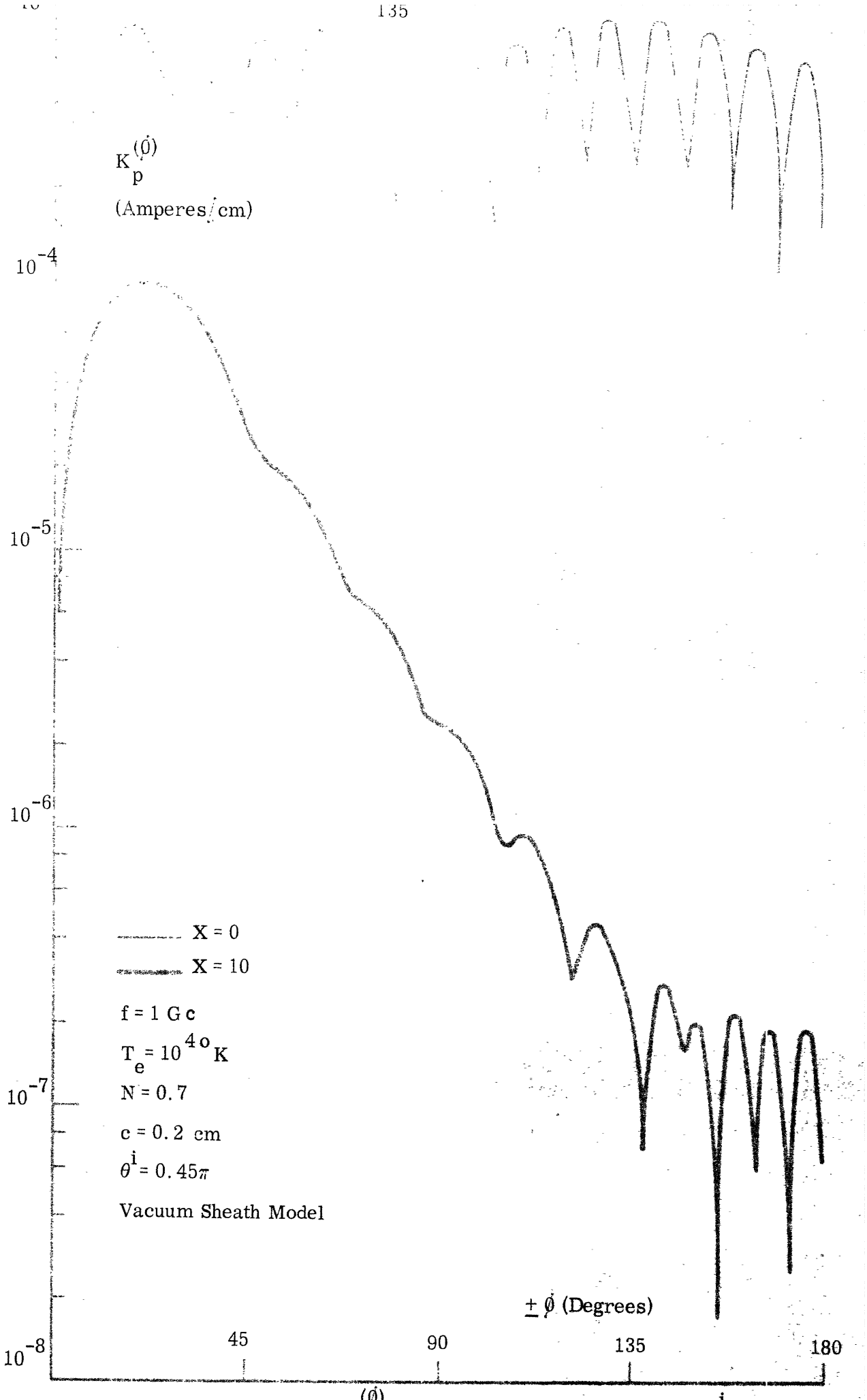

FIG. 3.28: MAGNITUDE OF $K_p^{(\phi)}$ vs. AZIMUTHAL ANGLE ϕ FOR $\theta^i = 0.45\pi$ AND NOMINAL VALUES OF OTHER PARAMETERS

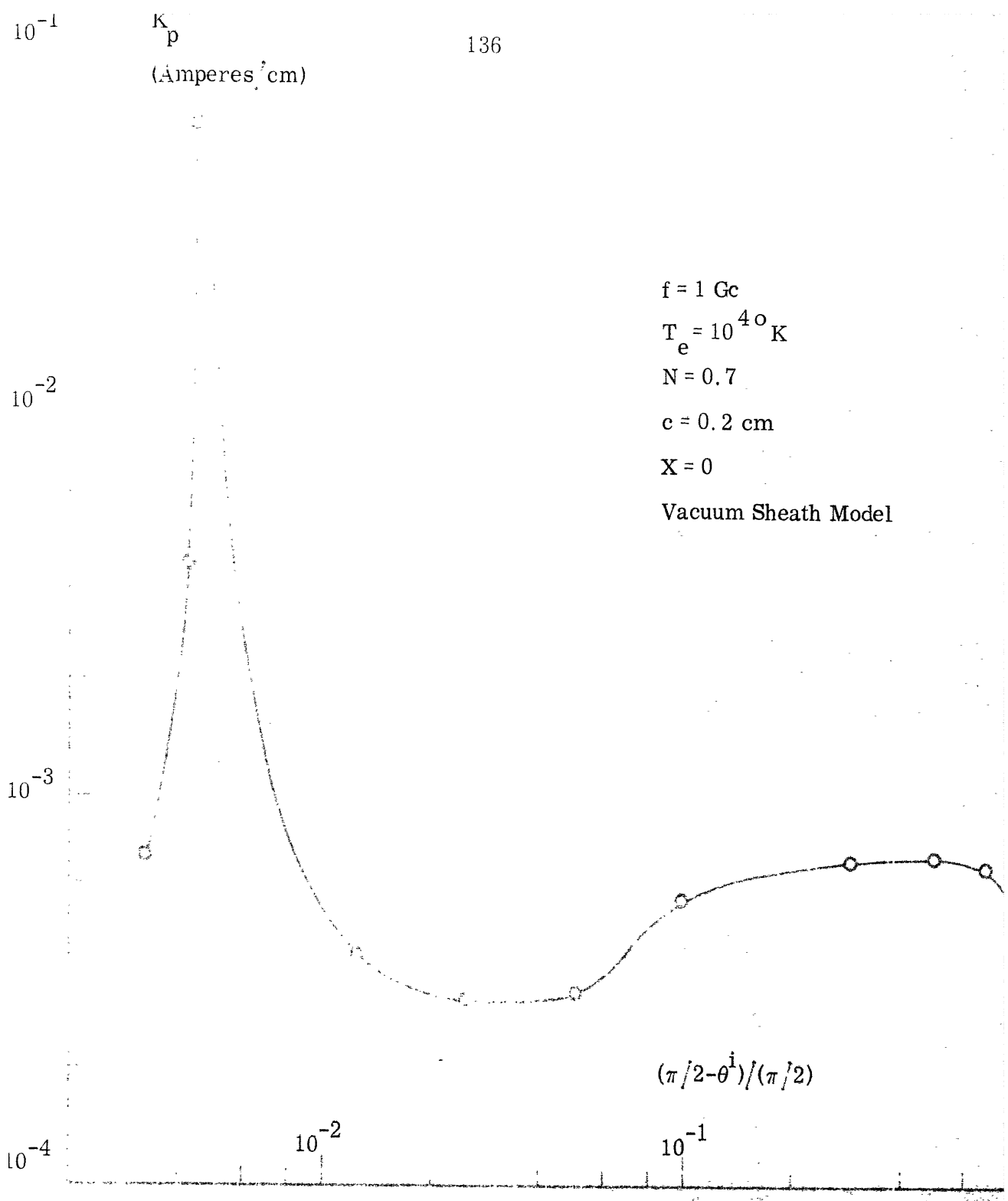

FIG. 3.29: MAGNITUDE OF MAXIMUM VALUE OF $|K_p^{(z)}|$ AS A FUNCTION OF ANGLE OF INCIDENCE AND NOMINAL VALUES OF OTHER PARAMETERS

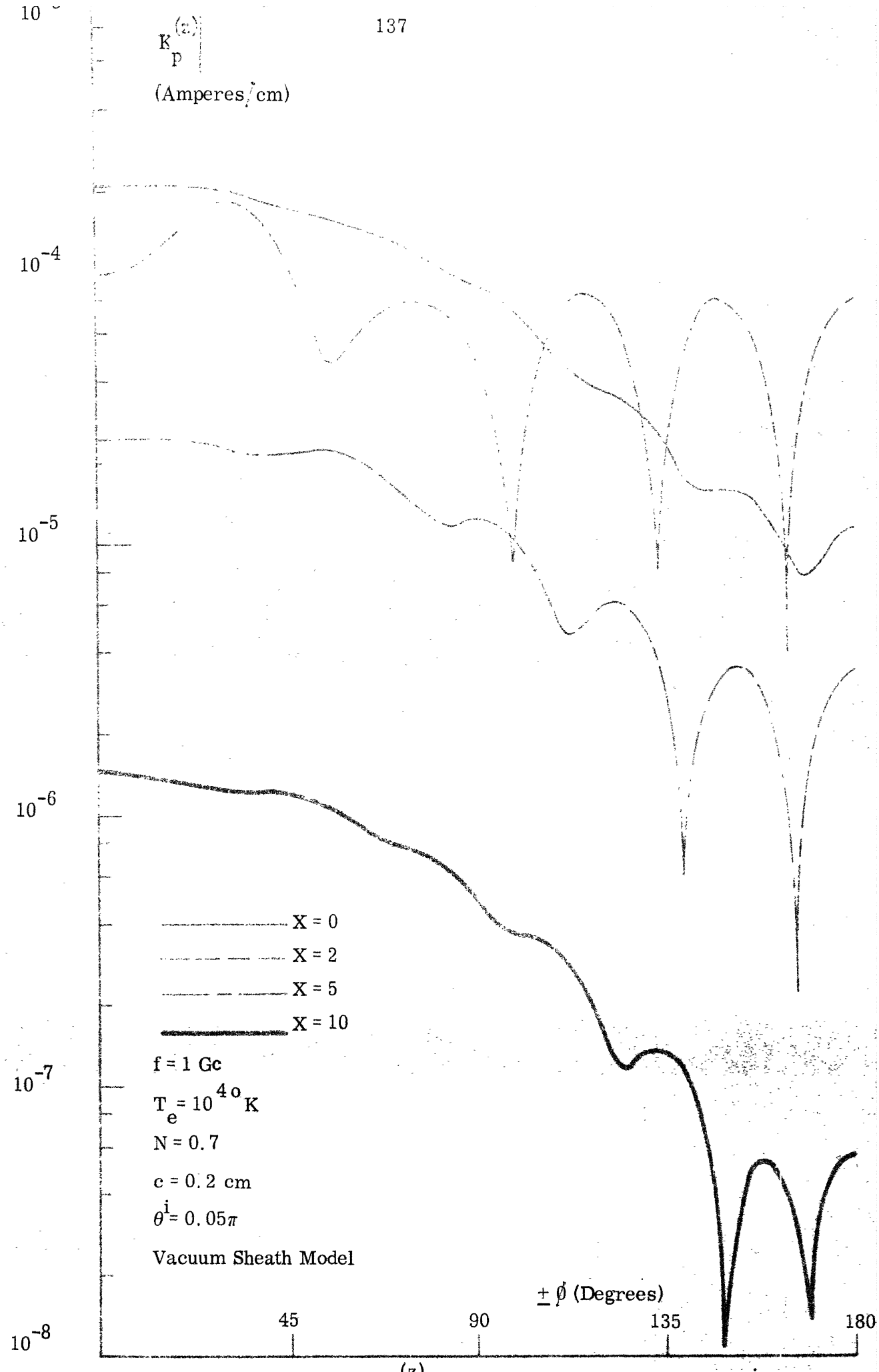

FIG. 3.30a: MAGNITUDE OF $K_p^{(z)}$ vs. AZIMUTHAL ANGLE ϕ FOR $\theta^i = 0.05\pi$ AND SHEATH THICKNESS X A PARAMETER

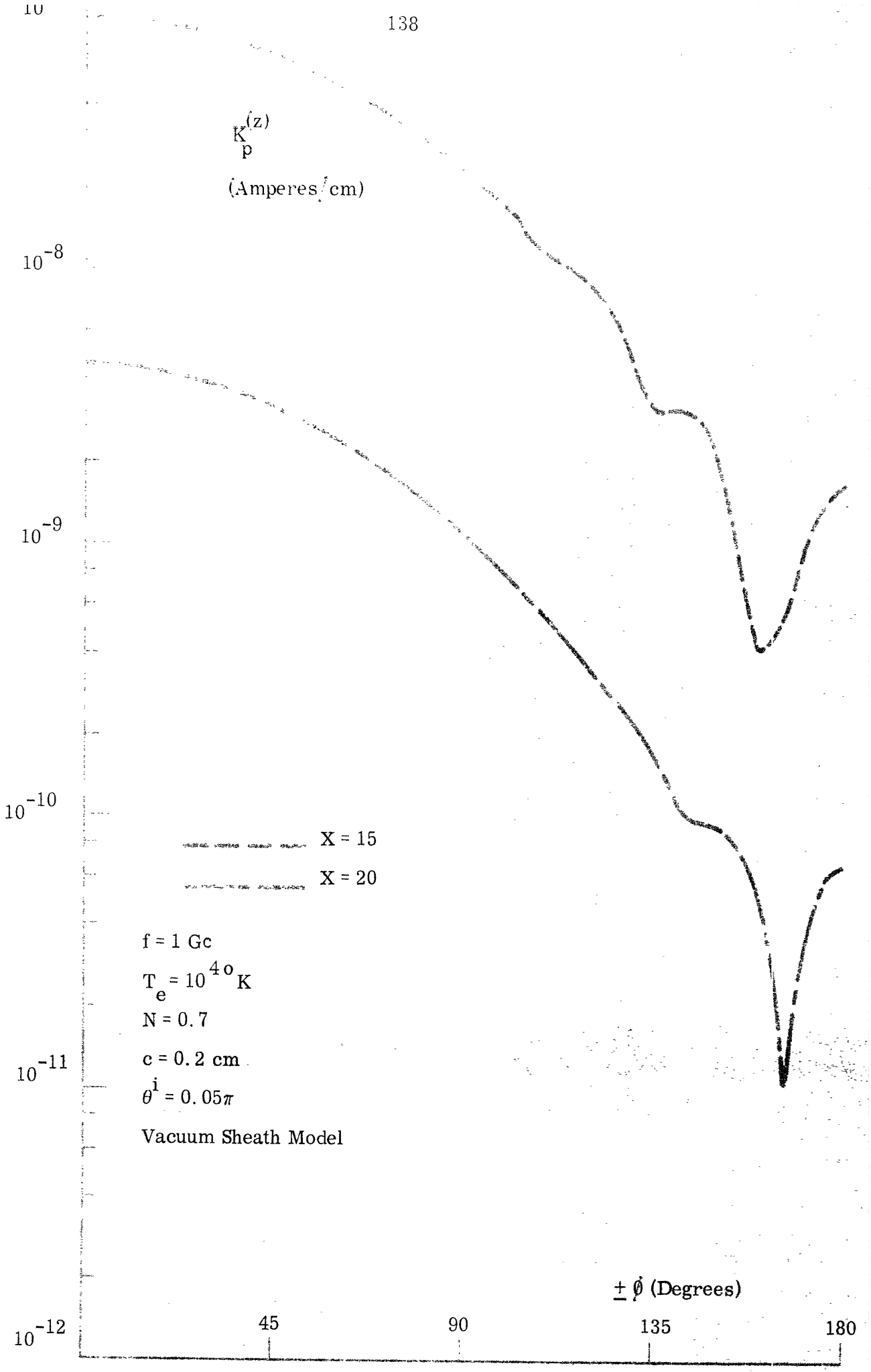

FIG. 3.30b: MAGNITUDE OF $K_p^{(z)}$ vs. AZIMUTHAL ANGLE ϕ FOR $\theta^i = 0.05\pi$ AND SHEATH THICKNESS X A PARAMETER

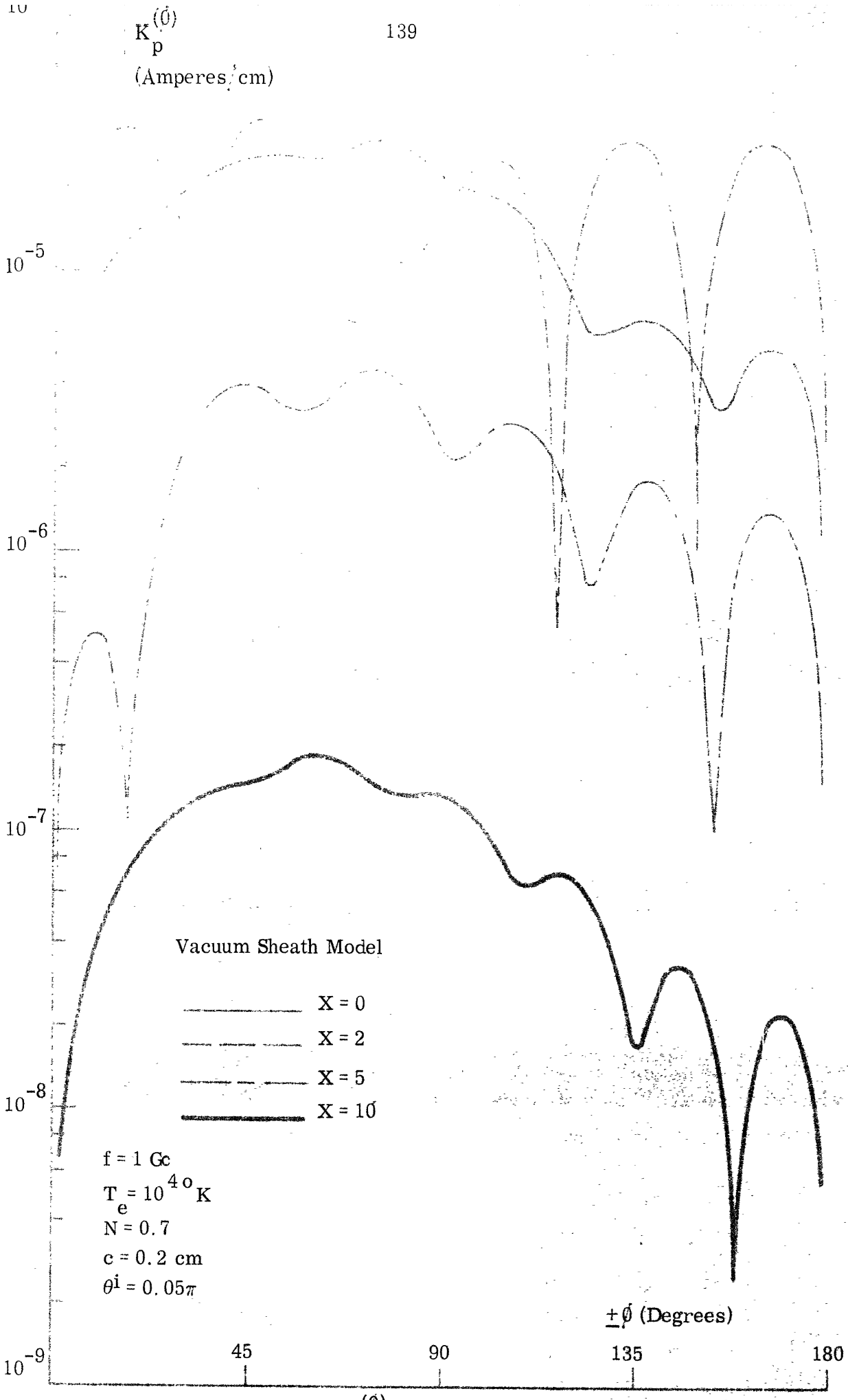

FIG. 3.31a: MAGNITUDE OF $K_p^{(\phi)}$ vs. AZIMUTHAL ANGLE ϕ FOR $\theta^i = 0.05\pi$ AND SHEATH THICKNESS X A PARAMETER

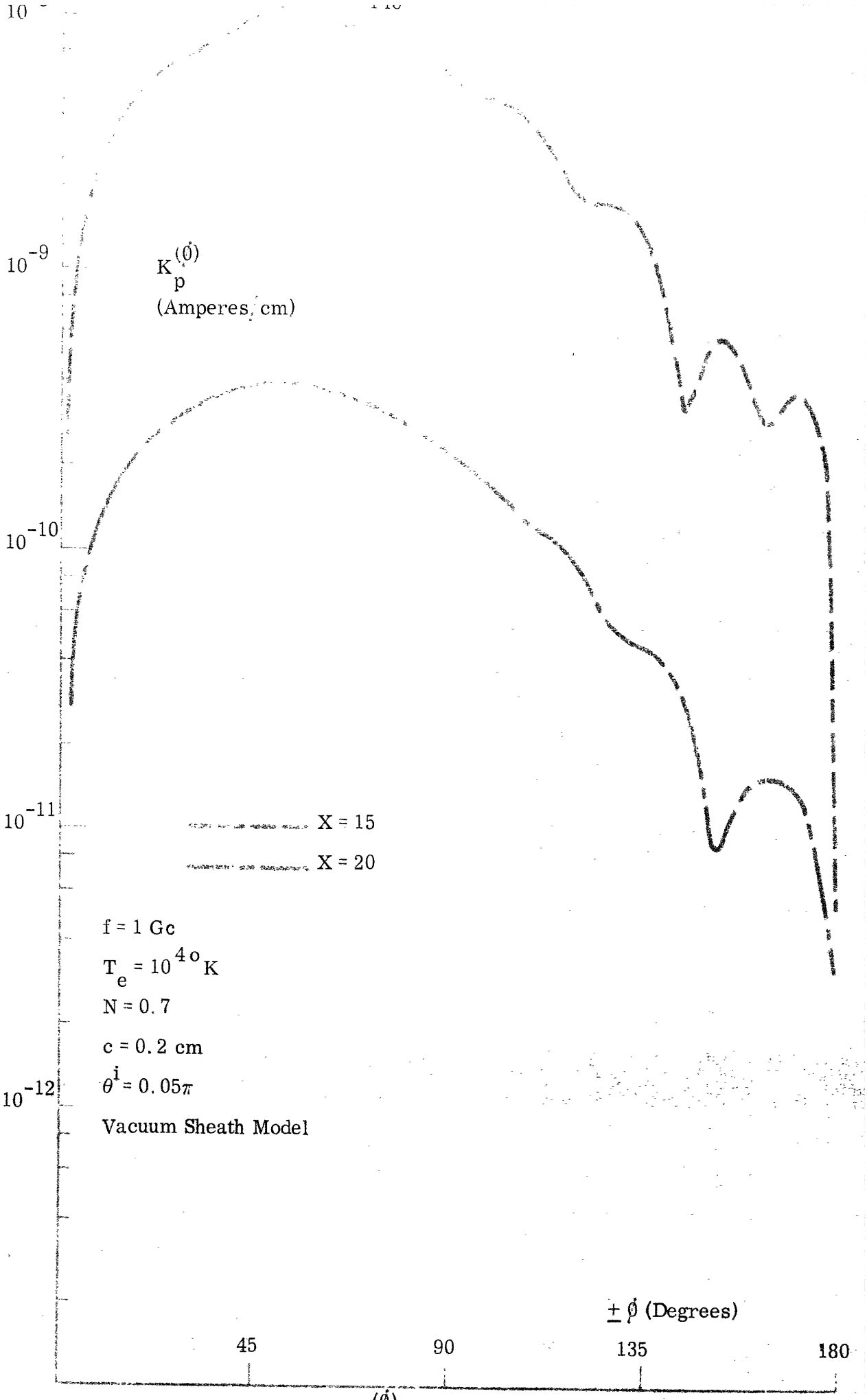

FIG. 3.3lb: MAGNITUDE OF $K_p^{(\phi)}$ vs. AZIMUTHAL ANGLE ϕ FOR $\theta^i = 0.05\pi$ AND SHEATH THICKNESS X A PARAMETER

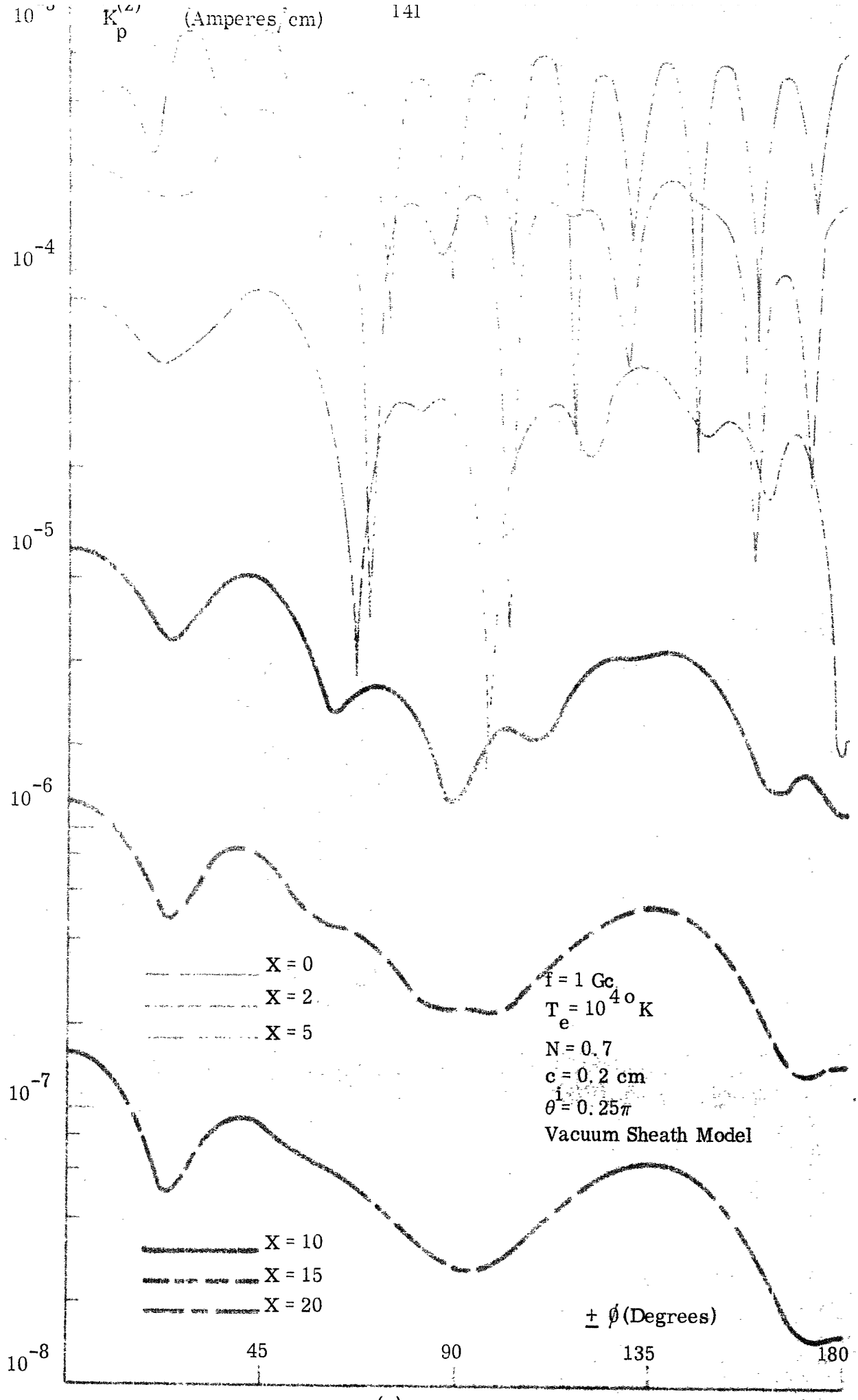

FIG. 3.32: MAGNITUDE OF $K_p^{(z)}$ vs. AZIMUTHAL ANGLE ϕ FOR $\theta^i = 0.25\pi$ AND SHEATH THICKNESS X A PARAMETER

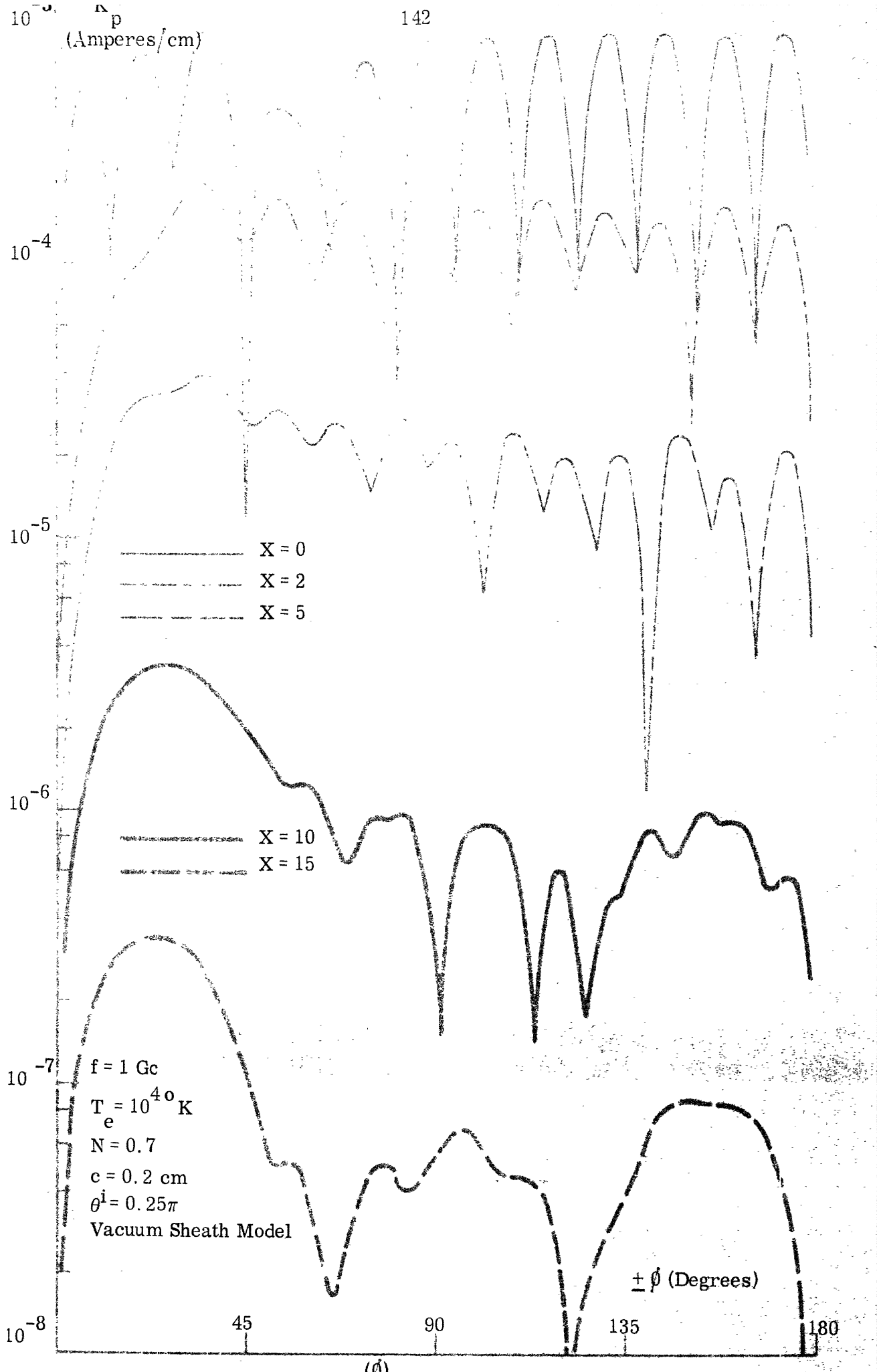

FIG. 3.33a: MAGNITUDE OF $K_p^{(\phi)}$ vs. AZIMUTHAL ANGLE ϕ FOR $\theta^i = 0.25\pi$ AND SHEATH THICKNESS X A PARAMETER

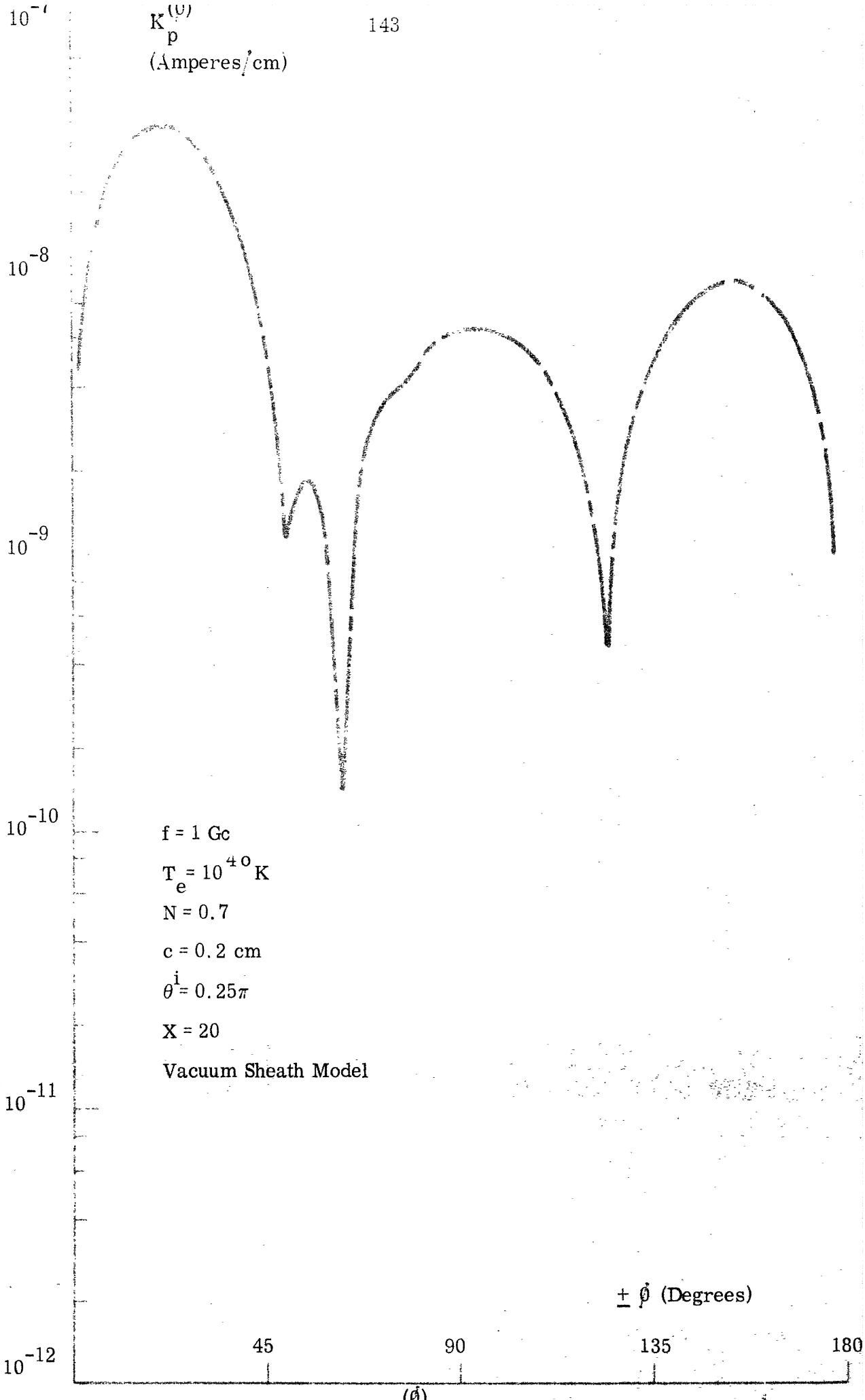

FIG. 3.33b: MAGNITUDE OF $K_p^{(\phi)}$ vs. AZIMUTHAL ANGLE ϕ FOR $\theta^i = 0.25\pi$ AND SHEATH THICKNESS X A PARAMETER

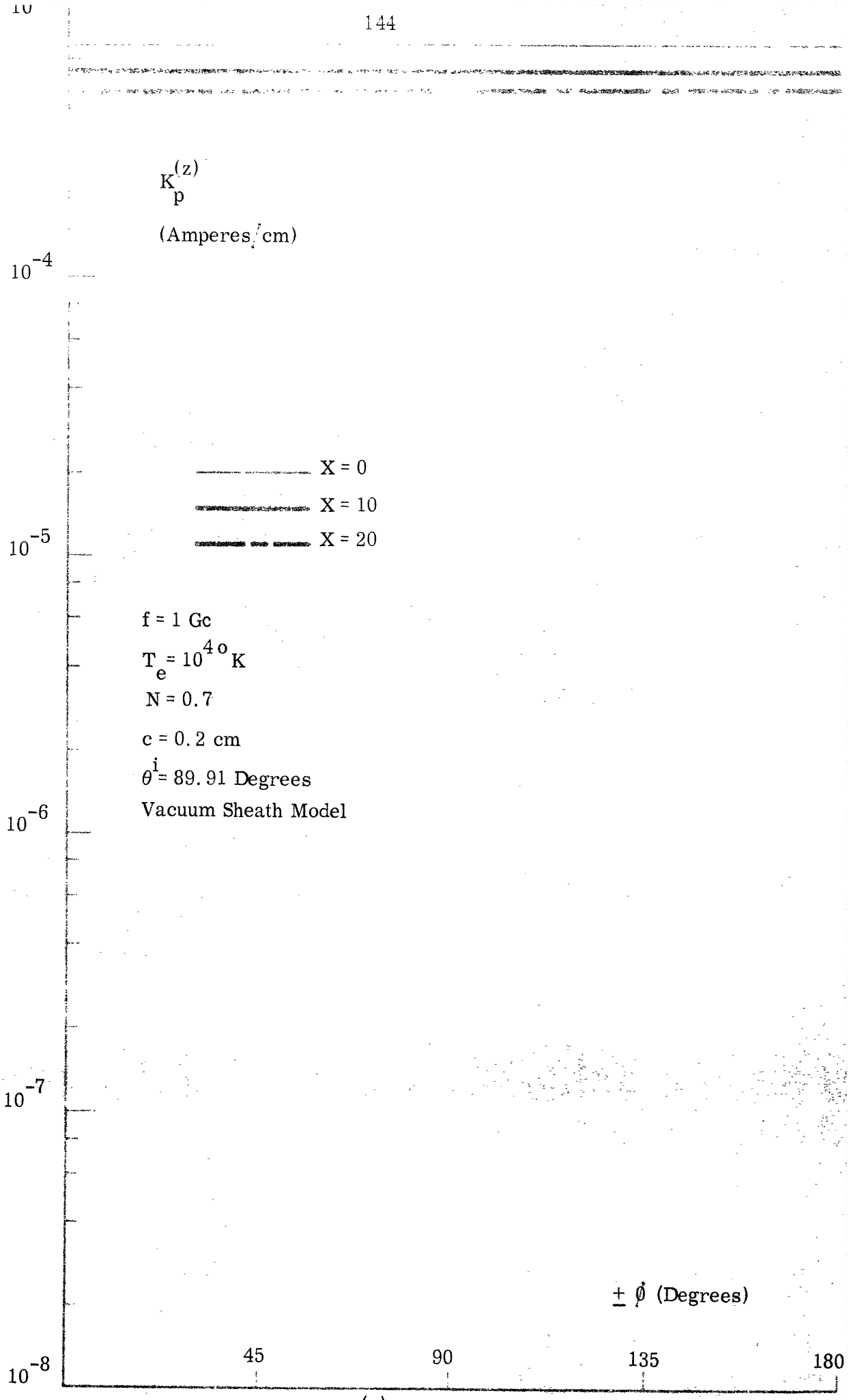

FIG. 3.34: MAGNITUDE OF $K_p^{(z)}$ vs. AZIMUTHAL ANGLE ϕ FOR θ^i = 89.91 DEGREES AND SHEATH THICKNESS X A PARAMETER

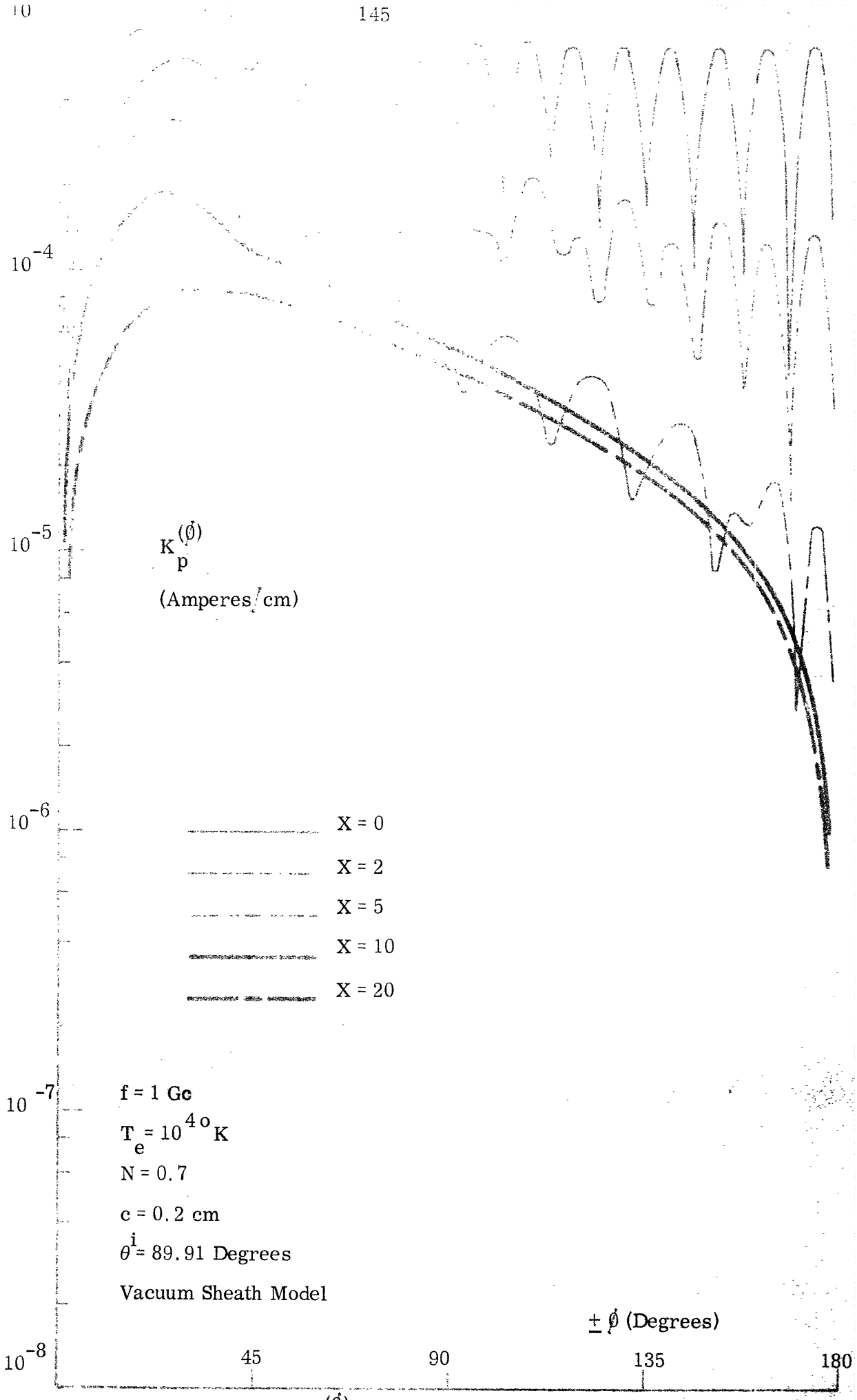

FIG. 3.35: MAGNITUDE $K_p^{(\phi)}$ vs. AZIMUTHAL ANGLE ϕ FOR θ^i = 89.91 DEGREES AND SHEATH THICKNESS X A PARAMETER

There are several features of the results presented above which are interesting in their own right, but there are two which are of the greatest significance from the viewpoint of measuring these currents in order to detect an incident EK wave. The most important is the shielding effect of the vacuum sheath, which was found to produce as much as 60 db attenuation in the surface currents for sheath thicknesses up to $20D_\ell$. The implication of this is obvious, in that the sheath may act to screen the EK wave from the cylinder and thus prevent its detection. Figures 3.36 and 3.37 summarize the sheath effect, showing the maximum current values for changing sheath thickness, at three angles of incidence. The attenuation due to the sheath is seen to be nearly exponential, with a scale factor $\alpha(\theta^i)$, determined by the angle of incidence, and may be approximately represented by

$$A(\theta^i, X) \approx \exp\left[-\alpha(\theta^i) X\right] \tag{3.1}$$

X is the sheath thickness in D_ℓ and should exceed 2 for (3.1) to be valid. This is a useful result since an approximate magnitude of the current for an arbitrary angle of incidence and sheath thickness can be obtained from the current value at a reference point, once $\alpha(\theta^i)$ is known.

This exponential dependence of the attenuation on the sheath thickness was deduced from the approximations to the exact solutions, given in Appendix E. There it is shown that the sheath attenuation may be approximately accounted for by a factor given by

$$\frac{1}{\cosh\left[\lambda_{eo}(s-c)\right]} = \frac{1}{\cosh\left[\beta(s-c)\right]} \tag{3.2a}$$

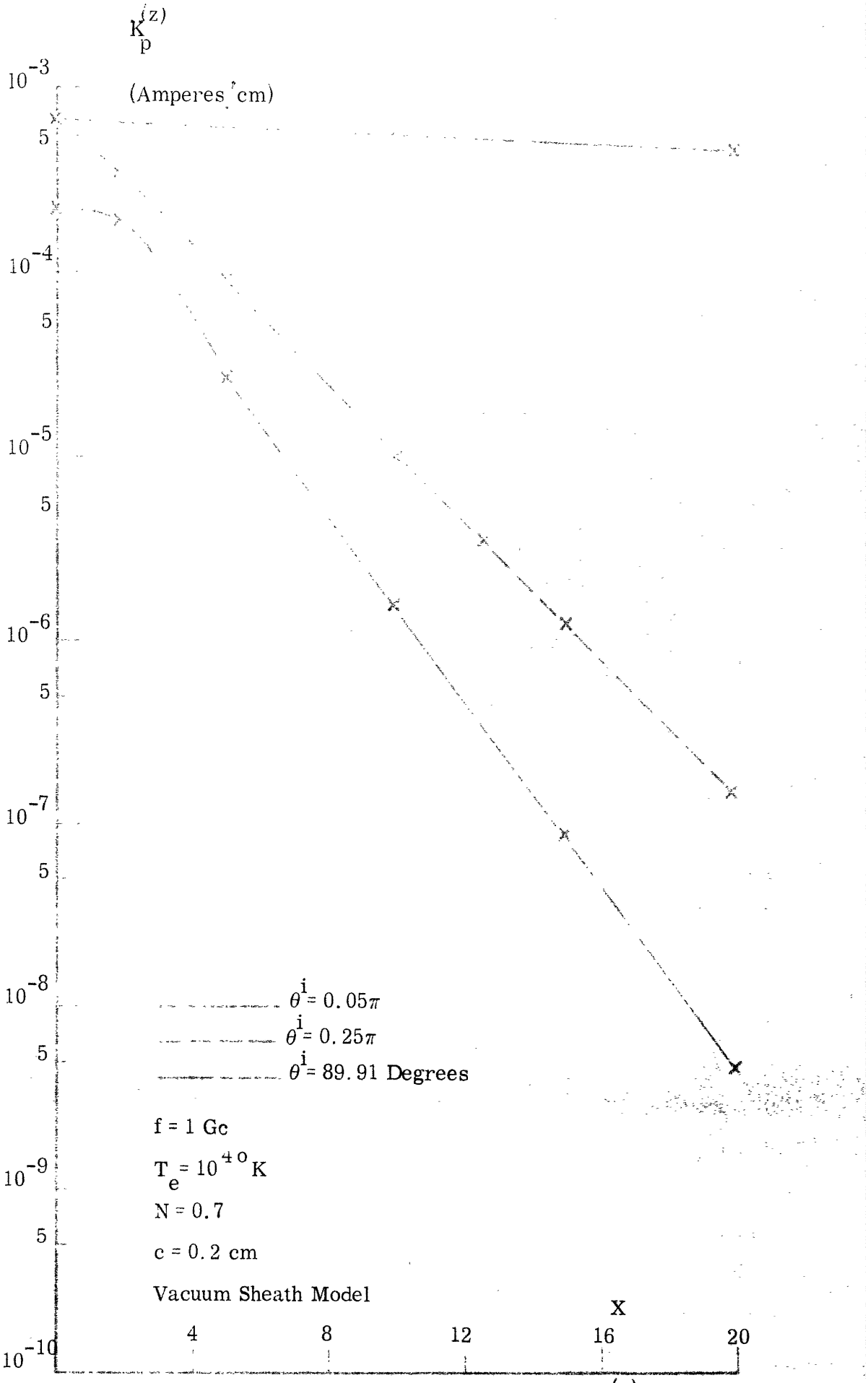

FIG. 3.36: MAGNITUDE OF MAXIMUM VALUE OF $|K_p^{(z)}|$ vs. SHEATH THICKNESS X WITH θ^i A PARAMETER

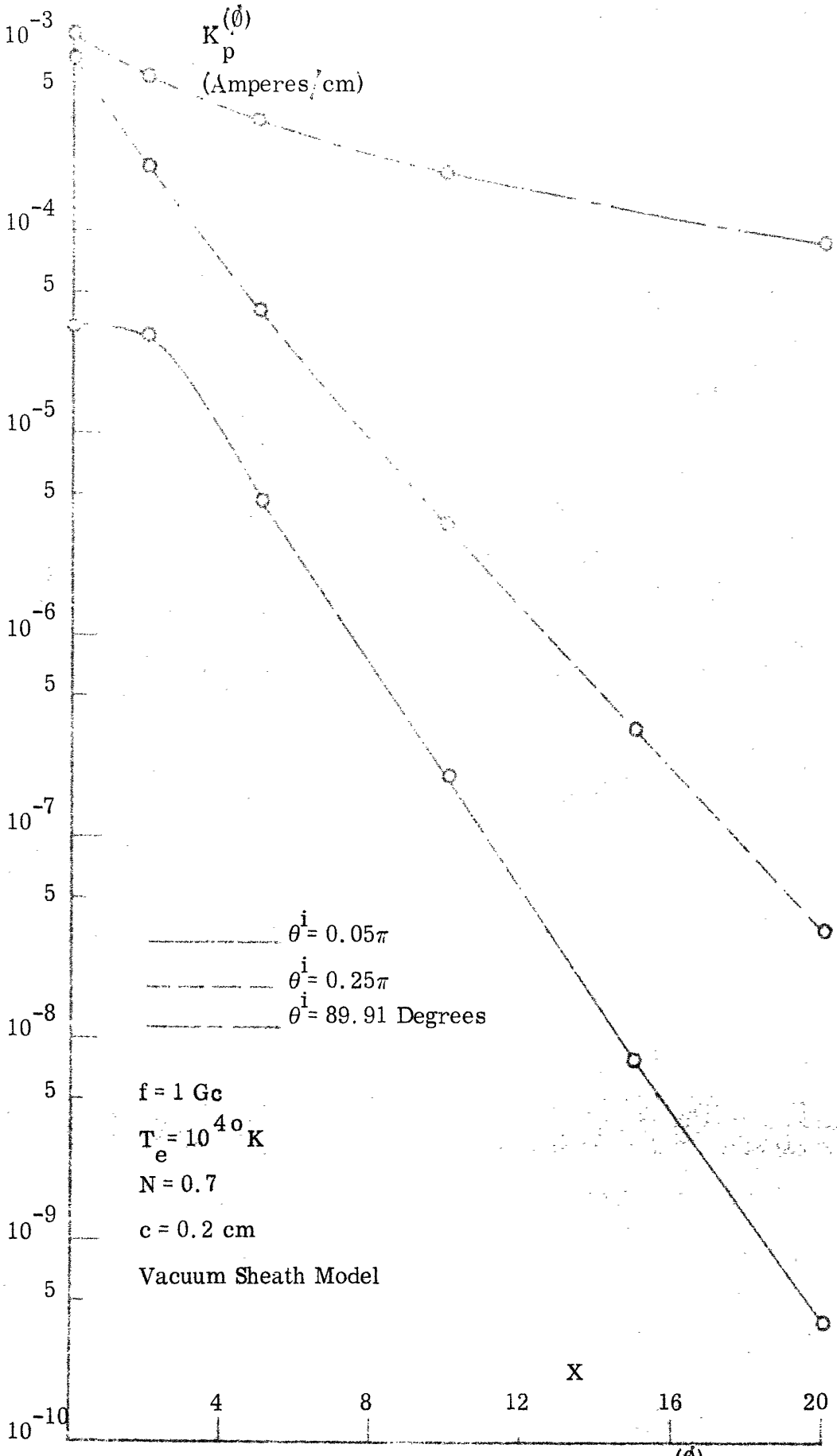

FIG. 3.37: MAGNITUDE OF MAXIMUM VALUE OF $|K_p^{(\phi)}|$ vs. SHEATH THICKNESS X WITH θ^i A PARAMETER

when $\cos\theta^i \quad v_r / v_\ell$. When $\beta(s-c) \quad 1$ this becomes

$$\frac{1}{\cosh \beta(s-c)} \cong 2 \exp \left[-\beta(s-c) \right] \tag{3.2b}$$

Thus we should have

$$\alpha = \quad - \quad = \quad - \quad \tag{3.3}$$

As a check $\beta D_\ell = 0.418$ and 0.562 for $\theta^i = 0.25\pi$ and $.05\pi$ respectively. Using the graphs, we obtain the corresponding values for α as 0.46 and 0.636 from $K_p^{(\phi)}$ and 0.417 and 0.575 from $K_p^{(z)}$. The agreement between the maximum current values from the exact solutions and the approximations is thus quite good. Note that α can be written in a more general way as

$$\alpha = \sqrt{1-N^2} \cos\theta^i / N \tag{3.4}$$

The physical explanation for the attenuation of the currents by the sheath is straightforward. It has been pointed out previously that the radial separation constant of the EM fields becomes imaginary when θ^i of the incident EK wave differs sufficiently from normal incidence. Further attention was directed to the fact that the modified cylindrical functions serve then to describe the radial dependence of the EM fields. These modified cylindrical functions exhibit an exponential dependence on ρ for large arguments. Consequently the fields in the plasma outside the sheath far from the cylinder decay exponentially, and are known as evanescent waves. They carry no energy in the outward radial direction, but instead form surface waves along the sheath-plasma interface ($\rho = s$). The fields within the sheath also decay with the radius moving away from the sheath interface ($\rho = s$), so that the fields at the cylinder may be significantly less than

those at the sheath interface. If we consider the sheathless case, the currents on the cylinder are determined by the magnetic field at the cylinder surface, which is also then the sheath-plasma interface. As the sheath interface is gradually moved away from the cylinder surface, it may be deduced that the magnetic field at the sheath interface is not very sensitive to the cylinder radius, as shown by the graphs of figures 3.9 and 3.11. The magnetic field at the cylinder however is decreased in value from that at the sheath interface by the amount of attenuation caused by the sheath, so that the sheath attenuation of the magnetic field is proportionately reflected in a decrease of the vacuum sheath current compared with the sheathless current.

A second feature which is of considerable interest is the ϕ variation of the EK induced currents (note also the z variation $e^{i\beta z}$ which is not plotted graphically here). Since the variation is on the order of the EK wave length, which is less by the ratio v_r/v_ℓ than the EM wave length at the same frequency, then this variation may possibly be used to discriminate between EM and EK induced currents. Note in this regard however, that with increasing sheath thickness, the ϕ variation is correspondingly decreased.

Some of the other aspects of the preceding results deserve mention. One of these is the peaking of the z component of current at the angle where the scattered EM modes change from propagating to evanescent in the radial direction. This occurs for $\theta^i=\theta^i_c$ when there is no sheath, at which point the EM mode is a pure surface wave, propagating unattenuated in the z direction. A similar peaking of radiated power was observed by Balmain (1965) for the radiation from a slot in

an infinite plane. He concluded that while the maximum power in the peak is very large, the width of the peak is so narrow that its integrated power in comparison with the total power radiated by the slot, is negligible. The current peak in the present case is also very narrow, on the order of 0.1 degrees at the point where the current falls to 0.1 its maximum value. As a consequence of the extreme narrowness of this current peak as a function of the angle of incidence, it does not seem promising in a practical sense for detecting an incident EK wave. A similar observation was made above concerning the increase in the z directed current with decreasing cylinder radius.

Another striking property of some of the current graphs is the exponential attenuation of the current as a function of ϕ. This is particularly noticeable for an angle of incidence of 0.45π. It is characteristic of a surface wave in the ϕ direction, as was previously mentioned. While this may be accounted for as being a consequence of the energy reaching the cylinder's surface primarily from the front part of the sheath, it is difficult to find the combination of circumstances between cylinder radius, angle of incidence and sheath thickness which leads to this situation.

Three final graphs of this sequence are presented in figures 3.38 to 3.40 which summarize the maximum current value for the sheathless case and a sheath $10\,D_\ell$ thick, as a function of θ^i, N and c respectively, where θ^i for the latter two curves is $\pi/4$. In the first, where θ^i is the independent variable, it can be seen that the currents for the sheathless case are not very sensitive to θ^i, (except for the peak in $K_p^{(z)}$ discussed above which is not shown here). However, when the

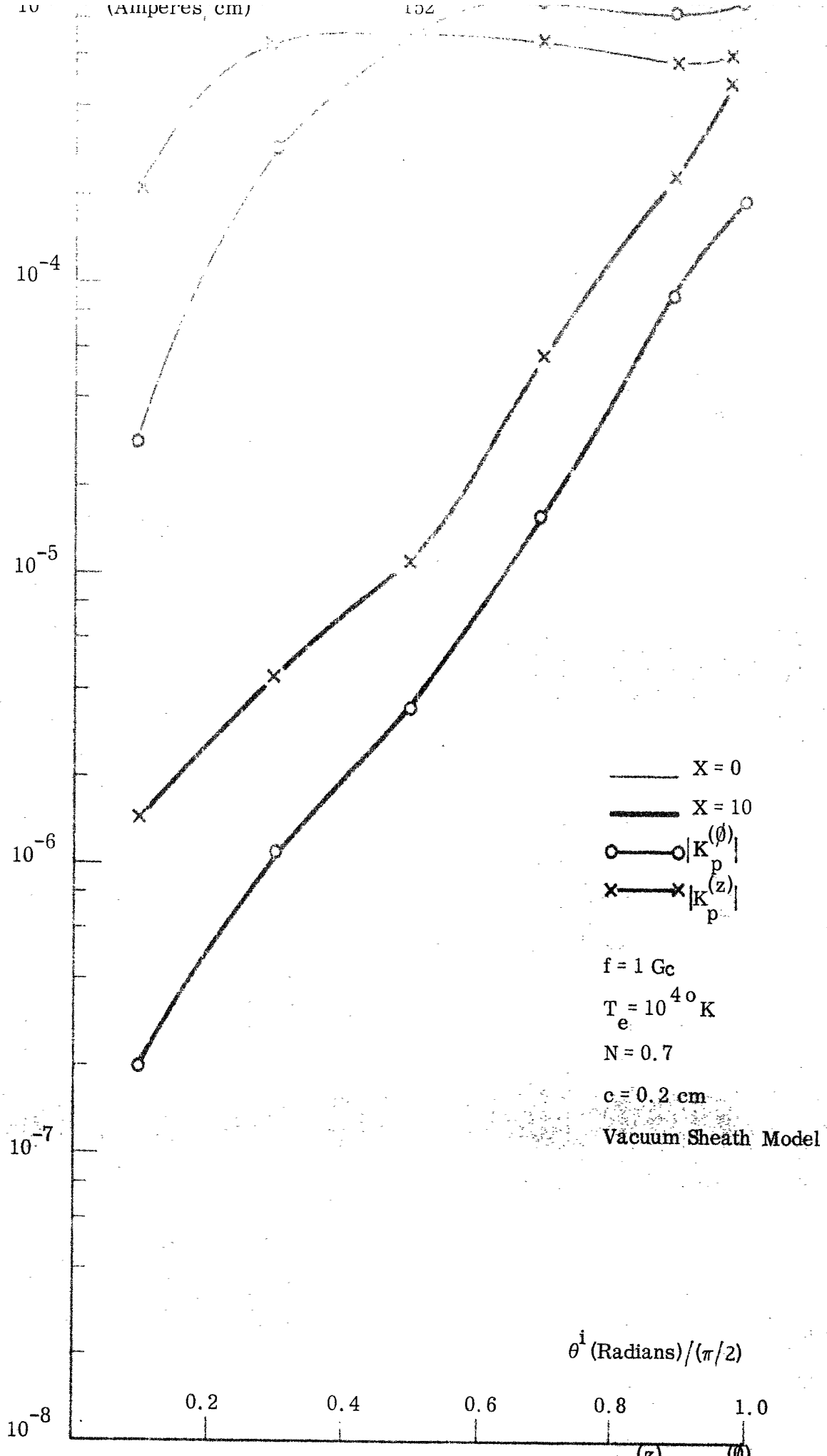

FIG. 3.38: MAGNITUDE OF MAXIMUM VALUES OF $|K_p^{(z)}|$ and $|K_p^{(\phi)}|$ vs. ANGLE OF INCIDENCE θ^i.

case where the sheath is $10\,D_\ell$ thick is considered, a strong dependence upon θ^i is found. This can be explained by the fact that the effective sheath thickness increases with increasing obliqueness of the angle of incidence, thereby producing greater attenuation. The approximate solution derived in Appendix E correctly predicts this behavior, since α, the sheath attenuation scale factor, as given by (3.4) above, increases proportionally to $\cos\theta^i$.

An examination of figure 3.39 reveals that the sheath attenuation decreases with increasing N, also in agreement with (3.4). There is in addition more than an order of magnitude decrease in the sheathless currents as N increases from 0.7 to 0.99. This is to be expected, since if N were exactly unity, there would be no propagation of energy and no currents would be excited on the cylinder.

Finally, in figure 3.40 where the cylinder radius varies from 0.005 cm to 1 cm, it can be seen that there is a fairly regular increase of $K_p^{(\phi)}$ and a decrease of $K_p^{(z)}$ with increasing cylinder radius for a $10\,D_\ell$ thick sheath. For the sheathless case, there does not appear to be any systematic current variation with changing cylinder radius. According to (3.4), the sheath attenuation is not a function of the cylinder radius, so that the sheathless and the $10\,D_\ell$ thick sheath currents might be expected to exhibit similar variations with changing cylinder radius. But (3.4) was based on a large argument approximation to the cylindrical functions, which becomes invalid for a radius less than 0.1 cm, so that (3.4) is not applicable then.

It should also be noted in this regard that the sheath attenuation as expressed by (3.4) depends on the order of the cylindrical function also being less than the

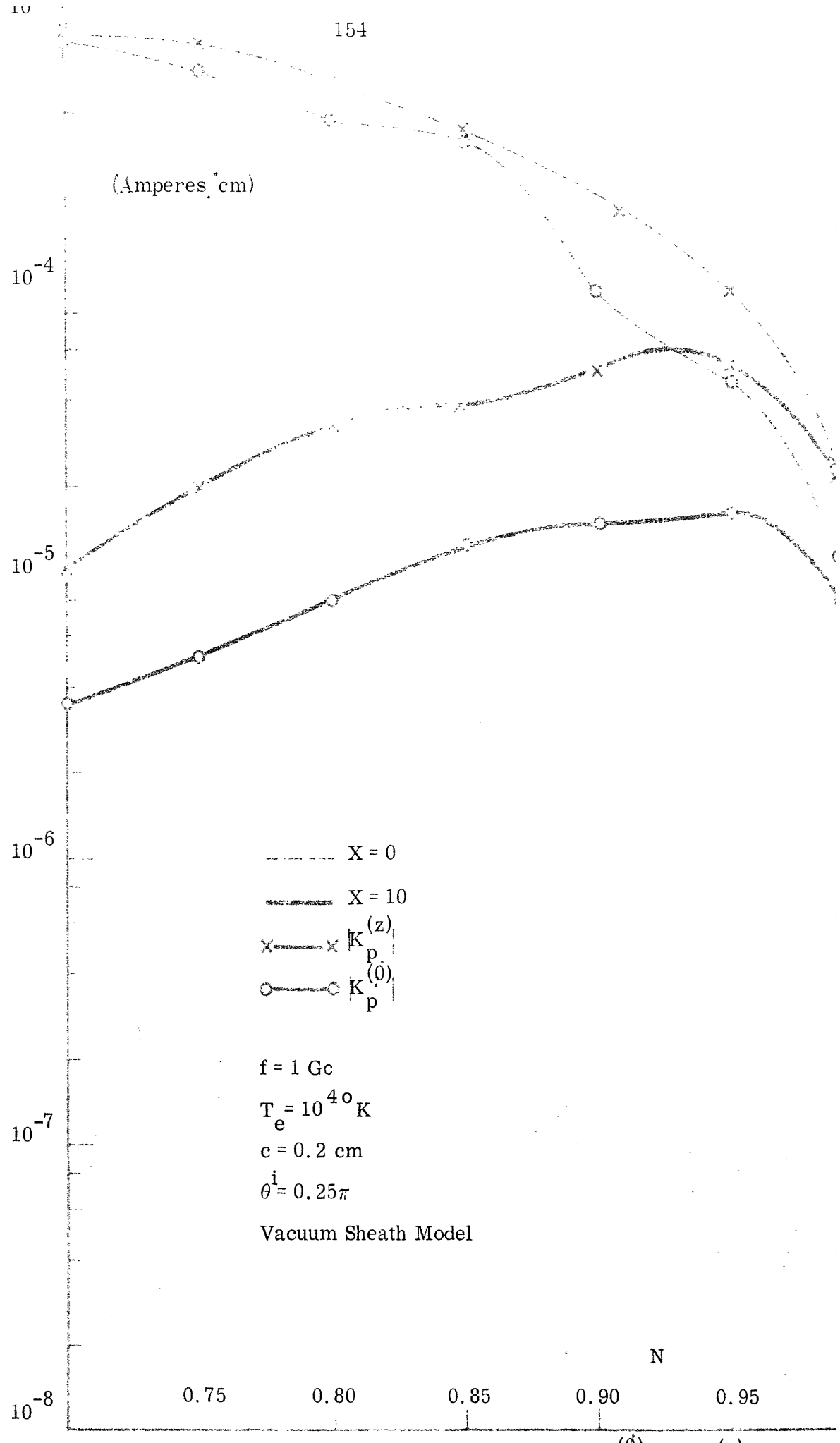

FIG. 3.39: MAGNITUDE OF MAXIMUM VALUES OF $|K_p^{(\phi)}|$ AND $|K_p^{(z)}|$ vs. RATIO OF PLASMA FREQUENCY TO INCIDENT WAVE FREQUENCY, N

MISSING
PAGE

argument. Since, as discussed in Appendix E, the Fourier series for the current does not converge before this requirement is violated, then the sheath attenuation may differ from (3.4), resulting in the curves of the five previous graphs being at variance from the behavior predicted by the approximate formula.

3.1.2 Incident EM Wave

The surface currents excited by the e and h waves for the nominal values of the parameters are shown as a function of ϕ in figure 3.41.* This graph is distinctly different from those for the incident EK wave in two important points. First the ϕ variation here is quite regular, being approximately $\sin\phi$ for $K_h^{(\phi)}$ and $K_e^{(z)}$ and almost independent of ϕ for $K_h^{(z)}$ and $K_e^{(\phi)}$. The second difference is in the fact that the vacuum sheath has considerably less effect upon the magnitudes of the currents excited by the incident EM wave compared with its effect in the case of the EK wave. It is of interest to observe however, that $K_h^{(\phi)}$ shows an increase in magnitude in the presence of the vacuum sheath. It should be noted in this regard, that the h wave when illuminating a perfectly conducting cylinder in free space, does not excite a ϕ component of current. In the present case, the compressible plasma and the sheath both act as a means for causing its excitation. It however is small in magnitude compared with the z component of current excited by the h wave.

Because the surface currents due to the h and e waves have a consistent ϕ variation, it is unnecessary to present them as a function of ϕ for each parameter value used. Instead the currents are shown directly as a function of the various parameters. The current values given in these curves will be the maximum values

*The magnitude of the currents only is presented since the phase is practically independent of ϕ.

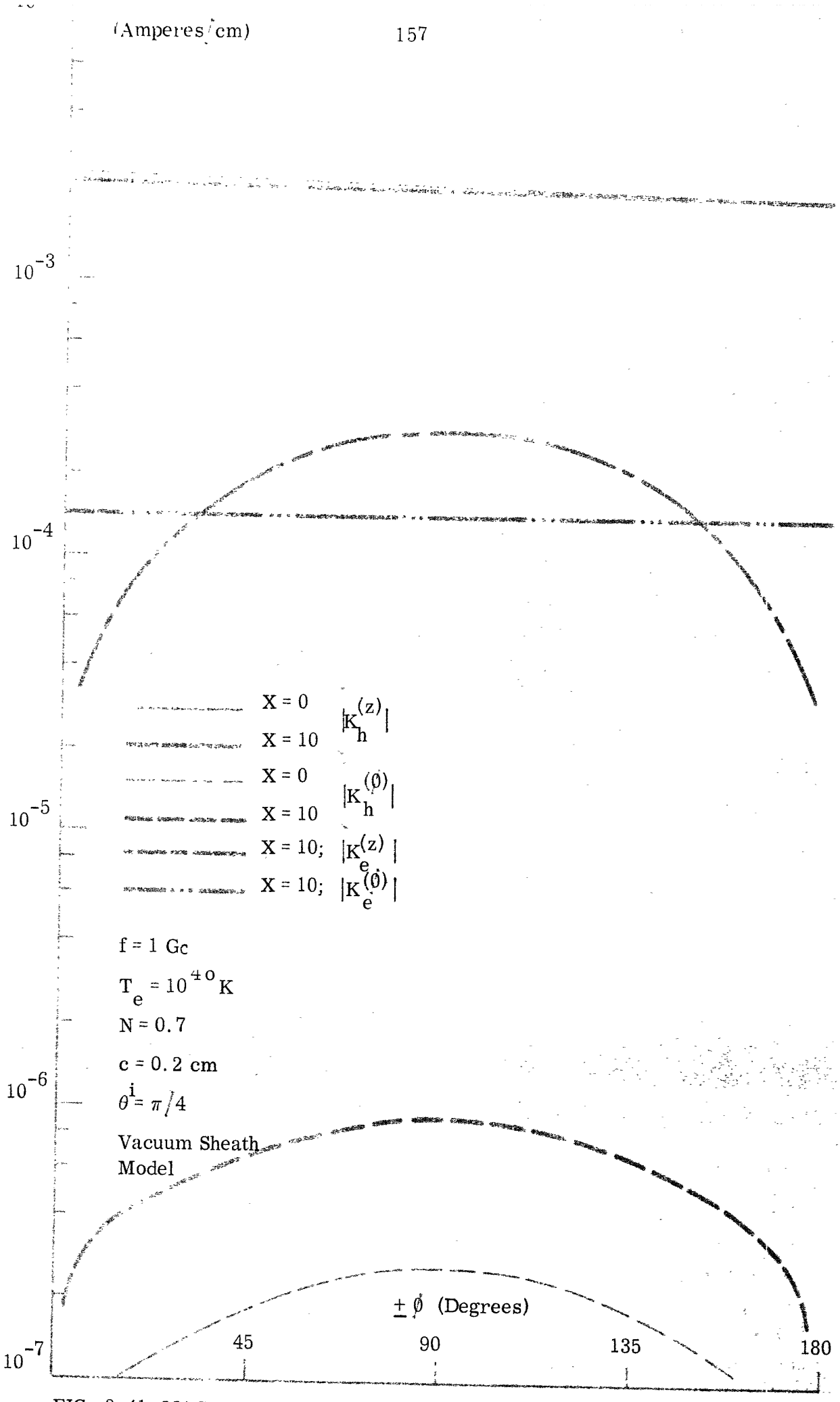

FIG. 3.41: MAGNITUDE OF CURRENTS EXCITED BY EM WAVE vs. AZIMUTHAL ANGLE ϕ FOR NOMINAL PARAMETER VALUES

from the ϕ variation of the current. Figures 3.42 to 3.45 show these results as a function of the cylinder radius, the ratio of ω_p to ω, the angle of incidence and the sheath thickness respectively. Two curves are presented for each current, one for the sheathless case and the other for a sheath 10 D_ℓ thick, when the difference between the currents for the two cases is large enough to show graphically. The most striking feature to be observed from these graphs is that, apart from $K_h^{(\phi)}$, these currents are relatively unaffected by the vacuum sheath. Another important point is that these currents, excepting again $K_h^{(\phi)}$, have magnitudes on the order of, or larger than, those produced by the incident EK wave. This will be taken up in greater detail in the next section.

It was mentioned in the preceding chapter that the incompressible plasma would also be investigated in connection with the incident EM wave. Taking the plasma to be incompressible means that the EK wave does not appear in the analysis and the plasma is treated simply as a dielectric as far as the EM wave is concerned. These calculations were also carried out, and the currents were changed less than 5 percent from the compressible plasma case except of course for $K_h^{(\phi)}$. This component of the current becomes zero when the plasma is incompressible and the sheath thickness is zero. It was found to depend primarily on the existence of the sheath for its excitation, and with a sheath of nonzero thickness, the plasma compressibility affected its magnitude less than 5 percent also.

An important consequence of these results is that when considering the scattering of EM waves from plasma-immersed obstacles (small compared with the EM wave length), the plasma can, for practical purposes be replaced by an equivalent dielectric whose permittivity is $\epsilon_o (1-N^2)$. This statement

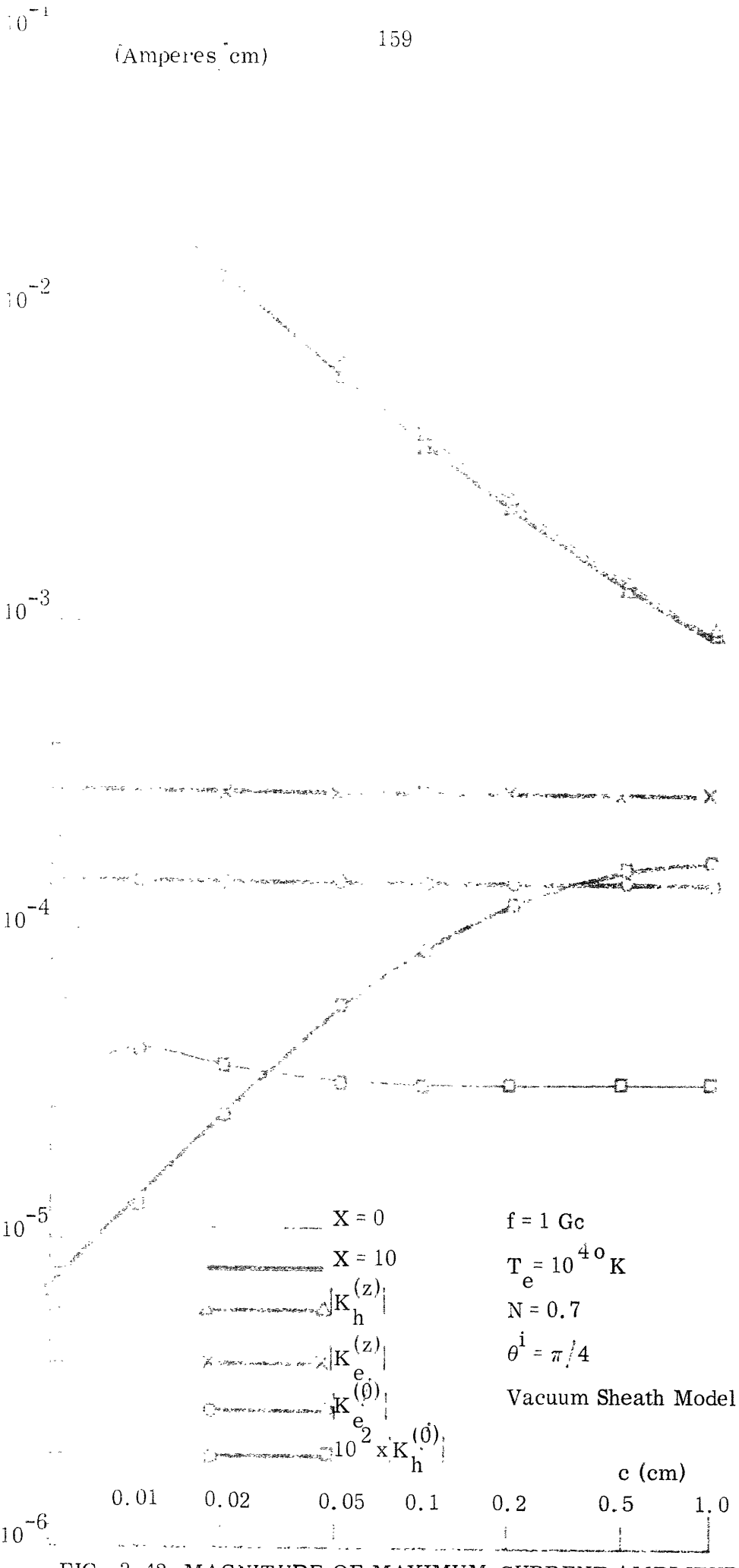

FIG. 3.42: MAGNITUDE OF MAXIMUM CURRENT AMPLITUDES EXCITED BY EM WAVE vs. CYLINDER RADIUS c .

MISSING
PAGE

MISSING
PAGE

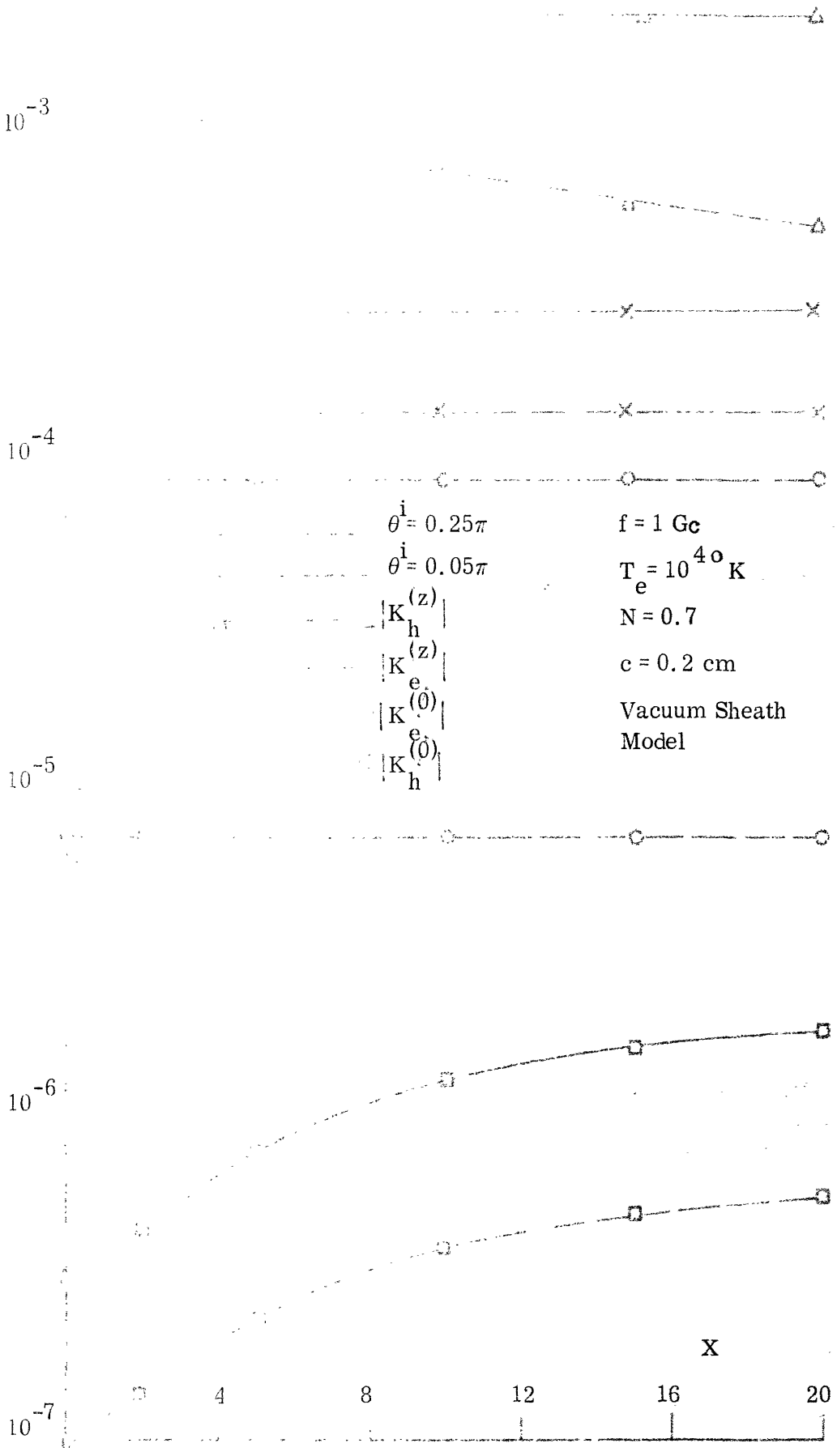

FIG. 3.45: MAGNITUDE OF MAXIMUM CURRENT AMPLITUDES EXCITED BY EM WAVE vs. THE SHEATH THICKNESS X.

can not be made for obstacles of arbitrary size since the present analysis has been restricted to a cylinder no larger than 1/15 EM wave lengths in diameter.

3.1.3 Comparison of EM and EK Induced Currents

We come now to the very important question of deciding the feasibility of making surface current measurements for the purpose of detecting an EK wave incident on the cylinder. Since such a measurement would conceivably have to be performed in a strong background of EM radiation, it is pertinent to compare the magnitudes of the currents excited by both kinds of waves. It was observed previously that the EM waves generally induced currents of equal or greater magnitude than those due to the EK wave for unit V^i . This may be misleading however since there are two considerations to be taken into account before the comparison is meaningful. These are: (1) the power flow density in each wave and (2) the satisfying of the linearity requirement upon which this analysis has been based. The former point is important to the relative magnitudes of the induced currents, which the latter places a limit on their absolute magnitudes in connection with a linearized analysis.

The only reasonable criterion for a comparison of the induced currents caused by the two kinds of waves would seem to be that when the incident power flow densities are equal A Poyntings vector for the power flow was given in Chapter II, from which it can be shown that the equal incident power flow requirement can be expressed as

$$V^i_p = \qquad V^i \tag{3.5}$$

where V^i represents both V^i_e and V^i_h. For an electron temperature of $10,000^o$ K, (3.5) reduces to

$$V^i_p = 4.74 \times 10^{-2} N \; V^i \tag{3.6}$$

which shows that in order to compare the curves of sections (3.1) and (3.2), the scale for the EK induced currents must be reduced by a factor of 0.0332 to 0.0470. This changes the picture considerably, since instead of having currents on the same order of magnitude induced by the two kinds of waves, the currents are a minimum of 15 to 20 db apart.

The linearization requires that the dynamic electron number density be small compared with the static number density, and in addition that the dynamic electron velocity be small compared with v_r so that the plasma is not heated by the dynamic fields. These requirements can be stated

(3.7a)

(3.7b)

T_e is 10^{4o} K in the numerical expressions. L is a parameter which is the ratio of the static to dynamic electron number density or the rms to dynamic electron

velocity, and is thus a measure of the validity of the linearization. It is interesting to note that in the case of the EK wave, the linearity conditions on both the dynamic density and velocity reduce to the same form given by (3.7a). If L = 10 and N = 0.7 then

$$V_p^i \leq 0.178 \text{ Volts} \tag{3.8a}$$

$$V_- \quad 1.59 \times 10^2 \text{ Volts} \tag{3.8b}$$

so that results obtained using $V_- = 1$ and V_p^i determined by (3.6) will satisfy both the linearity requirement and equal power flow criterion discussed above. Note however, that equations (3.7) apply to the incident plane wave only. It is possible that the interaction of this plane wave with the cylinder will give rise to fields in the vicinity of the cylinder which are so large that the linearization is invalid even though (3.7) are satisfied. These equations thus represent an upper limit for V_-^i and V_p^i. It is of interest to observe that when (3.8) holds the power flow density in the plane EM and EK waves respectively are 5.5×10^3 and 6.1 watts/(meter)^2.

When V_p^i is set at 0.0332, corresponding to N = 0.7, and for the sheathless case only, then we find the EK and EM induced currents for $\theta^i = \pi/4$ and $\theta^i = \pi/2$ given in figures 3.46 and 3.47. It can be seen that the z component of the current excited by the EK wave is about 0.003 that due to the h wave and 0.05 that due to the e wave for $\theta^i = \pi/4$. The ϕ component of the EK induced current is about 0.1 that excited by the e wave and about 100 times that produced by the h wave for $\theta^i = \pi/4$. The same relationship holds for the EK and e induced ϕ components of current for $\theta^i = \pi/2$. Thus apart from the $K_h^{(\phi)}$ current, the currents excited by the

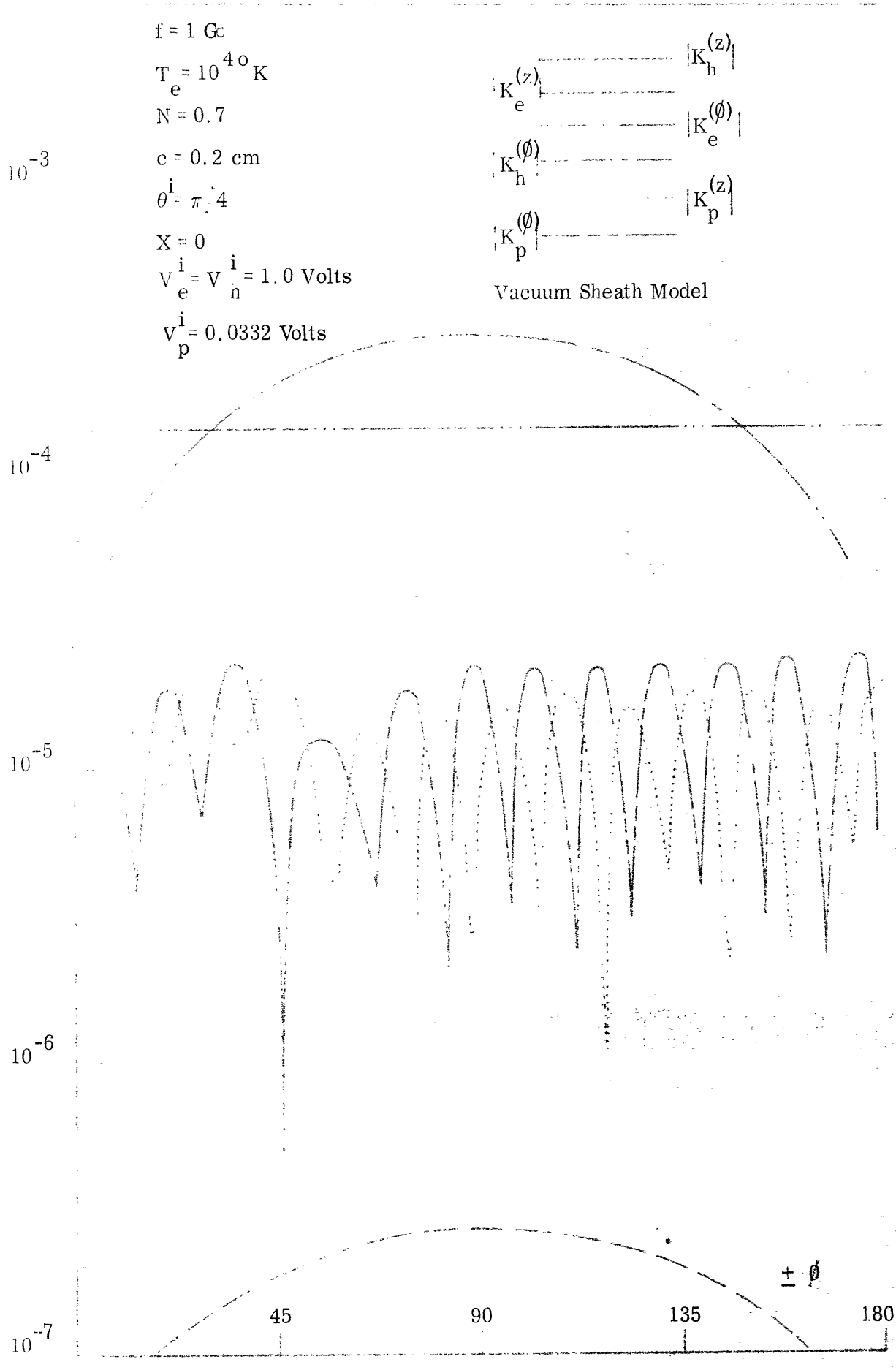

FIG. 3.46: MAGNITUDE OF CURRENTS EXCITED BY EM AND EK WAVES OF EQUAL POWER FLOW DENSITY vs. AZIMUTHAL ANGLE ϕ FOR $\theta^i = \pi/4$ AND NOMINAL VALUES OF OTHER PARAMETERS

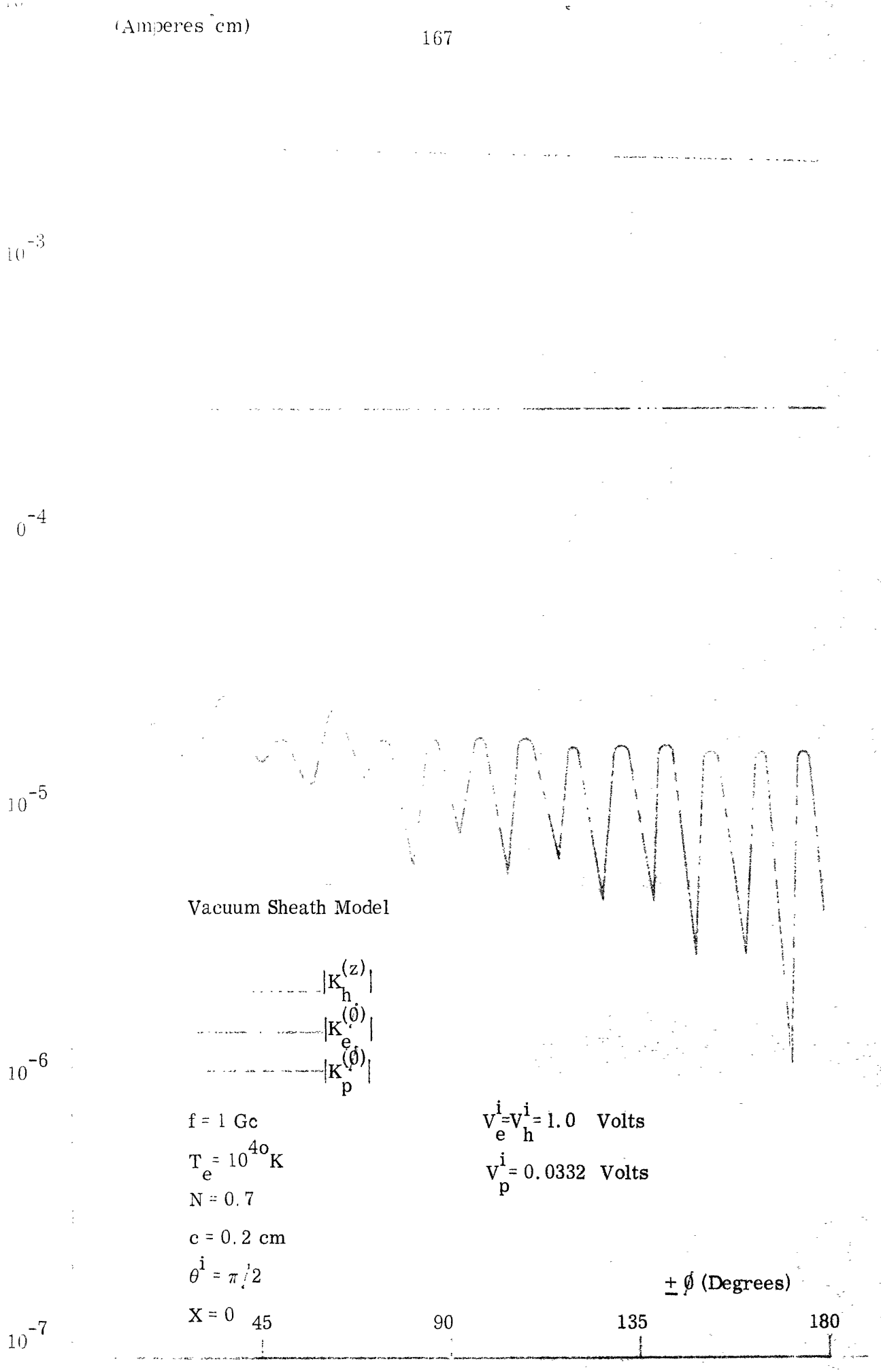

FIG. 3.47: MAGNITUDE OF CURRENTS EXCITED BY EM AND EK WAVES OF EQUAL POWER FLOW DENSITY vs. AZIMUTHAL ANGLE ϕ FOR $\theta^i = \pi/2$ AND NOMINAL VALUES OF OTHER PARAMETERS

EK wave for the sheathless case are 0.1 to 0.003 the corresponding currents caused by the EM wave. When the attenuation due to the vacuum sheath is taken into account, the EK induced currents are reduced by a further factor of 0.01 to 0.001 except for near normal incidence, where the attenuation factor may be 0.5 to 0.1. It can thus be concluded that the EK wave is considerably less effective than the EM wave in the excitation of currents on the plasma-immersed cylinder.

There is an additional factor to be taken into consideration here, from the viewpoint of practically measuring these surface currents. A slot which is very thin in the direction of the current flow has been previously mentioned as a means of carrying out these measurements. The effect of the slot is to perform a line integration of the magnetic field parallel to it, which is the current flow normal to the slot. If the current is of constant phase and amplitude over the surface of the cylinder, then the longer the slot the larger the voltage which can be measured across it, as long as the slot length does not approach the smallest length at which it will resonate. One of the distinct differences between the EK and EM wave induced currents is the much greater fluctuation with the azimuthal angle ϕ of the magnitude and phase of the EK currents. This limits the practical effective size of the slot and thus the magnitude of the signal to be obtained in measuring $K_p^{(z)}$, while the z component of the EM current is not subject to this limitation. A similar argument follows for the ϕ directed currents due to the difference in the z variation behavior of the EK and EM currents.

The curves of $K_p^{(z)}$ and $K_p^{(\phi)}$ on figure 3.46 show that the average separation of the current minima are on the order of 12° to 15°. Since these minima are

associated with rapid phase changes, the slot for measuring $K_p^{(z)}$ should thus subtend no greater angle than that enclosed by two successive minima, which leads to a slot length of about 0.0535 cm. Assuming that the slot is centered on a current maxima, the total component of the current available for measurement due to the EK wave would be no greater than $1.5 \times 10^{-5} V_p^i$ amperes, for the sheathless case. With V_p^i equal to its maximum value for which the linearization is valid, the current is about 3×10^{-6} amperes. If this current could be introduced to a 50 ohm transmission line without coupling loss, then a power on the order of 5×10^{-10} watts would be available at the output of the line. An rf power level of this magnitude is well within the capability of the more sensitive laboratory techniques commonly in use. An incident h wave with V_h^i related to V_p^i by (3.6) would produce an output power from the line on the order of 3×10^{-5} watts for the z component of the current. A consideration of the ϕ components of the surface current shows that due to the EK wave to be one tenth the current caused by the e wave, with respective output powers on the order of 5×10^{-10} and 5×10^{-8} watts.

It should be kept in mind that the calculations outlined above are for the sheathless case, so that the output power figures mentioned for the EK wave may be a factor of up to 10^{-6} less than those calculated above when the vacuum sheath is allowed for. Note also that the larger of the two current components excited by the h and e waves has been used in the comparison, since the incident EM wave must be assumed of arbitrary polarization. The prospect of detecting the EK wave in a background of EM radiation would thus appear to be a very difficult

one. The variation of the EK induced surface currents in the ϕ and z directions does however, suggest a means for observing them in the presence of the EM currents, since a relative motion between the slot and source would produce a variation in the output which is dependent upon the EK wave length. It would appear that the most favorable circumstances for experimentally detecting the EK current would be for normal incidence, since the sheath attenuation is a minimum there.

There is one additional observation which can be made concerning the ϕ component of the [illegible current], $K_h^{(\phi)}$. It was pointed out that this current is not excited in the absence of the sheath when the plasma is incompressible. Further, except in the sheathless case, the compressibility of the plasma has little effect on its magnitude while it is fairly sensitive to sheath thickness. Therefore, a measurement of $K_h^{(\phi)}$ would be informative in determining the effective sheath thickness.

3.2 Inhomogeneous Sheath

The numerical solution of the inhomogeneous sheath equations given in Chapter II take 20 times more computer time than the corresponding vacuum sheath calculations. Because of this, the range of parameter variations which could be investigated for the inhomogeneous sheath is much more limited. Furthermore, there are additional parametric quantities associated with the inhomogeneous sheath which are not encountered in the vacuum sheath analysis. They are the cylinder potential and the potential variation in the sheath, as well as the

boundary condition that the dynamic electron number density be zero at the cylinder. This boundary condition does not need to be considered in the numerical calculations for the vacuum sheath since the EK current is then zero. Consequently in order to obtain the maximum benefit from the computer time available, a judicious choice had to be made for the values of the parameters to be used.

Due to these considerations, the only vacuum sheath parameter varied here is the sheath thickness. N, c, ω, T_e and V^i have the nominal values given on page 107, while the angle of incidence is of course fixed at $\pi/2$. A limited number of values for the cylinder potential and for the exponent of the potential variation in the sheath are employed, for both boundary conditions, the vanishing of the dynamic electron number density, and the normal dynamic electron velocity at the cylinder surface. These will be referred to as the soft and hard boundary conditions for obvious reasons. While the number of cases which can be investigated numerically for the inhomogeneous sheath is small compared with the vacuum sheath, for the same computer time, there is a great deal of very useful and interesting information in addition to the surface currents which can be obtained from the inhomogeneous sheath results relating to power flow, energy density, etc., and which is not obtained in the vacuum sheath analysis. This material is presented after the surface current curves are given and discussed

3.2.1 Incident EK Wave

Figure 3.48 is a graph of the surface current (note that there is only the ϕ component for normal incidence of the EK and e waves) for both the hard and soft

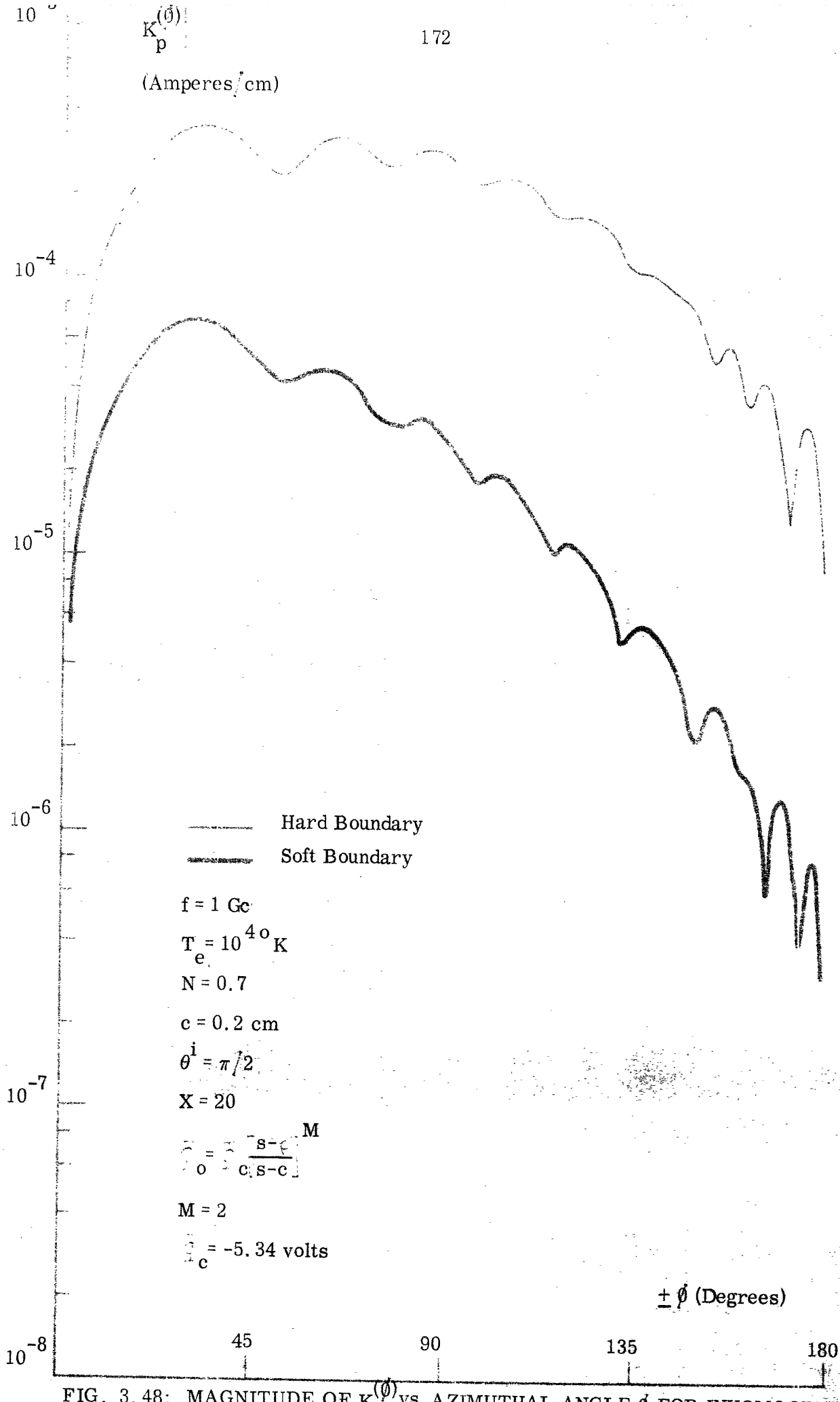

FIG. 3.48: MAGNITUDE OF $K_p^{(\phi)}$ vs. AZIMUTHAL ANGLE ϕ FOR INHOMOGENEOUS SHEATH MODEL WITH M=2 AND ξ_c = -5.34 VOLTS

boundaries. The sheath thickness is 20 D_ℓ. A parabolic sheath potential variation is used (M=2) and the cylinder potential is obtained from (2.17) for a mercury plasma (m_i=200 atomic mass units), which yields a value of -5.3 volts for ϕ_c.

An important feature of figure 3.48 is that the soft boundary condition leads to currents a factor of 5 to 20 times less than those obtained from the hard boundary. It was pointed out in Chapter II that the use of the soft boundary condition will give coupling between the EK and EM waves due only to the sheath inhomogeneity, and thus serves to separate the relative contributions of the inhomogeneity and boundary coupling for the inhomogeneous sheath. The tentative conclusion might thus be reached that inhomogeneity coupling is less effective by a factor of at least 5 than the hard boundary coupling.

A comparison of figures 3.48 and 3.7 is now very informative. It can be seen that the current from the sheathless case in figure 3.7 exceeds that for the inhomogeneous sheath and the hard boundary condition in figure 3.48 by 3 to 10 times, while the current for a vacuum sheath 10 D_ℓ thick is on the same order less than this. The two curves from the vacuum sheath model thus bracket the inhomogeneous sheath current, which is a desirable result from the viewpoint of establishing the validity of the vacuum sheath model. Before drawing any conclusions from this outcome, some further observations should be made.

First the vacuum sheath model, it should be remembered, has as its only coupling mechanism, that due to the hard boundary condition. The soft boundary condition produces no coupling for the vacuum sheath model. The inhomogeneous sheath on the other hand, has the additional coupling mechanism of the sheath

inhomogeneity. We might expect then that the inhomogeneous sheath, with both of these coupling mechanisms in effect, could produce larger surface currents than those obtained with the vacuum sheath, which has the single coupling mechanism. This does not turn out to be the case however, except when the vacuum sheath is more than 5 D_ℓ thick. The implication would seem to be that the inhomogeneous sheath serves more as an attenuator for the incident EK wave than it contributes to the coupling picture. The effective attenuation appears to be fairly well approximated by the vacuum sheath model with a sheath about 5 D_ℓ in thickness.

A second observation of importance concerns the uncertainty of the inhomogeneous sheath current results due to lack of knowledge about Y_B. We mention again that Y_B, introduced by Cohen in the boundary condition on the normal electron velocity at the bounding surface (equation 2.42), is set at 0 or ∞ in this analysis, corresponding respectively to complete reflection or complete absorption of the electrons. It is likely that the correct value for Y_B lies somewhere between these two extremes. Now it is shown in Appendix E, equation (E5), that for the sheathless case and EK wave incidence, Y_B appears only in the denominator for the e and h mode reflection coefficients. The surface currents induced by the EK wave thus show the same dependence on Y_B. Obviously then, when Y_B is large enough, the boundary contribution to the EK surface currents becomes inversely proportional to Y_B going to zero when Y_B is infinity. The boundary contribution to the surface current for the inhomogeneous sheath and vacuum sheath models may be concluded to exhibit a similar dependence on Y_B. In the

latter case, Y_B would correspond to a surface admittance at the sheath-uniform plasma interface.

We further note that an implicit assumption in the preceding discussion has been that the contributions to the magnetic field on the cylinder surface by the sheath inhomogeneity and the boundary are additive so that the two effects together, arising from use of the hard boundary condition, would lead to a larger surface current than would the sheath inhomogeneity alone as is the case for the soft boundary condition. An examination of the real and imaginary parts of the surface currents showed that the current phase for the hard boundary was generally within 45^{o} of that for the soft boundary. This result, together with the increased current magnitude obtained from the hard boundary condition indicates the approximate validity of this assumption.

Consequently, we are justified in conjecturing that, when the magnitude of the EK currents, obtained from the inhomogeneous sheath model is considered as a function of Y_B, a minimum is obtained for $Y_B = \infty$. Unfortunately, we cannot conclude that the current has correspondingly its maximum value when $Y_B = 0$. It may be seen in equation (E5) that the e and h reflection coefficients can be increased over those results obtained for $Y_B = 0$ by a value of Y_B which makes the denominator D_m smaller. As a matter of fact, (E5) shows that if Y_B is complex and of the proper value, D_m can be zero, leading to surface currents of infinite magnitude. This is unacceptable on physical grounds, indicating that the boundary condition relating the dynamic normal electron velocity to the dynamic electron density through Y_B is an over-simplification or this value for Y_B is not realistic.

It might be concluded from this that Y_A should not be set equal to zero in equation (2.42). We see that the question of the surface impedance of the boundary for the dynamic electron motion there is a complicated one which has a strong influence on the contribution of the boundary to the EK induced surface current. As a result of this uncertainty in the contribution of the boundary to the surface current as a function of Y_B, we cannot establish an upper limit to the EK induced current in the same way as a lower limit has been established, for the inhomogeneous sheath.

A final observation about these graphs concerns again the vacuum sheath results in comparison with those from the inhomogeneous sheath. It is apparent that the vacuum sheath currents for sheath thicknesses of up to 20 D_ℓ exceed the current obtained from the inhomogeneous sheath with the soft boundary condition. On the other hand, the vacuum sheath currents are in reasonably good agreement with those from the inhomogeneous sheath for the hard boundary condition. It thus appears that the vacuum sheath model using $Y_B=0$, provides a good approximation to the inhomogeneous sheath also using $Y_B=0$. It naturally fails, however, when $Y_B=\infty$ as a consequence of the fact that the boundary coupling becomes inversely proportional to Y_B alone, and the current goes to zero. Thus we see that the range of uncertainty in the EK induced current from the vacuum sheath model due to variation with Y_B is much greater than that for the inhomogeneous sheath where a lower limit to the current has been established. Also the validity of the vacuum sheath model is thus much more dependent upon the correctness of the hard boundary condition than is the inhomogeneous sheath model.

Figure 3.49 shows the inhomogeneous sheath surface currents for the same conditions as figure 3.48 except that M = 4. The principle effect of this change is to increase the current fluctuation with ϕ and to increase the magnitude of the curve resulting from the soft boundary condition by about 2 times while having little effect on the magnitude of that for the hard boundary. This increase in the inhomogeneity coupling is somewhat surprising, since the static electron density gradient and the static potential gradient for M = 4, the quantities which produce the coupling, are less than the M=2 values over more than half the outer part of the sheath, as can be seen in the graphs A2, A4 and A5 of Appendix A. Evidently the greater degree of sheath inhomogeneity near the cylinder surface more than compensates for the decreased inhomogeneity in the outer part of the sheath.

In order to determine the effect on the surface currents of varying the cylinder potential, the above calculations were repeated for the hard boundary condition only, for a hydrogen plasma, giving a cylinder potential of -3.06 volts. The results are shown in figure 3.50 where it can be observed that the currents are just slightly larger, by a factor of 1.5 to 2, than the corresponding curves at the higher potential. It can also be seen that the curve for the hard boundary condition with ϕ_c = -3.06 volts and M=4 resembles that of figure 3.7, for the sheathless case more closely than any of the other curves presented. This is reasonable, since the lower cylinder potential and larger M decrease the sheath inhomogeneity, so that in effect this case is now closer to resembling the sheathless model than the others for the lower cylinder potential and smaller value of M. Proceeding further with this line of reasoning, these computations

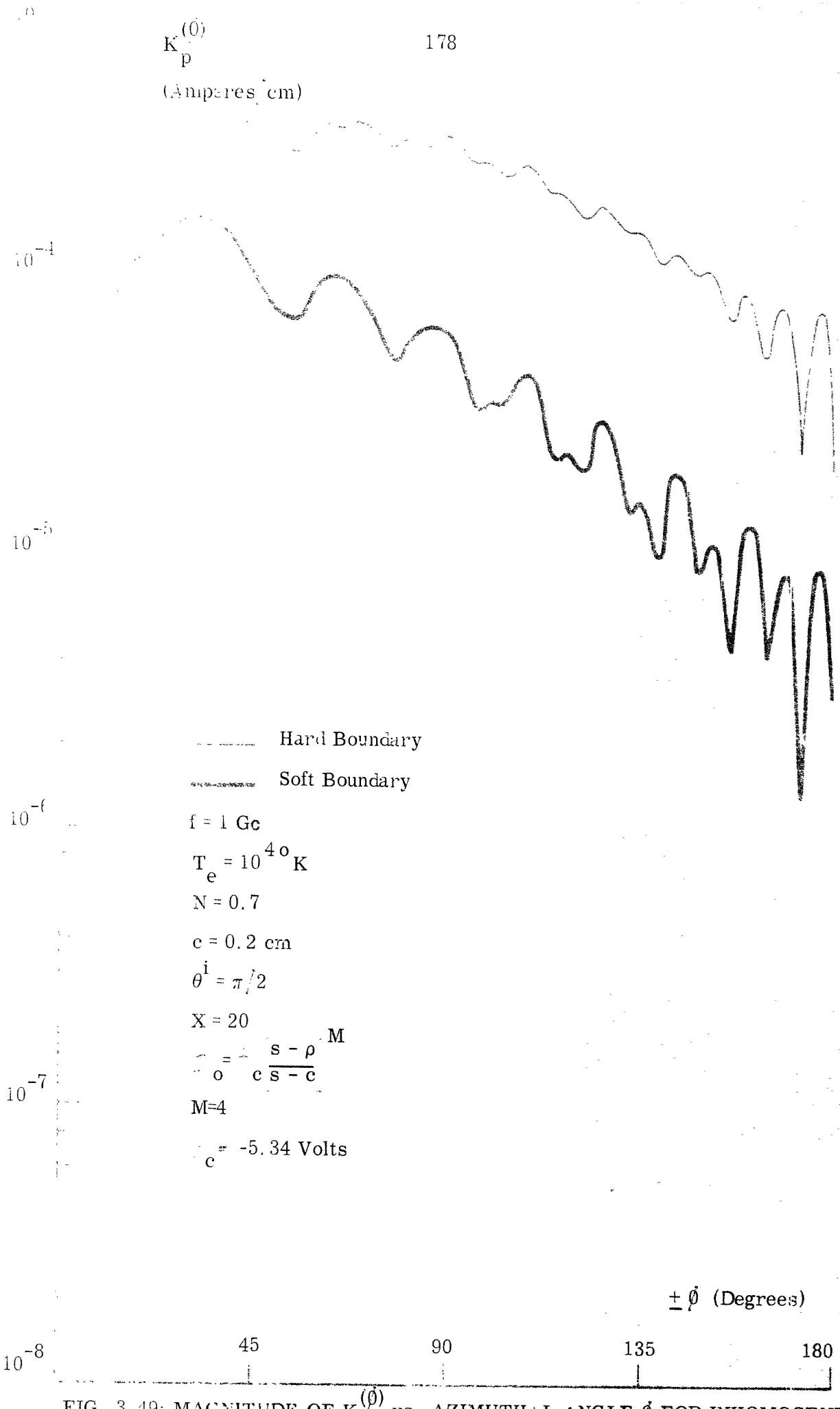

FIG. 3.49: MAGNITUDE OF $K_p^{(\phi)}$ vs. AZIMUTHAL ANGLE ϕ FOR INHOMOGENEOUS SHEATH MODEL WITH M = 4 AND V_c = -5.34 VOLTS

MISSING PAGE

for the hard boundary condition and the hydrogen plasma were repeated for M=10, the expectation being that with the sheath inhomogeneity thus further confined to a narrow region close to the cylinder surface, the surface current obtained from the inhomogeneous sheath should even more closely approach that for the sheathless case. That this is the case can be readily seen from a comparison of figure 3.51 which presents this result with the curve for zero sheath thickness of figure 3.7. There is a striking similarity between them.

While the use of sheath thickness on the order of 20 D_ℓ seems to be the most reasonable choice in light of both the theoretical and experimental information which is available, it is desirable to investigate at least one other sheath thickness to see if the results obtained are very sensitive to this parameter. A sheath thickness of 5 D_ℓ was used for the mercury plasma with M=2 for both the hard and soft boundary conditions. The currents are shown in figure 3.52. Comparing these results with those for a 20 D_ℓ sheath given in figure 3.48 reveals that the currents from both boundary conditions exhibit an increased magnitude and fluctuation as a function of ϕ. The soft boundary current shows the largest increase in magnitude which is consistent with the increased values of the coupling quantities, the static electric field and the static electron density gradient, in the thinner sheath. This would suggest that by making the sheath sufficiently thin, the inhomogeneity coupling would eventually exceed that caused by the hard boundary. Since a sheath thinner the 5 D_ℓ does not seem physically realistic, however, for the insulated plasma-immersed cylinder, this result is of more mathematical than physical interest. It is interesting to note in addition that the

$K_p^{(\phi)}$ (Amperes/cm)

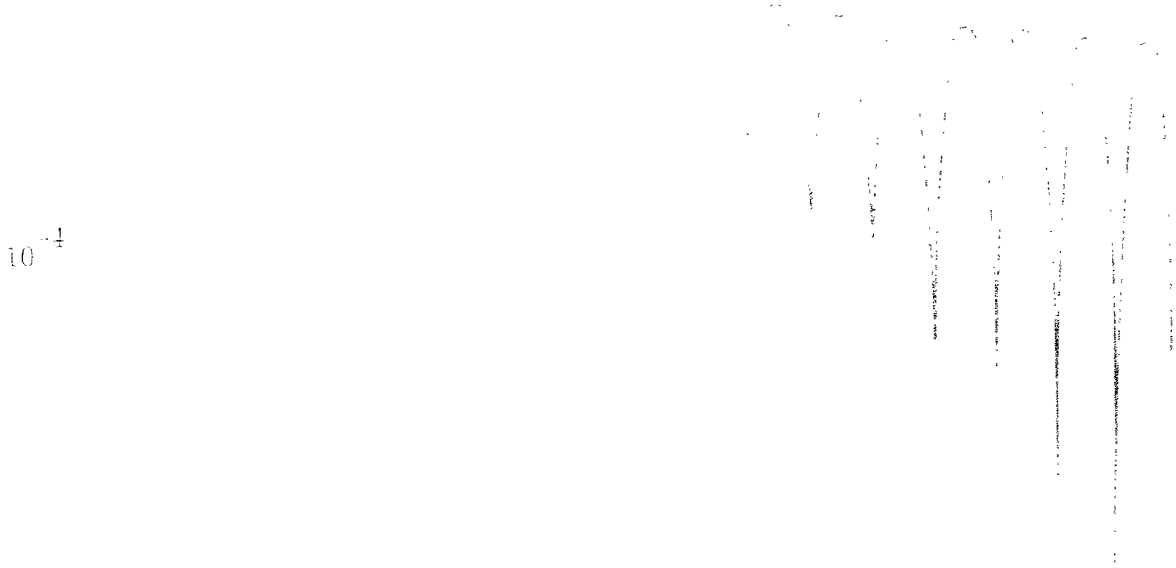

f = 1 GHz

$T_e = 10^4\ ^oK$

N = 0.7

c = 0.2 cm

$\theta^i = \pi/2$

$\rho_s = \frac{M}{c}\,\rho_{s-c}$

$\rho_{s-c} = -3.06$ Volts

M = 10

X = 20

$\pm\phi$ (Degrees)

45 90 135 180

FIG. 3.51: MAGNITUDE OF $K_p^{(\phi)}$ VS. AZIMUTHAL ANGLE ϕ FOR INHOMOGENEOUS SHEATH MODEL WITH M = 10 AND ρ_c = -3.06 VOLTS AND HARD BOUNDARY CONDITION

MISSING
PAGE

curves of figure 3.52 are very similar to those obtained from the vacuum sheath analysis given in figure 3.35.

This concludes the presentation of the surface currents excited by the incident EK wave coming from the inhomogeneous sheath analysis. Since the currents obtained for an incident EM wave from both the vacuum sheath and inhomogeneous sheath analyses were found to be the same for the first three significant figures, no graphs are included here for the latter case. This outcome strengthens the conclusion reached from the vacuum sheath analysis, that the sheath has a negligible effect on the scattering of EM waves from plasma-immersed obstacles. Since the current values produced by the inhomogeneous sheath analysis are in substantial agreement with those arising from the vacuum sheath model, the comparison which was previously made concerning the problem of measuring the EK and EM induced surface currents is essentially the same. There are however interesting results to be obtained from both EM and EK wave incidence and the inhomogeneous sheath model pertaining to power flow and energy density in the sheath which are given in the next section.

3.2.2 A Closer Examination of the Dynamic Sheath Behavior

There are some aspects of the inhomogeneous sheath solutions which are of considerable significance to better understanding the physical processes occurring within the sheath that are not revealed by the surface current results, which necessarily give a kind of spatial average of the dynamic sheath response to the incident waves. Such quantities as for example the dynamic electron velocity and number density, and the electric and magnetic fields, as they vary with position in the

sheath, may provide a more detailed picture of the sheath behavior. In particular the inhomogeneity coupling is one phenomenon that can be more closely examined. There is also the question of whether the requirements on the incident wave amplitude which were necessary for the linearization to be valid for the vacuum sheath are also adequate for the inhomogeneous sheath, since the static electron number density decreases by two or more orders of magnitude as the cylinder is approached through the inhomogeneous sheath.

It is obvious that with the many quantities which vary with both the angular and radial coordinate in the sheath, it is impractical to find the complete spatial variation of each or of even one for a given situation. Rather, it is necessary to limit the examination to some selected paths in the sheath, the results of which may serve to form an overall picture of the sheath behavior. The decision was made to look at the radial variation for some particular azimuthal angles, since the dependence on the radius is of more interest than the ϕ variation in connection with the static sheath which has a functional dependence on radius alone. In addition, the angular variation of the surface currents provides some indication of the dependence of the other dynamic quantities on ϕ.

The dynamic electron number density, and the dynamic electric and magnetic fields are the dependent variables of the differential equations for the inhomogeneous sheath, and consequently are of possible significance as quantities to be investigated as discussed above. While these are quantities which can provide an answer to the question concerning the linearization requirement, they are otherwise of limited usefulness in themselves in arriving at a fuller understanding

of the dynamic sheath behavior. However, they can be used to derive some physically interesting quantities which are perhaps more meaningful and more open to interpretation, in particular as related to the coupling of energy from one wave type to another.

To be specific, we return to the expression for the inhomogeneous sheath given by equation (2.31) of Chapter II, which is reproduced here as

(3.9)

As explained in Chapter II, the terms on the left hand side of this equation give the time average power flow density in the plasma while those on the right hand side yield the time average density of the various types of energy stored in the plasma. In addition the last term on the right also allows the possibility of a gain or loss of energy in the sheath. A comparison of the various energy storage terms should provide some insight into the conversion of the purely EM or EK energy of the incident wave into energy associated with the other type of wave.

Now it was observed in Chapter II, that while both the EM and EK waves in a homogeneous plasma have an electric field and also a dynamic electron velocity field, the EM wave alone has a magnetic field while the EK wave alone has a charge accumulation in the form of a dynamic electron number density. Thus the relative magnitudes of the magnetic and the potential energy density terms of

equation (3.9) should be especially informative about establishing the conversion of the incident wave energy. The remaining terms may provide additional information about the relative importance of the various energy storage mechanisms and their dependence upon the kind of incident wave.

The power flow terms on the other hand, since they do not incorporate field quantities associated with either wave alone when propagating in a non-uniform plasma, are not suited for investigating the conversion problem. It is of interest however, to know the power flow in the sheath in comparison with that of the incident wave to determine what effect the sheath has on the flow of energy towards the cylinder. An integration of the power flow across the sheath-uniform plasma interface also serves to establish the net power flow to the cylinder, which should be zero if the sheath is passive and lossless, and the cylinder itself absorbes no energy. The topics of the linearization requirement, conversion [illegible] and the possible loss of energy in the sheath are considered separately in turn below.

3.2.3 Linearization Criteria in Inhomogeneous Sheath

The linearization of the Boltzmann moment equations requires that the dynamic quantities be small compared with their static counterparts so that products of the dynamic terms may be neglected in the equations. In order to check this the dynamic quantities obtained in the inhomogeneous sheath solution were calculated as a function of radius in the sheath, at angular intervals in the ϕ variable of $\pi/8$ from the front to the back of the cylinder.

As before we regard the linearization condition to be that the amplitude of

the incident wave be such that the dynamic variables do not exceed a fraction, L, of the corresponding static quantity. Upon observing the magnitudes of these quantities, it was found that the linearization criterion established for the homogeneous plasma (see equation (3.7) did not hold for the inhomogeneous sheath. For a fixed value of L=10, it was found that the maximum allowable amplitude, for particularly the incident EK wave, was sensitive to the sheath model and the boundary condition on the dynamic electron number density at the cylinder wall. The use of the soft boundary condition, i.e. complete absorption of the incident electrons, generally resulted in smaller allowable values for V_p^i than the hard boundary, on the order of 10^{-4} for the former compared with 10^{-3} for the latter. Corresponding values for V_e^i are 0.25 and 0.5 respectively.

These values are considerably smaller than those obtained for the homogeneous plasma, which were $V_p^i = 0.178$ and $V_e^i = 159$. They are also less than the values used for the comparison of the EK and EM induced currents and the discussion on the possibility of measuring the currents in section 3.1.3, the values used there being $V_p^i = 0.0332$ and $V_e^i = 1$. The importance of pointing this out is that the surface currents which can be expected to be produced when the power in the incident wave does not exceed the maximum for which the linearized theory applies, may be an order of magnitude or so less than those discussed in section 3.1.3. This has the effect of rendering the measurement of the current produced by the EK wave, as predicted by the linearized theory, somewhat more marginal than over the previous discussion would.

The linearity condition for the homogeneous plasma was based on plane

wave propagation. It is interesting to see what effect the diverging waves in the vicinity of the cylinder may have on it, when there is no sheath. When the cylinder potential was set at zero, to check the sheathless case, it was found that with L= 10, V_p^i and V_e^i were required to be about 50 percent of those values given in (3.7), which was derived for the homogeneous plasma. It may be recalled that this possibility was mentioned in the discussion concerning the derivation of (3.7).

While the question of the linearity condition being satisfied is a necessary one in a discussion of the absolute magnitudes of the various quantities involved, it [illegible] when, as in the subsequent discussion, the relative magnitudes of the effects caused by the EK and EM wave are under consideration. What is more important then is that the incident power flow in the two waves be the same. Since the following discussion is concerned with quantities which are normalized with respect to the incident wave, the only restriction on V_p^i and V_e^i in the following is that (3.6) be satisfied.

3.2.4 Coupled Field Variation in Sheath

The conversion or coupling of EM to EK waves and vice versa in the inhomogeneous sheath and at plasma boundaries is one of the most interesting theoretical aspects of this problem. It is also of practical interest since without the coupling, there would be no excitation of surface currents due to an incident EK wave, and no mechanism for detecting it, in the context of the present study.

Before presenting some of the results dealing with this phase of the problem, it is informative to consider the magnetic energy density of the incident plane EM

wave and the potential energy density of the EK wave. Having some knowledge about the energy densities associated with the incident waves which may be compared with the corresponding energy densities in the reflected waves may provide a basis for establishing the relative coupling between the two kinds of waves.

If we use the formulas given in equations (2.45) to (2.47), (2.51), and (3.9), it is easy to show that the time average magnetic energy density, w_h, for a plane EM wave is given by

(3.10)

Similarly, the time average potential energy density w_p of a plane EK wave is

(3.11)

V_E^i and V_p^i are the magnitudes of the potentials from which the wave fields are obtained. Upon forming the ratio w_h to w_p, we find

(3.12)

This leads to the situation, when $V_p^i = V_E^i$, that w_p exceeds w_h by about $(v_f/v_r)^2$, which is also the square of the ratio of the EM to EK wave length. This is simply an illustration of the fact that, for a wave of a given amplitude, the energy density is inversely proportional to the square of the wave length. Now if we relate V_E^i and V_p^i by equation (3.5) so that the incident waves have equal

power flow density, then

(3.13)

Thus, even with the equal power flow requirement, which is used here, the magnetic and potential energy densities of the plane EM and EK waves respectively vary by the ratio of their propagation velocities.

Because of this large difference between w_h and w_p, a direct presentation of their magnitudes for the purpose of exhibiting the relative coupling between the EM and EK waves is not very [illegible]. Instead we generate normalized energy densities N_h^- and N_p^- defined as the ratio of w_h^- and w_p^- in the sheath to the respective values of w_h and w_p in EM and EK plane waves of equal power flow density. The superscript denotes the kind of incident wave, so that we have

(3.14a)

(3.14b)

An examination of the variation of the normalized energy densities about unity will serve two purposes. First, the normalized energy densities N_h^e and N_p^p provide an indication of the perturbing effects of the cylinder and sheath on the propagation of the incident wave near the cylinder. Second, N_h^p and N_p^e give a measure of the energy converted to the other wave form. For convenience in the discussion, we refer to the former as incident energy densities and the latter as coupled energy densities.

The graphs to be presented show the normalized magnetic and potential energy densities N_h^- and N_p^- as a function of ρ in the sheath at an angle 90^o from the

front of the cylinder. This angle was chosen since at the front of the cylinder, only the field variables associated with the incident wave are non-zero. A check of $\bar{N}_h$ and $\bar{N}_p$ at other values of azimuthal angle revealed no significant difference in their variation as a function of ρ.

Three sets of graphs are shown, for the sheath models that have been used in the current presentation and a cylinder radius of 0.2 cm. There is one graph in each set for the incident e wave and EK wave. Figures 3.53 and 3.54 show $\bar{N}_h$ and $\bar{N}_p$ for the sheathless case and the hard boundary. No corresponding curves are shown for the soft boundary since then there is no coupling. Figures 3.55 to 3.58 present similar results for the inhomogeneous sheath, with M=2 and m_i = 200 atomic mass units (ϕ_c = -5.34 volts), for both the hard and soft boundaries, and a sheath thickness of 20 D_ℓ.

Observation of figures 3.53 and 3.54 shows that for the sheathless case, there is some similarity between the results of e and EK wave incidence. In both cases, the incident energy densities are on the order of unity, while the coupled energy densities are about 5×10^{-3} and of very nearly the same magnitude at the cylinder's surface. Both the incident and coupled energy densities exhibit a different dependence on ρ however.

It is interesting to note that in the case of the incident e wave, N_h^e is approximately unity independent of ρ. This is simply an illustration of the Born approximation, which is that the total field in the vicinity of a scattering obstacle small compared with the wave length is approximately equal to the incident field. This also indicates that no coupling energy from the incident e wave is converted to

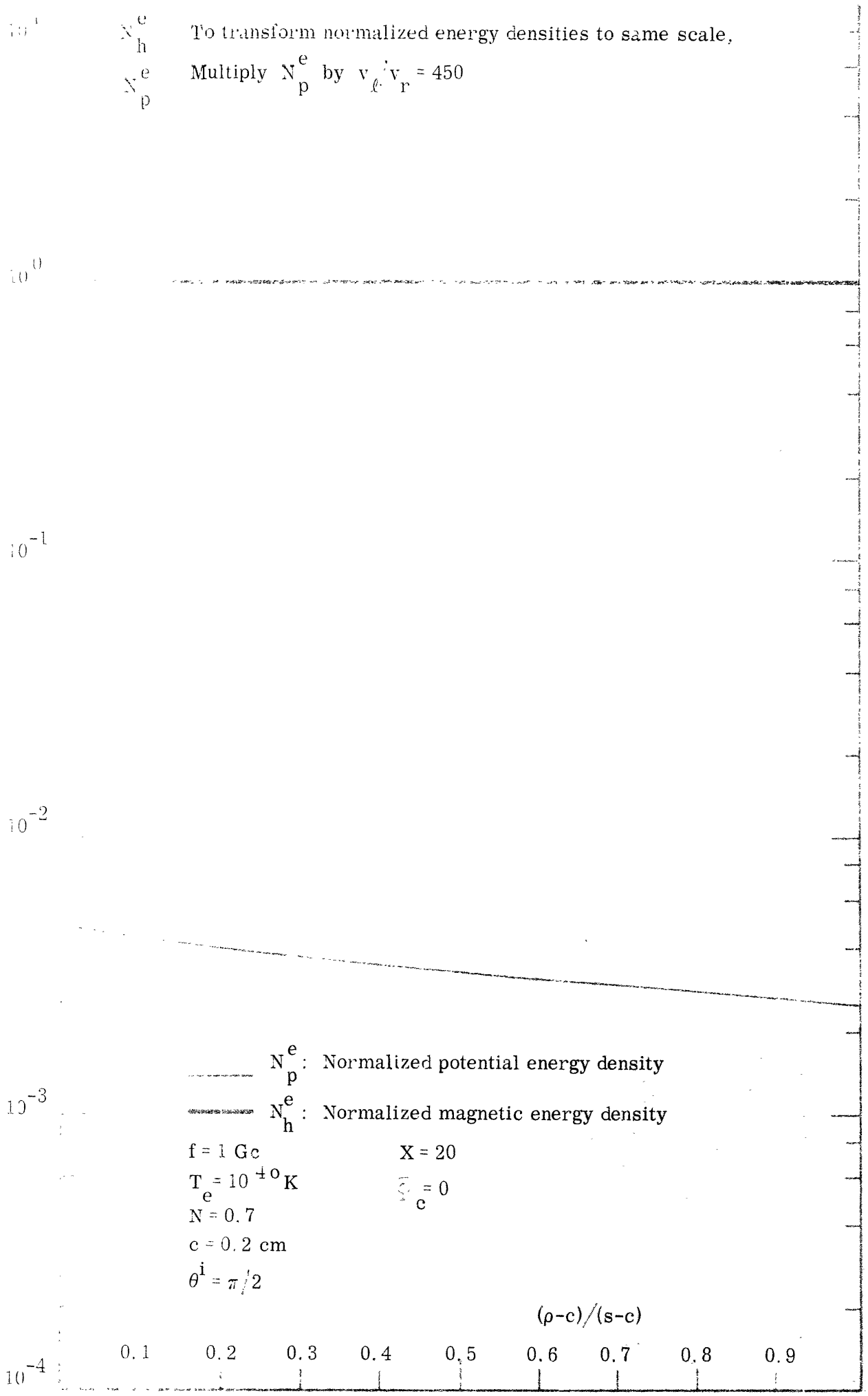

FIG. 3.53: THE NORMALIZED ENERGY DENSITIES N_p^e AND N_h^e vs. RADIAL DISTANCE FOR EM WAVE (e POLARIZATION) INCIDENCE AND SHEATHLESS CASE

MISSING
PAGE

scattered EK energy. A standing wave of N_p^p is produced by interference between the incident and scattered EK waves on the other hand since the cylinder diameter is almost 4 times the EK wave length and the scattered fields are not negligible.

When the coupled energy density terms are considered for the sheathless case, it is seen that N_h^p falls off more rapidly than N_p^e with increasing ρ. This is caused by the difference in the cylinder radius to wave length ratio of the two waves, since the larger this ratio, the more nearly the scattered fields resemble those produced by a planar obstacle.

Consider now figures 3.55 and 3.56 which present results corresponding to those just given but for the inhomogeneous sheath and the hard boundary. Again, the Born approximation is seen to be satisfied, for e wave incidence, as shown by figure 3.55 N_p^e is nearly unity throughout the sheath. The coupled energy density N_p^e now exhibits an oscillatory variation with ρ in the sheath, whereas in the sheathless case it was monotonically decreasing from the cylinder. This illustrates that there is now coupling within the inhomogeneous sheath, since the standing wave pattern requires energy to be propagating in both directions in the sheath. Apparently as a result of the inhomogeneity coupling, the coupled energy density N_p^e is about 4 times larger than it was for the sheathless situation.

When we look at the results for the incident EK wave in figure 3.56, there are observed to be standing wave patterns in both N_h^p and N_p^p, again showing the effect of inhomogeneity coupling. It is interesting to see that variations in N_h^p and N_p^p coincide quite closely in the outer part of the sheath, but that on approach-

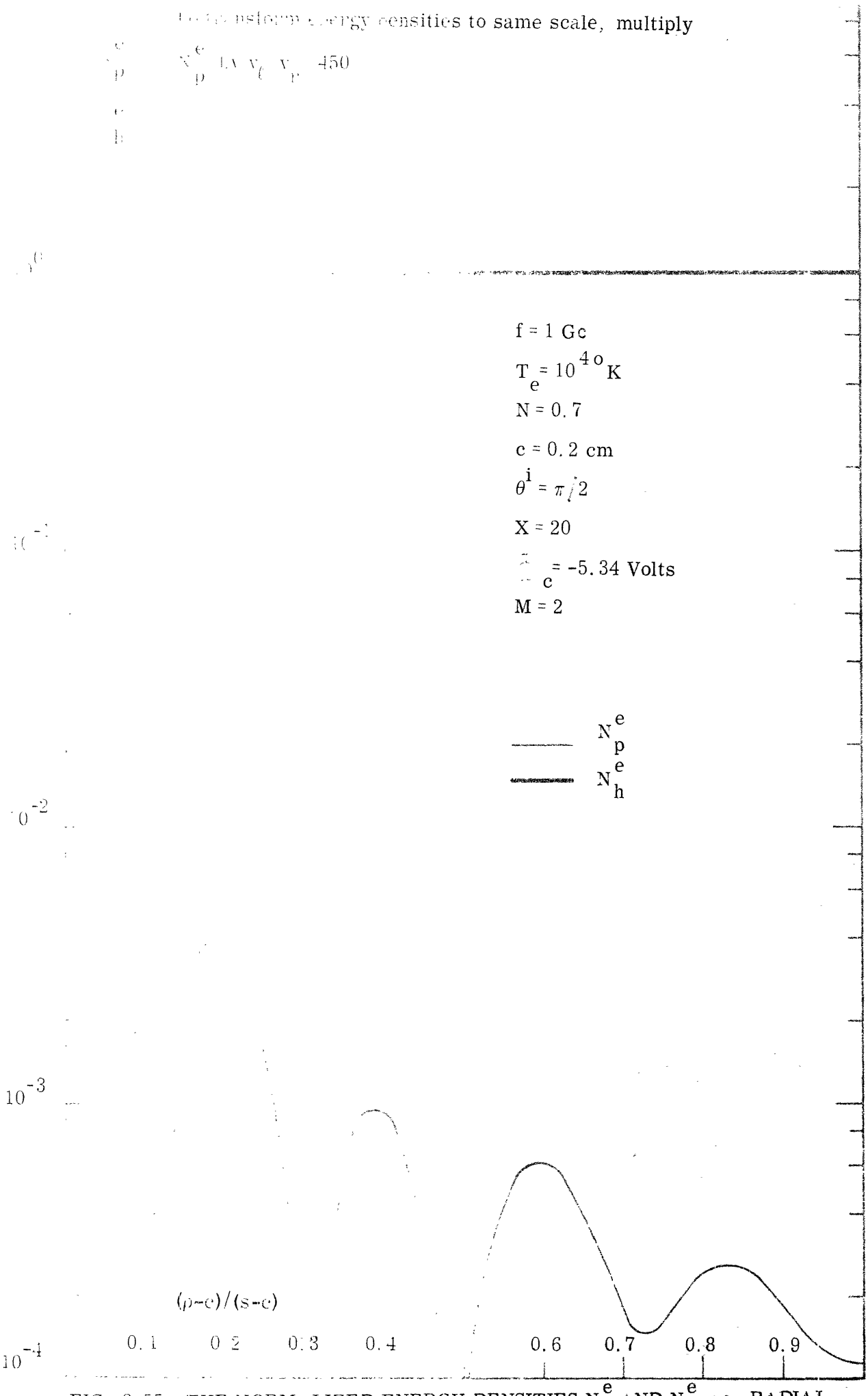

FIG. 3.55: THE NORMALIZED ENERGY DENSITIES N_p^e AND N_h^e vs. RADIAL DISTANCE IN SHEATH FOR EM WAVE (e_p POLARIZATION) INCIDENCE AND INHOMOGENEOUS SHEATH WITH HARD BOUNDARY CONDITION

MISSING
PAGE

ing the cylinder surface, N_h^p increases in nearly the same way as for the sheathless case. This indicates that the magnetic field near the cylinder is principally determined by the contribution from the boundary coupling, while farther out in the sheath, the inhomogeneity coupling effect is predominate. The increase in N_p^p upon nearing the cylinder would seem to be due to the fact that the potential energy density is inversely proportional to the static electron density, which of course becomes smaller with decreasing ρ. Since the increase in N_p^p is on the order of the decrease in static electron density, the implication is that the dynamic electron density is relatively unaffected by the sheath. This is a question which is considered further in the following.

Finally we direct our attention to figures 3.57 and 3.58 which show the results from the inhomogeneous sheath and soft boundary condition. It is strikingly evident that the soft boundary condition produces field variations in the sheath quite different from those obtained with the hard boundary especially for the EK wave incidence. In the case of the incident e wave, the difference is not so great, and there is again substantiation of the Born approximation. (Actually N_h^e may become less than 1.0, on the order of 0.99, a difference too small to show on the graph). The coupled energy density N_p^e however, is now about 400 times larger than that for the hard boundary. It is nearly the same at the cylinder as that produced in the sheathless case with the incident EK wave, but decays more quickly away from the cylinder, with more cycles of amplitude variations.

The situation where the EK wave is incident is characterized by extremely large increases of N_h^p and N_p^p with increasing radius contrary to that shown by the

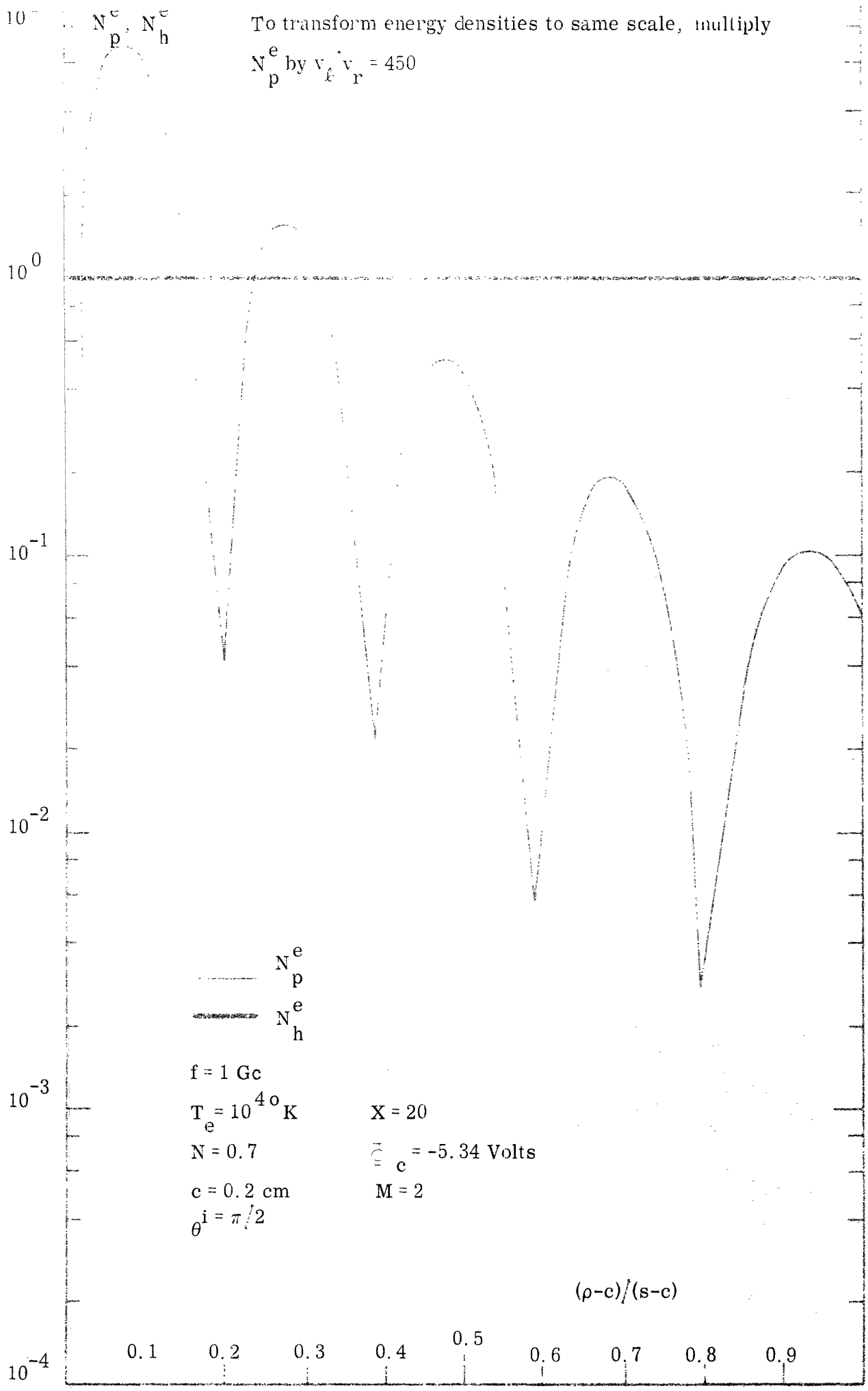

FIG. 3.57: THE NORMALIZED ENERGY DENSITIES N_p^e AND N_h^e vs. RADIAL DISTANCE IN SHEATH FOR EM WAVE (e POLARIZATION) INCIDENCE AND INHOMOGENEOUS SHEATH FOR THE SOFT BOUNDARY CONDITION

MISSING
PAGE

hard boundary results. Both of the normalized energy density terms now exceed unity at the sheath-uniform plasma interface, indicating a large accumulation of energy in the outer part of the sheath. Again, as for the hard boundary and inhomogeneous sheath, N_h^p varies in the same way through the sheath as N_p^p.

Now with the use of the soft boundary condition, there is only the inhomogeneity coupling mechanism in the sheath to produce the coupled energy densities observed. And yet, as is shown in the preceding graphs, the coupled energy densities can exceed those which are obtained when the additional coupling mechanism due to the boundary is included by the use of the hard boundary condition. It is further apparent that the soft boundary has much more effect on w_p than w_h, which is reasonable since the dynamic electron density is more intimately associated with the former, its effect on the latter occurring only through the coupling. This conclusion is based on the fact that for e wave incidence, w_h is unaffected by the change in boundary conditions, while for EK wave incidence, w_h follows the variation in w_p.

Thus for the particular sheath model that has been studied, we find that complete absorption of the electrons at the cylinder wall can produce effects which are substantially different from those obtained when the electrons are reflected, particularly in the sheath region, but which may also extend out into the uniform plasma In order to investigate the latter, some calculations were performed using a potential variation with M=10. Thus the sheath inhomogeneity is confined more closely to the cylinder, and the numerical integration over the outer part of the sheath is effectively carried out in the uniform plasma. It was

found for EK wave incidence that the soft boundary then produced N_p^p values close to those of figure 3.58 near the cylinder, but which decreased in the outer part of the sheath to about 10^{-4} of the maxima near the cylinder.

Some further calculations were carried out which differed from the sheath model used for figures 3.53 to 3.58 by incorporating a sheath 5 rather than 20 D_ℓ thick. The results of the EK wave incidence on such a sheath are shown for both the hard and soft boundaries in figures 3.59 and 3.60. These graphs exhibit variations of N_h^p and N_p^p in the sheath quite different from those for the 20 D_ℓ thick sheath. In particular, there is not the large increase in the energy densities that were found for the thicker sheath and the soft boundary.

The overall picture provided by the results above is one which shows both the inhomogeneous sheath and the boundary to strongly influence the behavior near the cylinder of the fields which are produced by an incident EK wave. Of these two influences, the soft boundary dominates the behavior of the dynamic electron number density in the sheath. The soft boundary condition leads to increases in the dynamic electron density with increasing radius, while the hard boundary has little effect on the dynamic electron density in the sheath. Significantly less effect is found to be exerted by the sheath and boundary on the fields arising from e wave incidence. This is particularly true of the magnetic energy density, which was found to be nearly that of the incident wave, indicating relatively little energy transfer to a scattered EK mode. The conclusion that the sheath and the compressibility of the plasma have negligible effect on the scattering by the cylinder of incident e plane waves, which was previously

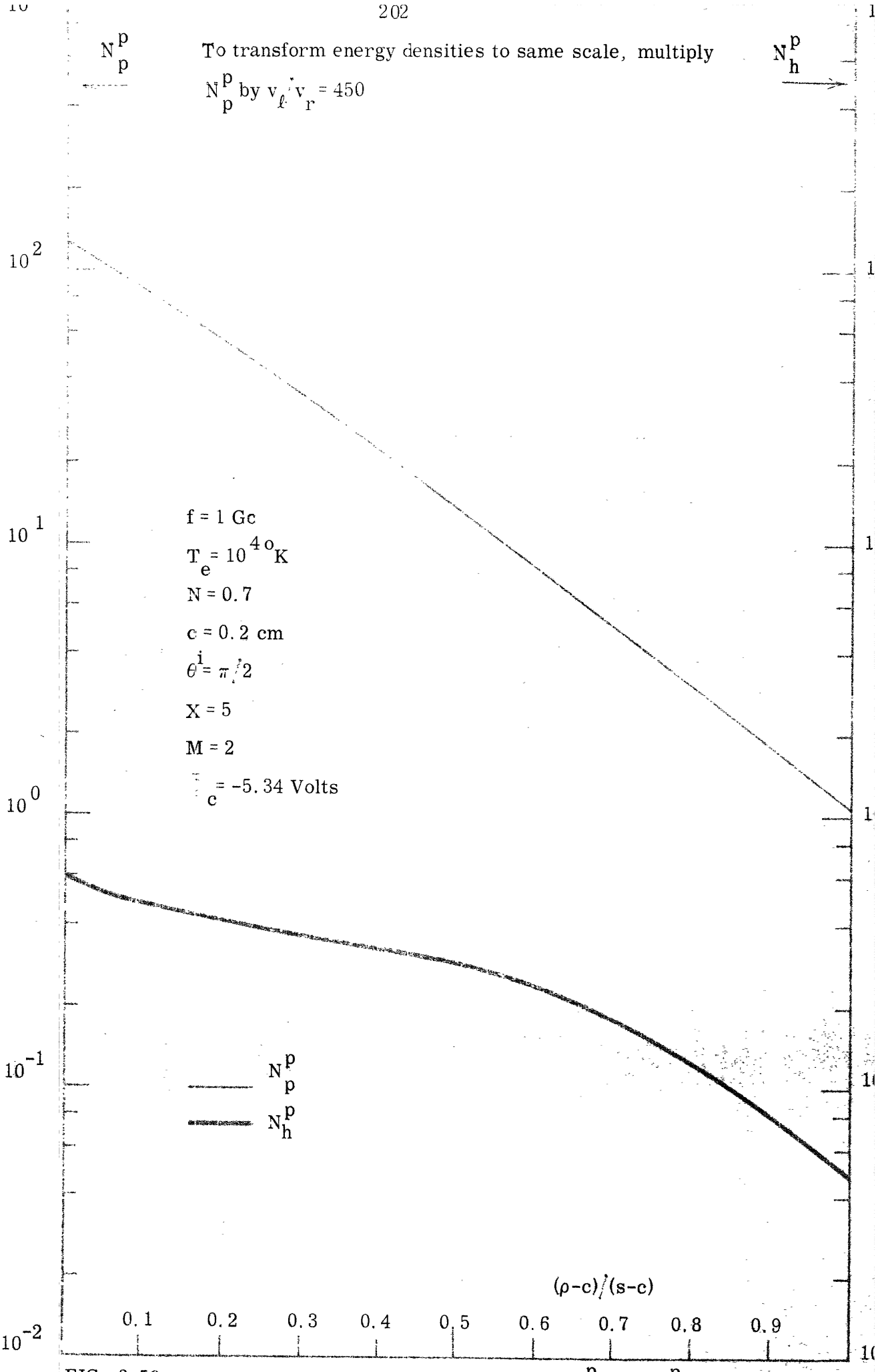

FIG. 3.59: THE NORMALIZED ENERGY DENSITIES N_p^p AND N_h^p vs. RADIAL DISTANCE IN SHEATH FOR EK WAVE INCIDENCE AND INHOMOGENEOUS SHEATH WITH X = 5 AND HARD BOUNDARY CONDITION

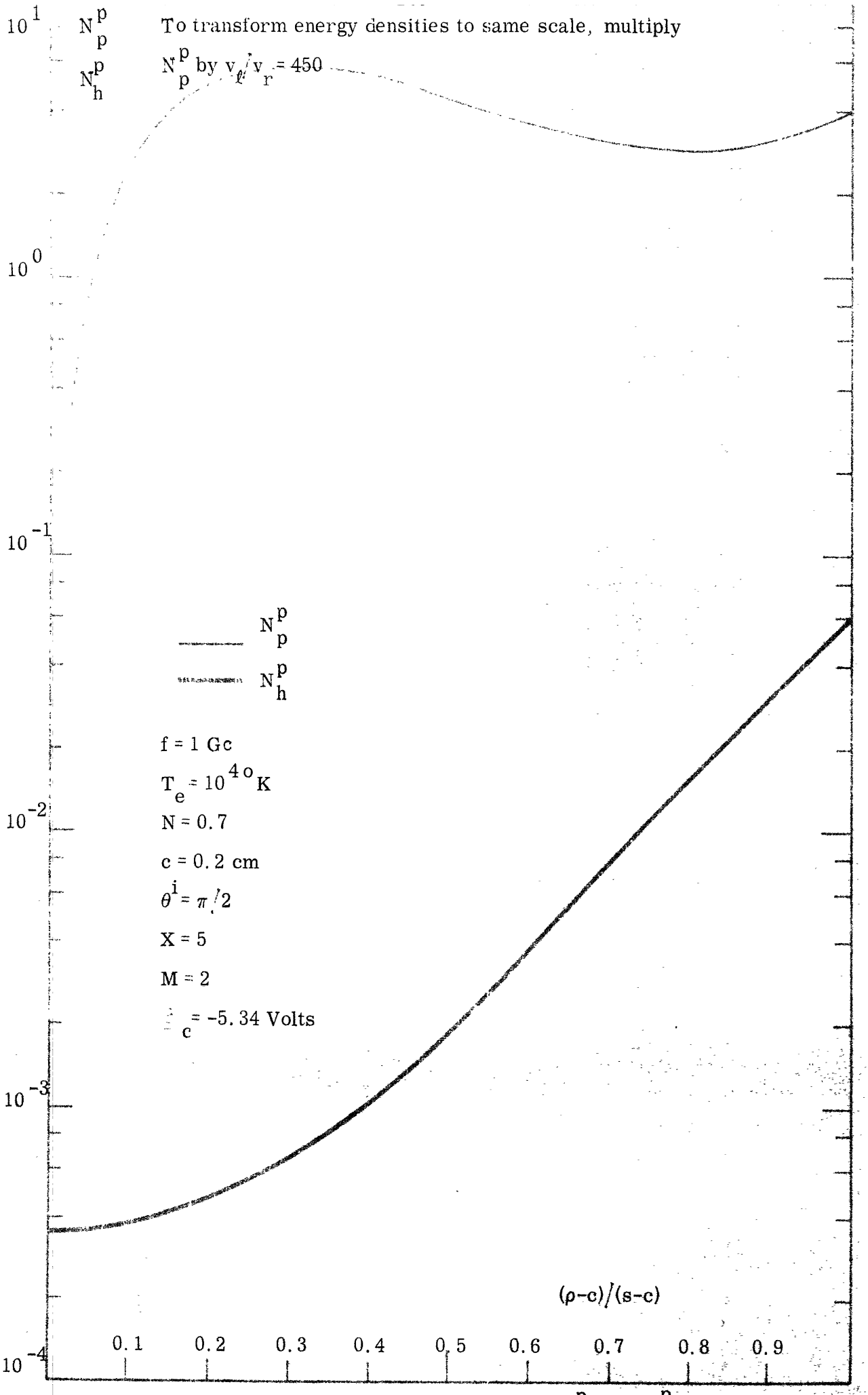

FIG. 3.60: THE NORMALIZED ENERGY DENSITIES N_p^p AND N_h^p vs. RADIAL DISTANCE IN SHEATH FOR EK WAVE INCIDENCE AND INHOMOGENEOUS SHEATH WITH X=5 AND SOFT BOUNDARY CONDITION

reached on the basis of the surface currents, is thus further reinforced from the energy density results.

A physical interpretation of the [illegible] accumulation in energy density in the sheath is that the cylinder and sheath have a focusing effect on the incident EK plane wave, causing energy concentrations appreciably larger than those found in the incident wave. Another way of looking at this is in terms of the effective area of the cylinder and sheath, which may become much greater than the physical area, as evidenced by the energy accumulation. This picture is also true on a particle basis, as the effect of the cylinder on the plasma may extend beyond its physical boundary.

We have as yet made no quantitative statement about the relative conversion of EK to EM energy and vice versa. It is difficult to give a definite answer to this question on the basis of the previous results because of the energy density focusing effect. This is especially true of the incident e wave. Thus there is seen in figure 3.57 a situation where N_p^e exceeds unity while N_h^e is nearly unity, indicating that a relatively small portion of the total energy has been removed from the incident e wave. It appears obvious however, that a small proportion, certainly no more than 1 percent of the incident e energy is converted to scattered EK energy, since the magnetic energy density is in all cases within 99 percent of that in the incident wave.

On the other hand, when the incident EK wave is considered, it seems reasonable that since it is more affected by the focusing action of the sheath and

cylinder than the EM wave, a direct comparison of N_h^p and N_p^p should give a meaningful measure of the conversion efficiency. Proceeding on this premise, it may be verified from the graphs of figures 3.54, 3.56 and 3.58 that in no case does the normalized magnetic energy density represent more than 1 percent of the normalized potential energy density. What is especially interesting to observe is that, at the surface of the cylinder, the largest value of N_h^p is obtained in the sheathless case, with the smallest value occuring for the soft boundary and the inhomogeneous sheath. This has of course been previously commented on in the discussion of the surface currents. By way of contrast, at the sheath-plasma interface the situation is reversed, and N_h^p is a maximum for the soft boundary condition, as a result of the rapid increase of N_h^p with increasing radius. This situation is somewhat perplexing, but may perhaps be explained by the following reasoning.

A prominent feature of N_p^p in figure 3.58 is that only one maxima occurs as a function of radius and that is located near the cylinder. As a consequence, it seems logical to conclude that the incident and reflected waves of potential energy are of about the same amplitude only near the cylinder. Since N_h^p increases on approaching the sheath interface, a further conclusion is that it is the outward traveling component of N_p^p which is predominate in the outer part of the sheath. This is based on assuming that the energy converted from potential to magnetic propagates in the same direction as the original energy, so that if the inward travelling part of N_p^p were larger, N_h^p would increase on approaching the cylinder.

If the proceding logic is correct, then there must be regions in the sheath

where the energy flow is predominantly towards the cylinder, to supply the flow away from the cylinder in other areas. A complete picture of this phenomenon would require mapping the power flow over the entire sheath region. The calculations which would be required to accomplish this are beyond the scope of the present investigation.

3.2.5 An Examination of Possibility of Ordered Energy Absorption by Sheath

A highly significant feature that appears in this analysis is the implication in the Poynting's theorem given in equation (2.32), that there exists a possibility for a gain or loss of energy in the sheath, by the incident wave. As was exaplained in connection with the derivation of this equation, we use the term loss to mean a net decrease in the ordered energy content of the plasma, varying at the frequency of the incident wave. Gain indicates the converse, a net increase of the ordered energy content. We shall in the following use loss to cover both eventualities, since gain can be described then as a negative loss. Used in this context then, there is no loss or gain of energy associated with the production of scattered EK radiation as a result of an incident EM wave, but rather a conversion of the ordered energy from one mode to another.

The implication for a loss of energy by the incident wave in equation (2.32) lies in the interpretation of the imaginary parts of the equation to represent stored or reactive energy and the real parts to represent real power flow. Thus a non-zero real part of the left hand side of (2.32) shows there to be a loss of power in the sheath since the net power flow across the sheath-uniform plasma interface is not zero. We are thus interested in examining

(3.15)

There is no surface integral over the cylinder surface since the boundary conditions there make the power flow into the cylinder equal to zero. Since (3.15) has been obtained using an outward pointing surface normal vector, we interpret a minus result from the integration to indicate a loss of power to the sheath from the incident wave.

It should be noted that the right hand side of (3.15) provides the loss mechanism for extracting energy from the incident wave, while the left hand side merely provides an inflow of ordered energy into the sheath to balance the losses which occur in the sheath. The term on the right hand side of (3.15) is thus a cause and that on the left an effect in the cause-effect relationship between energy loss and power flow. For this reason, while (3.15) requires both integrals to be numerically equal, we refer to the right hand side as the loss term.

The loss term was investigated by numerically integrating the power flow term on the left side and the loss term on the right side of (3.15) respectively over the sheath surface and volume. It is unnecessary to integrate both sides of the equation, since the same answer should be obtained from each. This however provides a check on the consistency of the numerical results.

We express the sheath loss per unit cylinder length by forming the ratio

of the net power flow across the sheath interface to the power flow density in the incident plane wave multiplied by the cross sectional sheath area per unit

(3.16)

where either V_p^i or $V_e^i = 0$. less than one indicates that the sheath's equivalent cross sectional area for absorbing the incident wave energy is less than its physical area, while greater than one indicates the converse.

These calculations were performed for several sheath models for both EK and e wave incidence. The results show that for e incidence regardless of the sheath model. Similarly there is found for EK wave incidence, and the hard boundary condition also. These numbers are too small to be of significance and most likely represent the limitation on the computer accuracy. They are useful in that they indicate the sheath to be lossless for practical purposes in these particular cases.

On the other hand, when the soft boundary condition is used for EK wave incidence, there is a very significant difference in the results, and is found to have values which range from 10^{-3} to 10. was found to vary

with sheath thickness, cylinder radius and the value used for the exponent of the potential distribution in the sheath. The significance of this result is discussed below.

Some interesting results were obtained by calculating both the real and imaginary parts of the volume integral appearing in (3.15), which is

(3.17)

The real part, to which the sheath loss is proportional, was found to be 10^{-6} or so, of the imaginary part for EK wave incidence and the hard boundary condition. Use of the soft boundary condition made little change in the imaginary part but increased the real part by 2 to 6 orders of magnitude. This means that in the case of the hard boundary the power flow across the sheath interface is almost wholly reactive, and the sheath volume serves primarily to store the energy from the incident wave.

The important point here is that the ratio of the real to the imaginary parts of (3.17) depends on the boundary condition used. Since the real and imaginary parts of (3.17) are obtained by simply rearranging the real and imaginary parts of the product nv, the change in this ratio with boundary condition appears to be numerically significant. This is particularly so because the change is larger in orders of magnitude than the number of significant places which are accurate in the calculations. The possibility for a loss of energy in the static sheath appears then to be a real one, rather than merely resulting from uncertainties in the cal-

culations. A more thorough investigation of this problem would have to be undertaken before definitive answers could be obtained, an analysis which was beyond the intended scope of this study.

Some results obtained by Paskovich and Kino (1964) are relevant to this discussion. A theoretical formulation of the variation of rf fields in a plasma sheath for a plane boundary was carried out based on an integration of the collisionless Boltzmann equation. An integral equation was developed for the rf electric field in the sheath which is related to the perturbed electron distribution function and the static sheath potential. The numerical results obtained from this analysis also indicate the possibility for a gain or loss of rf energy in the sheath.

Now, there is no question of a net gain or loss of energy by the system as a whole, since the total energy must be conserved. This being so, it is necessary to look into this question more carefully, to determine the possible sources or sinks of energy that may be associated with the cylinder and sheath. This is especially important since the present formulation does not show the other end of the energy exchange mechanism.

There may seem to be some inconsistency in a system of equations which admits of a loss of energy without indicating the new form into which this energy is converted. That this is not the case is illustrated by the interpretation of the loss term in connection with EM wave propagation in a medium with a complex permittivity. A term appears in the derivation of Poynting's theorem which is related to the imaginary part of the permittivity, ϵ', of the medium. This term

leads to a net flow of EM energy into the volume proportional to ϵ'. This is interpreted to mean that energy is lost from the EM wave propagating in such a medium, through the mechanism of the complex permittivity. It is informative to explain the loss of the ordered energy from the EM wave on the basis of there being in-phase components of the electric field and current flow as a result of ϵ''. A further analysis of the current flow in this situation leads to the conclusion that the ordered EM energy is dissipated as heat in the medium, and is thus randomized. Since the Poynting's theorem was derived to account only for the flow of ordered energy in the EM mode through the medium, then it is physically necessary that any transformation of energy to a form other than that in the given EM mode be manifested in a loss term. It is important to emphasize that the loss term cannot tell us what new form the energy lost from the EM wave will take, although it may provide a good indication of this. That can only be established by formulating a Poynting's theorem which takes into account all the types of energy appearing in the system.

It is instructive to examine more closely the loss term, given in (3 15), to see if some physical insight will provide a clue to the question of the ordered energy loss. We have previously observed that this term may be regarded from two viewpoints. In the first, there is observed to be a current flow in the sheath, arising from the ordered electron motion, $n\underline{v}$, which is acted upon by the static sheath electric field. Depending upon the relative directions of current and field, there may be a loss of energy either by the field or the ordered electron flow. The other viewpoint looks at the displacement of the sheath electrons from their

equilibrium positions as a change in their potential energy, again corresponding to a gain or loss, depending on the displacement relative to the field.

In either of these two equivalent viewpoints, there is seen to be a means of exchanging energy between the ordered electron motion and the static field. Now it has been an assumption all along that while the dynamic fields in the sheath are dependent on the static sheath, the converse is not true. It would seem that this assumption may have to be re-examined. This is because the EK wave propagates in a homogeneous plasma by a process of energy exchange between ordered kinetic energy and potential energy caused by charge accumulation. When the wave encounters an inhomogeneous region such as the sheath, with a static electric field, the kinetic energy can be exchanged with the static field as well as the potential energy of charge accumulation. The wave therefore can upset the energy distribution of the static sheath. At first thought, it might seem that such an effect would be inconsistent with the linearization of the original equations, but the same term can be obtained without recourse to linearization.

There are two observations which can be made here. First, it is apparent that whether or not there is a net transfer of energy to the sheath is strongly influenced by the static sheath itself, since the overall effect is obtained by an integration of (2.33) over the sheath volume. Second, assuming that there is such net energy transfer, then it must be concluded that the static sheath is indeed changed or perturbed by the incident wave. The change involved depends on how efficiently the sheath is able to redistribute the energy it receives from the wave.

a steady state should be attained where the redistribution by the sheath of the energy received from the wave proceeds at the same rate at which it is absorbed.

The way in which the sheath might redistribute this energy may be conjectured to occur in two ways, one involving the ions and the other the electrons. We have discussed in connection with the static sheath the motion of the ions under the influence of the accelerating potential in the sheath. The ions are the recipients of the kinetic energy lost by the plasma electrons energetic enough to reach the cylinder. There is in other words, an energy exchange mechanism at work in the static sheath which leads to the kinetic energy of the electrons being transferred to the ions. Ultimately, this energy reappears in the form of higher temperature neutral particles which result from the recombination of ions and electrons at the cylinder wall. Thus, an increase in cylinder potential brought about by the absorption of incident wave energy by the sheath could result in raising the temperature of the neutral gas particles.

An alternative to the mechanism discussed above involves the interaction of the plasma electrons with the perturbed sheath. As the individual electrons move through the sheath they are subject to the local potential. When they come under the influence of the perturbation in potential caused by the incident wave, their paths are altered in a different way than would be the case in the unperturbed static sheath. If the electrons are moving faster than the fields of the incident wave, they can, as a result, move into areas where their dynamic motion does not match that of the wave fields, thus leading to a decrease of ordered energy. The important point is that the sheath field provides a mechan-

ism for redirecting the electron motion with respect to the incident wave, or in other words, it effectively brings electron collisions into the picture.

An inherent limitation of the hydrodynamic approach is that the electron motion is averaged so the theory cannot show effects on a microscopic scale. It becomes apparent here also, that our neglect of the heat flux tensor in the plasma cannot be strictly correct when there are losses, for the ordered energy lost in the sheath by the wave must be removed from the sheath by a heat flow arising from a temperature gradient.

CHAPTER IV

CONCLUSIONS AND RECOMMENDATIONS FOR FURTHER STUDY

4.1 Summary and Conclusions

A theoretical investigation of the surface currents excited on a plasma-immersed metal cylinder by incident plane electromagnetic and electrokinetic waves has been carried out. The associated problem of the static plasma sheath has also been examined. For normal incidence, the actual inhomogeneous plasma sheath has been accounted for, while for arbitrary incidence, the sheath has been replaced by a free space layer, called the vacuum sheath.

It has been shown that the static electron velocity in the inhomogeneous sheath surrounding the insulated cylinder has a negligible effect on the static electron density variation in the sheath. It was also shown that the effect of the static electron velocity on wave propagation within the sheath is negligible in comparison with the effect of the sheath inhomogeneity.

The most significant finding of the vacuum sheath analysis is the large attenuation which may be caused by the sheath of the surface currents excited on the cylinder by an incident electrokinetic wave. The attenuating effect of the sheath on the currents can be as great as 60 db compared with the currents when there is no sheath, depending on the angle of incidence and sheath thickness. The currents excited by the electromagnetic wave on the other hand are found to be unaffected, for practical purposes, by the vacuum sheath. In addition, the compressibility of the plasma also has little effect on the currents due to the electromagnetic wave. These results for EM wave incidence are based on cylinders with radii small compared with the EM wavelength, the case for which the numerical calculations have been performed.

An analysis of the inhomogeneous sheath for normal wave incidence further demonstrates the negligible effect of the sheath on the electromagnetically induced currents. The currents due to the electrokinetic wave for the hard boundary condition and an inhomogeneous sheath 20 D_ℓ thick are found to be in good agreement with the results of the vacuum sheath analysis for a sheath 5 D_ℓ thick. This result can be taken to indicate the credibility of the vacuum sheath anaylsis for oblique wave incidence.

Consideration was also given in both analyses to the effect on the surface currents of the boundary condition on the normal electron motion at the cylinder surface, as represented by the surface admittance Y_B. It was observed that when $Y_B=0$, corresponding to a perfectly reflecting or hard boundary, there are contributions to the surface current excited by the electrokinetic wave from both the boundary and sheath inhomogeneity. The other extreme value of $Y_B=\infty$, corresponging to the soft boundary, results in a surface current due to the sheath inhomogeneity alone, the boundary contribution then being zero. It was found that the hard boundary was more efficient in contributing to the surface current than the sheath inhomogeneity, for the inhomogeneous sheath models investigated.

We may briefly summarize the results of the surface current calculations with the following remarks:

(1)* The sheath and plasma compressibility can be neglected when the scattering of electromagnetic waves from a cylinder which is small in diameter compared with the electromagnetic wavelength is considered.

*Calculations performed after the writing of this thesis show this result to hold for a cylinder with a diameter of 4 (free space) EM wavelengths.

(2) The electrokinetic wave is screened from the cylinder by the sheath, with the screening effect increasing as the angle of incidence measured from the cylinder axis, is decreased.

(3) The electrokinetic wave is less efficient than the electromagnetic wave in exciting surface currents even when the screening effect of the sheath is not taken into account, by a factor of 10 to 500. It thus appears that detection of the electrokinetic wave in a background of electromagnetic radiation by measuring the surface currents would be difficult to accomplish.

A further significant finding of the inhomogeneous sheath analysis is that the potential and magnetic energy densities in the sheath are strongly influenced by the value of Y_B. In particular, the soft boundary condition leads to values of potential energy density in the sheath much larger than that in the incident electrokinetic wave. This indicates that the perturbing influence of the cylinder on electrokinetic wave propagation in the plasma extends far beyond the cylinder's physical boundary. In addition, there is found to be the possibility for the loss of energy from the incident electrokinetic wave in the sheath when the soft boundary condition is used.

When we compare the results obtained in this study for the scattering of electromagnetic waves from a plasma immersed cylinder with the results of Parker et. al. (1964) for the inverse problem, the scattering of electromagnetic waves from a plasma cylinder, an interesting observation can be made. For Parker's problem, both the plasma compressibility and sheath effects are required

to account for the resonances in the scattering properties of the plasma cylinder, whereas their effects are negligible concerning the scattering properties of a plasma immersed cylinder which is small compared with the electromagnetic wavelength. This implies that the treatment of electromagnetic wave scattering from obstacles in contact with plasmas requires allowing for inhomogeneity and compressibility effects in the plasma only if the geometry is such that standing electrokinetic waves may be excited in the plasma by the electromagnetic wave.

It is interesting to observe that the production of evanescent electromagnetic waves by electrokinetic waves incident on a plasma discontinuity has been previously pointed by Kritz and Mintzer (1960), Tidman and Boyd (1962), Cohen (1962b) and Fedorchenko (1962). The significance of this as far as screening the electrokinetic wave from surfaces bounding the plasma has not been mentioned however.

Finally, we should inquire as to the possible significance of the results obtained in this study in relation to the problem of the plasma immersed antenna. The analysis of Cohen (1962b) predicts very large effects, due to the excitation of the electrokinetic wave, on the radiation resistance of a linear filamentary current source in a plasma. The present results, as mentioned above, show however that the electrokinetic wave has little effect on the electromagnetic scattering properties of the cylinder. We can infer from this that the effect of the electrokinetic wave on the impedance characteristics of the plasma immersed cylinderical antenna would also be small. Wait (1965) arrived at this conclusion for an antenna large compared with the electrokinetic wave length.

4.2 Recommendations for Further Study

The results obtained in this study suggest some areas for further investigation. One of the most vital points which needs additional effort is the boundary condition on the electron motion at the cylinder surface. This is a question the importance of which has been recognized for some time, but little clarification concerning it has been accomplished. It appears that it would be worthwhile to carry out a parametric study on the surface admittance for the electrons, Y_B, concerning its effect on the surface currents and the energy distribution in the sheath.

It also would be valuable to extend the inhomogeneous sheath calculations which have been performed here to the case of oblique incidence. This would be especially important to further verify the screening effect of the sheath as obtained from the vacuum sheath analysis.

One additional significant subject that should be studied is the radiation by a cylindrical antenna immersed in a plasma. It has been conjectured here that, contrasted to a current filament in a plasma, a physical cylindrical antenna immersed in a plasma would not strongly couple to the electrokinetic wave. Before this can be accepted without reservation, a careful analysis of the radiation problem for the plasma immersed cylinder must be performed. Wait (1965) has recently begun an analysis of such a problem which does indicate the electrokinetic wave to exert only a minor influence on the cylindrical antenna. His treatment however neglects the inhomogeneous sheath. The inhomogeneous sheath should be taken into account before any definite conclusions are drawn from such an analysis.

Finally, a theoretical analysis of the experiment proposed in Appendix D should be performed, based on the formulation of this study. Numerical results obtained from such an analysis should indicate the likelihood for this experiment to be carried to a successful conclusion. If the indications are indeed that this is the case, the performance of such an experiment would seem to offer an attractive means for checking the validity of the theoretical formulation.

APPENDIX A

ANALYSIS OF ELECTRON NUMEER DENSITY IN STATIC SHEATH

An analysis of the static sheath problem is basically one of finding the potential in the sheath via Poisson's equation and integrals over the velocity of the electron and ion distribution functions. The difficulty in accomplishing this is determined primarily by what assumptions one is willing to make about the ion and electron distribution functions. Additional complications arise when electron generation is allowed for. Finally, the geometry of the plasma configuration, whether it is an internal or external problem which is being considered, also has a strong influence on the complexity of the analysis.

The intent here is not to solve the static sheath problem. Rather what is desired is to make use of some of the results previously obtained in order to specialize them to the particular problem of the plasma-immersed cylinder. For this reason, the potential variation in the sheath is not solved for here, but is assumed to be given by

(A.1)

The experimental work of Gabor et al (1955) and Harp and Kino (1964) confirm the validity of (A.1) with M 2, while the theoretical analysis due to Self (1964), La Frambois (1964) and Eernstein and Rabinowitz (1959) indicate that M is about 4.

It is an easy matter then to find the static sheath electron density from (A.1) and using a Maxwellian electron velocity distribution with a superimposed static drift velocity given by

(A.2)

where

(A.3a)

(A.3b)

(A.3c)

$\underline{v}_o$ is the static electron drift velocity towards the cylinder caused by electron-ion recombination at the cylinder wall. $N_e(\rho)$ is the usual Boltzmann distribution for particles in a potential well.

The quantities which we want to find are the electron density and velocity in the sheath. An integration of (A.2) over the velocity between the appropriate limits will yield the number density, while a similar integration of $f_e \underline{u}$ will give the velocity. The integration limits on u_e are $-\infty$ and u_m where u_m is the truncation point of the distribution function, determined by a deficit of fast

electrons reflecting from the sheath. (This method will be referred to as the truncation approach.) If the sheath is thin compared with the radius of curvature of the cylinder, so that at any point in the sheath all electrons which have sufficient radial velocity to reach the cylinder do so, then u_m is given by

(A.4)

When the integration which leads to the electron number density and velocity is carried out, there is obtained

(A.5)

(A.6)

where

(A.7)

and erf is the error function. By way of comparison, the result which was arrived at for $n_{eo}(\rho)$ from the integration of the Boltzmann equation for the electrons is, as shown by (2.18b)

(A.8)

The static velocity in (A.8) would be obtained from solving the set of equations (2.18) where v_{eo} is related to n_{eo} by (2.18d).

We now have available two expressions for the electron density in the sheath which if the two approaches are consistent, should produce the same results. Lam (1964) pointed out that (A.8) is an accurate representation for the electron number density in the sheath provided that few electrons are lost to the bounding surface, in this case the cylinder wall. Self (1964) on the other hand arrived at (A.5) from basically physical reasoning; however, he did not include the static electron velocity in (A.7). Both expressions obviously are the same when there is no electron flow to the wall.

A different analysis based on the orbital approach used by Bernstein and Rabinowitz may also be instructive for comparing with the preceding results. The basis of the formulation depends on the fact that when there are no collisions, the general solution of the Boltzmann equation is an arbitrary function of the constants of the motion. By assuming the form of the distribution function at an infinite distance from the body and with a knowledge of the reflective and absorptive properties of the body, the particle density and flux can be obtained in terms of an integration over the constants of the motion.

The essential difference of the Bernstein and Rabinowitz approach from that of Langmuir lies in eliminating the velocity co-ordinates and using instead

the constants of the motion in the integrals which give the particle number density and flux. In addition there was no assumption that the static electric field is confined to a well-defined sheath region. When the radius of the body is large enough so as to preclude the possibility of trapped ions, then the loss of particles to the body is accounted for by the appropriate integration path in energy-angular momentum (E, J) space. This integration path does essentially what the truncation of the distribution function in the preceding calculation accomplished. It excludes those electrons which reach the probe from being included in the integration of the outward-travelling electrons.

Following Lam's(1964) development of the Bernstein and Rabinowitz theory for electrons in a spherical geometry, we have for the cylindrical case

(A.9)

where

$E_{\parallel}$ and $E_{\perp}$ are electron energy components associated with electron motion parallel and perpendicular to the cylinder and J is the angular momentum. J_1 and J_2 are given by

(A.11a)

(A.11b)

The particle flux is

(A.12)

(A.13)

After performing the integrations over J and E , and with some simplification, there is obtained

(A.14)

(A.15)

where

$$-\qquad \text{(A.16a)}$$

$$-\qquad \text{(A.16b)}$$

Some observations are required before the numerical solution of (A.5), (A.6), (A.8), (A.14) and (A.15) are obtained. First, the same potential variation given by (A.1) is to be used for all three methods of obtaining the electron number density. Obviously if one could find the potential from each method of analysis, the result obtained in each case would be expected to be different. However, in using the same potential for these calculations, the relative consistency of the three analyses can be checked. At the same time an indication is given of the agreement which might exist between the potential solutions which could be obtained if one solved for the potential from each analysis rather than assuming its form. Second, in finding the number density from (A.8), the static velocity will be used from (A.6) rather than solving the transcendental equation (2.18d) for it. Third, the static velocity (A.6) contains a term which is the real electron drift velocity in the plasma and for which a numerical value is required. Now at the sheath edge, and for that matter all through the sheath, the electron and ion currents are equal. Since the densities are also approximately the same at the edge of the sheath, then the ion and electron drift velocities are equal there. If we use the Bohm (1949) sheath criterion, that the edge of the sheath

is the point where the ion drift velocity equals the ion rms velocity, or where the transition from subsonic to supersonic ion flow occurs, then

at the sheath edge. This term will be taken to be constant throughout the sheath.

The results of the numerical computations for a sheath thickness of $20D_\ell$, with $m_i = 1$ and 200 atomic mass units and M = 2 and 4 are shown in figures (A-1) to (A-4) as a function of position in the sheath. It is immediately evident that the electron number density obtained by the three methods outlined above is in agreement with the Boltzmann distribution to within 5 percent over almost the entire sheath. Further, it may be observed that the Bernstein and Rabinowitz method and the truncation analysis are shown as a single curve since they agree numerically to within 1 percent and cannot be separated on the graph. Finally we note that the curve showing the results from the Boltzmann equation integration lies between the Boltzmann distribution and the Bernstein and Rabinowitz results.

When we observe the curves for the electron velocity, there is seen to be remarkably good agreement between the two models with the difference never exceeding a factor of 2. Surprisingly the velocities are practically identical at the cylinder surface for both models regardless of the potential variation. This is explained by noting that the electron distribution function is one-sided at the surface, so that the electron drift velocity there is dependent only on the electron

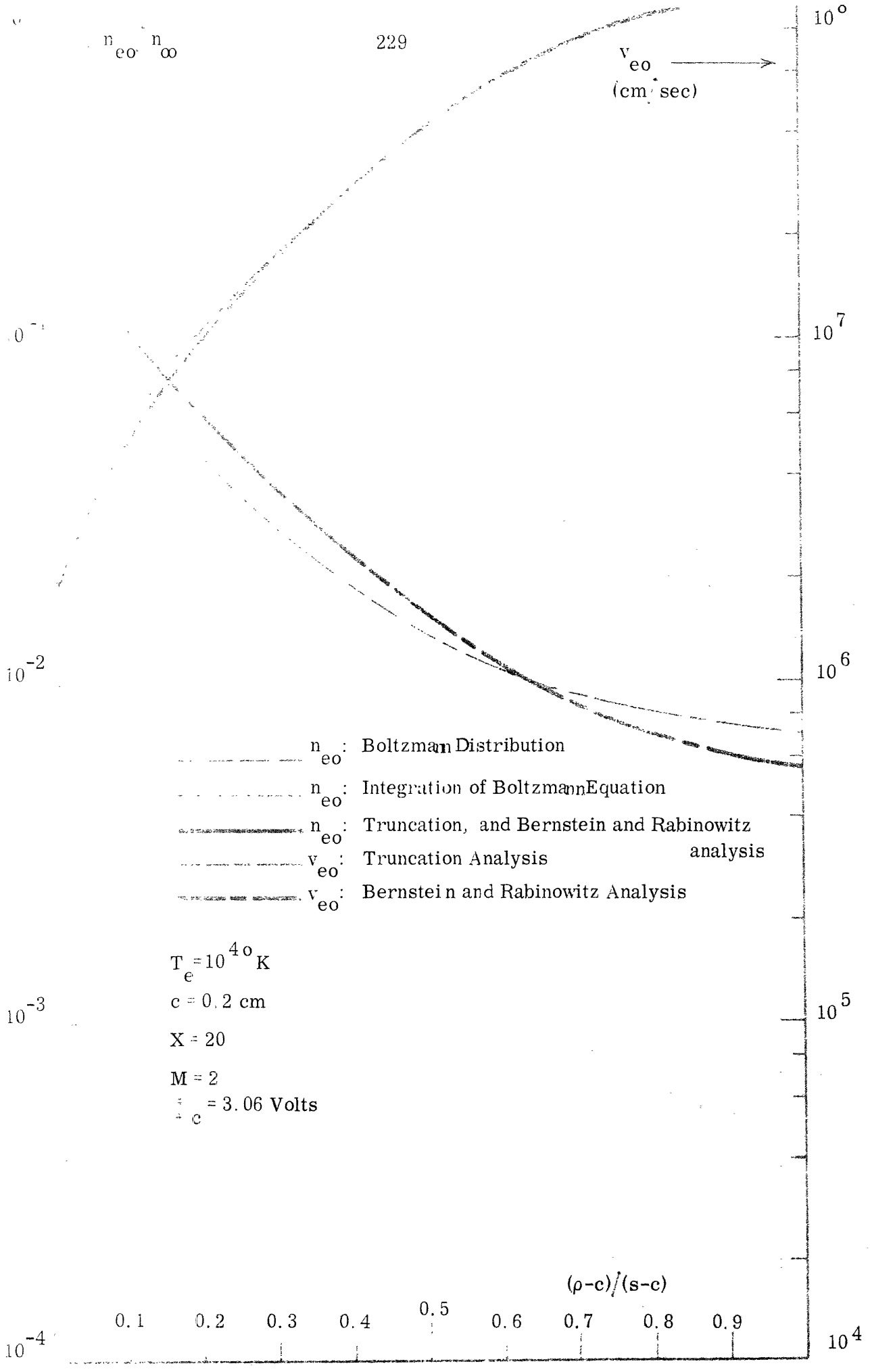

FIG. A1: STATIC ELECTRON DENSITY AND VELOCITY vs. RADIAL DISTANCE IN SHEATH FOR M = 2 AND Φ_c = -3.06 VOLTS

MISSING
PAGE

MISSING
PAGE

MISSING
PAGE

temperature and not upon the potential variation or the cylinder potential. The drift velocity at the cylinder is 0.468 that of the rms velocity in the uniform plasma.

The close agreement which is thus obtained by the three analyses outlined is gratifying. It justifies the use of the scalar electron pressure in the Boltzmann equation formulation since the results obtained from its use differ little from the other two analyses where the anisotropy of the electron velocity distribution function is taken into account. It should be realized that scalar electron pressure may not be generally valid however, as when the cylinder is biased to collect more electrons than ions. The scalar pressure depends for its validity on few of the particles involved reaching the cylinder, so it is a good approximation for the repelled particles only, which in this case are the electrons. This is why a determination of the density and velocity of the attracted particles requires a more rigorous analysis than indicated by (2.18). Further, since the Boltzmann distribution is so little different from the densities due to the other methods, it appears that the flow of electrons to the cylinder can be neglected as far as the static sheath picture is concerned. Consequently, the Boltzmann distribution will be used to calculate the static electron density in the sheath in the subsequent formulation of the dynamic sheath problem. The results for the static electron velocity in the sheath are used in Appendix B to examine the influence of this velocity on the dynamic sheath analysis.

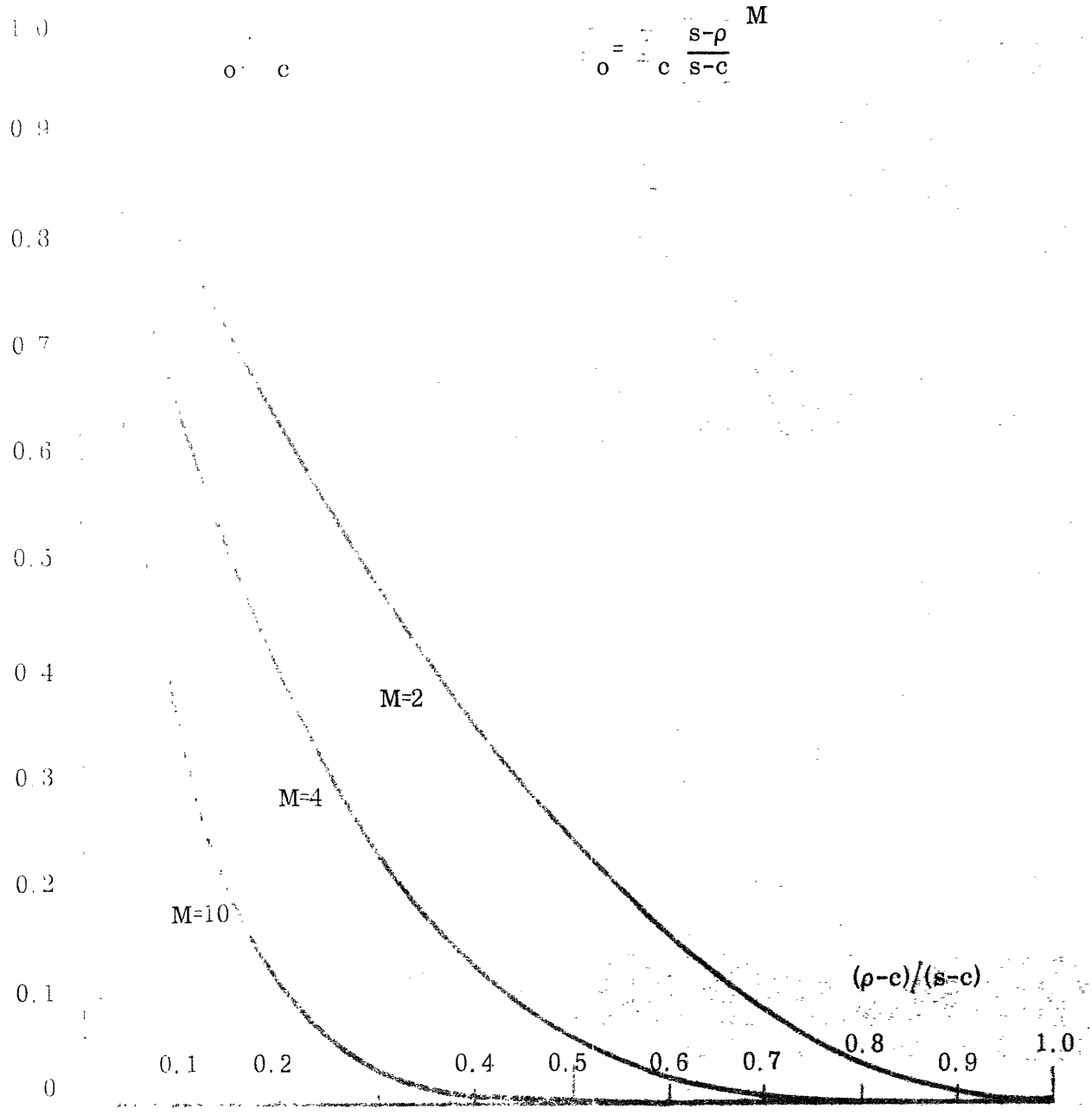

FIG. A.5: STATIC POTENTIAL VARIATION IN SHEATH vs. RADIAL DISTANCE

APPENDIX B

ELIMINATION OF THE STATIC ELECTRON VELOCITY TERMS IN THE DYNAMIC SHEATH EQUATIONS

The question of the influence on the dynamic sheath solution of the static electron velocity was found, in Chapter II, Section 2.5.2, to reduce to an evaluation of the ratios

The requirement for the approximation of omitting the static velocity from the dynamic equations to be valid is that R_1 and R_2 be small compared to unity; the smaller their values, the better the approximation.

R_1 and R_2 are calculated using a frequency of 10^9 cps and the velocity obtained by the Bernstein and Rabinowitz analysis in Appendix A. Figure B.1 shows R_1 and R_2 as a function of position in the sheath for M = 2 and M = 4 with plasma ions of 1 atomic mass unit. We see that the ratios are everywhere smaller for the larger value of M except for R_1 near the sheath-uniform plasma interface. This occurs since R_1 is inversely proportional to the gradient of the potential, which becomes increasingly concentrated towards the cylinder surface for increasing values of M.

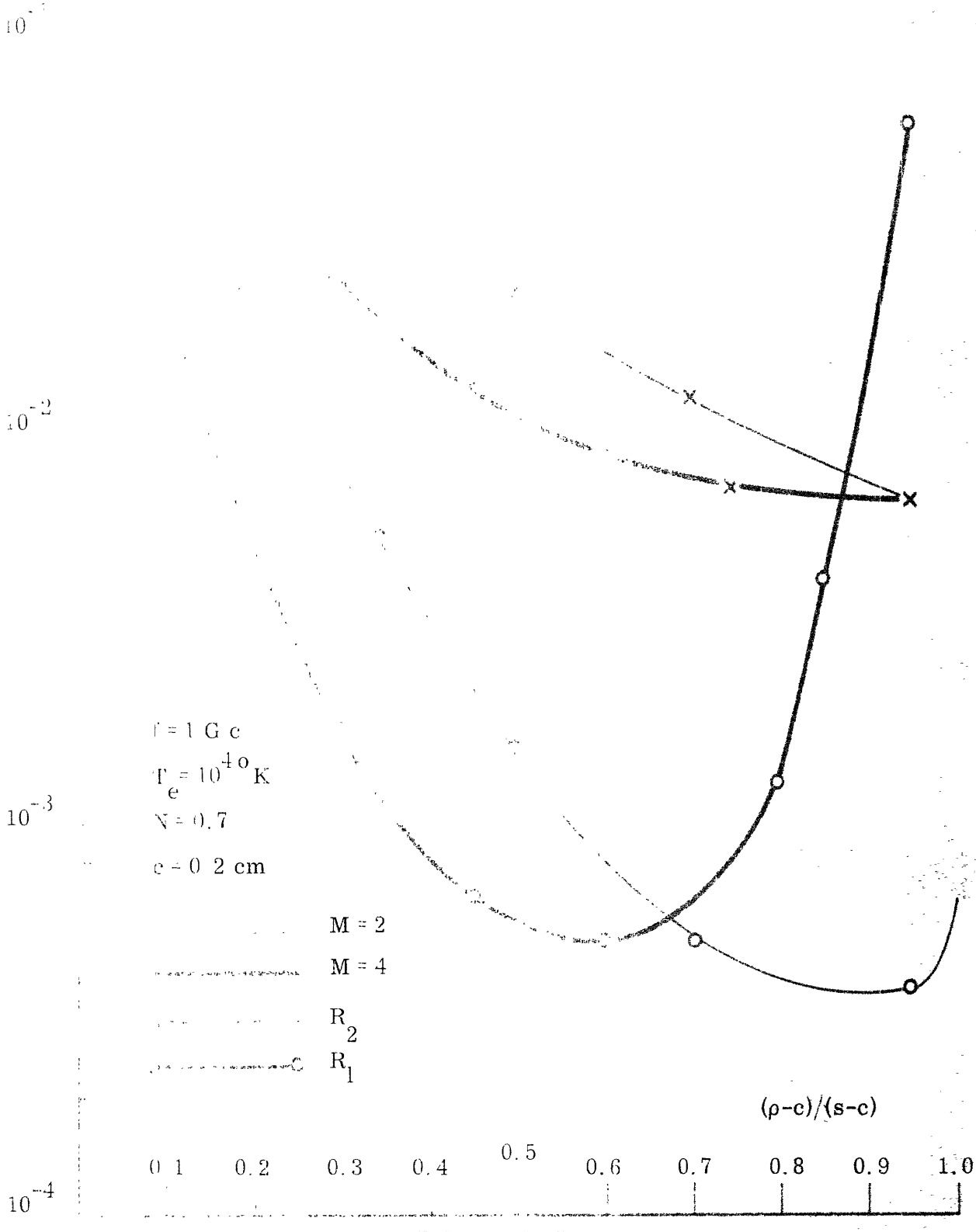

FIG. B1: THE RATIOS R_1 AND R_2 vs. RADIAL DISTANCE IN SHEATH

The ratios are less than 0.1 over 85 per cent of the sheath, with the average value of the largest 0.058. Similar results are obtained for a plasma with an ion mass of 200 atomic mass units. The omission of the static velocity terms from the dynamic equations, in view of the fact that the contribution of these terms is small in comparison with the terms which are retained thus seems to be a very reasonable approximation

APPENDIX C

DETAILS OF INHOMOGENEOUS SHEATH ANALYSIS

The solution of the inhomogeneous sheath model would follow in a fashion similar to that of the vacuum sheath model if analytic solutions could be obtained to the equations which describe the propagation modes of the inhomogeneous sheath. The application of the boundary conditions at the cylinder and the sheath-uniform plasma interface would lead to a matrix, which when inverted would yield the Fourier coefficients of the various modes propagating in the sheath and the uniform plasma.

Such a procedure cannot be followed when solutions must be obtained by numerical computation. The reason for this is that the boundary conditions are expressed at two boundaries by certain of the dependent variables being zero, as in (2.52g) to (2.52i), or in terms of linear combinations of the dependent variables and their derivatives, as in (2.52a) to (2.52c). Consequently, the boundary conditions at one boundary alone are not sufficient to specify the values of all of the dependent variables at that boundary. Part of this information is contained in the boundary conditions at the other boundary. But before starting the numerical integration of the differential equations at one boundary, the values of all the dependent variables at that boundary are required. In contrast to the situation where analytic solutions are attainable and the functions can be evaluated at the boundary by using the appropriate argument, the numerical solution has yet to be obtained.

The linearity of the differential equations allows the use of the superposition principle to surmount this difficulty. One unknown dependent variable is set

at unity, thus leading to values for the other variables related to it by the boundary conditions and the differential equations, at one boundary. The remaining variables are then set equal to zero to start a numerical solution at this boundary. An integration across the sheath to the second boundary is performed. This process is repeated for a different unknown variable equal to unity, and the process repeated as many times as there are boundary conditions at the second boundary. A linear combination of the solutions thus obtained is formed at the second boundary, and is required to satisfy the boundary conditions there, leading to a matrix. The required starting values for the dependent variables at the first boundary which were successively set at unity are proportional to the coefficients of the linear combination which are obtained from inverting the matrix. At the same time the boundary conditions at the first boundary are satisfied by finding the starting values for the remaining variables through the boundary conditions there.

To illustrate this procedure, we use the differential equations and boundary conditions given by (2.41) and (2.52). These equations can be written for normal incidence as

(C1a)

(C1b)

(C1c)

(C1d)

with the boundary conditions

(C2a)

(C2b)

at $\rho = c$ and

(C2c)

(C2d)

at $\rho = s$. Note that the prime above indicates derivatives with respect to ρ. S_p and S_e are given by

(C3a)

(C3b)

We put the equations into a more convenient form by transforming the real and imaginary parts of the dependent variables to $Y_1 \ldots Y_8$ as

$$
\begin{bmatrix} Y_1 \\ \cdot \\ \cdot \\ \cdot \\ \cdot \\ \cdot \\ \cdot \\ Y_8 \end{bmatrix} = \begin{bmatrix} H^{(z)}_{mr} \\ H^{(z)}_{mi} \\ Q_{mr} \\ Q_{mi} \\ E^{(\varsigma)}_{mr} \\ E^{(\rho)}_{mi} \\ E^{(\phi)}_{mr} \\ E^{(\phi)}_{mi} \end{bmatrix} \tag{C4}
$$

where the subscripts r and i indicate the real and imaginary parts respectively of the dependent variables. Then with

then (C6)

where

s the set of differential equations to be solved. The bo, ..., conditions are

hen at $\rho = c$

$$Y_7 = Y_{\cdot} = 0 \tag{C7a}$$

and

$$Y_3 = Y_4 = 0 \tag{C7b}$$

or

$$\cdot\cdot\ 1 \tag{C7c}$$

At $\rho = s$ we have, with

$$\frac{H_m^{(2)}\ (K_E s)}{H_m^{(2)}\ (K_E s)} \tag{C8a}$$

$$\frac{H_m^{(2)}\ (K_{\cdot} s)}{H_m^{(2)}\ (K_{\cdot} s)} \tag{C8b}$$

and

$$S_1 + iS_2 = S_e / H_m^{(2)}\ (K_E s) \tag{C8c}$$

$$S_3 + iS_4 = S_p / H_m^{(2)}\ (K_P s) \tag{C8d}$$

then

$$Y_{i\_}' = S_{i\_} + R_{ij}\ \ Y_{j\_} \tag{C8e}$$

$$i, j = 1, \ldots 4$$

where

(C8f)

$$\begin{matrix} R_E & -I_E & 0 & 0 \\ I_E & R_E & 0 & 0 \\ 0 & 0 & R_{\cdot} & -I_{\cdot} \\ 0 & 0 & I_{\cdot} & R_{\cdot} \end{matrix}$$

If now the numerical integration is begun at $\rho = c$, some of the starting values of Y_i and Y_i' are determined by the boundary conditions and the differential equations (C6). But it can be seen that, which ever set of the boundary conditions are used, corresponding to zero [illegible] velocity, not all dependent variables Y_i are specified at $\rho = c$. In the former case Y_1, Y_2, Y_5 and Y_6 are not known, while in the latter case Y_1 through Y_4 are not known. The information for determining those unknowns is contained in the boundary condition at the other boundary, (C8), which cannot be used until the integration has been performed across the sheath. This then is the reason for the indeterminancy of the starting values of the dependent variables.

We overcome this obstacle to the numerical solution by setting all but one of the unknown Y_i equal to zero at $\rho = c$, the one being set at unity. The numerical integration of (C6) is then performed with this set of starting values, leading to a set of $Y_i^{\alpha}(\rho)$ and $Y_i^{\alpha'}(\rho)$ where α has the value of the index of the particular unknown Y_i with the value 1 at $\rho = c$. This procedure is repeated for a new unknown Y_i equal to unity with the rest zero again at $\rho = c$, leading to a new set of $Y_i^{\alpha}(\rho)$ and $Y_i^{\alpha'}(\rho)$. When the integration has been performed as many times as there are unknown Y_i at $\rho = c$ (or equivalently the number of boundary conditions at $\rho = s$) a linear combination of these solutions is formed as

$$Y_i(s) = C^{\alpha} Y_i^{\alpha}(s) \tag{C9a}$$

$$Y_i'(s) = C^{\alpha} Y_i^{\alpha'}(s) \tag{C9b}$$

Then upon using (C8e) there is obtained

$$C^{\alpha} \; Y_i^{\alpha'}(s) - R_{ij} \; Y_j^{\alpha}(s) = S_i \qquad \text{(C10)}$$

The coefficients C^{α} are found from inverting the matrix of equation (C10). The significance of the C^{α} is that their numerical values give the correct starting values of the corresponding dependent variables at $\rho = c$. When the integration of (C6) is then carried out for the final time, with these starting values for the previously unknown $Y_i(c)$ and the rest determined by the boundary conditions at $\rho = c$, [illegible] will be satisfied.

The actual numerical integration of (C6) was started by using a Taylor series expansion up to the third derivative in the dependent variables for the first step. The Runge-Kutta technique was used for the next four steps in the integration, in order to set up the values for the Milne predictor-corrector technique which was employed for the remainder. A Taylor series expansion was required for the first integration point since the first and second order derivatives of some of the dependent variables was zero at $\rho = c$, while the third order derivative was not.

The number of integration points to be used was established after some experimentation. It was determined partly by comparison of the sheathless and inhomogeneous sheath results for the current when the cylinder potential was set equal to zero with an integration interval of varying magnitude. Also a determining factor here was the fact that the Milne predictor - corrector routine provides information giving the maximum error in each of the dependent variables at every integration point. A comparison of the error terms from the predictor-corrector routine and the results obtained from twice solving the same sheath model using 25

and then 50 integration points established the reliability of the error terms in correctly showing the accuracy of the calculations. As a result it was found that 25 integration points provided an acceptable degree of accuracy, on the average a minimum of three significant figures.

Another possible source of error in these results besides that arising from the numerical integration comes from the numerical evaluation of the cylindrical functions. The method used to calculate them and the relative accuracy obtainable is discussed in Appendix F. The accuracy of the inhomogeneous sheath computations was not limited due to this consideration.

Finally, errors are generated by the matrix inversion required to find the C^{α}. The inversion was carried out in a double precision routine on the computer, which provides an additional 8 significant places, for a total of 16. Consequently, the maximum possible errors in the C^{α} are determined not by the matrix inversion, which is accurate to about 8 figures, but by the uncertainty in the Y_i due to the numerical integration.

The overall accuracy of the solution was checked by calculating the ratio of the boundary condition (C8e) to the sum of the absolute values of the terms appearing in (C8e) at the conclusion of the final integration. If the fractional error in the largest terms appearing in the boundary condition is on the order of δ, then this ratio should also be on the order of δ. It was found that this ratio was consistently less than 5×10^{-4} and generally averaged about 10^{-7}, for the boundary condition equations in which S_i was not zero.

In order to show the accuracy of the inhomogeneous sheath numerical integration,

figure C1 is presented which gives the surface currents obtained for a cylinder potential equal to zero. This reduces the problem then to the sheathless case. A comparison of figures C1 and 3.7 shows that the current from the inhomogeneous sheath numerical integration and that from the vacuum sheath analysis cannot be differentiated to the limit of the graphical accuracy. Actually, the currents obtained from the two models in this case were found to agree to an average of three to four significant figures, after the summation of the Fourier series. This provides an excellent verification of the accuracy which may be expected of the numerical results obtained from both the vacuum sheath and the inhomogeneous sheath analyses.

As a final check, the numerical integration of (C6) was performed for $\tilde{Q}_c = 0$ and the soft boundary condition with EK wave incidence. This is equivalent to the sheathless case also, but there is no coupling for this boundary condition and hence no surface currents should be excited. The currents obtained from (C6) were found to be about 10^{-6} of those values obtained for the hard boundary. Consequently, since the limitations on the computer accuracy keep the computer from obtaining exactly zero, this result can be interpreted to mean that the overall accuracy of the calculations is on the order of 5 or 6 significant figures for this particular case.

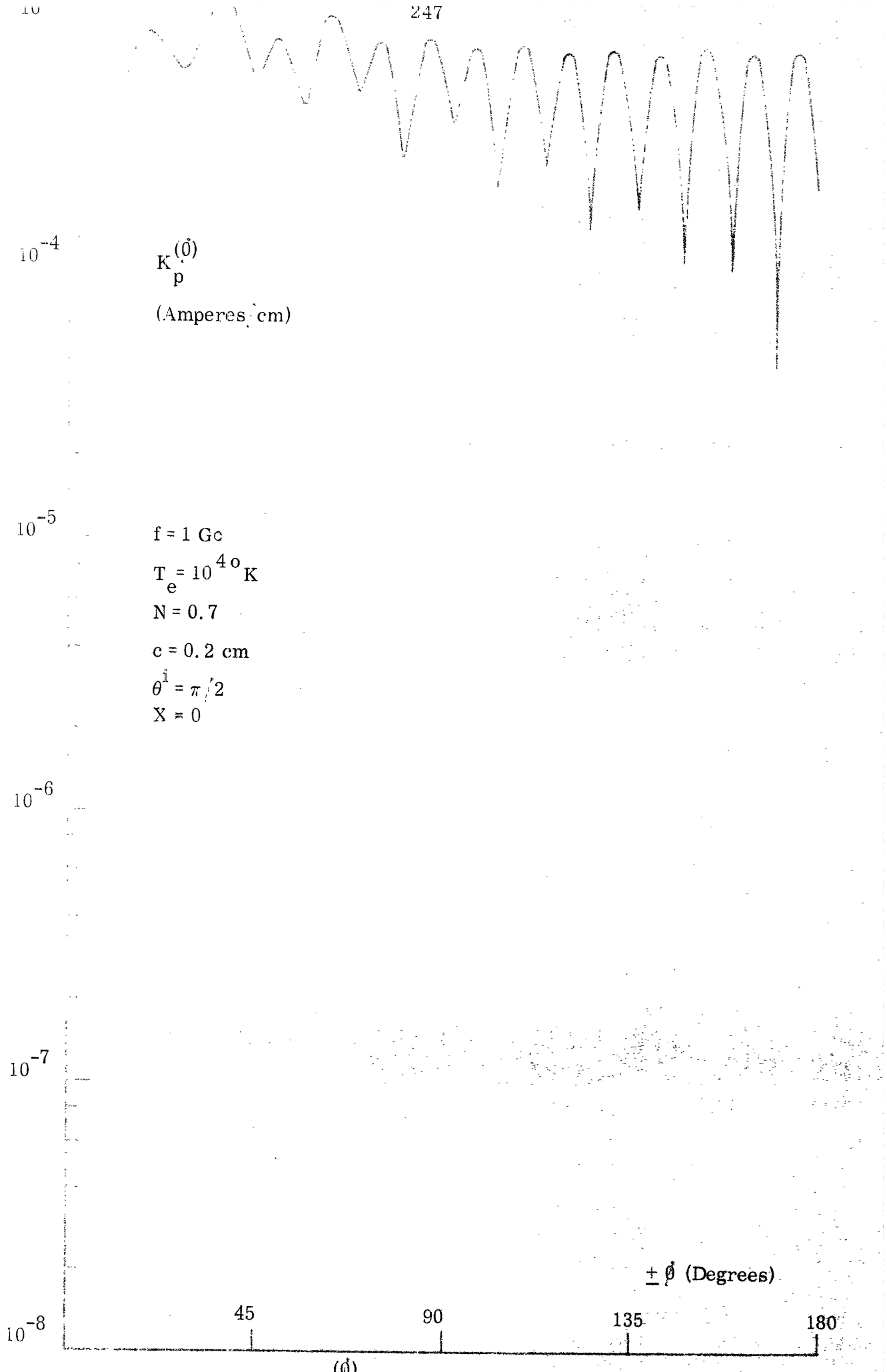

FIG. C1: MAGNITUDE OF $K_p^{(\phi)}$ vs. AZIMUTHAL ANGLE ϕ FOR SHEATHLESS CASE CALCULATED FROM INHOMOGENEOUS SHEATH COMPUTER PROGRAM

APPENDIX D

A SUGGESTED EXPERIMENT ON THE ELECTROKINETIC WAVE

It would be desirable to perform an experiment for the purpose of determining the validity of the theoretical results obtained in this study. Unfortunately, the practical problems associated with conducting an experiment designed to conform to the plasma-cylinder geometry for which this analysis has been performed seem to preclude this possibility. This is particularly so because of the requirement for an incident plane EK wave. If we were to attempt generating this wave by causing a plane EM wave to impinge on a planar plasma slab, it appears from this and other analyses (Tidman and Boyd (1962), Kritz and Mintzer (1960)) that relatively little energy could be expected to be converted to a plane EK wave in the plasma. Consequently, the possibility of discriminating between the currents excited by the EM and EK waves on the plasma-immersed cylinder would seem to be unlikely, especially in view of the fact the theory indicates this to be a marginal prospect even with equal power flow densities in both waves. However, if we do not require a plane wave incident on the plasma-immersed cylinder at an arbitrary angle, but instead confine the experimental investigation to normal incidence, an experiment with more likelihood of success can be visualized.

We may recall from the introduction that Parker et. al. (1964) recently performed an experiment involving the scattering of EM waves from a plasma cylinder. Their experiment was motivated by the heretofore unexplained resonances in the scattering properties of the plasma cylinder. The good

agreement which they obtained between their experimental observations and theoretical predictions indicates that an EK wave is excited in the plasma by the EM field with a maximum amplitude at the resonance frequencies. In order to excite a single mode in the plasma, they arranged dipole and quadrapole excitation structures, parallel to and concentric with the cylindrical glass envelope containing the plasma, thus effectively selecting only one mode at a time from the modal expansion of an incident plane wave.

The arrangement which Parker et. al. used would seem to be one which could be employed in our situation also. The only change to be required would be the addition of a metal cylinder along the axis of and inside the cylindrical glass envelope containing the plasma. By observing the resonances in the excitation circuit, one could determine the point of maximum EK wave amplitude so as to optimize the possibility of detecting the surface currents which the EK wave would induce on the plasma-immersed cylinder. Similar measurement of the surface current in the absence of the plasma would provide a means of separating the EM induced current from that due to the EK disturbance. In addition, since the EM current would vary as cos $m\phi$ while the EK current varies as sin $m\phi$, where m is the mode number and ϕ the azimuthal angle, a determination of the angular variation of the currents would provide an additional means for separating out the two components. Finally, by using a metal cylinder whose diameter c is such that $K_P c \ll 1$ and $K_E c \gg 1$, then an increase in the ratio of EK to EM currents can be achieved by increasing the mode number m, since the EK current is relatively insensitive to m when $K_P c > m$ while on the

other hand, the E M current decreases approximately as $(K_E c)^m$.

This experiment would have two important aspects. First, it would provide a source for the EK wave in a well-defined geometry and the indications are from the present study that the currents would be large enough to measure. The most critical point here would be the practical one of how efficiently the surface currents could be coupled to a transmission line which would carry the signal to an external receiver. Due to the magnetic field having a z-component only for normal incidence of the EK wave, it does not appear that a coaxial line could be efficiently coupled to the surface current. However, by using a hollow metal tube cut with 2m axial slots as the plasma-immersed cylinder, where m is the mode number of the exciting structure, one would have a circular wave guide that would be excited by the surface currents in the TE_{m1} mode and which could carry the signal to the receiver. For the TE_{11} mode and a cutoff frequency of 1.0 Gc, a cylinder about 4.4 cm in diameter would be required, but this size could be reduced by loading the waveguide with a dielectric. A diameter of this size is not unreasonable.

A second feature of this experiment would be an extension of Parker et. al. (1964) work on the plasma resonances. It seems likely that the resonance spectrum of the plasma column would be modified by the presence of the metal cylinder, an effect which could be studied in the experiment outlined.

There would be some further analysis required to that done in this study to predict the results of such an experiment. In this respect then, we are proposing to solve a problem different from that which we have already done. How-

ever, what we desire is a check on the theoretical formulation which has been used for the present study of the cylinder immersed in an infinite plasma medium. This would be accomplished by using the same formulation for the problem which is outlined here, for which the experimental check could be made.

APPENDIX E

DEVELOPMENT OF VACUUM SHEATH FORMULATION AND APPROXIMATE SOLUTIONS

The solution of the boundary condition equations arising from the vacuum sheath model for the Fourier coefficients of the scattered, transmitted and reflected fields requires the inversion of the matrix given by equation (2.61). A straightforward approach to performing this task leads to expressions that are complicated and lengthy and which as a result convey little information. A close examination of the matrix reveals that due to the number of zeros in it, some of the coefficients can be easily found in terms of the others, so that the order of the matrix can be reduced and its inversion consequently simplified. Proceeding in this way, the matrix was reduced to 3x3, with A^{S}_{m-p}, A^{R}_{m-h} and A^{R}_{m-e} appearing in it as the coefficients to be determined. The advantage of using the coefficients of the reflected waves is that they are required for calculating the surface currents and are related in a simple way to the transmitted wave coefficients which are also needed for this purpose.

The remainder of the coefficients are expressed in terms of these three as

(E.1a)

(E.1b)

(E-1c)

(E-1d)

where

(E-2a)

(E-2b)

(E-2c)

(E-2d)

(E-2e)

The dash subscript represents the kind of incident wave, p, e or h and the prime denotes differentiation with respect to argument. The resulting three

equations for determining A^{S}_{m-p}, A^{R}_{m-e} and A^{R}_{m-h} are then

(E-3)

where

(E-4a)

(E-4b)

(E-4c)

(E-4d)

(E-4e)

(E-4f)

(E-4g)

(E-4h)

(E-4i)

The terms in the source vector are

(E-4j)

(E-4k)

(E-4ℓ)

The solutions for $A^{S}_{m\text{-}p}$, $A^{R}_{m\text{-}h}$ and $A^{R}_{m\text{-}e}$ are given in equations (2.66) to (2.69) and the surface currents in (2.70). The correctness of these solutions was established by verifying that the original boundary condition equations were satisfied when these results were put into them. In addition the sheathless

model was treated as a separate problem, and the solutions obtained there were compared with those of the vacuum sheath when the sheath thickness goes to zero. The results obtained from those two different approaches were identical.

The results obtained for the sheathless case and EK wave incidence for arbitrary Y_B are of value. They are

(E-5a)

(E-5b)

(E-5c)

where

(E-5d)

and

(E-5e)

We see that A^R_{mpe} and A^R_{mph} become inversely proportional to Y_B as $Y_B \to \infty$, so that the current excited by the EK wave also is inversely proportional to Y_B. The same result is found for the cross-coupling coefficients for e and h wave incidence which are not included here.

We repeat now, for emphasis, what was mentioned in the discussion of Chapter II, section 2.6 concerning the radial variation of the scattered fields. β, the z-direction separation constant, is determined by the incident wave, so that the radial separation constants are obtained from

(E-6a)

(E-6b)

(E-6c)

where

(E-6b)

and K_i is the propagation constant of the incident wave. If in particular, $K_i = K_p$ then

(E-7a)

(E-7b)

(E-7c)

Due to the fact that v_r is generally much less than v_ℓ, then whenever

(E-8a)

and

(E-8b)

λ_E and λ_{Eo} respectively, become imaginary. This leads to the possibility for large sheath attenuation when the EK wave is obliquely incident on the cylinder, as will be shown below. Note that as θ_p^i is varied from normal incidence, λ_E first becomes imaginary, followed by λ_{Eo}. This means that there can exist trapped unattenuated EM waves in the vacuum sheath. Since v_r in this study has been fixed at 6.67×10^7 cm/sec, and the nominal value of N is 0.7, then the angular interval for θ_p^i in which this phenomenon could occur is about 0.05^o. For angles greater than about 0.18^o from normal, both λ_E and λ_{Eo} are imaginary, and the EM wave becomes a surface wave propagating on the sheath-uniform plasma interface and the cylinder surface.

When $\cos\theta_p^i < v_r/v_\ell$ then in a fashion similar to (E.7), we can write

(E.9a)

(E.9b)

where θ_E and θ_{Eo} are the "scattering" angles of the EM waves in the plasma and vacuum sheath. Physically, they represent the direction of the vector sum of the power flow in the scattered fields in the radial and the z-directions from the front of the cylinder, i.e., the backward scattering angle of the EM mode. It is convenient to specify the angle of incidence of the EK wave in this situation by giving the angle θ_E, which varies from $\pi/2$ to 0 when θ_p^i varies from $\pi/2$ to $\pi/2 - v_r/v_\ell$, and is thus easier to visualize than θ_p^i.

The situation is very different when $K_i = K_E$, for then

(E.10a)

(E.10b)

(E.10c)

Since $v_r/v_\ell \ll 1$, then $\lambda_P \approx K_P$, and the scattered EK fields propagate away

from the cylinder in a nearly normal direction. There is no possibility for the excitation of surface waves in this case.

In order to check the results obtained from the computer calculations involving the exact expressions for the current, given by (2.70), some formulas were derived using approximate forms for the cylindrical functions appearing in these equations. The approximate expressions which are obtained in this way provide the additional benefit of reducing the complicated appearance of the equations giving the currents to a form more easily interpreted.

The radius of the cylinder chosen for this investigation was on the order of 1 cm, a size dictated partly by theoretical considerations which required that a solution be obtained with a reasonable number of terms, and partly by practical considerations associated with the feasibility of performing an experiment. These tend to be opposing restraints, the former leading to smaller radii and the latter to larger. In the end a third consideration resulted in decreasing the nominal radius to 0.2 cm, due to the oscillation of the EK currents as a function of ϕ being so rapid that plotting the currents on 8-1/2 x 11 inch graph paper was made impractical. For the nominal choice of other parameters used, such as T_e, f, etc., $K_E \approx 0.14\,cm^{-1}$ and $K_P \approx 66\,cm^{-1}$. Thus $K_E s \ll 1$ and $K_P s \gg 1$, so that small argument approximations can be used for the cylindrical functions of argument proportional to $K_E s$ while large argument approximations can be used for those of argument proportional to $K_P s$. The leading term in the ascending series for the cylindrical functions is used as the small argument approximation and Hankel's asymptotic expansion is used for the large argument approximation.

The currents excited by the two types of EM waves are given by the following approximate expressions, where only the leading term in the series is included to be consistent with the approximations used.

(E.11a)

(E.11b)

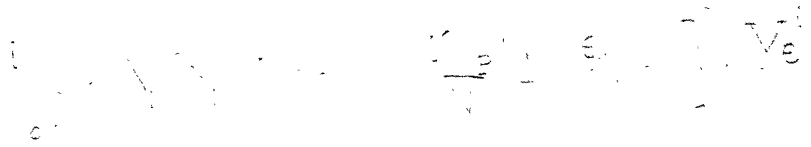

(E.11c)

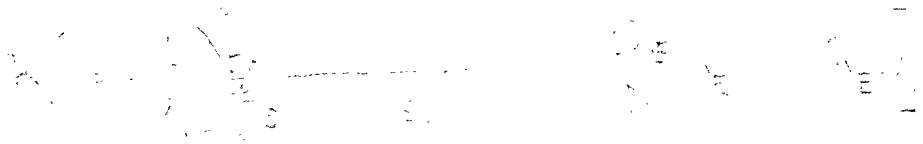

(E.11d)

D_0 and D_1 are

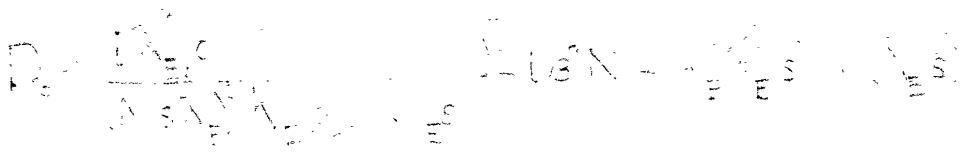

(E.11e)

(E.11f)

D_1 is shown as a function of m since it is used also for the EK current expressions. m = 1 when D_1 is used in the equations above.

These currents do not show a strong dependence on the sheath, in contrast to the case for the EK wave discussed below. Numerical results obtained using (E.11) were found to be in good agreement with those calculated from the exact expressions. In addition, since the exact results showed the currents to be unaffected by the sheath and the compressibility of the plasma, it is instructive to rewrite (E.11) for s = c and with the terms resulting from the EK wave omitted, as

(E.12a)

(E.12b)

(E.12c)

(E.12d)

where it should be recalled

(E.12e)

The behavior predicted by these expressions is exhibited by the graphs of figures 3-42 to 3-45 which show the currents as a function of ϕ, N, c and θ^i calculated without approximation. Note that $K_n^{(\phi)}$ is not excited unless there is a sheath or the plasma compressibility is allowed for.

When the EK induced currents are considered, a different problem is encountered in making the approximations. There is, first of all, the fact that some of the cylindrical functions can have imaginary arguments. Secondly, the convergence of the current expressions with m is controlled by the ratio of the EK wavelength to the cylinder radius, so that the first term in the series no longer accurately represents the sum of the series. As a matter of fact, if we wish to represent the entire series, different approximations would be required when the argument $\gg$ m and unity, when the argument m and when the argument $\ll$ m. There is nothing to be gained from going through this lengthy

procedure, since the calculations are to be carried out using the exact expressions anyway, but by deriving the first few terms in the series from the approximations, a check can be made on the exact results, and we may also be able to deduce something about the dependence of the currents on the various parameters.

Thus the equations which follow are reasonable approximations for the leading terms in the series, based on $K_P s \gg 1$ and $K_P s \gg m$. The first set of equations is for the case where the EM modes produced by the incident EK wave have real arguments and the second for the case where their arguments are imaginary.

Case 1: Real EM mode arguments

With $\lambda_{Eo}c$, $\lambda_E c \ll 1$ and real; $\lambda_P c \gg 1$ and m

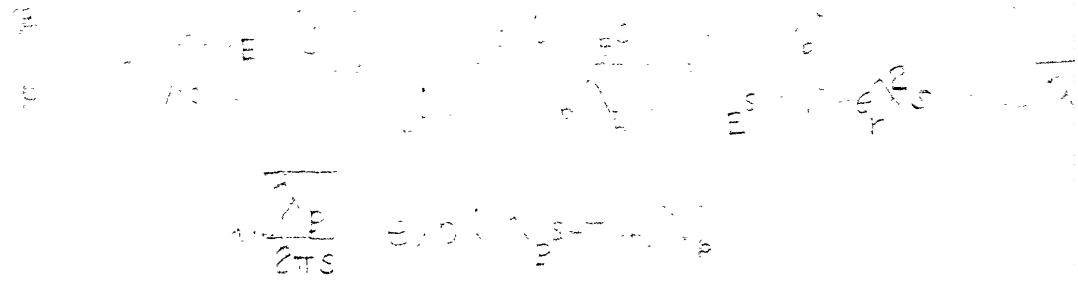

(E.13a)

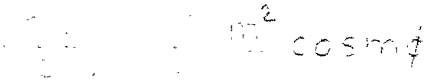

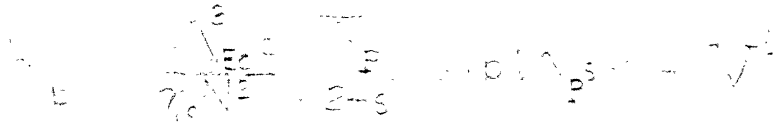

(E.13b)

D_1 is as given by (E.11f). It is interesting to observe that when $s = c$, then $K_p^{(z)}$ is given the $m = 0$ term only, a result which, incidentally, is dependent only upon $\lambda_{Eo} c \ll 1$ being true. This result explains the relatively little influence of the sheath on $K_p^{(z)}$ and also the little variation shown by $K_p^{(z)}$ as a function of ϕ that is exhibited by the graphs in Chapter III.

The peaking of $K_p^{(z)}$ which changing θ^i near normal incidence can also be shown from (E.13a). This peaking occurs essentially because the last two terms in the denominator of (E.13a) for the $m = 0$ term may become small or equal to zero. Since the β^2 term for these angles of incidence is much less than either of the other two terms, until θ^i approaches $\pi/2 - v_r/v_\ell$, then the magnitude of $K_p^{(z)}$ is inversely proportional to the terms in λ_E and λ_{Eo}. Consequently, as λ_E and λ_{Eo} decrease in value with increasing obliqueness of θ^i, $K_p^{(z)}$ shows a corresponding increase in magnitude, which for the sheathless case becomes maximum when $\lambda_E = 0$. When $s \neq c$, the peaking of $K_p^{(z)}$ is not so accentuated, since λ_E and λ_{Eo} do not go to zero at the same time.

The dependence of $K_p^{(z)}$ on c can also be observed from (E.13a). When the sheathless case is considered, we see that for c 1 cm, $K_p^{(z)} \alpha c^{-3/2}$ approximately. This dependence on c is shown by the graph of Fig. 3-14.

Case 2: Imaginary EM mode arguments.

The situation where $\cos\theta^i \gg v_r/v_\ell$ leads, by the use of equation (E.7), to

(E.14a)

(E.14b)

The minus sign is chosen for the imaginary root to ensure the proper behavior of the fields as $\rho \to \infty$. Now with $\cos\theta^i \gg v_r/v_\ell$, β can vary from $\sim 0.01\, K_P$ to K_P with decreasing θ^i. But over the range $\theta^i < 85^o$, $\beta > 0.1\, K_P$ so that with the nominal value of K_P 66 cm^{-1}, and with c 1 cm, $\beta c \gg 1$ holds over most of this range in θ^i. We are thus interested in the large argument approximations for all the cylindrical functions occurring in the exact formulas.

If we require then

where $\lambda_E = \lambda_E$ and $\lambda_{Eo} = \lambda_{Eo}$, there is obtained

(E.15a)

(E.15b)

D_i is given by

(E.15c)

and (E.15d)

These expressions are quite involved and would be of little use other than serving to check the numerical computations, if it were not for the fact that they show the effect of the sheath on the first few terms in the series for the currents. We see that $\cosh \delta'^{-1}$ appears as a factor in these equations. When $\delta' \gg 1$, then

(E.16a)

(E.16b)

Thus the terms which are proportional to $\tanh\delta'$ do not become large in relation to the other terms, but the $\cosh\delta'$ factor exerts an overall influence, tending to decrease the current magnitudes. The sheath influence can be represented by an attenuation factor

(E.17a)

With the sheath thickness given in D_ℓ, this becomes

(E.17b)

where X is expressed by

(E.17c)

It is enlightening to give the sheath attenuation A_{db}, in db, as

(E.17d)

With $N = 0.7$, $X = 10$, and $\theta^i = \pi/4$, $A_{db} = -15.1$ db.

This attempt to predict the sheath attenuation is a very rough approximation of course, based on the first few terms in the Fourier series for the currents.

I gives surprisingly good results however, when compared with the attenuation found in the currents calculated from the exact expressions.

APPENDIX F

DETAILS OF THE CYLINDRICAL FUNCTION EVALUATION

The accuracy of the numerical results presented in this study is determined to a great extent, and particularly in the case of the vacuum sheath analysis, almost wholly by the accuracy with which the cylindrical functions could be obtained. A wide range of order and argument values had to be considered for the cylindrical functions of both real and imaginary arguments. As a result, no single method of evaluating these functions could be used, but instead a number of various paths had to be available depending upon the area to be covered in argument-order space.

This was due to some extent to limitations of the computer, which since it must work within the constraints of a finite memory, can handle only numbers of limited magnitude and numbers of significant places. Thus for example, while the ascending series solution for the Bessel function of the first kind, $J_m(z)$, is nicely convergent for large (m/z) ratios, the numbers which are generated in the individual terms in the series may be quite large and overflow the computer, i.e., exceed the computer capacity. It also happens that in a representation such as Hankel's asymptotic expansion, with an imaginary argument, the answer is much smaller than the individual terms of alternating sign which occur in the series, thus requiring their difference to be smaller than the last significant figures carried along by the computer in summing the series. Inaccurate or wholly incorrect results are then obtained. Another consideration, of course, is the inherent maximum accuracy which can be obtained in an asymptotic expansion.

These considerations led to the use of three distinct methods for calculating the cylindrical functions. The formulas used are the ascending series, Hankel's asymptotic expansion and Olver's uniform asymptotic expansion, given by Olver (1964) in Eqs. (9.1.10) to (9.1.14), (9.2.5) to (9.2.10), and (9.3.35) to (9.3.41) respectively, for real arguments. When the arguments are imaginary, the corresponding expressions are given in Eqs. (9.6.10) to (9.6.13), (9.7.1) and (9.7.2), and (9.7.7) to (9.7.11) respectively, in the same reference. The advantage of using Olver's uniform asymptotic expansion in spite of its much greater complexity is due to the fact that his formulas are valid for any argument to order ratio for large orders, so that it complements the other methods which are useful primarily for small orders.

The accuracy of the programs which were used to calculate the cylindrical functions was checked against the tables listed by Olver (1964). The various methods were also checked against each other to better establish the more desirable formula to use for a given order and argument. The series appearing in these formulas were calculated to the point where the last term taken was no larger in absolute value than 10^{-6} of the first.

If we denote the ascending series by AS, Hankel's asymptotic expansion by HE and Olver's uniform asymptotic expansion by OE, then the region of order-argument space where each was used in the calculations can be depicted as shown in figure F.1. The line dividing OE from HE is $m = \sqrt{10z}$, as it was found for m much closer to z than this, that HE began to lose accuracy, particularly for imaginary arguments.

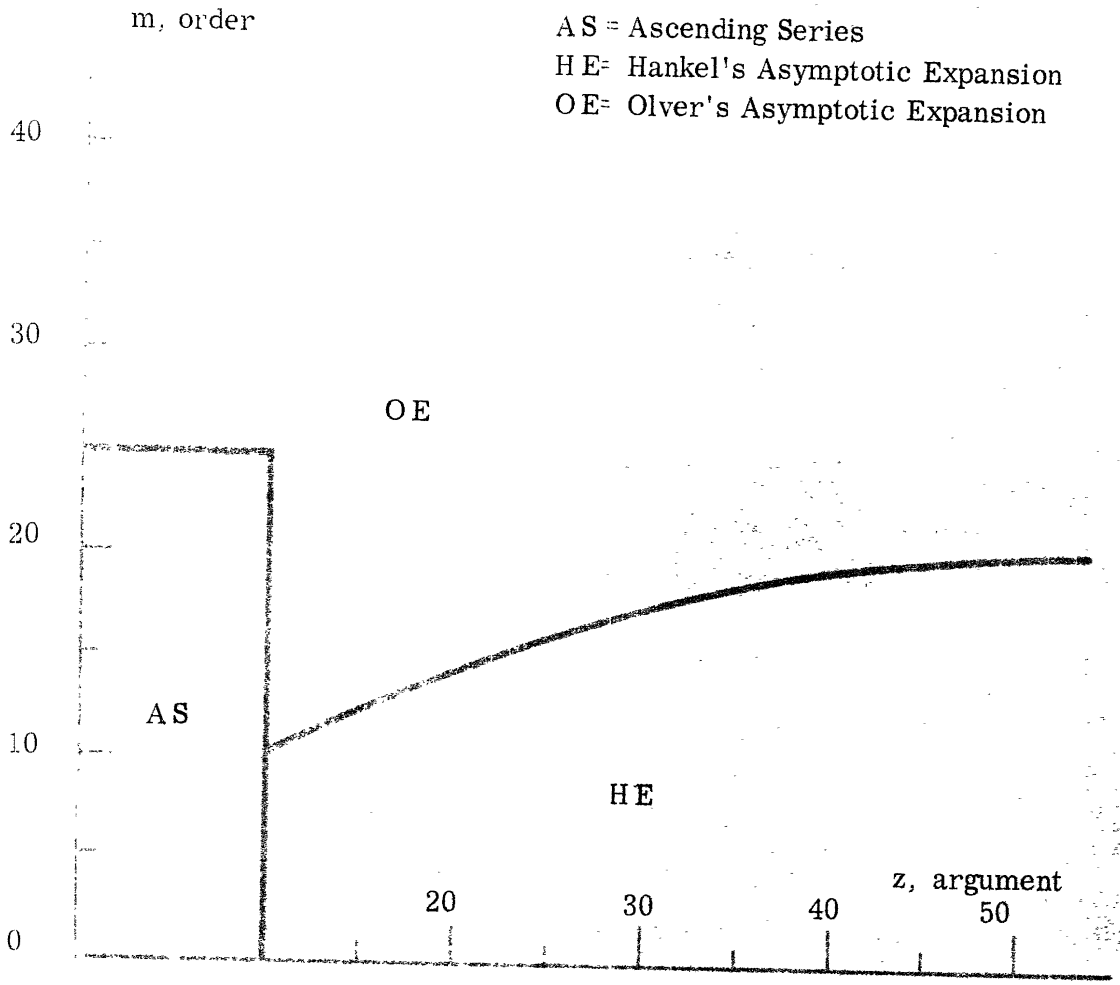

FIG. F1: THE DIVISION OF ARGUMENT - ORDER SPACE AMONG VARIOUS METHODS OF COMPUTING THE CYLINDRICAL FUNCTIONS

The minimum overall accuracy achieved for the cylindrical functions used in this study was about one digit in the fourth significant place. On the average, the accuracy was no less than one digit in the fifth place, and frequently the calculated values checked those tabulated out to seven and eight places. This should not be taken to mean that better results could not be obtained if they were desired. That would be a matter of taking more terms in the series from which the functions are obtained and possibly also of resorting to fancier computer techniques such as double precision operation. In such a way, one could achieve an arbitrary accuracy up to the limit of the theoretical accuracy obtainable using the asymptotic expansion, at the expense of requiring more computer time. This was not done in the present study since the results which were obtained were felt to be adequate. It may be of interest to note that the average time required for calculating a cylindrical function was about 0.05 seconds

If we observe the expressions which lead to the vacuum sheath surface current (2.70), it is apparent that the only source of random error in the calculations is that due to the cylindrical functions. A systematic inaccuracy is represented by the uncertainty in such parameters as the value of the velocity of light (or equivalently μ_o and ϵ_o) Boltzmann's constant, the electronic charge, etc., over which we have no control. The values used for these parameters in the calculations are:

$$\epsilon_o \quad 8.854 \times 10^{-12} \text{ farads/m}$$

$$\mu_o = 4\pi \times 10^{-7} \text{ henrys/m}$$

$$v_\ell = 2.997 \times 10^{8} \text{ m/sec}$$

$$k = 1.8304 \times 10^{-23} \text{ Joules/}^{o}\text{K}$$

$$e = 1.60207 \times 10^{-19} \text{ coulombs}$$

$$m_e = 9.1072 \times 10^{-31} \text{ kg}$$

Due to the complexity of the expressions for the currents, a detailed error analysis is impractical. The situation leading to the greatest inaccuracy occurs when two nearly equal numbers are subtracted since the errors are additive, and can become larger than the result. Multiplication and division lead to roughly an N - fold increase in the errors when N nearly equal numbers with equal uncertainty are involved.

Upon taking into account the number of multiplications and divisions involving the cylindrical functions occurring in the current equations, it seems unrealistic to suppose that the inaccuracy would increase by more than a factor of 10 due to this consideration. In order to check for errors arising from subtraction, various computation points in the process of obtaining the solution were printed out. The situation where nearly equal numbers were being subtracted was identifiable by these check points consistently having zeros in the several last significant figures. A check of the results for the current in such a case revealed numbers which varied erratically from those otherwise obtained. The only time this was found to occur was for angles of incidence of the EK wave

near $\pi/2 - v_r/v_\ell$. Numerical results for the current in this case were obtained from the approximate expansions. An overall accuracy of at least three significant figures is felt to have been maintained in the individual terms in the Fourier series for the current. The convergence of the Fourier series is not a factor here, since the terms were calculated out to the point where the last term is no bigger in absolute magnitude than 10^{-6} times the $m = 1$ term.

This estimate of the accuracy is probably somewhat conservative, as evidenced by the fact that the inhomogeneous sheath and vacuum sheath results agreed to 3 and 4 places after the summation of the Fourier series had been performed. An additional factor in establishing the credibility of the results is the agreement of the calculated curves with the expressions obtained from approximating the exact equations. Finally, the regular variation of the currents with the azimuthal angle ϕ indicates the relative absence of random errors in the calculations. In this regard it should be noted that current minima less than 10^{-3} of the maxima should be regarded with caution since a three figure accuracy in the Fourier coefficients for the currents would indicate that the total error could then exceed the total of the Fourier series at the minima.

NOTATION

A	:	Proportionality coefficient for electron velocity distribution function.
$A(\theta^i, X)$	:	Sheath attenuation function.
AS	:	Abbreviation for ascending series method of calculating cylindrical functions.
$\bar{A}_{---}$	:	Fourier coefficient for expansion of fields arising in the vacuum sheath analysis. Superscript indicates scattered, transmitted or reflected mode, and subscripts indicate mode number, incident wave type and mode type respectively. Example: A^S_{mph}.
α	:	Dummy coordinate.
$\alpha(\theta^i)$	:	Sheath attenuation scale factor.
$\alpha(\ _o)$	:	Factor which shows the decrease in the static electron number density in the sheath due to collection of electrons by cylinder, arising from truncation analysis.
B	:	Proportionality factor appearing in exponential term for electron velocity distribution function.
β	:	z direction separation constant; determined by angle of incidence with respect to cylinder axis of incident wave.
C^α	:	Coefficients which determine the starting values of the final integration in the inhomogeneous sheath analysis.
C	:	Matrix which shows the relation between the various Fourier coefficients obtained in the vacuum sheath analysis.
C_m	:	General cylindrical function of real argument and order m.
c	:	Cylinder radius.
cm	:	Centimeter.
cps	:	Cycles per second.

γ	:	Ratio of specific heats for electron gas.
D_0	:	The m=0 term for the determinant expansion of the vacuum sheath analysis obtained with approximate expressions for cylindrical functions.
D_m	:	The determinant expansion for m greater than zero, corresponding to D_0.
D	:	Electron Debye length for uniform plasma.
D_1	:	The exact expression for the determinant expansion of the vacuum sheath analysis.
d^3v	:	Increment of volume in velocity space.
Δ	:	Coefficient matrix for determining the Fourier coefficients of the vacuum sheath analysis.
Δ	:	Coefficient matrix of reduced order.
∇_r	:	Gradient operator in physical space.
∇_v	:	Gradient operator in velocity space.
δ'	:	Sheath thickness multiplied by 3.
E	:	Total electron energy.
E	:	Used as subscript to indicate plane wave propagation constant and radial separation constant of electromagnetic wave.
E_z	:	Component of electron energy parallel to the z axis.
E_r	:	Component of electron energy perpendicular to the z axis.
E_o	:	Static part of electric field.
E_1	:	Time-varying part of electric field.

$E_m^{(\ )}$: Electric field of inhomogeneous sheath analysis. Superscript indicates component relative to co-ordinate system and subscript shows mode number.

E_E : Electromagnetic component of total electric field, in uniform plasma.

E_P : Electrokinetic component of total electric field, in uniform plasma.

EK : Abbreviation for electrokinetic wave.

EM : Abbreviation for electromagnetic wave.

$\underline{E}$: Total electric field.

e : Electronic charge.

e : Subscript which denotes quantities associated with transverse electric wave and abbreviation for transverse electric wave.

e_j : Charge of j'th plasma species.

erf : Error function.

ϵ : The plasma permittivity.

ϵ_r : The dielectric constant of the plasma.

ϵ_o : Permittivity of free space.

ϵ'' : Imaginary part of permittivity.

F_1 : Integrand of integral for determining the electron number density from the Bernstein and Rabinowitz analysis.

F_2 : Integrand of integral for determining the electron velocity from the Bernstein and Rabinowitz analysis.

$\underline{F}_e$: Electron force term.

$\underline{F}_i$: Ion force term.

$\underline{F}_j$: Force on j'th plasma species appearing in the Boltzmann equation.

f : Frequency of incident wave.

f_{--}^{--} : Factor which relates the various Fourier coefficients of the electromagnetic wave in the vacuum sheath analysis. Superscripts indicate wave types as scattered, transmitted or reflected and subscripts indicate polarization. Example: f_{eh}^{SR} .

f_{eo} : Static electron velocity distribution function.

f_e : Electron velocity distribution function.

f_i : Ion velocity distribution function.

f_j : Distribution function of the j'th plasma species.

f_p : Electron plasma frequency .

Gc : 10^9 cps .

H_o : Static magnetic field.

H : Total magnetic field.

H_1 : Time varying component of the magnetic field.

H_E : Abbreviation for $H_m^{(2)}(\lambda_E s)$.

H_{Eo} : Abbreviation for $H_m^{(1)}(\lambda_{Eo} c)$.

H_P : Abbreviation for $H_m^{(2)}(\lambda_P s)$.

$H_m^{(1)}(z)$: Hankel function of first kind of order m and argument z.

$H_m^{(2)}(z)$: Hankel function of second kind of order m and argument z.

HE : Abbreviation for Hankel's asymptotic Expansion method of evaluating cylindrical functions.

$H_m^{(\ )}$: Magnetic field of inhomogeneous sheath analysis. Superscript indicates component relative to co-ordinate system, and subscript indicates mode number.

$\underline{H}$: Total magnetic field.

h : Denotes transverse magnetic polarization of electromagnetic wave, and used as subscript to indicate quantities associated with transverse magnetic wave.

η : Impedance for electromagnetic wave in plasma.

η_o : Free space impedance for electromagnetic wave.

I : Static electron and ion particle flux density in sheath.

I_E : Imaginary part of the ratio $H_m^{(2)'}(K_E s)/(H_m^{(2)}(K_E s)$ where ' indicates differentiation with respect to argument.

I_P : Imaginary part of the ratio $H_m^{(2)'}(K_P s)/H_m^{(2)}(K_P s)$ where ' indicates differentiation with respect to argument.

I_m : General cylindrical function of imaginary argument and order m.

i : Denotes imaginary quantities.

J : Angular momentum of electron.

J_m : Bessel function of order m.

J_P : Abbreviation for $J_m(\lambda_P s)$.

J_1 : Integration limit of electron angular momentum in Bernstein and Rabinowitz analysis.

J_2 : Integration limit of electron angular momentum in Bernstein and Rabinowitz analysis.

$\underline{J}$: Current density.

K_E : Propagation constant of electromagnetic waves in plasma.

K_{Eo} : Propagation constant of electromagnetic waves in free space.

K_i : Propagation constant of incident wave.

K_P : Propagation constant of electrokinetic waves.

K_m : Cylindrical function of second kind and imaginary argument.

^oK : Degrees Kelvin.

$\underline{K}^{(\ )}$: Cylinder surface current. Superscript indicates component relative to co-ordinate system and subscript indicates incident wave type.

k : Boltzmann's constant.

L : Parameter which relates the magnitudes of the time varying quantities to their static parts in the linearization of the plasma equations.

ℓn : Logarithm to the base e.

λ_E : Radial separation constant of electromagnetic wave in uniform plasma.

λ_{Eo} : Radial separation constant of electromagnetic wave in vacuum sheath.

λ_P : Radial separation constant of electrokinetic wave.

M : Exponent of static potential variation in sheath.

MFP : Electron Mean Free Path.

m : Azimuthal separation constant, an integer.

m_e : Electron mass.

m : Electron mass.

m_i : Ion mass.

m_j : Mass of j'th species in Boltzmann equation.

μ_o : Permeability of free space.

N : Ratio of electron plasma frequency to radio frequency.

$N_e(\rho)$: Denotes Boltzmann distribution for static electron number density variation in sheath.

N_m : Neumann function of order m.

$\bar{N}_{-}$: Normalized energy density of kind indicated by subscript with incident wave indicated by superscript.

n : Time varying electron density variation.

n_e : Electron number density.

n_{eo} : Static electron number density.

n_i : Ion number density.

n_{io} : Static ion number density.

n_o : Static particle density.

n_1 : Time varying electron number density.

n_o : Static electron number density.

n_∞ : Electron and ion number density in uniform plasma.

0E : Abbreviation for Olver's asymptotic Expansion method of evaluating the cylindrical functions.

ω : Angular frequency of incident wave.

ω_p : Angular plasma frequency.

P_e : Electron pressure.

P_i : Ion pressure.

P_{ij} : The ij component of the pressure tensor.

P_o : Non time varying pressure.

P_1 : Time varying pressure.

P : Subscript to indicate electrokinetic plane wave propagation constant and radial separation constant.

$\underline{P}$: Measure of gradient of plasma inhomogeneity.

p : Denotes quantities associated with incident electrokinetic wave or scattered electrokinetic mode.

Φ_c : Cylinder potential.

Φ_o : Static potential in sheath.

Φ^{-} : Denotes potential of wave type indicated by subscript with superscript indicating incident, reflected, transmitted or scattered potential.

ϕ : Azimuthal co-ordinate.

Q : Quantity proportional to time varying electron number density.

Q_m : Q of mode number m.

Q_{ijk} : The ijk component of the heat flux tensor.

R : Superscript denoting quantities associated with reflected mode.

R_E : Real part of the ratio $H_m^{(2)'}(K_E s)/H_m^{(2)}(K_E s)$, where ' indicates differentiation with respect to argument.

R_P : Real part of the ratio $H_m^{(2)'}(K_P s)/H_m^{(2)}(K_P s)$, where ' indicates differentiation with respect to argument.

$\underline{R}$: Matrix used to write boundary condition equations at sheath interface for inhomogeneous sheath analysis.

R_1, R_2, R_3 : Ratios to determine validity of dropping static electron velocity from equations.

r : Space point.

rms : Abbreviation for root-mean-square velocity.

ρ : Radial co-ordinate in cylindrical co-ordinate system.

$\boldsymbol{\rho}$: Unit vector in radial direction.

S : Used as superscript to denote scattered mode.

$S_{\_}$: Source term due to incident wave type indicated by subscript in inhomogeneous sheath analysis.

S_1, S_2, S_3, S_4 : Real and imaginary parts of S_p and S_e, respectively.

$\tilde{S}_{\_}$: Source term due to incident wave of type indicated by subscript for vacuum sheath analysis and boundary equation matrix of reduced order.

$\bar{S}_{\_}$: Source term due to incident wave of type indicated by subscript in vacuum sheath analysis.

s : Sheath radius.

: Summation symbol for Fourier series.

ℓ : Normalized absorption cross-section for inhomogeneous sheath.

T : Superscript which denotes transmitted mode.

T : Particle temperature.

T_e : Electron temperature.

T_i : Ion temperature.

$\bar{T}$: Matrix of coefficients for the inhomogeneous sheath equations.

t : Time.

θ^i : Angle of incidence of incident wave.

θ_c^i : Angle of incidence of electrokinetic wave at which the radial separation constant of the electromagnetic wave becomes imaginary.

θ_s : Angle of incidence of electrokinetic wave at which the backward scattering angle of the electromagnetic wave is 45 degrees from the z axis.

u_e : Total electron velocity.

u_i : Total ion velocity.

u_j : Velocity of j'th species in the Boltzmann equation.

u_m : Velocity at which the integration is terminated in the truncation analysis.

V_E^i : Denotes amplitude of either polarization of incident electromagnetic plane wave.

V_-^i : Amplitude of incident wave of type indicated by subscript.

$V_m^{(\ )}$: Electron velocity of inhomogeneous sheath analysis. Superscript indicates component relative to co-ordinate system and subscript shows mode number.

v : Time varying electron velocity.

v_{eo} : Static electron velocity.

v_{er} : Electron root-mean-square velocity.

v_{io} : Static ion velocity.

v_{ir} : Ion root-mean-square velocity.

v_ℓ : Velocity of light in free space.

v_r : Electron root-mean-square velocity.

v_i : The i component of fluid velocity.

v_1 : Time varying electron velocity.

v_o : Static electron velocity.

W_E : Time average electric energy stored in sheath volume. (Lower case letters denote time average energy density.)

W_H : Time average magnetic energy stored in sheath volume.

W_K : Time average electron kinetic energy stored in sheath volume.

W_P : Time average electron potential energy stored in sheath volume.

$W(\_,\_)$: Abbreviation for Wronskian relation involving cylindrical functions of two different arguments.

w_i : The i component of particle random velocity.

X : Sheath thickness measured in electron Debye lengths.

x : Electron displacement from equilibrium.

Y_A : Admittance relation between electron normal velocity and normal electric field at cylinder surface.

Y_B : Admittance relation between electron normal velocity and time varying electron number density at cylinder surface.

Y'_B : Quantity proportional to Y_B.

Y_i : Dependent variable of inhomogeneous sheath equations.

Y_i^{α} : Value for Y_i obtained at sheath interface from αth integration of inhomogeneous sheath equations.

y : Dummy variable of integration.

Z_c : Integration limit proportional to cylinder potential.

Z_o : Variable proportional to static sheath potential.

z : z variable of cylindrical co-ordinate system.

z : Dummy argument of cylindrical functions.

REFERENCES

Allen, J. E., R. L. F. Boyd and P. Reynolds (1957) "The Collection of Positive Ions by a Probe Immersed in a Plasma", Proc. Phys. Soc. of London 70, Pt. 3, 297-304.

Auer, P. L. (1961) "The Space Charge Sheath in Low Pressure Arcs", Ionization Phenomena in Gases, Munich, Vol. 1, 297-305.

Balmain, K. G. (1965), "The Radiation Resistance of a Slot Antenna in a Compressible Plasma," 1965 Spring USNC-URSI Meeting, Washington, D. C.

Bernstein, I. B. and I. N. Rabinowitz (1959) "Theory of Electrostatic Probes in a Low-Density Plasma", Phys. of Fluids 2, 112-121.

Bohm, D. (1949) The Characteristics of Electrical Discharge in Magnetic Fields, Chapter 3, (Edited by A. Buthrie and R. K. Wakerling; McGraw Hill, New York).

Caruso, A. and A. Cavaliere (1962) Nuovo Cimento 26, 1389.

Chen, K. M. (1961) et. al., "Studies in Non-Linear Modeling III : On the Interaction of Electromagnetic Fields with Plasma", Radiation Laboratory, Ann Arbor, Michigan, Report 4134-2-F.

Cohen, M. H. (1962a) "Radiation in a Plasma II: Equivalent Sources", Phys. Rev. 126 389-397.

Cohen, M. H. (1962b) "Radiation in a Plasma III: Metal Boundaries" Phys. Rev. 126, 398-404.

Dattner, A. (1957) Ericsson Technics 2, 309.

Dattner, A. (1963a) Ericsson Technics 8, 1.

Dattner, A. (1963b) "Resonance Densities in a Cylindrical Plasma Column", Phys. Rev. Letters 10, 205-208.

Dittmer (1926) Phys. Rev. 28, 507.

Fedorchenko, A. M. (1962) "Conversion of a Transverse Electromagnetic Wave into a Longitudinal Wave at a Dielectric-Plasma Boundary", Sov. Phys. Tech. Phys. 7, 428-430.

Field, G. B. (1955) "Radiation by Plasma Oscillations", Astrophys. Journal 124, 555-570.

Gabor, D., E. A. Ash and D. Dracott (1955) "Langmuir's Paradox", Nature 176, 916-919.

Gierke, E., W. Ott and F. Schwirzke (1961) Proc. Fifth Internat. Conf. on Ionized Gases, Munich, Vol. 2, 1412.

Gould, R. W., (1959) Proc. of the Linde Conf. on Plasma Oscillations, Indianapolis.

Harp, R. and G. S. Kino (1963) "Experiments on the Plasma Sheath", VIth International Conference on Ionization Phenomena in Gases, Paris, France.

Harrison, E. R. and W. B. Thompson (1959) "The Low Pressure Plane Symmetric Discharge", Proc. Phys. Soc. 74, Pt. 2, 145-152.

Hessel, A., N. Markuvitz and J. Shmoys (1962) "Scattering and Guided Waves at an Interface Between Air and a Compressible Plasma", IRE Trans. Antennas and Propagation, AP-10, 48-54.

Hessel, A. and J. Shmoys (1962) "Excitation of Plasma Waves by a Dipole in a Homogeneous Isotropic Plasma", Proc. Symposium on Electromagnetic and Fluid Dynamics of Gaseous Plasma, Polytechnic Press of Polytechnic Institute of Brooklyn, New York, 173-183.

Hok, G. (1958) "Electrokinetic and Electromagnetic Noise Waves in Electronic Waveguides", Proc. of Symp. on Electronic Wave Guides, Polytechnic Press of the Polytechnic Institute of Brooklyn.

Kritz, A. H. and D. Mintzer (1960) "Propagation of Plasma Waves Across a Density Discontinutiy", Phys. Rev. 117, 382-386.

La Frambois, J. (1964) "Theory of Electrostatic Probes in a Collisionless Plasma at Rest", Fourth International Symposium on Rarified Gases, Toronto

Lam, S. H. (1964) "The Langmuir Probe in a Collisionless Plasma," Aeronautical Eng. Dept., Princeton University Report No. 681.

Looney, D. H. and S. C. Brown (1964) "The Excitation of Plasma Oscillations", Phys. Rev. 93, 965-969.

Merrill, H. J. and H. W. Webb (1939) "Electron Scattering and Plasma Oscillations", Phys. Rev. 55, 1191-1198.

Olver, F.W.S. (1964), Handbook of Mathematical Functions, Chapter 9, "Bessel Functions of Integer Order," NBS Applied Mathematics, Series 55.

Oster, L. (1960) "Linearized Theory of Plasma Oscillations", Rev. of Mod. Physics, Vol. 32, pp. 141-163.

Parker, J. V. (1963) "Collisionless Plasma Sheath in Cylindrical Geometry", Phys. of Fluids 6, 1657-1658.

Parker, J. V. , and J. C. Nickel and R. W. Gould (1964) "Resonance Oscillations in a Hot Nonuniform Plasma", Phys. of Fluids 7, 1489-1500.

Pavkovich, J. and G. S. Kino (1963) "RF Behavior of the Plasma Sheath", Sixth Internat. Conf. on Ionization Phenomena in Gases, Paris.

Romell, D. (1951) Nature 167, 243.

Rose, D. J. and M. Clark (1961) Plasmas and Controlled Fusion, MIT Press; John Wiley and Sons, New York.

Self, S. A. (1963) "Exact Solution of the Collisionless Plasma Sheath Equation", Phys. of Fluids 6, 1762-1768.

Spitzer, L. (1962) Physics of Fully Ionized Gases, Interscience Publishers.

Stratton, J. A. (1941) Electromagnetic Theory, McGraw-Hill Book Co., Inc.

Tidman, D. A. (1960) "Radio Emission by Plasma Oscillations in a Nonuniform Plasma", Phys. Rev. 117, 366-374.

Tidman, D. A. and G. H. Weiss (1961) "Radio Emission by Plasma Oscillations in Nonuniform Plasmas", Phys. of Fluids 4, 703-710.

Tidman, D. A. and J. M. Boyd (1962) "Radiation by Plasma Oscillations Incident on a Density Discontinuity", Phys. of Fluids 5, 213-218.

Tonks, L. (1931) Phys. Rev. 37, 1458: Phys. Rev. 38, p. 1219.

Tonks, L. and I. Langmuir (1929a) "General Theory of the Plasma of an Arc", Phys. Rev. 34, 876.

Tonks, L. and I. Langmuir (1929b) "Oscillations in Ionized Gases", Phys. Rev. 33, 954.

Wait, J. R. (1964a) "Theory of a Slotted Sphere Antenna Immersed in a Compressible Plasma, Part I", Radio Science, 68D, 1127-1136.

Wait, J. R. (1964b) "Theory of a Slotted Sphere Antenna Immersed in a Compressible Plasma, Part II", Radio Science 68D, 1137-1143.

Wait, J. R. (1965), "On Radiation of Electromagnetic and Electrokinetic Waves in a Plasma," Appl. Sci. Res., Section B, Vol. 12, p. 1.

Wasserstrom, E., C. H. Su and R. F. Probstein (1964) "A Kinetic Theory Approach to Electrostatic Probes", Fluid Mechanics Report No. 64-5, Dept. of Mech. Eng., MIT.

Wehner, G. (1951) "Electron Plasma Oscillations", J. Appl. Phys. 22, 761-765.

Yildiz, A. (1963) "Scattering of Plane Plasma Waves from a Plasma Sphere", Nuovo Cimento 30. 1182-1207.